UNIVERSITAT DE BARCELONA

Role of p38α kinase in myeloid cells during lung metastasis and inflammation

Clara Borràs Eroles

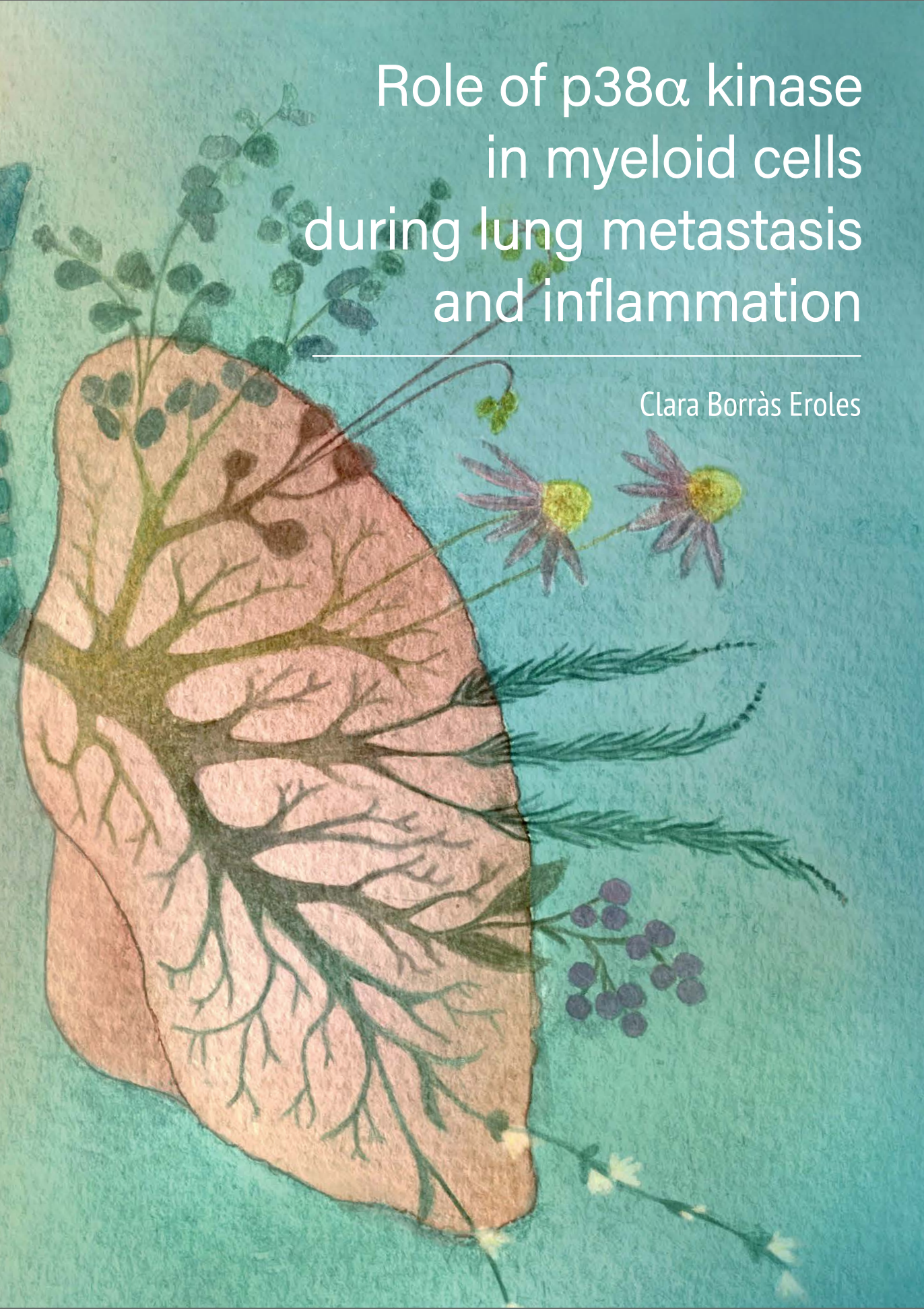

Role of p38α kinase in myeloid cells during lung metastasis and inflammation

Clara Borràs Eroles

UNIVERSITAT DE BARCELONA

INSTITUTE FOR RESEARCH IN BIOMEDICINE
IRB BARCELONA

UNIVERSITAT DE BARCELONA

Facultat de Biologia
Programa de doctorat en Biomedicina

Role of p38α in myeloid cells during lung metastasis and inflammation

Memòria presentada per Clara Borràs Eroles
per optar al grau de doctora per la Universitat de Barcelona

Aquesta tesi s'ha realitzat a
l'Institut de Recerca Biomèdica de Barcelona (IRB Barcelona)

DOCTORANDA	DIRECTOR	CODIRECTORA	TUTORA
Clara Borràs Eroles	Dr. Ángel Rodríguez Nebreda	Dra. Mónica Cubillos	Dra. Annabel Valledor Fernández

Barcelona, Desembre 2022


A la Lourdes, el Jaume,
l'àvia Teresa
i l'avi Pere

"It seems to me that the natural world is the greatest source of excitement; the greatest source of visual beauty, the greatest source of intellectual interest. It is the greatest source of so much in life that makes life worth living."

DAVID ATTEMBOROUGH

"L'art i la naturalesa lluiten sempre fins que es sedueixen l'un a l'altre, la victòria és el mateix traç i línia: aquell que és conquerit, conquereix al mateix temps."

MARIA SIBYLLA MERIAN

"Quan observes, coneixes; quan coneixes, estimes; i si estimes, protegeixes."

JORDI SABATER I PI

El 3 de setembre del 2018 començava la tesi, amb la il·lusió d'estrenar sabates noves. Després de 4 anys escric aquestes línies, i tot i que les sabates estan una mica gastades, no m'he cansat de caminar i sé que em portaran molt més lluny. Acabo la tesi plena de bons records, després de dies de sol, de vent i de tempesta. El que he après durant aquests anys és molt, com a científica i com a persona. Tot i això, aquesta tesi no només ha estat possible amb el meu esforç, sinó també gràcies a tot un teixit de persones que hi han contribuït tant a nivell intel·lectual com a nivell personal. Dedico unes paraules a totes elles.

Ángel, gracias por confiar en mi des del primer día. Contigo he aprendido de la ciencia, de la rigurosidad y del esfuerzo. Siempre recordaré una frase que dijiste en uno de mis primeros lab-meetings y qué me inspiró mucho, "En ciencia, o descubrimos algo nuevo o redescubrimos algo con métodos nuevos". Gracias por dejar fluir mis ideas entre placas de cultivo y pipetas; tus consejos han hecho que éste sea un trabajo del que estoy extremamente orgullosa.

Mónica, has sido una parte imprescindible de todo esto. Me has apoyado en momentos de todos los colores, cuando salían los experimentos y las innumerables veces que no. Hemos picado piedra juntas, reído y llorado, pero sobretodo nos hemos acompañado; cuando una no, la otra sí, y al revés. Muchísimas gracias por estar siempre dispuesta, a todas horas, haces que el lab funcione como un reloj y cuando no estás, ¡estamos perdidas! Al pequeño **Santi**, tus fotos y audios nos han hecho reír en muchos momentos!

Moltes gràcies també als membres del comitè de seguiment de tesi pel consells i recolzament durant aquests 4 anys, **Roger Gomis**, **Juan Ángel Recio** i en particular a l'**Annabel Valledor,** que ha contribuït en aquest projecte amb bons consells, ratolins i reactius.

Sense dubte, agrair també a les del lab, heu fet que el viatge de la tesi hagi sigut molt més fàcil i sobretot, molt més divertit. Moltíssimes gràcies per les preguntes i comentaris tant als lab meetings, com menjant croissants a la oficina, tots han contribuït en algun paràgraf d'aquesta tesi. Gracias **Elisa**, por empezar el proyecto de las mieloides y el pulmón, abriste las puertas de un proyecto muy bonito. **Eli**, ets la persona que em va ensenyar el lab el primer dia, i després, quantes vegades hem rigut juntes! Amb la teva energia fas que el el laboratori sigui una llar. **Bego**, muchas gracias por tu visión científica y por ser la dinamizadora de juegos y actividades del lab! **Laura**, t'he trobat molt a faltar! Vas ser un suport molt important en els primers anys i vaig riure molt amb tu. Per més tallers de dibuixar fulles seques! Pero bueno,

Lorena!!! Mi salsera! Gràcies per ser tu sempre, pels riures, el *perreo* al cotxe, les barbacoes a la Garrotxa i els vermuts una tarda qualsevol. **Nevenka**, I loved sharing the path with you, all the conversations we had to change the world and our world, the cinema sessions and the vermouths! **Dan**, thanks for your sweet view and enthusiasm, I really liked learning from you while enjoying beautiful things together. El meu pollet **Jordi** ! Se'm fa curt el temps amb tu, moltes gràcies pel teu suport i sobretot, pels mil riures per aquí i per allà (i pel bitllet de la loteria). L'altre pollet **Nerea**! Gracias por tu súper entusiasmo y energía, son contagiosos! I endavant amb el català! **Anna**, moltes gràcies per ser-hi i pels ànims, ets super dolça, o en el teu idioma químic, $C_6H_{12}O_6$… **Diana**, thanks for your scientific view and enthusiasm during these past months! **Melisa**, gracias por estos últimos experimentos antes de escribir, eres una crack! **Núria**, gràcies pels teus consells quan començava el doc i per ensenyar-me la meva tècnica preferida, el western blot! Merci també a la **Marga**, la **Raquel** i la **Mariana**, i a tots els estudiants de màster, treballs de recerca i *crazies* que heu passat pel lab, el vostre entusiasme fa que la rutina de la ciència tingui sentit.

Als de les *facilities*, sou els engranatges de l'IRB! Els del FACS; **Jaume**, **Sònia** i **Ricard**, sou amor, gràcies per la vostra paciència infinita. Gràcies **Lídia** i **Camille** per fer que les cèl·lules mieloides hagin donat el millor de sí! Gràcies **Neus** per les sessions al microscopi, sempre m'encanta la teva visió de la biologia. Gràcies **Muriel** per les mil activitats que hem fet, m'han inspirat molt i han fet el camí més artístic i expressiu. Vull agrair també a tota la comunitat de l'**IRB**, gràcies per la disponibilitat de *tothom* a deixar *de tot* sempre, sense això la ciència no funciona!

Gràcies a la **Rosa Ardèvol**, de l'escola el Cim, la **Marta Domingo**, de l'ESO, i la **Virginia Alsedà**, de Batxillerat. Totes vau contribuir a que el meu interès per la biologia creixés i em seguis volent preguntar el perquè de tot. Many thanks to all my lovely internship supervisors, which have carefully contributed to my today' hard and soft skills, without asking anything in return. In Sanquin Amsterdam, **Emile** and **Martijn**, which showed me the first steps in science, from how to pipet to do spotless cell culture. **Vincent**, from Utrecht, *dankjewel* for the patience and rigour you taught me. Your scientific method was exquisite and has accompanied me ever since. **Diana**, my forever mentor, I cannot express how much I learned with you in the Crick, you are definitely one of my referents, both scientifically and personally. Thank you so much for all ☺

Als meus amics PhDs, **Adrià**, **Paula**, **Pep**, **Hania**, **Nico**, **Elena** i **Marina**. Merci per fer d'aquest camí molt més divertit amb sortides, concerts i cerveses per oblidar els experiments que no sortien! Gràcies també a tots els de l'IRB amb qui hem conversat i passat bones estones; **Sara**, **Anna**, **Diego**, **Blazej** i tots els que em deixo. A la **Marieta**,

fa més de 12 anys que compartim camí tu i jo. Moltíssimes gràcies per ser-hi, per les mil converses a dins i fora de l'IRB, els dinars amb el *timer* que sona, els consells immunitaris, i les conferències en les que hem rigut de tot *quisqui*. A la **Sara**, que encara que estiguis a 6.400 km t'he sentit ben a prop sempre, moltes gràcies per ser-hi i per molts anys més dels àudios de 10 minuts. **Elena**, des d'Utrecht que quan ens ajuntem és un no parar de riure, merci per fer-ho tot més dolç. A les amigues de la carrera amb qui ens anem seguint en aquest camí; **Roser**, **Cristina**, **Maria F**, **Marina**, **Èlia**, **Txema**, **Ion**, gràcies pels sopars, sortides i tots els bons moments compartits en companyia!

A les boniques deesses de la meva vida, **Gemma**, **Ari**, **Jana**, **Sarai**, **Natalia**, **Esther**, **Tejo**, **Lorena**, **Maria** i **Olga**. Les estones en companyia amb vosaltres no tenen preu i feu sempre de bàlsam en moments durs. Gràcies pel vostre interès, les llargues converses i el vostre suport durant aquest viatge. **Xavi**, merci pel recolzament i, ànims! que el següent ets tu!

Cristina i **Joan Miquel**, pel vostre suport sempre i en totes les decisions. També al **Quim** i la **Pepa**, pel suport i les rialles.

Moltes gràcies a tota la **família Eroles**, pels sobretaules parlant de ciència i pel vostre interès en mi i en la meva recerca. Als germans Borràs, en especial al **Jan**, pels mil riures compartits i per ensenyar-me Holanda.

A les àvies i als avis **Teresa** i **Pere**, **Josefina** i **Jaume**, sempre us porto amb mi.

Simone, gracias por estar, en días de sol y alguno de tormenta, y hacer que parte del largo camino haya sido más suave y llevadero.

Marta, moltes gràcies per ser part de mi i fer-me part de tu. Per fer-me sentir acompanyada sempre, amb tot, de totes les maneres i en tot moment. Sense tu, molt poques coses tindrien sentit.

Finalment, als meus pares, **Lourdes** i **Jaume**, moltes gràcies per tot allò incondicional i invisible als ulls; gràcies per acompanyar-me en totes les decisions i per donar-me una llanterna en dies foscos. Gràcies per ensenyar-me de la constància, l'esforç, la passió i l'amor a la natura i a la bellesa.

Contents

Summary/Resum

Summary

The lungs are constantly exposed to external particles and microbes, so their particular immune environment is immunosuppressive to avoid unnecessary inflammatory responses. This increases the susceptibility of this organ to lung metastasis, a hallmark of advanced cancer constituting an important cause of dead. Among immune cells in tumors, myeloid cells are very predominant and strongly influence the outcome of primary tumours and metastasis. They promote an immunosuppressive environment and several studies indicate that a high infiltration of myeloid cells in tumours correlates with worse prognosis in patients. In the lungs there is a specific type of tissue-resident myeloid cells, alveolar macrophages (AMs), which are crucial for the fitness of the lungs. These cells are found patrolling the alveolar surface and maintain the immune tolerance of the lungs. A tight regulation of the inflammation pathways is central in AMs. Here, we have studied the influence of the stress-activated protein kinase p38α in lung myeloid cells to determine its role in lung tumorigenesis. By using a mouse model in which we deleted p38α kinase from myeloid cells (p38αΔ^{Lys}), we observed that those mice presented less lung metastasis, accompanied by an increase in activated T cells. Further transcriptomic analysis allowed us to determine that p38α is of particular importance in the biology of AMs, especially in their antigen presentation capacity via the major histocompatibility complex class II (MHCII). *In vitro* experiments using bone marrow derived macrophages (BMDMs) have allowed us to determine that the regulation of MHCII by p38α is through transcriptional regulation of class II transcriptional activator (CIITA). Our results indicate that p38α could regulate CIITA by controlling histone deacetylase 6 (HDAC6) through MK2, a key p38α substrate. We have also observed that AMs highly depend on p38α for other crucial functions such as phagocytosis, efferocytosis and cholesterol homeostasis, processes which were also found affected in AMs from p38αΔ^{Lys}. Additionally, *in vivo* lung inflammation experiments of asthma and acute lung injury revealed that p38α is crucial to maintain lung immunosuppression, a condition which benefits immune evasion of cancer cells. Our results support the importance of a balanced p38α signalling both in homeostasis and in different lung inflammatory pathologies.

Resum

Els pulmons estan sota constant exposició a partícules externes i microbis, de manera que el seu ambient immunitari és immunosupressor per evitar reaccions inflamatòries innecessàries. Això incrementa la susceptibilitat d'aquest òrgan a la metàstasi pulmonar, malaltia que actualment constitueix una important causa de mort. Entre les cèl·lules immunitàries dels tumors, les cèl·lules mieloides són molt predominants i influencien de manera important al desenvolupament tumoral i la metàstasis. Promouen un ambient immunosupressor que beneficia el tumor i de fet, molts estudis correlacionen una alta infiltració de cèl·lules mieloides als tumors amb una pitjor prognosi dels pacients. Als pulmons hi ha un tipus especial de cèl·lules mieloides residents de teixit, els macròfags alveolars (MAs), que són clau per mantenir el bon funcionament pulmonar. La regulació de les cascades de senyalització inflamatòries és central en els MAs. En aquesta tesi, hem estudiat la influència de la proteïna cinasa activada per estrès p38α en cèl·lules mieloides per veure la seva funció en la formació de tumors pulmonars. Per fer-ho, hem fet servir un model de ratolí en què la proteïna p38α està delecionada en les cèl·lules mieloides (p38αΔ^{Lys}). Amb aquest model, hem observant que els ratolins p38αΔ^{Lys} presentaven menys metàstasis que els control, i això estava acompanyat d'un increment en les cèl·lules T activades. Amb anàlisis de transciptòmica hem pogut veure que p38α és crucial en la biologia dels MAs, particularment en la seva capacitat de presentació d'antígens via el complex major d'histocompatibilitat de classe II (MHCII). Experiments *in vitro* usant macròfags derivats de medul·la òssia ens han permès determinar que la regulació de MHCII per p38α és mitjançant la regulació de l'activador transcripcional de classe II (CIITA). Els nostres resultats indiquen que p38α podria regular CIITA mitjançant la regulació de la histona desacetilasa 6 (HDAC6) per mitjà de la cinasa MK2, un dels principals substrats de p38α. També hem observat que els MAs depenen de p38α per altres funcions importants, com la fagocitosi, esferocitosi i la regulació de la homeòstasi del colesterol. Experiments *in vivo* d'asma i lesió pulmonar aguda han revelat que p38α és crucial en el manteniment de la immunosupressió pulmonar, una condició que, per altra banda, és beneficiosa pel creixement tumoral. Els nostres resultats suporten la importància de la senyalització de p38α en homeòstasi i en diferents patologies inflamatòries pulmonars.

Abbreviations

A

5-AZA	5-azacytidine
ActD	Actinomycin D
ALT	Alanine aminotransferase
AM	Alveolar macrophage
APC	Antigen presenting cell
ARDS	Acute respiratory distress syndrome

B

BAC	Bacterial artificial chromosome
BAL	Bronchoalveolar lavage
BCR	B Cell receptor
BMDM	Bone marrow-derived macrophages
BrdU	Bromodeoxyuridine

C

CARD	Caspase activation and recruitment domain
CD-	Cluster of differentiation
cDC	Classic dendritic cell
CDK	Cyclin-dependent kinase
Cef	Ceftriaxone
CIITA	Class II transcriptional activator
CLIP	Class-II associated Ii chain peptide
COPD	Chronic Obstructive Pulmonary Disease
CREB	Cyclic-AMP-responsive-element-binding protein
CTLA4	Cytotoxic T-lymphocyte antigen 4

D

DC	Dendritic cell
ddH2O	Double distilled H_2O
DMSO	Dimethyl sulfoxide
DSS	Dextran sulphate sodium
DUSP	Dual specificity phosphatase

E

EMT	Epithelial to Mesenchymal Transition
ER	Endoplastic reticulum
ERK	Extracellular signal regulated kinase

F

FACS	Fluorescent-activated cell sorting
FBS	Fetal Bovine Serum
FC	Fold change
FDR	False discovery rate
FS-A	Forward scatter area

G

GM-CSF	Granulocyte-macrophage colony-stimulating factor
GO	Gene Ontology
GSEA	Gene Set Enrichment Analysis

H

h	Hours
H/E	Hematoxilin/Eosin
HAT	Histone acetylase
HDAC	Histone deacetylase
HDM	House dust mite
HSPC	Haematopoietic stem and progenitor cells

I

i.p.	Intraperitoneal
IFN	Interferon
IHC	Immunohistochemistry
Ii	Invariant chain
IL	Interleukin
ILC	Innate lymphoid cell
IM	Interstitial macrophage
IP	Immunoprecipitation
IRF	IFN-regulatory factors

J

JAK	Janus kinase
JNK	C-Jun N-terminal kinase

K

KO	Knock-out

L

LPS	Lipopolysaccharide

M

MAPK	Mitogen-activated protein kinases
MAPKAP	MAPK-activated protein
MDSC	Myeloid-derived suppressor cell
MFI	Mean Fluorescence Intensity
MHC	Major histocompatibility complex
MK2	MAPK-activated protein kinase-2
MNK	MAPK interacting kinase
MPO	Myeloperoxidase
MSK	Mitogen and stress activated kinase

N

NES	Normalized Enrichment Score
NEX	Nexturastat
NFKB	Nuclear factor k-light chain enhancer of activated cells
NFY	Nuclear transcription factor Y
NK	Natural killer
NLR	NOD-like receptor
NSCLC	Non-small cell lung carcinoma

O

OVA	Ovalbumin

P

P/S	Penicillin/streptomycin
PCR	Polymerase chain reaction
PD-1	Programmed cell death 1
PD-L1	Programmed death-ligand 1
pDC	Plasmacytoid dendritic cell
PG E2	Prostaglandin E2
PPAR-	Peroxisome proliferator-activated receptor
PRR	Pattern recognition receptor
pval	P-value

R

RBC	Red blood cell
RFX	Regulatory factor X
RNA-Seq	RNA Sequencing
ROS	Reactive oxygen species
RT	Room temperature
RT-qPCR	Reverse transcription-quantitiative PCR

S

sc-RNA-Seq	Single cell RNA Sequencing
SD	Standard Deviation
SEM	Standard Error of the Mean
siRNA	Silencing RNA
STAT	Signal transducer and activator of transcription

T

T-regs	Regulatory T cells
TAM	Tumor-associated macrophage
TAN	Tumor associated neutrophil
TCR	T cell receptor
tDC	Tumor-associated dendritic cell
TGF	Transforming growth factor-
TLR	Toll like receptor
TME	Tumor microenvironment

TNF	Tumor necrosis factor
TSA	Trichostatin A

U

UMAP	Uniform Manifold Approximation and Projection
UV	Ultraviolet

V

VEGF	Vascular endothelial growth factor

W

WT	Wild-type

Introduction

Metastasis

Described as one of the main hallmarks of cancer (Hanahan, 2022), metastasis is usually a final and fatal stage in solid tumor progression and accounts for the majority of deaths from cancer (Dillekås et al., 2019). In this process, cancer cells from the primary tumor detach, intravasate and travel through the circulatory or lymphatic system, evading immune attack, to finally extravasate at distant capillary beds, to proliferate and colonize distant organs (Fares et al., 2020; Ganesh & Massagué, 2021).

Metastatic cells have selective pressure all over the process. The ones that reach and colonize a secondary organ have succeeded in all the previous stages of the metastatic cascade, surviving in a foreign microenvironment and protecting themselves against immune surveillance. Thus, a fine cross-talk between the tumor cells and the microenvironment is required for the colonization of the distal organ. Mechanisms of tumor cells to successfully colonize secondary organs include evasion of the immune system, promotion of survival signals in the stem/resident cell niches in the local microenvironment and recruitment of cells that remodel the host microenvironment to match the requirements of cancer cells. The metastatic niche can form after the tumor cell arrival (post-formed niche) or start forming before the tumor cell arrives (premetastatic niche). In this premetastatic niche, factors from the primary tumor travel through circulation and prepare the niche in the secondary organ before metastatic cell arrival (H. Wang et al., 2021).

Primary tumors have a unique and recurrent tropism for certain organs to metastasize. For instance, lung cancer usually metastasizes to liver, brain, bone and lung; breast cancer spreads to bone, liver, lung and brain; colon cancer to liver and lung (Obenauf & Massagué, 2015). The fact that specific primary tumors usually metastasize to the same tissues and that these tissues are common amongst different cancers points at a combination of certain cellular traits in the cells of origin and a specific "permissive" composition of the target organ microenvironment that determine this specific tropism (Obenauf & Massagué, 2015). Already described in 1889, the "seed and soil" hypothesis proposed that for a tumor to metastasize, the "seed" (cancer cell) and the "soil" (target or secondary organ) have specific characteristics that facilitate the metastatic process (Fidler & Poste, 2008; Q. Liu et al., 2017; Paget, n.d.).

The lungs constitute a very common metastatic destination for a variety of primary tumors, including breast cancer, gastrointestinal tumors, renal carcinomas, melanoma, sarcomas and lung cancer (Budczies et al., 2015; Riihimäki et al., 2018).

Lung metastasis is a hallmark of advanced malignant cancer and constitutes an important cause of dead in cancer patients (Obenauf & Massagué, 2015). The lungs present a very particular immune environment that might be responsible for the susceptibility of this organ to tumor metastasis. The lung facilitates the process of metastasis at different stages; by developing a premetastatic niche by inflammatory factors produced by the primary tumor and/or when the tumor cells arrive to the lungs. The characteristic physiology of the lungs, with immune suppression and tolerance to maintain an immune balance, makes this tissue a perfect target organ for metastasis. A better understanding of the lung functions in homeostatic conditions can provide clues about the biology of the lung metastatic process.

The tumor microenvironment

Tumors include several types of non-malignant cells that shape the processes of tumor initiation, growth, invasion and metastasis. Early in tumor formation, there are already reciprocal interactions between malignant cells and the components of the stroma that support cancer cell survival, local invasion and metastatic dissemination (Anderson & Simon, 2020). To help overcome the acidic and hypoxic conditions, the tumor microenvironment (TME) orchestrates a program promoting angiogenesis to supply nutrients and remove metabolic waste. Tumors become infiltrated with immune cells that can perform anti-tumor or pro-tumorigenic functions. Moreover, the TME can also affect the response to cancer therapy. The participation of the TME in cancer is considered one of the hallmarks of cancer given its importance in the biology of this disease (Hanahan & Weinberg, 2011). Some authors even consider factors beyond the TME, the tumor organismal environment, as key important factors for the development of this disease (Laplane et al., 2019). For these reasons, increasing research efforts are put into the development of new therapies to target specific components of the TME. However, the clinical efficacy of these new therapies remains still unsatisfactory.

The TME comprises cancer cells and non-malignant cells such as fibroblasts, immune cells, endothelial cells, and neural cells, as well as the extracellular matrix components (Anderson & Simon, 2020; Jin & Jin, 2020). The TME is complex and heterogeneous and can exert different functions depending on the tumor type and stage. Interactions between the different components can promote anti-tumoral or pro-tumoral activities. The types of stromal cells found in the TME are heterogeneous and depend on the tumor type. Cancer cells and immune cells establish complex relationships though the expression of cytokines and the release of exosomes, which finally determine the

stage and outcome of the disease (Farc & Cristea, 2021). Given their potential use for anti-cancer therapy, immune cells are one of the most important players in the TME (**Figure 1**).

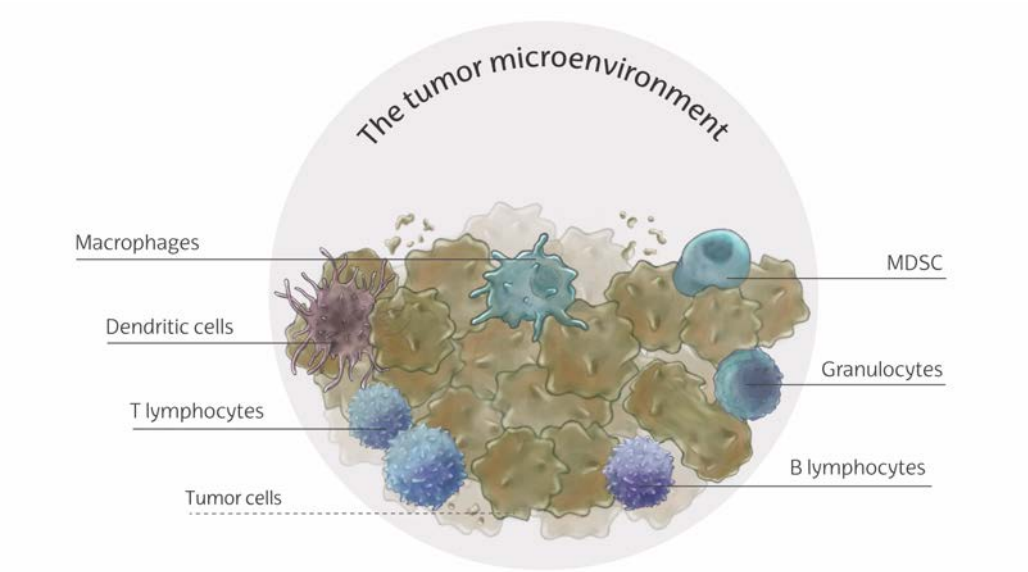

Figure 1. Immune cells in the tumor microenvironment
Different immune cell types in the tumor microenvironment play crucial roles in tumor progression. Macrophages include both monocyte-derived and tissue-resident macrophages, T lymphocytes include both $CD4^+$ and $CD8^+$ T cells, and granulocytes include neutrophils, eosinophils, basophils and mast cells. MDSC= myeloid derived suppressor cells.

Immune cells in the TME

Immune cell infiltrates are usually abundant in biopsies of human tumors. Their role in tumor progression is crucial, so their study is of major importance. Immune cells in the TME can be classified in different ways, although a common one is to distinguish between adaptive and innate cellular components (**Figure 1**). Adaptive immunity is activated by specific antigens and uses "memory" to evaluate the threats and enhance the immune responses. Adaptive immunity in the tumors comprises the function of $CD4^+$ and $CD8^+$ T lymphocytes, and B lymphocytes (Farc & Cristea, 2021). Although the adaptive response is the one actually promoting the ultimate anti-tumoral response, it is clear that innate immune mechanisms are also involved in the recognition of tumors by the immune system and play a crucial role in tumorigenesis (Gajewski et al., 2013). As the first line of defence, innate immunity is a non-specific defence mechanism that starts within hours after a foreign antigen enters the body. The innate cells mainly come from the myeloid lineage of the hematopoietic system

and comprise macrophages and monocytes, dendritic cells (DCs), granulocytes, natural killer (NK) cells, NK T cells, γδ-T-cells and innate lymphoid cells (ILCs).

The cancer immunity cycle

Tumor cells can be detected and eliminated by the immune system through the cancer immunity cycle (Chen & Mellman, 2013), which is the basis for most current immunotherapies. In this process, genetic alterations and de-regulation of normal cellular processes in the cancer cells result in the expression of neoantigens, differentiation antigens or cancer testis antigens (**Figure 12**). These are released when cancer cells die being captured and processed by professional antigen presenting cells (APCs) which, together with proinflammatory signals, present the captured antigens to T cells in the proximal lymph nodes (Chen & Mellman, 2013) (**Figure 12**). This results in the priming and activation of T cells to effector responses, which travel and infiltrate the tumor mass to kill the tumor cells. This death releases additional tumoral antigens, which boost and re-start the cycle again (**Figure 12**). In fact, tumor infiltration by $CD4^+$ and $CD8^+$ T lymphocytes is often a marker of good prognosis in different cancer types (Barnes & Amir, 2017). However, this simplified process does not perform optimally in cancer patients. The cycle is not sustained as there are handicaps and tumor hijacks in all the stages of the cycle. The tumors gradually evade from this immune surveillance by shaping the TME to become immunosuppressive and allow cancer cell growth.

Immunosuppression in the TME

The TME may include both immune cells that attack or supress the tumor and immune cells that promote tumor growth. Immunosuppressive environments promote tumor progression, protecting the tumor from immune attack and limiting the efficacy of immunotherapies. However, immunosuppressive responses are not a *de novo* mechanism of tumors, in fact, they are physiological responses that are crucial to promote tolerance, limit the inflammatory response and promote wound healing and tissue repair (Byun & Gardner, 2013). Therefore, tumors not only survive and disseminate, but they can also co-opt pre-existing mechanisms of the immune system to boost conditions that favour tumor immune tolerance and escape the immune attack (Byun & Gardner, 2013).

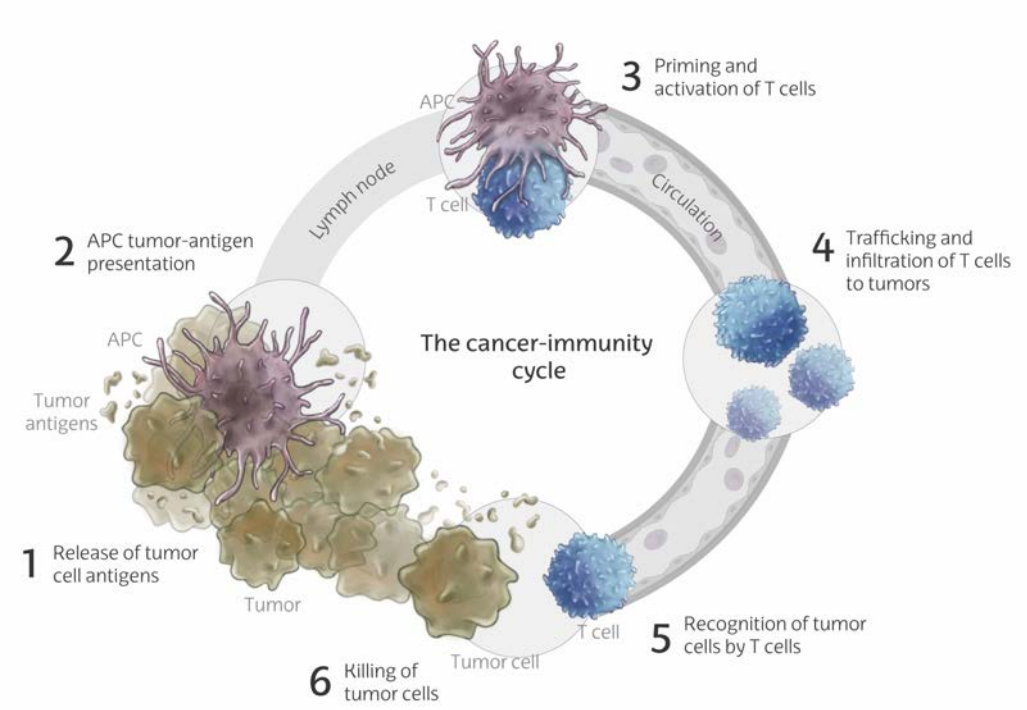

Figure 12. The cancer-immunity cycle
The immune response against cancer is a cyclic process divided in some major steps. It starts with the release of tumor cell antigens generated upon tumor cell death (1), those antigens are taken by antigen presenting cells (APC) as macrophages and DCs (2) and presented in the local lymph nodes to prime T cell activation (3). Activated T cells travel through the circulation to the tumor site (4) where they recognise the tumoral antigens (5) and promote the killing of tumor cells (6), which releases additional antigens that can further propagate the cycle. Adapted from (Chen & Mellman, 2013).

The immunosuppressive microenvironment of tumors is composed of a variety of cellular and soluble components. The main cells that play a role in the immunosuppressive phenotype of the TME are different types of myeloid cells and adaptive immune cells like the regulatory T cells (T-regs) (Tie et al., 2022). A vast amount of research effort is being devoted to developing therapies that target these cells in cancer (Tie et al., 2022). The final outcome of the tumor will depend on the complex balance between anti-tumor and immunosuppressive responses. For instance, large amounts of T-regs compared to effector T cells in tumors tilt the balance in favour of a more tolerogenic environment (Zou, 2005). Changes in the APC subsets with an increased expression of co-inhibitory molecules and IL-10 production also tilt the balance towards a more immunosuppressive environment (Zou, 2005). Besides, small molecules released by cancer cells or immune cells are also involved in the immunosuppressive phenotype, such as vascular endothelial growth factor (VEGF), transforming growth factor (TGF)-β, and cytokines like interleukin (IL)-10

(Aguilera et al., 2014; S. Li et al., 2020; Ouyang & O'Garra, 2019). In addition, cancer cells can also evade the immune response by decreasing the expression of neoantigens and antigen presentation molecules, or by upregulating the expression of immune checkpoint molecules to avoid immune recognition (Sade-Feldman et al., 2017; Vinay et al., 2015). Amongst all the immune cells in the TME, myeloid cells are major players in the immunosuppressive response in tumors.

Myeloid cells in the TME

Myeloid cells are the most abundant cell type in the TME, and emerging evidence indicates that their presence in tumors influences patient survival (Engblom et al., 2016). Myeloid cells are a type of innate immune cells crucial for the defence against infection and are also very important in tissue homeostasis, as well as by the initiation, maintenance and termination of T cell adaptive immune responses.

Myeloid cells comprise various cell types including mononuclear phagocytes, as macrophages and DCs, and granulocytes, as neutrophils, eosinophils, mast cells and basophils. However, in the context of a tumor, the TME can define and remodel both infiltrating and resident myeloid cells into tumor-associated macrophages (TAMs), tumor-associated neutrophils (TAN), tumor-associated DCs (tDCs) and others. Myeloid-derived suppressor cells (MDSC) are exclusively found in tumors, and include an heterogeneous population of myeloid progenitors and monocyte/granulocyte-like cells, defined by their functional ability to supress T cells *in vitro* (Lu et al., 2011). However, macrophages can also suppress T cell activity, and it is disputed whether MDSC are a different myeloid cell population or just a different cell state (Engblom et al., 2016; Pittet et al., 2022). Macrophages perform local functions including the regulation of tissue homeostasis, inflammation and immune surveillance. TAMs from monocytic or tissue-resident origin can affect tumor growth and have a variety of functions (Pittet et al., 2022). DCs consist on different subsets; classic DCs (cDCs), which are specialized in sampling antigens, migrating to the draining lymph node and activating the T cell adaptive response, and plasmacytoid DCs (pDCs), which produce interferon (IFN)-α (IFNα) and also regulate cancer progression (Swiecki & Colonna, 2015). Within tumors, tDCs can affect the fate of tumor infiltrating T cells shaping the adaptive immune response against tumors (Gerhard et al., 2021). Granulocytes can accumulate in disease states and release potent inflammatory agents that protect the host against various inflammatory insults (Galli et al., 2011; Nathan, 2006; Rosenberg et al., 2013). Although the role of eosinophils and basophils in tumor progression remains still unresolved, neutrophils have been linked to cancer progression and their presence in tumors is associated with poor prognosis (Coffelt et al., 2016).

The functions of myeloid cells in tumorigenesis have been linked mainly to tumor-promoting abilities, but they also have anti-tumoral functions. The tumor-promoting functions include promotion of cancer proliferation by secreting cytokines and growth factors, increased tumor vascularization by production of angiogenic factors, increased tumor cell invasion by enzymes and other factors, and suppression of NK and T cells by intracellular, cell surface and secreted molecules (Engblom et al., 2016). Anti-tumoral functions include direct cell killing or elimination by other immune cells as NK or $CD8^+$ T cells (Engblom et al., 2016).

Tumors may also use myeloid cells to promote cancer cell proliferation not only within the local TME but also in distant body organs. Some tumors express soluble factors that travel and act in other parts of the body and induce myeloid cell production from haematopoietic stem and progenitor cells (HSPCs) (Bayne et al., 2012; Casbon et al., 2015; Cortez-Retamozo et al., 2013). In that line, enriched myelopoiesis has been observed in human cancer patients (W. C. Wu et al., 2014), and mice with tumors also show an increase in myeloid progenitors in the bone marrow (Casbon et al., 2015). Moreover, the primary tumor can prime other tissues to form a supportive metastatic environment, called the premetastatic niche (Sceneay et al., 2013), and myeloid cells have emerged as crucial players in this process. Various studies have reported tumor-produced factors that promote mobilization of bone marrow derived myeloid cells and their recruitment to premetastatic sites (Granot et al., 2011; Hiratsuka et al., 2006; S. Kim et al., 2009; Kowanetz et al., 2010; Sceneay et al., 2012; Wculek & Malanchi, 2015; Yan et al., 2010). These cells produce integrins, chemokines, growth factors, inflammatory mediators and angiogenic factors in response to the tumor-released soluble molecules which together promote a niche that facilitates tumor cell invasion of the secondary organ (Sceneay et al., 2013).

Macrophages in the TME

Amongst the myeloid cells in the TME, macrophages represent a very heterogeneous population which is particularly abundant in tumors, and are present throughout all the stages of tumor progression (Noy & Pollard, 2014; Pittet et al., 2022). Macrophages have been described to perform pro-tumoral functions in the primary and metastatic sites, including suppression of T cell responses, promotion of angiogenesis, tumor cell invasion and motility, intravasation and stimulation of cancer cell proliferation (Biswas et al., 2013; Coussens et al., 2013; Nielsen & Schmid, 2017; Qian & Pollard, 2010; Redente et al., 2010). Therefore, macrophages represent a very promising target for cancer therapy (DeNardo & Ruffell, 2019), including both

enhanced chemotherapy response and immune checkpoint blockade immunotherapies like anti-cytotoxic T-lymphocyte antigen 4 (CTLA4) or anti-programmed cell death 1 (PD-1) or anti-programmed cell death ligand 1 (PD-L1) (Cassetta & Kitamura, 2018).

In the early 2000, the M1 and M2 paradigm of macrophage polarization was introduced continuing the Th1/Th2 lymphocytic polarization (Mills et al., 2000). This classification resulted from *in vitro* stimulation experiments and considers that M1 macrophages express pro-inflammatory factors, while M2 macrophages express anti-inflammatory and wound-healing mediators. In a general canonical sense, M1 macrophages are "classically-activated" under IFNγ or lipopolysaccharide (LPS) stimulation, and produce high levels of tumor necrosis factor (TNF)α, IL-6, IL-12, IL-1β and reactive oxygen species (ROS) to promote inflammation and activate an immunological response against foreign pathogens (Italiani & Boraschi, 2014). On the other side, M2 macrophages are "alternative-activated" in response to IL-4 or IL-13, and express high levels of arginase and anti-inflammatory IL-10 and TGFβ, promoting tissue repair, angiogenesis and modulating effector functions of lymphocytes to resolve inflammation (S. Gordon, 2003). Further classification of M2 macrophages has been suggested according to the agents they are exposed to: M2a exposed to IL-4/IL-13, M2b to immune complexes and toll like receptor (TLR) agonists, M2c to IL-10 and glucocorticoid hormones, and M2d to TLR agonists through adenosine receptor (Benoit et al., 2008; Shapouri-Moghaddam et al., 2018). However, with recent technical advances in genomics and transcriptomics, this M1-M2 concept has become oversimplified. The reality *in vivo* is that there is a continuum of macrophage populations with various functions that exhibit high plasticity and can switch from phenotypes when exposed to different environmental cues. There have been some attempts to standardize the nomenclature of macrophages, but a unifying language to describe macrophage phenotypes is still missing (F. O. Martinez & Gordon, 2014; Murray et al., 2014). However, although simplistic and with some limitations, the M1-M2 paradigm has proven useful to classify macrophage functions in cancer. Pro-tumoral states of macrophages in cancer have been described as M2-like, whereas anti-tumoral properties have been attributed to M1-like phenotypes. However, TAMs can express M1 and M2 markers at the same time or express other markers not included in this paradigm. A further important distinction is whether the TAMs are recruited or have a tissue-resident origin, since their functions related to the development of the tumor can differ. Hence, techniques like RNA Sequencing (RNA-Seq) or single cell RNA-Seq (sc-RNA-Seq) are becoming crucial to understand macrophage functions in cancer.

Origin of macrophages

Macrophages have two distinct developmental origins; they can form from hematopoietic stem cell-derived circulating monocytes or from embryonic precursors (Perdiguero & Geissmann, 2016). In mice, circulating monocytes can be either classical/Ly6C^{hi} or patrolling/Ly6C^{lo} monocytes. Classical or Ly6C^{hi} monocytes are recruited to the tissues in response to injuries, infections, inflammation or neoplastic transformation (Kratofil et al., 2017; L. Liu et al., 2017). Patrolling or Ly6C^{lo} monocytes, on the other hand, are primarily involved in vasculature maintenance (Lichanska & Hume, 2000). The majority of tissue-resident macrophages are seeded in the organs before birth and derive from embryonic precursors (Perdiguero & Geissmann, 2016). After birth, the tissue-resident macrophages are mainly maintained by self-renewal. Under certain conditions like ageing or inflammation, circulating monocytes can also give rise to tissue-resident macrophages with self-renewal capacities (Gomez Perdiguero et al., 2015; Molawi et al., 2014; Van Hove et al., 2019).

Tissue-resident macrophages

Tissue-resident macrophages are a heterogeneous population with a substantial tropism to their niche and are less plastic than the recruited macrophages (Guilliams & Svedberg, 2021). Although sharing the same developmental origin, there is significant genetic diversity amongst tissue-resident macrophage populations (Gautiar et al., 2012). However, almost all of them are dependent on CSF1/CSF1R signalling for their development and survival (Cotechini et al., 2021), except alveolar macrophages (AMs), which depend on granulocyte-macrophage colony-stimulating factor (GM-CSF) (Guilliams et al., 2013). Tissue-resident macrophages are critical to maintain tissue homeostasis and control tissue remodelling. Given their anatomical position, they are sentinels of the immune system and play important roles in antigen presentation, control of inflammation and resolution (Mu et al., 2021). They also coordinate the maintenance of tolerance in their target organs, for instance, by expressing tolerogenic transcriptional programs and immune checkpoint inhibitors, or by controlling the generation of FoxP3^{+} T-regs (Balhara & Gounni, 2012; Soroosh et al., 2013).

There are tissue-resident macrophages in the majority of adult organs. The populations described so far comprise lung AMs, dermal macrophages, large peritoneal macrophages, pancreatic macrophages, osteoclasts, epidermal Langerhans cells, brain microglia, liver Kupffer cells, splenic red pulp macrophages,

kidney, adipose tissue, mammary gland and cardiac macrophages (Perdiguero & Geissmann, 2016; T'Jonck et al., 2018).

Tissue-resident macrophages in cancer

Given their specific localization, tissue-resident macrophages are amongst the first cellular components that interact with the tumor cells. For this reason, they play an important role in tumorigenesis, both in tumor initiation, when the tumors are established, and in pre-metastatic and metastatic lesions. However, little is known about their specific roles in tumor progression partly due to the only recent knowledge of their ontology. It seems that their origin and tissue specificity differentially impact tumor progression. For instance, depletion of resident macrophages, but not recruited monocyte-derived macrophages, reduced tumor progression in a mouse model of pancreatic ductal adenocarcinoma (Y. Zhu et al., 2017). In the context of the M1/M2 paradigm, tissue-resident macrophages fall into the M2-like category, since their function is fundamentally to coordinate tissue development, resolve inflammation and maintain tissue integrity activating repair mechanisms (Davies et al., 2013). These characteristics have been suggested to contribute to the establishment of a "soil" or premetastatic niche for eventual metastatic cancer. In fact, the main sites of metastasis in patients and in mouse models are lung, liver, brain and bone, all populated by tissue-resident macrophages. In experimental models of metastasis, tissue-resident macrophages correlate with tumor growth (Loyher et al., 2018). For example, in an ovarian tumor model, tissue-resident macrophages facilitate the epithelial to mesenchymal transition and their targeted depletion prevents peritoneal metastatic disease (Etzerodt et al., 2020). Thus, tissue-resident macrophages contribute to tumor progression and could be considered as therapeutic targets to help preventing malignant progression.

Macrophage-targeted therapies to boost anti-tumoral response

Many research efforts are devoted to understand the role of macrophages in cancer, and a vast amount of therapeutic strategies have been developed to target macrophages in tumors (Cotechini et al., 2021; Pittet et al., 2022). Some strategies aim at preventing the recruitment of macrophages by the tumors, such as treatments with inhibitors of CSF1/CSF1R, CCR2-CCL2 or CXCR4. Other strategies aim at depleting macrophages, such as TREM1/2 or CSF1/CSF1R inhibitors. Also, inhibitors of SIRP1α-CD47 and SIGLEC10-CD24 are being studied to exploit the antitumoral functions of TAMs. A recent interesting strategy is to reprogram the TME to a more anti-tumoral

state, characterized by increased infiltration of cytotoxic T cells, with M1-like macrophages and decreased numbers of M2-like cells. This is being explored by the use of CD40 or TLR agonists, anti-PD-L1 antibody, and TREM, PI3K and histone deacetylase (HDAC) inhibitors, which all aim at reprogramming TAMs to a M1-like phenotype. The development of engineered macrophages is also under study to reprogram the TME or to eliminate cancer cells (Cotechini et al., 2021; Pittet et al., 2022; Xu et al., 2022).

It is important to note that those treatments used alone rarely lead to tumor elimination, and their efficacy lays in the combination with other treatments, such as the use of immune checkpoint blockade antibodies that further boost the anti-tumoral phenotype of T cells (Pittet et al., 2022; Xu et al., 2022).

Lung immunity in health and disease

The lungs are one of the main and most important organs in our body. They are part of the respiratory system and their main function is to perform respiration, the gas exchange that provides oxygen to the rest of the organs and removes carbon dioxide from the blood. This function is vital for the organism, so the fitness of airways and their cellular components are of crucial importance. The lungs are formed by lobes and the respiratory airways; the larynx and trachea, branching to the bronchus, continuing through bronchioles and finally terminating in millions of highly-vascularized alveoli, which are microscopic air-filled sacs where the gas exchange occurs (Popper, 2017).

Lungs filter around 11.000 litters of air every day in an airway surface area of 90 m^2, which compared to the 10 m^2 of the guts, is a quite large surface. This means that airways are under continuous exposure to many external particles, which may be harmful or not, as well as to allergens and microbes. Lungs represent the most frequently targeted organ by pathogens, so this organ faces the challenge of a continuous demand of gas-exchange while fighting against foreign pathogens in a controlled manner ("The Lungs at the Frontlines of Immunity," 2014). Inappropriate inflammatory responses can cause various diseases such as asthma, pulmonary edema, fibrosis and emphysema, which can damage the organ and result in life-threating lung failure (Kopf et al., 2015). Some of the mechanisms by which the lungs protect against foreign particles are physical or soluble. Big particles remain trapped in the upper areas of the respiratory tract in the nasopharynx or tonsillar regions and expelled with coughing or sneezing. Further down, foreign particles are expelled

back up in the mucus layer through rhythmic movements of the microscopic cilia, a process called the mucociliary "escalator" (Bustamante-Marin & Ostrowski, 2017). The mucus layer of the airways also contains various antimicrobial components like surfactant proteins, collectins and complement components that bind to microbial peptides allowing their uptake by innate immune cells. Moreover, lung airways count on immune cells that repel pathogens and, equally important, repair injury in an inflammation-restrained manner. In this context, the lung immune system has evolved to simultaneously repel pathogens and restrain damage caused by inflammation to maintain gas exchange. Importantly, as mentioned above, the lung represents one of the most common sites of tumor metastasis.

Lungs are full of immune cells which maintain this delicate balance between immunity and tolerance. There are cells both of myeloid and lymphoid lineages, which reside in the lungs and provide a localized tissue-specific immune protection (Ardain et al., 2020). Lung resident immune cells comprise macrophages (alveolar and interstitial), DCs, neutrophils, eosinophils, basophils, mast cells, NK cells, ILC, B cells and T cells. Lung-resident macrophages are found near the epithelial surface and sample the air-borne material. Together with DCs and alveolar epithelial cells, they determine the threshold and quality of the immune response.

Lung-resident macrophages

In the lungs, the majority of macrophages are AMs, which reside in the alveolar space, while a small population of interstitial macrophages (IMs) resides in the lung parenchyma. The population of IMs is complex and has been less studied than AMs. However, they are important given that they function as neuroimmune communicators, provide chemoattractant signals for leukocytes, are involved in wound healing and repair, and secrete immunoregulatory cytokines like IL-10, TGFβ, IGF-1 and others (Ardain et al., 2020; Bedoret et al., 2009; Ural et al., 2020). Although less numerous than AMs, IMs can also phagocyte particles and bacteria (Bedoret et al., 2009; Fathi et al., 2001). Their antigen presentation capacity is superior than AMs and can drive T cell proliferation and T-regs differentiation (Chakarov et al., 2019). Unlike AMs, IMs mainly rely on the replenishment by blood monocytes (Aegerter et al., 2022; Ardain et al., 2020). On the other hand, AMs have been more studied in both homeostasis and pathological conditions and have been implicated in both processes.

Alveolar macrophages

AMs are the very first line of defence in the alveoli and the lung airways. As tissue-resident macrophages, they perform functions to keep homeostatic and metabolic conditions which are required to maintain the organ fit. At the same time, they also perform repair functions and are sentinel phagocytic cells (Aegerter et al., 2022; Bissonnette et al., 2020). AMs are localized in the luminal side of the alveolar space, in close contact with alveolar epithelial cells type I and II, capillary endothelial cells and interstitial fibroblasts (Westphalen et al., 2014) (**Figure 13**). Like most tissue-resident macrophages, AMs are sessile and crawl through alveoli patrolling the zone to keep it clean from pathogens and potentially hazardous factors (Neupane et al., 2020). Both AMs and epithelial cells are the gatekeepers of the lungs and together they exert the functions needed to preserve lung homeostasis (Bissonnette et al., 2020).

Origin of AMs

It was initially believed that AMs were derived and replenished from the differentiation of circulating monocytes, following the mononuclear-phagocytic theory proposed over 50 years ago (Van Oud & Van Furth, 1979). Although this has proven true for some AMs, more recent research has shown that AMs develop from embryo yolk sac and foetal liver cells, occupy the alveolar niche and self-maintain though a local low-grade proliferation in absence of inflammation and during inflammatory responses. They remain in the lungs after inflammation gets resolved (Gomez Perdiguero et al., 2015; Schulz et al., 2012; Yona et al., 2013). Gene expression profiles of resident AMs remain stable during inflammation (Mould et al., 2017). Replenishment of AMs from circulating monocytes is minimal if the lungs experience no major insult or injury (Hashimoto et al., 2013; Jakubzick et al., 2013). Depending on the degree of inflammation, the pool of AMs can be restored by self-proliferation of the remaining AMs or if the injury is more severe, macrophages are recruited from circulating monocytes to replenish the population (Janssen et al., 2011; Machiels et al., 2017; Mould et al., 2017).

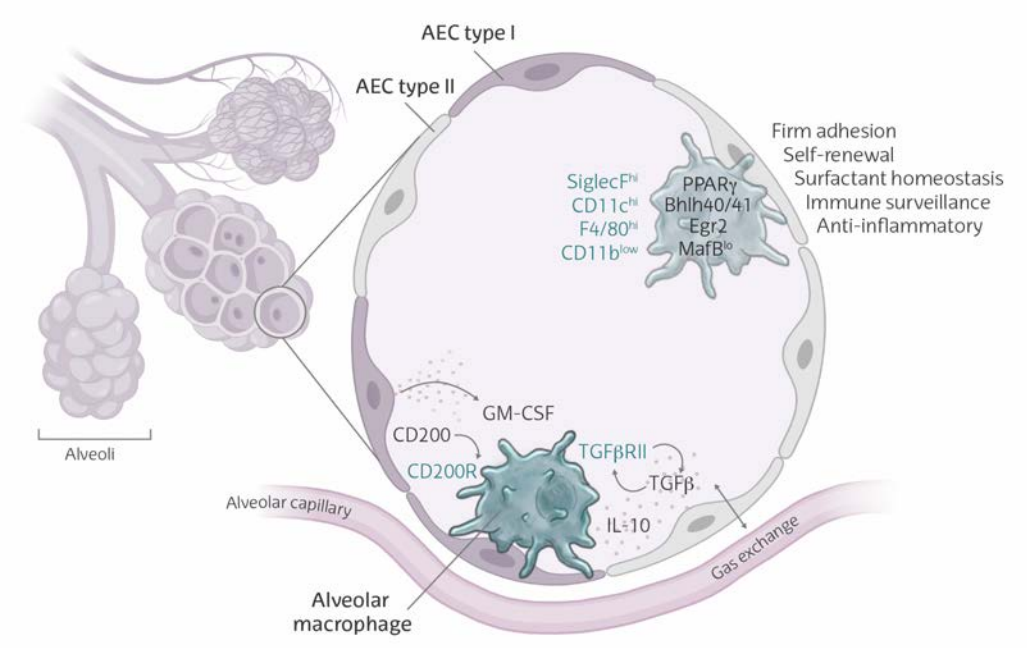

Figure 13. Alveolar macrophages are crucial cells for lung immunity
Alveolar macrophages (AMs) are tissue-resident macrophages that are exposed to various signals from the alveolar space. They reside in the alveolus, the anatomic structure where O_2 and CO_2 gas exchange occurs. GM-CSF produced by alveolar epithelial cells (AEC) type I, TGFβ and IL-10, which are abundant in the lungs, maintain some AM functions, which include immune surveillance, anti-inflammatory roles and surfactant homeostasis. Moreover, the firm adhesion of AMs to the epithelium is triggered by the CD200 expression in AEC type I cells, which binds to CD200R in AMs and further restricts the inflammatory response. Those alveolar cues activate PPARγ, a crucial transcription factor for AMs, and other transcription factors such as Bhlh40/41, Egr2 and MafB, which maintain the self-renewal capacity and other crucial functions of AMs. Some of the markers that define AMs are high expression of SiglecF, CD11c and F4/80, and low expression of CD11b. Inspired from (Aegerter et al., 2022; Bissonnette et al., 2020; Hussell & Bell, 2014). Figure partially designed with Biorender.

Signals and regulators of AMs

AMs have a transcriptional signature which is specifically dictated by the unique environment conferred by the alveolar signals (Gautiar et al., 2012; Lavin et al., 2014). Already on the first weeks of life, AM proliferation from foetal monocytes requires GM-CSF, derived from alveolar epithelial cells (Gschwend et al., 2021). This process is also enforced by autocrine signalling of TGFβ (X. Yu et al., 2017) (**Figure 13**). These signals induce the stable expression of the transcription factor peroxisome proliferator-activated receptor γ (PPARγ), which is known to regulate several lipid handling enzymes and transporters involved in surfactant turnover (Schneider et al., 2014). Apart from the generic macrophage transcription factors C/EBPβ and PU.1, AM self-

renewal and development also rely on other transcription factors like Bhlhe40, Bhlhe41, Egr2, Klf4 and Car4, which bind to enhancer regions of AM specific genes (Daniel et al., 2020; Gorki et al., 2021; Lavin et al., 2014; Mass et al., 2016; Rauschmeier et al., 2019; Sajti et al., 2020; Schneider et al., 2014) (**Figure 13**).

Patrolling the alveolar luminal area, AMs are in a constant exposed position, which allows them to capture, phagocyte and neutralize a large number of foreign particles (Westphalen et al., 2014) (**Figure 13**). However, this is done in an immunologically "silent" way without triggering excessive inflammation or neutrophil influx. AMs efferocytose apoptotic cells and phagocyte debris through scavenger receptors MARCO and Axl, and keep inflammatory response low through the transcription factors Klf2 and Klf4 activated by tissue-specific signals (Fujimori et al., 2015; Roberts et al., 2017). Apart from scavenger receptors, AMs also express high immunoglobulin (f_cR), complement and mannose receptors which facilitate phagocytosis of opsonized and non-opsonized particles (Allard et al., 2018; Dahl et al., 2007; Fadok et al., 2001; Rajaram et al., 2017; Zhang et al., 2008). Only when the phagocytic capacity is surpassed, AMs start producing pro-inflammatory factors such as cytokines and chemokines (type I IFNs, TNFα and IL-1β) that activate other players of the innate immune response: neutrophils, monocytes and DCs (Goritzka et al., 2015). In addition to their function as initiators of the immunological response, AMs are also responsible for the resolution of inflammation through the secretion of immunoregulatory cytokines like TGFβ, IL-1RA and prostaglandins (Branchett et al., 2021; Jardine et al., 2019; Thepen et al., 1991).

AMs in homeostasis and inflammation

In homeostatic conditions, AMs are found in an immunosuppressed (M2-like) state and promote immune tolerance. They prevent unnecessary inflammation by phagocytosis of foreign particles and facilitate resolution of inflammation by producing anti-inflammatory factors such as IL-10, TGFβ and prostaglandin E_2 (PGE_2) (Hussell & Bell, 2014; Ménard et al., 2007; Zissel et al., 1996). In that sense, the cross-talk with the alveolar epithelium is responsible for a multitude of AM phenotypes (Bissonnette et al., 2020). In basal conditions, AMs adhere to the epithelium via expression of proteins such as CD200R, PD-1 and SIRP1α, whose ligands CD200, programmed death-ligand 1 (PD-L1) and CD47 are expressed by epithelial cells (**Figure 13**). These protein interactions not only maintain the cells in close proximity, but also keep AM activation at low levels avoiding unnecessary inflammation (Barclay & Van Den Berg, 2014; Hu et al., 2020; Jiang-Shieh et al., 2010; Lauzon-Joset et al., 2015; Oumouna et al., 2015; Shinohara et al., 2006; Snelgrove et al., 2008; B. Zhu et

al., 2019). Epithelial damage or sensing of pathogens in the airways can cause the loss of these regulatory interactions, leading to the activation of AMs and initiation of the inflammatory response. Thus, the alveolar niche tightly controls the activation state of AMs. Some studies have also reported that TGFβ expression by AMs can suppress immune responses by inhibiting the DC-mediated activation of T cells (P. G. Holt et al., 1993; Strickland et al., 1996; Thepen et al., 1989). The production of TGFβ together with retinal dehydrogenases 1 and 2 induces retinol, which results in the generation of $FoxP3^+$ T-regs from naïve $CD4^+$ T cells (Soroosh et al., 2013). T-regs induce immune tolerance to inhaled innocuous antigens by inhibiting spontaneous and antigen-induced Th2-type inflammation (Josefowicz et al., 2012; Lloyd & Hawrylowicz, 2009).

The state of immunosuppression and tolerance is lost when inhaled pathogens and other dangers trigger the activation of pattern recognition receptors (PRRs) including TLRs, NOD-like receptors (NLRs) and C-type lectin receptors (S. B. Gordon & Read, 2002; C. H. Liu et al., 2017; E. C. Martinez et al., 2019). AMs switch from the tolerogenic to the inflammatory state through induction of TNFα, NO, IL-1β, IL-6, IFNs and MIP-1α (Kolli et al., 2014; Menard & Bissonnette, 2000; Soroosh et al., 2013). However, over-production of those mediators is dangerous, and contributes to the pathogenesis of diseases such as acute lung injury, asthma and chronic obstructive pulmonary disease (COPD) (Fricker & Gibson, 2017; Lomas-Neira et al., 2006; Russell et al., 2002). Hence, a very tight regulation of AMs is essential to maintain lung homeostasis.

Surfactant and lipid metabolism of AMs

A very important function of AMs in maintaining lung homeostasis is the internalization and catabolism of surfactant, a phospholipid that keeps the surface tension of the lungs and is crucial for the lung biomechanical function (Knudsen & Ochs, 2018; Lopez-Rodriguez et al., 2017; Ochs et al., 2020; Stern et al., 1986). Pulmonary surfactant is composed by 90% of lipids, whose main components are phospholipids and cholesterol. Proteins compose the remaining 10% of surfactant and actively contribute to its properties and are involved in the immunity of the lungs (Veldhuizen et al., 1998). AMs are the primary cells involved in the clearance of surfactant by phagocytosis of its lipids and catabolism of cholesterol through PPARγ (A. D. Baker, Malur, Barna, Ghosh, et al., 2010) (**Figure 13**). Deficiency in GM-CSF signalling leads to an impaired surfactant clearance by AMs causing the accumulation of proteins and phospholipids in the airways that can lead to pulmonary alveolar proteinosis in humans and mice (Carey & Trapnell, 2010; Dranoff et al., 1994).

The lipidic microenvironment of the lung alveoli also influences the metabolism of AMs. To prevent bacterial outgrowth, the lung environment has a good supply of oxygen and lipids but is actively depleted of glucose (E. H. Baker & Baines, 2018). Given the low capacity of AMs to use glucose, their energy metabolism mainly uses fatty acid oxidation, in contrast to IMs, which mainly use glycolysis, possibly due to their monocytic origin (Mould et al., 2017; Svedberg et al., 2019). The nuclear receptor PPARγ regulates genes related to lipid metabolism and fatty acid β-oxidation, and this TF is crucial to maintain the metabolism in AMs (Schneider et al., 2014).

Antigen presentation function in AMs

Antigen presentation in the lung is mainly performed by DCs (P. G. Holt et al., 1993; T. Kawasaki et al., 2022), which sample foreign antigens and migrate to the lung draining lymph node, where they encounter naïve $CD4^+$ and $CD8^+$ T cells and activate their clonal proliferation. Antigen-specific T cells will then migrate to the lungs for pathogen clearance, and in the lung environment, T cells encounter other local APCs, such as other DCs, AMs and IMs and even lung endothelial cells, which can also perform antigen presentation promoting further T cell activation (T. Kawasaki et al., 2022; Low et al., 2020).

Although AMs are the most abundant immune cell in the lung, their role in antigen presentation is still unclear (T. Kawasaki et al., 2022). AMs have been described to have poor antigen-presentation capacity (Chelen et al., 1995), supported by their low MHCII expression compared to IMs or DCs (Misharin et al., 2013). Although they can suppress DC function and migration to avoid inflammation against innocuous particles (Jakubzick et al., 2006), they have also been shown to play a functional role in antigen presentation in mice and during different infections in humans (P. Holt & Leivers, 1985; Ina et al., 1991; Vecchiarelli et al., 2012). Finally, some studies show that AMs have the ability to transport antigens to the lung draining lymph nodes (Kirby et al., 2009). Hence, the role of AMs role in *in vivo* antigen presentation is not well known yet.

AMs in tumorigenesis

The function AMs in tumorigenesis has been less studied than other macrophage populations like recruited TAMs or MDSC. However, some studies point at the implication and relevance of AMs in the development of lung tumors. It is conceivable that their distinct embryonic origin and their specialized local functions in the alveolar niche provides them with specific properties that can affect tumor formation.

Considering their physiological immunosuppressive and tolerogenic functions and their presence in the organ prior to tumor formation, AMs represent the perfect allies for tumoral growth.

Already in the 80's, AMs were described as an immune suppressor population that facilitated pulmonary LLC metastasis by inhibiting T cell activity and NK-cytotoxicity (Young et al., 1987). *In vitro* studies of human, mice and rat AMs also proved their immunosuppressive capacity through T cell inhibition (Aubas et al., 1984; Hengst et al., 1985; P. G. Holt, 1979; McCombs et al., 1982, 1984; Shellito & Kaltreider, 1985). More recently, a study on breast cancer metastasis showed that AMs promote metastasis in the lungs by suppressing Th1 and promoting Th2 response (Sharma et al., 2015). In the same study, AMs were also shown to modulate DC activity through TGFβ production. The depletion of AMs with clodronate liposomes reversed the immunosuppressive state increasing Th1 cell responses that reduced lung metastasis (Sharma et al., 2015). Moreover, a new study using state-of-the-art sc-RNA-Seq technology has reported that AMs localize close to tumor cells during early metastatic development of non-small cell lung carcinoma (NSCLC) (Casanova-Acebes et al., 2021). These macrophages help tumor progression by inducing tumor-promoting functions and increasing T-regs that protect the tumoral cells from $CD8^+$ cytotoxic activity. Specific depletion of AMs reduced tumor development and T reg number in both the NSCLC and a melanoma metastatic model (Casanova-Acebes et al., 2021). Hence, evidence exists on the implication of AMs in lung tumorigenesis, but the underlying molecular mechanisms remain unsolved.

Antigen presentation

Antigen presentation is a fundamental process in the immune system as it is the bridge between innate and adaptive immunity. It is a finely tuned mechanism to expose peptides in the optimal context to activate T and B cells, which will ultimately lead to a specific adaptive immune response against harmful microbes, pathogens or cells. The process comprises antigen uptake, processing and display, which together with co-stimulatory molecules has the capacity to successfully activate specific T and B cells (Zuniga et al., 2008).

For activation on the adaptive immune response, naive T cells need to be activated or "primed" (**Figure 14**). When they encounter the matching antigen, lymphocytes undergo clonal expansion and differentiation to their specific functions. Active $CD8^+$ or cytotoxic T cells can promote death in infected or malignant cells while active $CD4^+$

or helper T cells activate other immune cells as macrophages, CD8+ T cells or B cells. On the other hand, B cells become plasma cells that can secrete antibodies, which will bind to the specific antigen. In contrast to B cells, which can bind directly to the soluble antigens with the B cell receptor (BCR), T cells can only recognize antigens with the appropriate T cell receptor (TCR) that are displayed on the surface of cells bound to major histocompatibility complex (MHC) molecules. There are two types of antigen presentation, one performed by all nucleated cells, which comprises presentation via MHC class I (MHCI), and the other one performed by a specialized group of leukocytes named professional APCs via MHCII. $CD8^+$ T cells detect peptides bound to MHCI, while $CD4^+$ T cells bind to MHCII.

The "three signals" hypothesis

Distinct signals need to be delivered to $CD4^+$ T cells for their priming (**Figure 14**). The first signal is antigen recognition by the MHCII-TCR synapse. The second signal is provided by co-stimulatory molecules in the surface of APCs which can affect T cell response providing activatory or inhibitory co-stimulation (Liechtenstein et al., 2012) (**Figure 14**). For instance, binding of CD80/CD86 expressed in APCs to CD28/CD27 in T cells induces T cell proliferation and acquisition of cytotoxic properties (Nurieva et al., 2006). Other interacting molecules are CD40/CD40L, or OX40/OX40L, whose binding between APCs and T cells promotes activation of T cells (Hubo et al., 2013). On the other hand, CD80/CD86 binding to CTLA4 will engage an inhibitory signal to T cells which can lead to anergic T cells or T-regs (Collins et al., 2002; Fooksman et al., 2010). Likewise, binding of the PD-L1 in APCs to its receptor PD-1 on T cells causes the inhibition of T cells at multiple levels (Karwacz et al., 2011; Latchman et al., 2004; S. C. Liang et al., 2006). Modulation of these signals has allowed the development of checkpoint inhibitor therapies for cancer, including the antibodies against CTLA4 and PD-1/PD-L1, which inhibit the negative co-stimulatory signals to T cells, therefore activating T cell responses.

Additionally, there is a third signal that can polarize T cells to particular subsets and modulate the type of immune response towards tolerance, antibody responses or cytotoxicity (**Figure 14**). This signal is provided by cytokines, chemokines and other inflammatory mediators present during antigen presentation (Curtsinger et al., 1999; Liechtenstein et al., 2012). Only APCs provide the three signals which are needed to activate T cell response to recognise, destroy or tolerate certain antigens. When this occurs, T cells differentiate into different effector T cells such as CD4 Th1, Th2, Th17, T-regs or enhance CD8 T cell responses to weakly immunogenic antigens. Cytokines such as IL-12, IL-15, IL-6 or TNFα provide different cues for T cell modulation

(Curtsinger et al., 2003; Ramanathan et al., 2011). In general, T cells exposed to IL-12 and IL-18 differentiate to Th1, whereas IL-4 induces differentiation to Th2 (Leung et al., 2010). Combination of TGFβ, IL-6, IL-21 and IL-23 dictate Th17 differentiation, and TGFβ alone induces T-regs, which can inhibit Th1 and Th2 response (Leung et al., 2010).

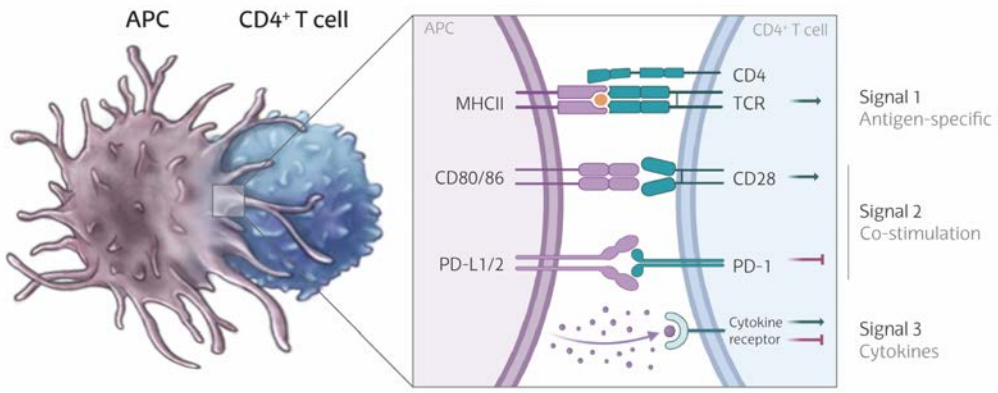

Figure 14. Antigen presentation via MHCII
Antigens bound to MHCII in the antigen presenting cells (APC) provide with the first signal to activate CD4+ T cells. For successful priming of T cells, a second signal is needed, which is given by co-stimulatory molecules like CD80 or CD86 that can bind to CD28 and promote stimulation, or by co-inhibitory signals like PD-L1 or PD-L2, which bind to PD-1 in T cells and promote inhibition. A third signal is provided by cytokines, which bind to cytokine receptors and will ultimately determine the final phenotype of CD4+ T cells. Adapted from (Velazquez-Soto et al., 2022). Figure partially designed with Biorender.

However, it is important to notice that a single costimulatory molecule is not restricted to tolerogenic or immunogenic functions. It is rather the combined effect of several costimulatory events, the interactions with soluble co-factors and the differentiation state of interacting T cells that will ultimately dictate the specific immune response.

Molecular basis of MHCII antigen presentation

To present exogenous proteins in MHCII, APCs internalize pathogens or other factors by endocytosis, phagocytosis or micropinocytosis (Blum et al., 2013; Jurewicz & Stern, 2018; Roche & Furuta, 2015) (**Figure 15**). Internalized antigens are degraded by lysosomal proteases, which takes place in a series of progressively more acidic and proteolytically active compartments described as early endosomes, late endosomes and lysosomes (Huotari & Helenius, 2011) (**Figure 15**). Cytoplasmic or nuclear antigens can also be trafficked into the endosomal network for antigen presentation via autophagy.

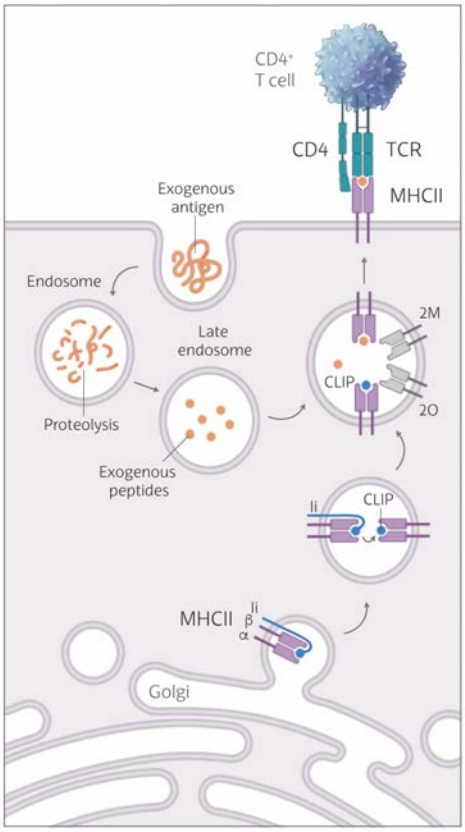

Figure 15. Generation of MHCII-bound peptides in antigen presenting cells.
Extracellular antigens are taken by endocytosis and proteolytically processed into peptides in the endolysosomal compartment. These exogenous peptides are later bound to the groove of the MHCII αβ dimer complex by displacing CLIP, which is derived from the proteolysis of MHCII-associated invariant chain (Ii), and impairs binding of unspecific peptides to the MHCII groove. MHC-2M (2M) and MHC-2O (2O) regulate the process of antigen-loading. The MHCII complex presents antigens to CD4+ T cells to activate the adaptive immune response. Adapted from (Kobayashi & Van Den Elsen, 2012; Roche & Furuta, 2015). Figure partially designed with Biorender.

Simultaneously, newly synthesized MHCII α and β dimers are loaded with the specific chaperone invariant chain (H2-Ii or CD74) in the endoplasmic reticulum (ER) and translocated to the endosomes or lysosomes. In the proteolytic endosomes, H2-Ii is degraded into smaller fragments, called class II-associated Ii chain peptides (CLIP) (**Figure 15**). CLIP loading blocks unspecific peptides from binding MHCII (Landsverk et al., 2009; Riberdy et al., 1992; Sette et al., 1992). CLIP is later removed from MHCII by the interaction with another unconventional MHCII molecule, MHC-2M, which causes a conformational change that promotes CLIP release and permits MHCII binding to foreign degraded antigen peptides (Cresswell, 1994; Denzin & Cresswell, 1995; P. Morris et al., 1994) (**Figure 15**). Premature release of CLIP leads to autoimmunity conditions since it allows MHCII biding to autoantigens from self-peptides from the different endosomal compartments (R. Busch et al., 2005; Mohan et al., 2011; Pu et al., 2004). Then, the vesicles are fused to the cell membrane where functional antigen-bound MHCII is ready to perform synapsis to the TCR on T cells (**Figure 15**). Later, surface expressed peptide–MHCII complexes can be internalized through the ubiquitin-dependent endocytosis pathway and be targeted for lysosomal degradation or be recycled back to the plasma membrane (Shin et al., 2006).

Transcriptional control of MHCII by CIITA

The regulation of MHCII is mainly controlled at the level of transcription by a group of factors that are ubiquitously expressed which include cyclic-AMP-responsive-element-binding protein (CREB), regulatory factor X (RFX) and nuclear transcription factor Y (NFY). All those factors are assembled together by the Class II transcriptional activator (CIITA) (Boss & Jensen, 2003) (**Figure 16**). Mutations in CIITA or RFX factors are found in bare lymphocyte syndrome, a condition in which patients do not have expression of MHCII and suffer from a severe immunodeficiency (DeSandro et al., 1999; Reith et al., 1995). Also, models of CIITA deficient mice have a global loss of MHCII and lack T cell antigen-specific responses (Chang et al., 1996; Itoh-Lindstrom et al., 1999). Several reports have showed that expression of CIITA is necessary and sufficient for MHCII expression (Chang et al., 1994; Steimle et al., 1994), and there is a close relationship between CIITA and MHCII levels in diverse tissues (Otten et al., 1998). For these reasons, CIITA is considered as the "master regulator" of MHCII expression (León Machado & Steimle, 2021) (**Figure 16**).

There is no evidence that CIITA can bind to DNA. Instead, it seems to activate transcription initiation and elongation by different mechanisms. For instance, CIITA can activate transcriptional machinery like TFIID and TFIIB, and its ability to phosphorylate RNA polymerase II has also been reported. CIITA can also recruit chromatin remodelling factors like p300, CBP, PCAF and BRG1, and has been reported to be associated with histone acetyltransferase (HAT) activity (Choi et al., 2011; Devaiah & Singer, 2013; León Machado & Steimle, 2021).

Transcriptional regulation of CIITA

CIITA is mainly regulated at transcriptional level. Three different isoforms of CIITA that differ in their N-terminal region can be generated by the expression from three different promoters (pI, pIII and pIV), which differ in their 5' regions and are spread over around 13 kb (León Machado & Steimle, 2021; Reith et al., 2005) (**Figure 17**). Although all the isoforms share the downstream exons, isoforms I and III have their own AUG, while isoform IV has the AUG in the common exon 2 of the gene. Moreover, the N-terminal region of isoform I contains a region of weak homology to a caspase activation and recruitment domain (CARD), which confers a slightly more efficient transcriptional activation of MHCII (Nickerson et al., 2001).

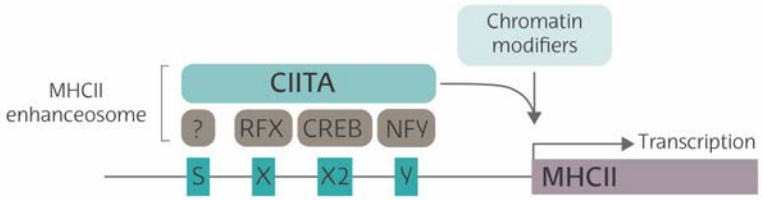

Figure 16. Transcriptional control of MHCII
The expression of MHCII classical genes is transcriptionally regulated by the SXY module, which is bound by the cooperation of four factors: the heterotrimeric X-box-binding factor RFX, the X2-box-binding factor CREB; the Y-box-binding factor NFY; and a yet-unidentified S-box-binding factor. This multiprotein complex, which is known as the MHC class II enhanceosome, is assembled by CIITA, which recruits additional factors that are involved in chromatin modification, and ultimately activate MHCII transcription. Modifyed from (Reith et al., 2005).

The different isoforms were initially proposed to play differential roles in cell lines and primary-cell populations (Reith et al., 2005) (**Figure 17**). The pI was described to be mainly used by DCs, pIII by B cells and pIV is induced by IFNγ stimulation (Muhlethaler-Mottet et al., 1997, 1998). However, later experiments using CIITA promoter-specific knock-out (KO) mice challenged this simplistic view (LeibundGut-Landmann, Waldburger, Krawczyk, et al., 2004; León Machado & Steimle, 2021; Reith et al., 2005). These studies concluded that pI is expressed in myeloid cells, such as macrophages and DCs, and pIII is mainly expressed in lymphoid cells, such as B cells, T cells in humans and plasmocytoid DCs (LeibundGut-Landmann, Waldburger, Reis e Sousa, et al., 2004) (**Figure 17**). However, DCs have also been shown to express pIII if they lack pI, indicating a certain level of flexibility in the expression of the different isoforms. Finally, pIV is induced by IFNγ in cells of non-hematopoietic origin, as those responsible for $CD4^+$ T cell selection, the thymic cortical epithelial cells (Waldburger et al., 2001).

The transcription factors regulating the different CIITA promoters have been described mainly for pIII and pIV. In response to INFγ, Janus kinase (JAK) 1 and JAK2 get activated and induce the phosphorylation, dimerization and nuclear transport of signal transducer and activator of transcription (STAT) 1. STAT1 homodimers in association with USF-1 bind to an IFNγ-activated (GAS)-E-box motif of the pIV promoter. STAT1 also activates the transcription of IFN-regulatory factors (IRF), and IRF1-IRF1 or IRF1-IRF2 dimers activate the promoter (A. C. Morris et al., 2002; Ni et al., 2005; Reith et al., 2005). The pIII promoter is a bit more complex and requires the interaction of different factors in different cell types. These include Oct1, NF-1, CREB

or ATF family members, RUNX3 and heterodimers of Pu.1 with IRF4 or IRF8 (Wright & Ting, 2006). Recent research has also identified NFAT5 as a crucial regulator of the pI promoter in primary macrophages (Buxadé et al., 2018).

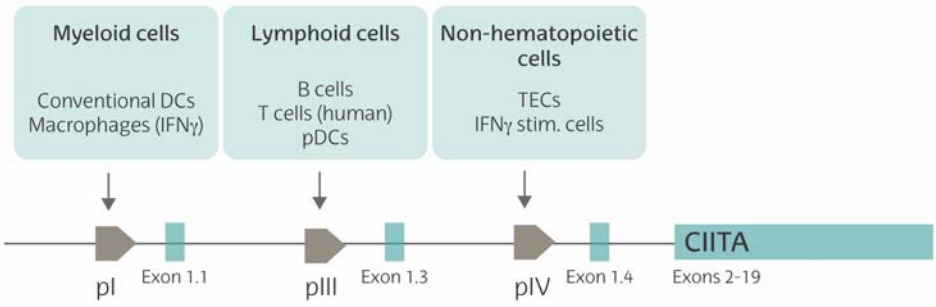

FIGURE 17. Transcriptional control of CIITA and MHCII
The three regulatory promoters (pI, pIII and pIV) of CIITA differ in distinct cell types. Promoter pI is mainly a myeloid-cell-specific promoter, sufficient to drive CIITA expression in conventional dendritic cells (DCs) and IFNγ-activated macrophages. Promoter pIII is a lymphoid-cell-specific promoter that is essential for CIITA expression in B cells, activated human T cells, and plasmacytoid DCs (pDCs). Promoter pIV is essential to drive CIITA expression in thymic epithelial cells (TECs) and for mediating the induction by IFNγ in cells of non-haematopoietic origin, such as endothelial cells, epithelial cells, fibroblasts and astrocytes. Adapted from (Reith et al., 2005).

Distal regulation of CIITA transcription

Apart from its proximal promoters, CIITA is also regulated by distal regulatory elements, which have been specially studied in IFNγ-induced pIV and in B cell lines for pIII. Epigenetic mechanisms have a crucial role in the regulation of CIITA, and have also been reported as CIITA-silencing mechanisms to promote immune escape in tumor cells (Blanck, 2002). Histone modifications and the recruitment of p300 and CBP have been reported in the CIITA promoter region, and are suggested to be induced by the chromatin remodelling enzymes BRG1 and PRC2 (Abou El Hassan et al., 2015; Ni et al., 2008). Studies with IFNγ-unresponsive trophoblast-derived cell lines and with tumor cells, which silence MHCII to avoid immune response, revealed in both cases an hypermethylation in the pIV of CIITA, which could be rescued by 5-azacytidine (5-AZA), an inhibitor of DNA methylation. The HDAC inhibitor trichostatin (TSA) also restored IFNγ inducibility in trophoblasts and tumor cells, proving that both methylation and deacetylation are able to silence the pIV promoter of CIITA (Holtz et al., 2003; Morimoto et al., 2004; A. C. Morris et al., 2000, 2002; Radosevich et al., 2007; Satoh et al., 2004; Van den Elsen et al., 2000; Van Der Stoep et al., 2002). Although less studied, the pIII promoter is also epigenetically regulated. The histone

deacetylases HDAC1 and HDAC2 and other chromatin silencers like G9a have been suggested to regulate CIITA (Gyory et al., 2004; Piskurich et al., 2000; J. Yu et al., 2000). Murine T cells and T-cell acute lymphoblastic leukaemia cell lines have pIII hypermethylation, which could be rescued by 5-AZA. In a B-cell lymphoma line, CIITA expression was rescued by the HDAC inhibitor TSA, indicating that various mechanisms coexist in the regulation of pIII CIITA depending on the context and the cell type (Chou et al., 2005; Holling et al., 2004; Murphy et al., 2002; Schooten et al., 2005). Finally, little is known about the epigenetic regulation of pI, except from the observation that this promoter is silenced during DC maturation, which correlates with decreased histone acetylation (Landmann et al., 2001). Thus, epigenetic regulation is important for CIITA transcriptional regulation.

The regulation of MHCII in different APCs is likely controlled by cell-specific CIITA transcription mechanisms (Boss & Jensen, 2003; Reith et al., 2005). However, the specific regulation of CIITA in steady-state myeloid cells is poorly characterised. Although macrophages and DCs are thought to have similar mechanisms of transcriptional regulation of CIITA and MHCII, their MHCII expression differences indicate that each cell type might have specific molecular elements that regulate the basal expression of MHCII. Moreover, the regulation of MHCII in tissue-resident macrophages has not been studied and remains crucial, given the importance of those cells for the maintenance of tolerance and homeostasis in different tissues. Besides, little is known on the identity and *in vivo* relevance of upstream regulators of CIITA expression in myeloid cells beyond IFNγ.

The p38α MAPK pathway

To be able to integrate cues from the environment, cells rely on signalling pathways that lead to activation or inhibition of intracellular programs allowing the specific responses. Amongst those, an important pathway is the group of the mitogen-activated protein kinases (MAPK). The MAPK family consists of highly conserved serine/threonine protein kinases which in mammalian cells includes p38 (Freshney et al., 1994; Han et al., 1994; J. C. Lee et al., 1994; Rouse et al., 1994), the extracellular signal regulated kinase (ERK) 1-4 (Boulton & Cobb, 1991), ERK5 (J. D. Lee et al., 1995; G. Zhou et al., 1995) and the c-Jun N-terminal kinase (JNK) 1/2/3 (Dérijard et al., 1994; Kyriakis et al., 1994). In general, the ERK1/2 cascade is activated by mitogen signals, while JNK and p38 MAPK cascades are activated mainly by stresses and pro-inflammatory cytokines.

The transmission of signals in MAPK signalling pathways happens through an evolutionary conserved mechanism of sequentially acting kinases. In the canonical activation pathway, a MAP3K receives an upstream signal and in turn activates a MAP2K, which will activate the MAPK. When active, MAPKs can phosphorylate a variety of downstream targets as transcription factors, other protein kinases, RNA-binding proteins, etc (Keshet & Seger, 2010) (**Figure 18**).

The p38 MAPK signalling pathway is especially important in immune cells as it is activated by pro-inflammatory cytokines (Canovas & Nebreda, 2021). The p38 MAPK family includes 4 different members, p38α/MAPK14, p38β/MAPK11, p38γ/MAPK12, p38δ/MAPK13 (**Figure 18**). Their amino-acid sequences share around 60% of homology, but the different family members have diverse tissue expression patterns, target preferences and sensitivity to inhibitors. p38α was the first one identified and it is the best studied family member, given its high abundance in most cell types. Expression of other family members is more restricted to specific tissues: p38β to brain, p38δ to muscle and p38γ to endocrine glands (Cuadrado & Nebreda, 2010), although the relevance of p38δ and p38γ has been described in a variety of processes and inflammatory conditions (Cuenda & Sanz-Ezquerro, 2017).

In general, the p38 pathway starts with the activation of a MAP3K, which includes up to ten different protein kinases, such as ASK1, MEKK3, TAK1, and DLK. The activation of the MAP3K can be induced by cytokines, TLR ligands, growth factors, hormones and environmental stresses like oxidative and osmotic stress, ultraviolet (UV), DNA damage and gamma radiation. MAP3K phosphorylation leads to activation of the MAP2Ks MKK3 and MKK6 (**Figure 18**). The full activation of p38α requires dual phosphorylation at the residues of threonine (Thr)-180 and tyrosine (Tyr)-182 (Han et al., 2020). The contribution of each MAP2K to p38α activation depends on the signal, the cell type and the expression level of each MAP2K (Remy et al., 2010). p38α can be localized either in the cytoplasm or in the nucleus, and the translocation upon activation is bi-directional (Maik-Rachline et al., 2020).

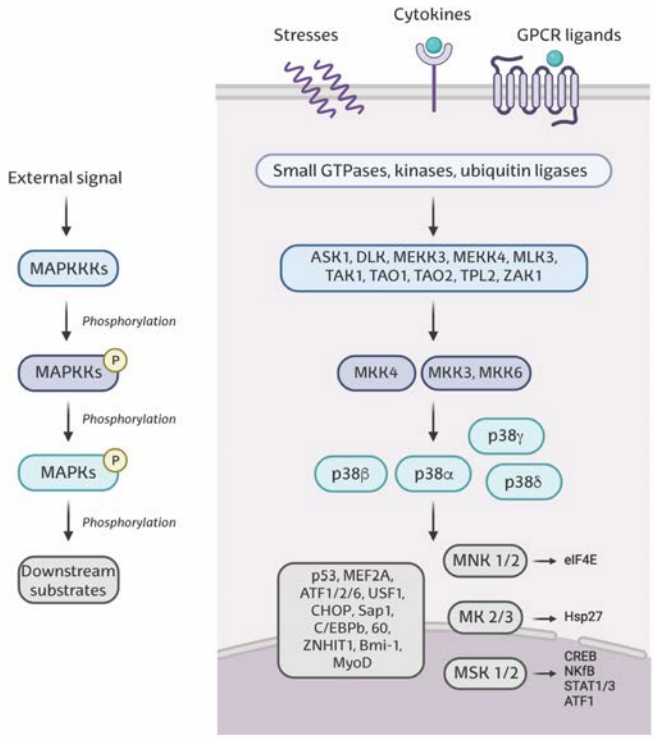

FIGURE 18. The p38α MAPK signalling cascade
Canonical activation of MAPK signalling cascades is depicted in the left, and involves the activation by an external signal of a cascade of 3 kinases acting sequentially leading to the phosphorylation of MAPK downstream substrates, which will promote the appropriate response to each particular signal. The right panel shows the activation of p38 MAPKs by environmental stress, inflammatory cytokines, and GPCR ligands, which involves the indicated MAPKKKs and MAPKKs, and will end up with the phosphorylation of 4 different p38 family members (α, β, γ and δ). p38α is ubiquitously expressed and can activate a diversity of substrates as indicated, including the kinases MNK1/2, MK2/3 and MSK1/2. These kinases can further phosphorylate additional substrates that will perform different functions. Adapted from (Canovas & Nebreda, 2021; Cuadrado & Nebreda, 2010). Figure designed with Biorender.

The responses orchestrated by the p38α pathway depend on the cell type and the context, and provide a variety of outcomes. There is evidence that p38α can directly phosphorylate more than 150 proteins (Han et al., 2020; Trempolec et al., 2013), so the outcomes of the pathway activation can vary from regulation of transcription factors, chromatin remodelling, mRNA stability, translation, protein degradation and localization, metabolism, differentiation, migration, apoptosis or proliferation (Canovas & Nebreda, 2021). Some p38α substrates are protein kinases, transcription factors and chromatin modifiers, which expand the versatility of the pathway by regulating a vast amount of different processes.

In particular, MAPK-activated protein (MAPKAP) kinase 2 (MK2) is of special relevance. p38α and MK2 form a complex that regulates the activation of both kinases. MK2 is involved in post-transcriptional regulation of mRNA stability by phosphorylating ARE-binding proteins. MK2 is also described to phosphorylate HSP-27, which can remodel the actin filaments, and eEF2K that regulates protein synthesis (Gaestel, 2016; Knebel et al., 2002) (**Figure 18**). Other important p38α substrates are MNK1 and MNK2, which can control protein synthesis though the activation of the initiation factor eIF4E (Sonali & Leonidas C., 2014) (**Figure 18**). p38α also phosphorylates MSK1 and MSK2, which are important players in the control of gene expression by phosphorylating components of the nucleosome, such as histone H3 (Knauf et al., 2001; Reyskens & Arthur, 2016) (**Figure 18**).

Several mechanisms can terminate or attenuate the signal of the p38α pathway, mainly by dephosphorylation, but also through other mechanisms (Cuadrado & Nebreda, 2010). Dephosphorylation usually occurs by dual-specificity phosphatases like MKP-1 or DUSP1, which target Thr-180 and Tyr-182 (Moosavi et al., 2017). Moreover, DUSP1 itself is activated by p38α signalling, inducing a negative feedback loop that inactivates the pathway. Also, p38α controls the expression of MKK6, one of its activators, limiting in that way the activation of the pathway (Ambrosino et al., 2003).

Pathophysiological functions of the p38α pathway

Several studies have described the role of p38α in pathophysiological conditions, especially in heart, neurodegenerative and inflammatory diseases and in cancer (Canovas & Nebreda, 2021; Cuadrado & Nebreda, 2010) (**Figure 19**). Mice with defects in p38α die during embryonic development due to defects in placental formation (Adams et al., 2000; Mudgett et al., 2000; Tamura et al., 2000), thus the studies of p38α in adult mice have been done using conditional alleles. In homeostatic conditions, p38α has been implicated in a variety of different processes. Inactivation of p38α affects lung homeostasis due to its function in the proliferation and differentiation in lung epithelial cells (Hui et al., 2007; Ventura et al., 2007). Also, p38α is important for skeletal muscle differentiation, proliferation of hepatocytes and hematopoietic cells, and several neuronal processes amongst other functions (Canovas & Nebreda, 2021). Studies using a mouse model that expresses inactive p38α showed increased proliferation and regeneration in pancreas, liver and spleen, which correlated with lower levels of cyclin-dependent kinase (CDK) inhibitors in those tissues, supporting a role for p38α in ageing (Wong et al., 2009).

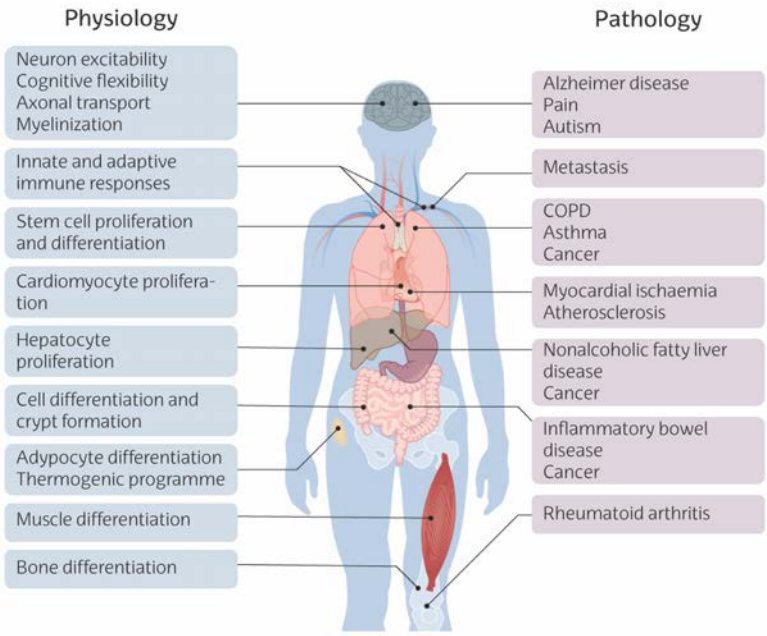

Figure 19. Roles of p38α in human physiology and pathology
p38α has been reported to be implicated in several physiological functions (left). Its dysregulation has been linked to diverse diseases (right). Modified from (Canovas & Nebreda, 2021).

p38α is also implicated in several pathologies, many of which are inflammatory conditions (**Figure 19**). As detailed later, numerous studies using chemical inhibitors of p38α have reported beneficial effects in asthma and COPD (Pelaia et al., 2021). Beyond controlling cytokine production and innate immunity, p38α can also regulate the adaptive immunity (J. S. C. Arthur & Ley, 2013; Rincón & Davis, 2009). It has been shown that p38α inhibition improves T cell expansion and expression of stemness markers, and promotes genomic stability in T cells, enhancing the efficacy of T cell-based immunotherapy (Gurusamy et al., 2020). Also, p38α inhibition in macrophages or DCs reduces colon inflammation and the associated tumorigenesis in mice (Youssif et al., 2018; T. Zheng et al., 2018). Moreover, inhibition of p38α has been shown to stabilize IFNAR1, which improves the viability of cytotoxic T lymphocytes and boosts the anti-tumour immune responses, which results in a reduction of colorectal tumours (Katlinski et al., 2017). In a model of premetastatic niche formation, the inhibition of p38α induces chemokine expression that enables neutrophil infiltration into lungs suppressing tumour growth (Gui et al., 2020).

Overall, p38α is a crucial regulator of immune cell functions and inflammatory responses, however, the ability of p38α to control both proinflammatory and anti-

inflammatory functions complicates the clinical use of pharmacological inhibitors of this pathway.

Immune functions of the p38α pathway

p38α signalling is involved in a variety of immune cell functions and plays a major role during inflammatory responses. Several *in vivo* and *in vitro* studies link p38α signalling with production of inflammatory mediators (Gupta & Nebreda, 2015). Also, factors and cytokines like TNFα, IL6, IL1β, IL18, PMA or TGFβ are known activators of the p38α pathway (Tzavlaki & Moustakas, 2020; Yang et al., 2014). Bacterial and microbes also trigger p38α activation through TLRs like LPS and other PRRs. In turn, p38α regulates the production of inflammatory cytokines in diverse immune cell types, epithelial cells, fibroblasts and endothelial cells (Canovas & Nebreda, 2021). Inflammatory mediators can be controlled by p38α through general transcription regulators, or by specific transcription factors like NFκB, or by regulating the stability, processing or translation of mRNAs usually through MK2 (Cuenda & Rousseau, 2007; Gaestel, 2016; Wagner & Nebreda, 2009). Besides regulating inflammatory mediators, the p38α pathway controls the expression of cytokine receptors such as the IFNαβ receptor IFNAR1, important in the response to pathogens and inflammation (Bhattacharya et al., 2011). Furthermore, p38α has been shown to induce VCAM-1, which plays a role in cell proliferation and immune cell differentiation (Pietersma et al., 1997).

The p38α pathway also has anti-inflammatory roles that involve phosphorylation of the transcription factor CREB and histone H3 by MSK1/2, which lead to the expression of anti-inflammatory genes like IL10 (Reyskens & Arthur, 2016). Other anti-inflammatory functions of p38α in myeloid cells are mediated by a negative feedback mechanism that limits TLR signalling via TAK1 inhibition (J. S. Arthur & Ley, 2013) or by the MSK1 and MSK2-mediated activation of dual specificity phosphatase (DUSP)-1 transcription, a phosphatase that deactivates p38α (Ananieva et al., 2008; C. Kim et al., 2008).

Given its implication in immune functions, p38α has been extensively described to be important in inflammatory diseases such as asthma and COPD (Pelaia et al., 2020, 2021), rheumatoid arthritis, multiple sclerosis, atherosclerosis and inflammatory bowel disease (Canovas & Nebreda, 2021; Gupta & Nebreda, 2015). Focussing on lung inflammation, analysis of alveolar walls and AMs in COPD and asthma patients shows increased p38 phosphorylation (Bhavsar et al., 2008; Gaffey et al., 2013; Renda et al., 2008). The use of p38α chemical inhibitors have shown promising results in several pre-clinical asthma models. Intranasal administration of ovalbumin (OVA) to

induce asthma in mice has shown to cause less infiltration of immune cells in the bronchoalveolar lavage (BAL), less production of cytokines and overall better survival in p38α-inhibitor treated animals (Choudhury et al., 2002; Dahl et al., 2007; Duan et al., 2005; Jaiswal et al., 2020; L. Liang et al., 2013; J. Y. Ma et al., 2008; Martucci et al., 2017; Nath et al., 2006; Underwood et al., 2000; Q. Wu et al., 2018). Similarly, using mouse models of COPD and LPS-induced acute lung injury, p38α was implicated in disease pathogenesis and the p38α inhibitors decreased neutrophil recruitment by decreasing inflammatory cytokine release before and during the inflammatory response (Amano et al., 2014; D. Li et al., 2018; Nick et al., 2000, 2002). Furthermore, in a MK2 KO mouse model, reduced TNFα promoted a better resistance to LPS-induced endotoxic shock (Kotlyarov et al., 1999). Similarly, p38α deletion in myeloid cells using the LysM-Cre mouse model led to improved survival of the mice and reduced TNFα levels in serum (Kang et al., 2008). However, the anti-inflammatory role of p38α in myeloid cells has also been reported using the LysM-Cre animal models (J. S. Arthur & Ley, 2013). In an experimental model of rheumatoid arthritis, myeloid specific deletion of p38α resulted in increased disease severity and reduced ability to resolve the inflammation in comparison with the wild type (WT) mice (Guma et al., 2012). This was also observed in a mouse model of UV-B-induced skin inflammation, in which the deletion of p38α in myeloid cells using the LysM-Cre system induced more severe swelling in the skin of the mice (C. Kim et al., 2008).

p38α in macrophages

MAPK pathways are important for the activation and proliferation of macrophages (Neamatallah, 2019). The stimulation of macrophages with various agents usually leads to the activation of MAPKs (Murali & Rao, 2001), which regulate transcription factors such as Ets-1, Elk/TCF and AP-1, all involved in the expression of early, intermediate and late inflammatory genes (Lloberas et al., 2016). However, there is variability in the kinetics of MAPK activation in macrophages, which might be due various factors, including the cell-surface expression of receptors, and the differential activation of pathways under the ligand-engaged receptor. For instance, although M-CSF and LPS both activate ERK1/2 though the same molecules (Ras, Raf, MEK1/2), their timings to initiate phosphorylation are different (Kolch, 2005). Thus, it remains very important to define the stimuli and the context of MAPK activation.

In particular, p38α is well known to regulate genes of the innate immune response and the polarization state of macrophages *in vitro* and *in vivo*. However, p38α can have both pro- and anti-inflammatory functions, thus remaining crucial to define the cell type, stimulus, kinetics and mode of kinase activation. In bone marrow-derived

macrophages (BMDMs) and peritoneal macrophages, IL-4 induction of M2 markers was dependent on p38α signalling (Li et al. 2019; Jiménez-Garcia et al. 2015). Regulation of TNFα and the anti-inflammatory cytokine IL-10 was also reported to be dependent on p38α in macrophages, including the MH-S alveolar macrophage cell line (C. Kim et al., 2008; Krementsov et al., 2014; Meng et al., 2014; Raza et al., 2017) Similar observations were found when blocking MK2, which reduced the expression of M2 markers CD206 and IL-10 after IL-4 stimulation in BMDMs (Suarez-Lopez et al., 2018). Using a mouse model of autoimmune multiple sclerosis, specific deletion of p38α in macrophages was shown to reduce the disease severity by decreasing M2 macrophage polarization (B. Li et al., 2019). MK2 KO in myeloid cells also reduced M2 markers in macrophages, decreasing colitis-associated cancer (Suarez-Lopez et al., 2018). Moreover, a study comparing the action of different p38α inhibitors and genetic p38α deletion in macrophages, showed that the function of p38α is context-dependent since each type of inhibition gave a different outcome in terms of cytokine production (Raza et al., 2017). In another study comparing the kinetics of p38α inhibition, the effects were found to vary amongst macrophage type and time of inhibition (Q. Shi et al., 2015). Taken together, these observations stress the importance of the context when studying p38 MAPK signalling.

Apart from macrophage polarization, p38α has also been implicated in phagocytosis, one of the main functions of macrophages. Different studies show that the chemical inhibition of p38α promotes a reduction in the capacity of macrophages to phagocyte bacteria (Blander & Medzhitov, 2004; Kang et al., 2008; Olman et al., 2022; Shiratsuchi & Basson, 2005). However, other studies show no effect of p38α inhibition on the macrophages' phagocytic capacity (Bewley et al., 2016; X. Li et al., 2003). Interestingly, a recent study has shown the role of p38α in efferocytosis (phagocytosis of apoptotic bodies) in human macrophages though regulation of the TIM4 receptor by the HAT p300 (De Maeyer et al., 2020).

However, very little is known on the contribution of the p38α pathway to the functions of tissue-resident macrophages like AMs both in homeostasis and during inflammation and tumorigenesis.

p38α in tumorigenesis

The role of p38α in tumorigenesis is dual as it has both tumour suppressor and promoting functions. Similar to the homeostatic conditions and in other diseases, the role of p38α in cancer is context-dependent. Several *in vitro* studies have demonstrated the ability of p38α to suppress malignant cell transformation by

inhibiting cell proliferation or promoting cell death or differentiation. This has been also observed in different mouse models of liver, lung, colon and skin cancer, where p38α downregulation *in vivo* enhances tumor growth (Igea & Nebreda, 2015). However, the pathway can also be harnessed by cancer cells and ultimately support primary tumor growth by controlling cell survival and proliferation by different mechanisms. In metastasis, p38α has also been implicated in the regulation of epithelial to mesenchymal transition (EMT), migration and extravasation. Moreover, it has also been described that p38α inhibition promotes the normalization of blood vessels, which can potentially enhance drug delivery and avoid leaky walls that can lead to metastasis (Batlle et al., 2019). MK2 has been shown to promote tumor formation in mouse models of DSS-induced colitis by inducing macrophage recruitment into the colon (Ray et al., 2016). Also, p38α-MK2 signalling induces upregulation of PD-L1 in cancer cells by increasing its mRNA stability, favouring tumor immunosuppression (Coelho et al., 2017). In summary, the p38α pathway plays an important role in keeping homeostatic conditions and is a caretaker in normal cells. However, when tumors have initiated, p38α favours tumor growth via diverse mechanisms.

There is also evidence that p38α has crucial functions in various cells of the tumor microenvironment. Thus, p38α in fibroblasts promotes the expression of cytokines, chemokines and other factors that recruit pro-tumoral myeloid cells to the tumor niche or that remodel the niche towards a pro-tumoral environment (Curtis et al., 2019; Gui et al., 2020). Other studies have shown that p38α deletion in myeloid cells promotes inflammation-induced colon tumorigenesis though IGF-1 (Youssif et al., 2018). In $CD4^+$ T lymphocytes, p38α activation leads to a pro-tumorigenic inflammatory state that promotes pancreatic cancer (Alam et al., 2015). Furthermore, in a model of lung pre-metastatic niche formation, deletion of p38α in fibroblasts suppresses lung metastasis by decreasing different factors, cytokines and chemokines as well as pulmonary neutrophil infiltration (Gui et al., 2020). Altogether, this proves the importance of p38α in different cells of the tumor stroma, and stresses the importance of carefully studying each of them to have a general idea of the possible beneficial effects of a systemic p38α chemical inhibition.

Inhibitors of p38α in clinics

Efforts have long been focused in investigating the effects of inhibiting the p38α pathway in clinics, given the role of p38α in a variety of pathological processes. Initially to target inflammatory diseases such as asthma, COPD and rheumatoid arthritis, p38α inhibitors were developed and supported by favourable results in preclinical models

(Canovas & Nebreda, 2021; Pelaia et al., 2021). More recently, p38α inhibitors have entered clinical trials for other diseases, such as Alzheimer disease, Huntington disease, multiple myeloma, muscular dystrophy and more COVID-19 (Canovas & Nebreda, 2021). In cancer, p38α inhibitors have been proposed in combination with other therapies, such as tamoxifen or gemcitabine and carboplatin in breast and ovarian cancer, respectively (Patnaik et al., 2016; Vergote et al., 2020). However, the use of the inhibitors in clinical settings has not given the expected results so far and none of them has progressed to phase III. The diversity of the functions regulated by p38α in different cells and contexts might contribute to the failure of p38α inhibitors in clinical trials, together perhaps with certain lack of selectivity of the inhibitors and secondary undesired toxicity. For these reasons, new strategies to target p38α signalling are emerging, such as the inhibition of downstream substrates of the pathway, p38α degradation using PROTACs, or specific targeting of the pathway in a tissue- and/or cell-specific manner.

Objectives

The aim of this thesis is to unravel the role of the p38α kinase in myeloid cells in the regulation of lung immunity, in homeostasis and in pathological conditions such as lung metastasis.

Specific objectives

- Determine the role of myeloid p38α in the development of lung metastatic melanoma.

- Study the function of myeloid p38α in lung inflammation using models of asthma and acute lung inflammation.

- Characterize a mouse model that overexpresses p38α.

Materials and methods

Mouse work

Mouse holding

Experimentation animals were housed in the specific pathogen-free (SPF) mouse facility of the Parc Científic de Barcelona (PCB). Animals were maintained under a standard 12 h light-dark cycle, at 21°C, with free access to regular chow diet and autoclaved sterile water. Breeding pairs were set at a minimum age of 6 weeks. Litters were weaned at 21 days of age and marked with an ear tag. The mice used in this present work were all in a C57BL/6J background. Experiments were performed following the European Union, national and institutional guidelines and experimental protocols were approved by the Animal Ethics Committee of the PCB.

Generation of mouse models

p38$\alpha\Delta^{Lys}$ transgenic mice

Myeloid-specific p38α KO mice were generated by crossing MAPK14lox/lox mice (Ventura et al., 2007), which have loxP sites upstream of exon 2 and downstream of exon 3 of the p38α-encoding gene MAPK14, with constitutive LysM-Cre mice (Clausen et al., 1999). Offsprings were maintained in a C57BL/6J background. MAPK14lox and Cre alleles were amplified by PCR to verify the genotype of the offspring in each crossing. To check the efficiency of p38α deletion, peritoneal macrophages were obtained and p38α protein was evaluated by western blot. The Cre transgene was always kept in heterozygosis. Littermate animals without Cre were used in all experiments as controls. In some experiments, animals with Cre but without MAPK14lox/lox alleles were also used as controls.

OT-II-TCR transgenic mice

OT-II transgenic mice were kindly provided by Dr. Eduard Batlle laboratory at Institut de Recerca Biomèdica de Barcelona (IRB Barcelona).

STAT1-KO transgenic mice

STAT1-KO and littermates mice were a kind gift of Dr. Annabel Valledor from the University of Barcelona.

p38α-BAC transgenic mice

The strategy to generate p38α overexpressing mice was designed by Dr. Stephen Forrow and Dr. Angel R. Nebreda. The mice were generated by the Mouse Mutant core facility at IRB Barcelona. Briefly, A bacterial artificial chromosome (BAC) covering the entire MAPK14 coding region and 20 kb of upstream sequence, named #RP24-137E7, was obtained from CHORI-BACPAC (http://bacpac.chori.org). Inverted terminal repeats were engineered into the vector to allow for transposase mediated integration. C57BL/6 zygotes were injected with the BAC vector and piggyBAC transposase mRNA. The zygotes were implanted into pseudo-pregnant female mice and the offspring was genotyped for integration of the vector in the genome. Maintenance of the line was done by crossing p38αBAC/+ with WT C57BL/6 mice. To generate homozygous animals, two p38αBAC/+ mice were crossed and the offspring was genotyped by copy number analysis (see section Mouse genotyping).

Mouse genotyping

Mouse tails were digested in 750 µl of Tail buffer (100 mM NaCl, 50 mM Tris-HCl pH 8, 10 mM EDTA pH 8, 1% SDS in sterile dH_2O) with proteinase K (0.5 µg/µl) at 56°C. After overnight digestion, 250 µl of saturated NaCl was added, mixed for 5 min and centrifuged at 1600xg 10 min at room temperature (RT). The supernatant was poured into a new tube containing 500 µl of isopropanol. Tubes were inverted several times and centrifuged again at full speed for 10 min at RT. The supernatant was carefully discarded without disturbing the DNA pellet. Pellet was washed with 70% ethanol and, after drying, resuspended in 150 µl of autoclaved dH_2O.

The polymerase chain reaction (PCR) mixture was prepared with 50 ng of genomic DNA (gDNA), 2 µl of 10x Taq buffer, 1.5 µl of each primer (10 µM), 0.5 µl of dNTP mix (10 mM), 0.3 µl Taq polymerase (BioTaq, Ecogen #21060) and double distilled H_2O (ddH_2O) to a final volume of 20 µl. Primers were purchased from Sigma and sequences are shown in **Table M1**. The mix was subjected to the following PCR program in a BioRad thermocycler: 94°C for 5 min; 35 cycles of 94°C for 30 s, 57°C for 30 s, 72°C for 45 s; and 72°C for 10 min, then cool down to 4°C. PCR products were resolved by electrophoresis in a 2% agarose gel.

p38α-BAC genotyping by copy number analysis

Copy number analysis was done as previously reported (Chandler et al., 2007; L. Ma & Chung, 2014). Briefly, mouse tails were digested as described above, gDNA was

quantified and a total of 7,5 ng was used for each quantitative PCR reaction. RT-qPCR was performed using primers for MAPK14 exon 2 and exon 12 (**Table M1**). For normalization, primers for Actin and GAPDH were used. RT-qPCR was run as described below (see section Molecular biology) except for the following considerations. A standard curve with increasing concentration of DNA was run in parallel to assess sensitivity of the technique using Actin. RT-qPCR was always run with known WT and heterozygous as controls for the BAC cassette (offspring of a WT and a p38αBAC/+ animal). For the analysis, the sample CTs were compared to the WT and p38αBAC/+ controls to assess the number of MAPK14 genetic copies present in each sample. Animals with 2 copies were considered WT, with 5 were considered heterozygous for the BAC cassette, and with >10 copies were deemed to be homozygous for the BAC cassette.

Table M1 |

Primers for genotyping				
Cre tg FW	ACGAGTGATGAGG TTCGCAAG	Cre tg RV	CCCACCGTCAGT ACGTGAGAT	520 bp
MAPK14 FW	CTACAGAATGCACC TCGGATG	*MAPK14* RV	AGAAGGCTGGAT TTGCACAAG	*MAPK14* WT: 121 bp *MAPK14* lox: 188 bp *MAPK14* del: 411 bp
MAPK14-BAC FW	GTGAGGCGTGCTTG TCAATG	*MAPK14*-BAC RV	CATCAATGCCTGT CAAGGGC	402 bp

Mouse experiments

Subcutaneous primary tumor generation

To generate subcutaneous tumors, 2.5 x10^5 B16/F10 cells or 5x10^5 B16/F10-OVA cells were subcutaneously injected in the right flank of the mice. Around 12-14 days later, when tumor volume was around 80-100 mm^3, tumors started to be measured with a caliper every day. Volume of the tumor was calculated by multiplying the biggest measure for the square of the smallest one.

Lung metastasis studies

To generate the experimental metastasis model,1.5x10^5 B16/F10 cells were injected intravenously in the tail vein of 8 weeks-old female mice at a density of 1.5x10^6

cells/mL. Mice cages were heated up with an infrared lamp and a heat blanket. Cells were thoroughly resuspended to avoid clumps right before each injection and loaded in a 25G needle syringe which was changed for every mouse. The tail was cleaned with 70% ethanol right before injection, and after injection was kept pressed with a tissue to stop bleeding, and mouse health state was monitored for 5 min. Lung tumors were allowed to grow for 21 days (unless otherwise specified). At the end of the experiment, lungs were carefully collected for analyses.

Mouse treatments

For p38α inhibition, mice were administered PH-797804 or LY-2228820 at a final concentration of 15 mg/kg every day during 2 weeks. Compounds were administered in 250 μL via oral gavage.

For anti-PD1 treatment, the antibody was diluted in PBS and 250 μg/mouse in 100 μL were administered via intraperitoneal (i.p.) injection. Treatment was started when tumors were 80-100 mm^3 and mice were administered a total of 5-6 doses every 3-4 days.

For gram-negative bacteria depletion, Ceftriaxone at 50 mg/kg was injected i.p. every day during 7 consecutive days.

House dust mite-induced asthma model

Mice were anesthetized with isoflurane until breathing pace was continuous. At that point, they were intranasally inoculated with 20 μl of house dust mite (HDM) at 1.25 μg/μl (kind gift from Dr. Annabel Valledor, Universitat de Barcelona). This procedure was repeated for 10 consecutive days. Control animals were inoculated with 0.9% sterile physiological saline buffer. After 10 days, Bronchoalveolar Lavage (BAL) fluid was extracted and lungs were carefully collected for analyses.

LPS-induced acute lung inflammation

Mice were anesthetized with isoflurane until breathing pace was deep. At that point, they were intranasally inoculated with 20 μl of LPS at 1.25 μg/μl or 5 μg/μl. Control animals are inoculated with 0.9% sterile physiological saline buffer. After 24 h, BAL fluid was collected and lungs were carefully collected for analyses.

DSS-induced colitis

To induce acute colitis, mice received 1.5% dextran sulphate sodium (DSS) in the drinking water. After 6 days, DSS was removed and mice were back to plain drinking water. Body weight was recorded daily to keep track of the mouse health. At sacrifice, colon region was collected and separated from the cecum at the ileocecal junction and flushed with cold PBS to remove faeces and blood. After removing excess fat, the colons were opened longitudinally and were fixed as "swiss-rolls" in 10% formalin. Tissue processing for immunohistochemistry (IHC) was followed as described later in this section.

Acute liver damage model

Liver damage experiments were performed with male mice between 8 and 10 weeks of age following previous reports (Fortier et al., 2019). CCl_4 was dissolved in corn oil in a ratio of 1:9 and was administered i.p. at 0.56 g/kg of mouse body weight. Facial blood collection was performed at the indicated times for ALT analysis, which was performed in the Animal Facility of the PCB. Mice were euthanized 48 h post-CCl_4 treatment. If indicated, 2 h before tissue harvest, mice were i.p. injected with 50 mg/kg of Bromodeoxyuridine (BrdU). After sacrifice, liver tissue was collected for histological or biochemical analyses.

Bronchoalveolar lavage

BAL was performed as previously reported (Sun et al., 2017). In brief, mice were euthanized using Pentobarbital (200 mg/kg) and trachea was exposed. Using a 24-G shielded catheter, trachea was carefully cannulated around 5 mm just below the larynx. The catheter was secured in place with surgical threat. A 1 mL syringe was attached to the catheter and around 7 mL of 37°C BAL Buffer (2 mM EDTA, 0.5% FBS in sterile PBS) were injected and recovered in turns of 1 mL each time (recovery around 800-900 μl each time). Collected BAL was kept at 37°C. Cells were pelleted at 300xg 5 min. If pellet was red, red blood cell (RBC) lysis Buffer (5% PBS, 0.8% NH_4Cl in sterile H_20, filtered) was added for 1 min at RT. Cells were used for culture or for Flow cytometry analyses.

Blood extraction

For facial vein extraction, mice were carefully pierced in the facial vein using a 20G needle. A maximum of 200 µl was collected in a 1.5 mL Eppendorf tube. For serum extraction, tubes were left for 1 h at RT and centrifuged 15 min at 1500xg and 4ºC. Next, yellowish supernatant (serum) was carefully collected and analysed or stored at -80ºC until use.

Immunohistochemistry (IHC)

Tissues, with the exception of the lungs, were directly fixed in formalin for 24 h at RT. Lungs were fixed by insufflating 10% neutral buffered Formalin with a 25G-needle syringe in the lobes, and incubated overnight at RT in 10 mL 10% neutral buffered Formalin. After that, samples were kept in 70% ethanol at 4ºC before processing. Then samples were washed with PBS and dehydrated in a tissue processor (Sakura). Finally, samples were embedded in paraffin blocks using a paraffin embedding module (Leica), and blocks were cut with a microtome (Leica) into 4 µm-thick sections. After a de-wax step in xylene for 10 min, samples were rehydrated in a descending series of 3 min in ethanol solution at decreasing concentrations (100%, 95%, 75%, 50% and ddH_2O). Lung sections were then either stained with H&E following the standard protocol, or used for IHC staining. See **Table M2** for antibodies used in IHC.

Table M2 |

IHC antibodies		
Antibody	Company	Reference
CD4	Abcam	14976680
CD8	Abcam	209775
Myeloperoxydase (MPO)	Dako	A0398
CD68	Biorbyt	ORB47985
CD45	Abcam	208022

Histopathological scores

Scoring for histopathological traits of the HDM-induced asthma model and the LPS-acute lung inflammation model was performed by Dr. Neus Prats from the Histopathology Facility at IRB Barcelona.

Scoring for colon epithelial damage was quantified as the average of two different scores. First score was given to the state of the crypts: 1-intact crypts, 2-basal/one third damaged, 3-basal/two thirds damaged, 4-damaged surface epithelium. The second score was given to the percentage of affected total colon area: 1 for 25%, 2 for 25-50%, 3 for 50-75% and 4 for 75-100%.

Cell culture

Cell line maintenance

Cells were cultured in humidified atmosphere in a 37°C incubator at 5%. For passageing, cells were washed once with PBS and incubated with trypsin/EDTA solution at 37°C until detached; cells were then diluted in culture medium and plated in a new dish in a ratio of 1:3- 1:10 depending on the experiment.

The B16/F10 melanoma cell line was bought from ATCC. B16/F10-OVA were a kind gift from Dr. Marisol S.Soengas (CNIO, Madrid). These cell lines were cultured in high glucose DMEM medium supplemented with 10% fetal bovine serum (FBS), 1% penicillin/streptomycin (P/S) and 1% glutamine.

Jurkat cells were a gift from Dr. Raul Méndez from IRB Barcelona. Cells were cultured in RPMI supplemented with FBS (10%) and 1% P/S.

L9-cell conditioned medium generation

Conditioned medium (L-cell) to generate macrophages from bone marrow precursor cells was obtained from the mouse fibroblast cell line L929 (ATCC CCL 1, NCTC clone 929). $7x10^5$ L929 cells were cultured in high glucose DMEM supplemented with 1% P/S, 10% FBS at 37°C and 5% CO2. Cells were grown in 150 mm plates up to confluence and 7 days later the supernatant was removed, filtered with a 0.22 µm vacuum filter and stored in aliquots at -80 °C. Once thawed, the aliquots were stored at 4 °C.

Cell freezing and thawing

For freezing, cells from a 70-85% confluent 10 cm culture dish were collected and resuspended in freezing media consisting of 90% FBS and 10% DMSO and transferred

to 1 or 2 1.5 mL cryo-tubes. Cryo-tubes were stored at -80°C for up to one week and then transferred to liquid nitrogen for long term storage.
For thawing, frozen cells were placed in a 37°C water bath until completely thawed. Then cells were transferred to a 5 cm plate with 5 mL of media. Next day, the media was replaced with fresh medium or passaged if needed.

Mycoplasma detection

All cell lines were checked routinely for mycoplasma using Mycoplasma Detection Kit. 100 µL of media from cells grown for a minimum of 48 h were collected and centrifuged for 5 min at 200xg. The supernatant was transferred to a test tube. 100 µL of MycoAlert reagent (A) were added and luminescence was measured after 5 min incubation. Then, 100 µL of MycoAlert substrate (B) were added and luminescence was measured after 10 min incubation. The ratio of B/A was used to determine the mycoplasma status according to manufacturer´s parameters. This assay was always performed using a positive control.

Generation of primary cell cultures

Isolation of bone marrow-derived macrophages (BMDMs)

8 weeks-old male mice were sacrificed by cervical dislocation and legs were removed to isolate tibia and femur, which were kept in PBS. Bones were cleaned from skin and muscle with the help of a clean tissue. Epiphysis of the bones was cut with sterile scissors and bones were flushed with a 5 mL of DMEM through the hole with a 25G syringe into a non-adherent 6 cm dish. The process was repeated until the bone looks white and empty. This procedure was repeated for the 4 bones of the same animal. 1 mL of bone marrow-containing medium was added to a non-adherent 15 mm plate with 40 mL of warm medium (DMEM (2% P/S) + 30-40% L9 cell medium + 20% FBS). Cells were cultured at 37°C for 6-7 days until confluent.

Isolation of alveolar macrophages (AMs)

AMs were isolated from BAL fluid as previously reported (C. Busch et al., 2019). Briefly, BAL was extracted from mice (see above) and cells were counted. $3x10^5$-4 $x10^5$ cells per well were plated into non-treated 6-well plates with 3mL of pre-warmed RPMI supplemented with 1X glutamine, 1X pyruvate, 1% P/S and 10%FBS. After incubating the cells for 6-18 h, medium was replaced with fresh medium and recombinant GM-

CSF was added to the culture at 5 ng/mL. Medium was changed every 2 days considering that alveolar macrophage culture is 20% in suspension, so cells in the supernatant were pelleted and fresh medium was used to resuspend them and add them back to the well. For cell passage, 30-45 min of incubation with Accutase was used to detach cells.

Isolation of peritoneal macrophages

Mice were euthanized and a small incision was performed in the abdominal skin to carefully expose the intact peritoneal area. Then, 5 mL of sterile PBS was injected in the peritoneal cavity using a 21G needle and, after a peritoneal massage, PBS was recovered with the same syringe. Peritoneal macrophages were isolated from peritoneal lavage by pelleting the collected PBS at 300xg for 5 min at 4°C. Cells were seeded onto non-treated 6-well plates with DMEM containing 1% P/S. After 1 h incubation at 37°C, cells were washed twice with PBS to remove erythrocytes and non-adherent cells. Then, DMEM containing 20%FBS, 30% L9-cell and 1%P/S was added to the cells, which were left to proliferate for 2-4 days depending on the starting cell number.

Isolation of naïve CD4$^+$ T lymphocytes

For isolation of CD4$^+$ T cells, 7-8 weeks-old OT-II-TCR mice were euthanized by CO_2 inhalation and spleen and lymph nodes (inguinal, axillar and mesenteric) were extracted. Samples were maintained all time on ice. Tissues were mashed through a 70 μm strainer with a 10 mL-syringe plunge and loaded into a 50 mL tube using cold PBS to flush residual material stuck in the strainer. Samples were washed with PBS and spun 10 min at 350xg. Pellet was resuspended in 1 mL RBC lysis Buffer and incubated no more than 1-3 min at RT. Reaction was quenched by adding 15 mL of PBS and filtered through a 40 μm strainer. Next, cells were centrifuge 5 min at 350xg. Pellet was resuspended in 1 mL PBS and cells were counted. At this point, cells can be stored in liquid nitrogen for future use.

CD4$^+$ T cells were isolated from the cell suspension using the Dynabeads Untouched Mouse CD4 Cells following the manufacturer's instructions. In brief, cells were set to a dilution of $5x10^7$ cells in 500μL of cold Isolation buffer. Then, 100 μL of Antibody mix were added together with 100 μL of FBS. The mix was incubated for 20 min at 4°C and after that, it was washed with 10 mL of Isolation buffer. The pellet was resuspended in 4 mL of Isolation buffer and 1 mL of clean magnetic beads was added and incubated for 15 min with gentle tilting. Then, 5 mL of isolation buffer were added and the mix

was resuspended with a narrow 1 mL tip avoiding foam formation. The mix was transferred to 2 mL Eppendorf tubes and placed in a magnetic stand for 2 min. After that, the clear supernatant containing CD4+ T cells was carefully transferred to a new tube to perform experiments. T cells were cultured in RPMI 1640 supplemented with 10% heat-inactivated FBS, 0.5 mM Sodium Pyruvate, 1X Non-essential amino acids, 2 mM L-glutamine, 1% P/S, 10 mM HEPES and 50 μM β-mercaptoethanol.

Cellular biology

BMDMs stimulation

After 6-7 days of BMDMs differentiation, cells were washed with PBS and 5 mL of fresh DMEM supplemented with glutamine, P/S and 10% FBS was added to the plates (starving medium). Cells were collected with the help of a cell scrapper and were placed in non-treated 6-well plates in the starving medium for 16-18 h to attach (overnight). After that period, inhibitors were added and left for 2 h before stimulation with cytokines. Working concentrations of inhibitors and cytokines are described in **Table M3** and **Table M4**. PH-797804 (PH) was used to inhibit p38α unless otherwise indicated. Stimulated cells were cultured for 20-24 h until they were collected for analysis by FACS, RT-qPCR or western blot.

Table M3 |

Cell treatments with inhibitors				
Compound	Activity	Concentration	Company	Reference
PH-797804	p38α/β inhibitor	2 μM	Selleckchem	S2726
LY-2228820	p38α/β inhibitor	200 nM	MedChem	HY-13241
NR-7H (PROTAC)	p38α/β degradation	1 μM	-	-
NR-11C (PROTAC)	p38α degradation	1 μM	-	-
PF-3644022	MK2 inhibitor	10 μM	Sigma	PZ0188
SB-747651A	MSK1/2 inhibitor	10 μM	Axon	1897
Tomivosertib	MNK1/2 inhibitor	10 μM	MedChem	eFT508
Trichostatin A	HDAC inhibitor	20 nM	Sigma	T1952
5-Aza-2'-deoxycytidine	DNA-methylation inhibitor	10 μM	Sigma	A3656
C646	p300 inhibitor	20 μM	Sigma	382113
Nexturastat A	HDAC6 inhibitor	5 μM	Sellekchem	S7473
Actinomycin D	Transcription inhibitor	5 μg/ml	Sigma	A1410
Anti-TNFα	TNFα neutralizing antibody	2.5/5 μM	BIOTECHNE	MAB4101-SP

Table M4 |

Cell treatments with cytokines			
Cytokine	Concentration	Company	Reference
LPS	100 ng/ml	Sigma	L3129
TNFα	2 ng/ml	eBIOSCIENCE	14-8321-62
GM-CSF	20 ng/ml	Peprotech	315-03
IL10	20 ng/ml	eBIOSCIENCE	14810162
IL4	10 ng/ml	BD pharmingen	550067
TGFβ	5 ng/ml	Peprotech	100-21
IFNγ	50 ng/ml	Peprotech	315-05

BMDMs silencing RNA transfection

BMDMss were electroporated by using the Neon transfection system kit, pipette and pipette station. After differentiation, BMDMss ($20x10^6$) were resuspended in 100 µL of buffer R (provided in the kit). The cell suspension was mixed with 800 nM of silencing RNA (siRNA), which were ordered from Silencer Select Pre-designed siRNAs by Thermofisher and are shown in **Table M5**. Cells were electroporated with 2 pulses of 1400V for 20 ms. $2\text{-}3x10^6$ cells were transferred into 6 cm plates with pre-warmed medium (without antibiotics). Cells were left to recover overnight and then were stimulated as previously described. We observed better recovery when cells were cultured with Opti-MEM medium after electroporation.

Table M5 |

siRNAs			
	Sense	Antisense	Reference
siHDAC6	CAGUGUAUCUGCAUCCGAATT	UUCGGAUGCAGAUACACUGAA	4390771
control siRNA	Negative control (undisclosed)	Negative control (undisclosed)	4390843

Antigen presentation assay

The assay of antigen presentation was optimised for AMs following previously published protocols (Campisi, 2017).
AMs were isolated from BAL fluid and $4x10^4$ cells were placed in a low-adherent U-shaped 96-well plate in 40 µl of AM medium without GM-CSF. Cells were left to attach for 1 h and after that, 50 µg/mL OVA 323-339 was added to the culture with or without LPS and PH in 60 µl of fresh medium, and AMs were incubated with OVA overnight. The next morning, $CD4^+$ T cells were isolated from fresh or frozen cell suspensions (see section Cell culture) and stained with Celltrace Violet following the

manufacturer's instructions. After that, AM medium was carefully removed from the wells and $1x10^5$ stained $CD4^+$ T cells were added to the AM culture in 150 μl T cell medium containing IL-2 at 200 ng/mL. Cells were co-cultured for 7 days adding 25-50 μl of fresh T-cell medium with IL2 every 3 days. At day 7, the cells in suspension (mainly T cells) were collected and stained for FACS analysis. As a control, Violet stained $CD4^+$ T cells were cultured alone in the same plate and in the presence of anti-CD3 and anti-CD28 at 2 μg/μl to induce proliferation.

Bead phagocytosis assay

BMDMs or AMs were plated in low attachment 12-well plates at around $5x10^5$ cells per well on medium without L9-cell-conditioned medium or GM-CSF in each case. Cells were left overnight and the next morning, 4 h prior to adding the beads, PH was added to the cell medium (if specified) followed by LPS 2 h later. After 2 h of LPS stimulation, $5x10^5$ fluorescent latex beads were added to the culture and left for different times. The plate was then placed on ice, and macrophages were washed thoroughly 3-4 times with ice cold PBS to stop phagocytosis, collected with a cell scrapper and used for FACS staining and analysis.

Apoptotic cell efferocytosis assay

Efferocytosis assays were devised from previous reports (Kozmar et al., 2010). In short, Jurkat cells were labelled with Celltrace CFSE following manufacturer's instructions. Labelled cells were washed 2 times and resuspended in complete medium at $5x10^5$ cells/mL containing 40 μM of etoposide and cultured for 16-18 h. Meanwhile, the culture medium of BMDMs or AMs was changed to medium without L9-cell-conditioned medium or without GM-CSF, respectively. Next day, when indicated, macrophages were treated with PH and/or LPS for 4 h and 2 h, respectively, prior to the addition of Jurkat cells. Then, apoptotic Jurkat cells were washed twice with PBS, and $1.5x10^6$ cells were added to $5x10^5$ macrophages. After incubation for the indicated times, cells were collected with a cell scrapper and stained for FACS analysis.

mRNA decay assay with Actinomycin D

BMDMs were starved overnight from L9-cell-conditioned medium and PH and LPS were added to the culture as reported above. After 16 h of LPS treatment,

macrophages were treated with actinomycin D (ActD) at 20 ng/mL for the indicated times before collection in Trizol for RNA extraction.

Flow cytometry

Preparation of single cell suspensions for flow cytometry

Lungs with or without tumors were collected and were finely minced with the help of a scalpel. The tissue was enzymatically digested in 10 mL of protein-free DMEM containing 1 mg/mL Collagenase A (Roche), 0.2 mg/mL Dispase II (Sigma) and 0.2 mg/mL DNAse I (Roche), during 25 min at 37°C with rotation. The enzymatic reaction was quenched by the addition of 30 mL of ice-cold 10% heat-inactivated fetal bovine serum DMEM (10% HI-FBS DMEM). Cell suspension was filtered through a 70 µm cell strainer (BD) and the remaining pieces of tissue were smashed against the filter with the help of a 1 mL syringe plunge. The filter was washed with 10 mL of ice-cold 10% HI-FBS DMEM and the cells were pelleted at 280xg for 5 min at 4°C. Lysis of erythrocytes was performed in Red Cell Lysis Buffer during 4 min at RT and immediately washed with ice-cold 10% HI-FBS DMEM. After filtration through a 70 µm cell strainer and centrifugation, cells were resuspended in ice-cold PBS or FACS Buffer (1 mM EDTA, 4% FBS in PBS), depending on the FACS staining protocol.

Alveolar macrophages from BAL fluid and peritoneal macrophages from peritoneal lavage were centrifuged and haemolysis with Red blood cell lysis Buffer was performed for maximum 2 min at RT if the pellet was very red. After quenching the reaction and washing with PBS (if haemolysis was performed), cells were resuspended in FACS Buffer or PBS, depending on the FACS staining protocol.

Flow cytometry analysis of immune cell populations

Prior to surface staining with the conjugated antibodies, cells were incubated 20 min at 4° in the presence of anti-CD16/CD32 to block Fc receptor with or without Live/Dead Fixable cell dead stain kit, depending on the panel. This incubation was done in PBS buffer if Live/Dead Fixable cell dead stain kit was used or in FACS buffer otherwise. Cells were then centrifuged and the mix of conjugated antibodies was added and incubated during 20-30 min at 4° in the dark. Antibodies are detailed in **Table M6**, and the combination of antibody panels are described in **Table M7**. If no intracellular staining was needed, cells were washed once with FACS buffer and resuspended in FACS buffer with or without DAPI depending on the panel.

For intracellular staining, membrane-stained cells were washed with PBS and then were incubated with a fixing solution of PBS + 4% Paraformaldehide (PFA) for 20 min in the dark at RT. Samples were spun at 350xg for 5 min and the supernatant was discarded. Cells were resuspended in 200 µl of permeabilization solution (PBD + 0,5% Tween and 1% BSA) and centrifugued at 350xg for 5 min. This process was repeated twice. Next, samples were resuspended in permeabilization solution with the intracellular antibodies and incubated for 20 min in the dark. Samples were washed twice with permeabilization solution and finally resuspended in FACS Buffer for analysis.
For T reg intracellular staining, the FOXP3 Transcription Factor staining buffer kit was used following the Manufacturer's instructions.

Flow cytometry analysis and cell separation were performed in a Beckman Gallios Flow Cytometer or in a Beckton Dickinson FACS Aria Fusion flow cytometer. Data was analysed using the FlowJo software. Immune cell populations were defined as described in **Table M8**.

Table M6 |

FACS antibodies			
Antibody	Company	Reference	Clone
MHCII PECY7	Invitrogen	25-5321-82	M5/114.15.2
F4/80 FITC	Invitrogen	11-4801-82	BM8
CD11C BV785	BioLegend	117336	N418
F4/80 PE	BioLegend	123109	BM8
SIGLECF PERCP-CY5.5	BD-Bioscience	565526	E50-2440
CD11B BV711	BioLegend	101241	M1/70
CD45-BV510	BD-Bioscience	563891	30-F11
LY-6C FITC	BD-Bioscience	561085	AL-21
LY-6G APC Cy7	BD-Bioscience	560600	1A8
I-A/I-E APC	BioLegend	107613	M5/114.15.2
CD3 PERCP-CY5.5	BioLegend	100327	145-2C11
CD19 BV711	BioLegend	115555	6D5
CD4 FITC	Invitrogen	11-0041-81	GK1.5
CD8a APC	Invitrogen	17-0081-82	53-6.7
CD44 BV711	BioLegend	103057	IM7
CD62L PE-CY7	BioLegend	104417	MEL-14
FOXP3 PE	Invitrogen	12-5773-80	FJK-16S
CD69 PE	BioLegend	104507	H1.2F3
CD25 APC-CY7	BioLegend	101917	3C7

MHCI APC	Invitrogen	17-5958-80	AF6-88.5.5.3
CD103-BV421	BioLegend	121421	2E7
NK1.1-BV421	BD-Bioscience	562921	PK136
CD16/CD32	eBioscience	16-0161-85	93
CD4 APC	Invitrogen	17-0041-81	GK1.5

Table M7 |

FACS antibody panels		
Panel	Antibodies	Life/Dead
MHCII panel	MHCII-PE-Cy7, F4/80-FITC, (MHCI-APC)	Aqua Life/Dead staining kit
Myeloid cells	CD45-BV510, CD11b-BV711, CD11c-BV785, F4/80-PE, Ly6C-FITC, Ly6G- APC-Cy7, I-A/I-E-APC, CD103-BV421, SiglecF-PerCP-Cy5.5 (only lung)	DAPI
Lymphoid cells	CD45-BV510, CD3-PerCP-Cy5.5, CD19-BV711, CD4-FITC, CD8a-APC, NK1.1-BV421, MHCII-PE-Cy7	DAPI
T cell activation	CD45-BV510, CD3-PerCP-Cy5.5, CD4-FITC, CD8a-APC, CD44-BV711, CD62L-PE-Cy7	Yellow Life/Dead staining kit
Myeloid cells from BAL	CD45-BV510, CD11b-BV711, CD11c-BV785, F4/80-PE, SiglecF-PerCP-Cy5.5, Ly6C-FITC, Ly6G- APC-Cy7, I-A/I-E-APC	DAPI
Regulatory T cells	CD45-BV510, CD3-PerCP-Cy5.5, CD4-FITC, CD8a-APC, FoxP3-PE	Yellow Life/Dead staining kit
T cells for proliferation assay	CD4-APC, CD69-PE, CD25-APC-Cy7, Celltrace Violet	Yellow Life/Dead staining kit

Table M8 |

Cell population definition	
Myeloid cells	CD45+, total CD11b+ and/or CD11c+ cells
Alveolar macrophages	CD45+, CD11c+, F4/80+, CD11b low, Ly6C/G-, CD103-, SiglecF+
Neutrophils	CD45+, CD11c-, F4/80-, CD11b+, Ly6Cmed, Ly6G+, CD103-, SiglecF-, MHCII-
Dendritic Cells	CD45+, CD11c+, F4/80+, CD11b-, Ly6C/G-, SiglecF-, MHCII+
CD103+ DC	CD45+, CD11c+, F4/80-, CD11b-, Ly6C/G-, CD103+, SiglecF-, MHCII+
CD11b+ DC	CD45+, CD11c+, F4/80-, CD11b+, Ly6C/G-, CD103-, SiglecF-, MHCII+
Ly6C low monocytes	CD45+, CD11c-, F4/80+, CD11b+, Ly6Clow, Ly6G-, CD103-, SiglecF-
Ly6C high monocytes	CD45+, CD11c-, F4/80+, CD11b+, Ly6Chigh, Ly6G-, CD103-, SiglecF-, MHCII low or high
Interstitial macrophages	CD45+, CD11c-, F4/80+, CD11b+, Ly6Clow, Ly6G-, CD103-, SiglecF-, MHCII high
Eosinophils	CD45+, CD11c-, F4/80+, CD11b+, Ly6Clow, Ly6G-, CD103-, SiglecF+, MHCII-, SSC high
CD8 T cells	CD45+, class II MHC -, CD19-, NK1.1-, CD3+, CD4-, CD8+
CD4 T cells	CD45+, class II MHC -, CD19-, NK1.1-, CD3+, CD4+, CD8-

NK cells	CD45+, class II MHC -, CD19-, NK1.1+, CD3-, CD4-, CD8-
B cells	CD45+, class II MHC +, CD19+
Effector T cells	CD45+, CD3+, CD4/CD8+, CD44+, CD62L-
Central Memory T cells	CD45+, CD3+, CD4/CD8+, CD44+, CD62L+
Naïve T cells	CD45+, CD3+, CD4/CD8+, CD44-, CD62L+
Regulatory T cells	CD45+, CD3+, CD4+, CD8-, FoxP3+
Peritoneal macrophages (peritoneal lavage)	F4/80+
T cells (blood)	CD45+, CD3+
B cells (blood)	CD45+, CD19+

RNA-Seq of alveolar macrophages

Sample collection and RNA isolation

For this experiment, we used mice with and without lung metastasis. Mice with metastasis were left for 11 days after B16/F10 cell inoculation. We used 4 mice per condition divided and pooled into 2 biological replicates of each condition. AMs were extracted from BAL, pelleted at 350xg for 5 min at 4°C and the pellet was resuspended in 350 µl of Trizol. RNA isolation was performed with the PureLink RNA minikit. Total RNA extractions were quantified with the Qubit RNA Hs Assay kit (Invitrogen), and RNA integrity assessed with the Bioanalyzer 2100 RNA Pico assay (Agilent).

Library preparation and sequencing

Libraries for RNA-seq were prepared at IRB Barcelona Functional Genomics Core Facility. Briefly, mRNA was isolated from 140 ng of total RNA using the kit NEBNext Poly(A) mRNA Magnetic Isolation Module (New England Biolabs). Libraries for RNA-seq were prepared from the purified mRNA using the NEBNext Ultra II RNA Library Prep Kit for Illumina (New England Biolabs). Twelve cycles of PCR amplification were applied to all libraries. The final libraries were quantified using the Qubit dsDNA HS assay (Invitrogen) and quality controlled with the Bioanalyzer 2100 DNA HS assay (Agilent). An equimolar pool was prepared with the nine libraries and submitted for sequencing at the Centre for Genomic Regulation (Barcelona). A final qPCR quality control was performed before sequencing in one lane of an Illumina HiSeq2500. Sequencing output was 294 Million 50-bp single-end reads and a minimum of 29 million reads were obtained for all libraries.

Bioinformatics analysis of RNA-Seq

Bioinformatics analyses were performed by the Biostatistics/Bioinformatics Facility at the IRB Barcelona. In brief, RNA-seq was used to compare WT and p38αKO mice in healthy and metastatic lungs. RNA-seq reads were aligned to the mouse genome version mm10 using STAR (v.2.5.2b) (Dobin et al., 2013). SAM files were converted to BAM files and sorted using sambamba (v0.7.1) (Tarasov et al., 2015). The count matrix was generated with Rsubread with the built-in annotation for mm10 (Liao et al., 2019). DESEq2 (v1.30.1) was used for differential expression analysis with fold change shrinkage as implemented in the lfcShrink function (Love et al., 2014). Functional enrichment analysis was performed over gene sets defined in the Molecular Signatures Database (MSigDB) hallmark gene set collection, Gene Ontology database, and KEGG. The rotation-based approach for enrichment implemented in the R package limma was used to represent the null distribution (D. Wu et al., 2010). The max-mean enrichment statistic, under restandardization, was considered for competitive testing (Efron & Tibshirani, 2007).

For Venn diagram, Biovenn online tool was used (Hulsen et al., 2008).

sc-RNA-Seq of CD45$^+$ cells

Sample collection

We used a pool of 4 mice for each genotype in tumor-free conditions (1 replicate of each condition), and 2 pools of 2 mice of each genotype in the case of animals with lung metastasis (2 replicates of each condition). Mice with metastasis were left for 11 days after B16/F10 cell inoculation. Lungs were collected as described before and CD45$^+$ cells were sorted using an Aria Sorter.

Single cell and library preparation

The cell suspensions for single-cell transcriptome analysis were processed at IRB Barcelona Functional Genomics Core Facility. Briefly, the cell concentration of each sample was adjusted to approximately 1,000 cells/µl. Cell partition into GEMs was performed using Chip G and the 3' v3.1 chemistry (10X Genomics). Barcoded cDNA was amplified for eleven cycles, quantified, and quality controlled on the Bioanalyzer 2100 using a high sensitivity DNA assay (Agilent). Libraries were generated using only 10 µl (25%) of the total cDNA (40 µl), strictly following the manufacturer instructions. 13 amplification cycles were performed for each library. Purified libraries were quality

controlled on the Bioanalyzer 2100 and quantified. A 20 nM equimolar pool was prepared and a final qPCR validated libraries before cluster generation. Illumina sequencing was performed at CNAG using a NovaSeq6000 S2 with an asymmetric strategy (28+90) to reach 150 Gbp. Sequencing output was 1,589 million paired-end reads and a minimum of 233 million reads were obtained for all libraries.

Bioinformatics analysis of sc-RNA-Seq

Bioinformatics analysis were performed by the Biostatistics/Bioinformatics Facility at the IRB Barcelona. Briefly, Chromium single cell RNA sequencing reads were aligned to the reference transcriptome (refdata-gex-mm10-2020-A) with CellRanger (v4.0.0) (G. X. Y. Zheng et al., 2017). The count utility was used with default options to quantify gene expression. The subsequent processing steps and analysis were performed with Seurat package (v4.0.3) (Butler et al., 2018; Hao et al., 2021; Satija et al., 2015; Stuart et al., 2019). Cells having <20% mitochondrial read content and >500 UMIs were considered for downstream analyses. Ribosomal reads were removed. The proportion of mitochondrial reads was regressed out during the normalization and variance stabilization of raw counts, which was performed with the sctransform method (Hafemeister & Satija, 2019). SCT transformed counts were further imputed and smoothed with MAGIC (v.2.0.3) (van Dijk et al., 2018). Cell types were annotated with singleR using as reference the ImmGen expression dataset from celldex (Aran et al., 2019). The mitochondrial and UMI content thresholds were manually refined by inspecting their distribution in each cell type. A threshold of 1000 UMIs was set for Neutrophils, T cells, NK cells, B cells, ILC, NKT, Endothelial cells, Tgd, proB cells, Basophils, Stromal cells and Eosinophils. A threshold of 1500, 2000, 3000, 4000, and 4500 was set for Monocytes, Mast cells, Macrophages, Fibroblasts, and DCs, respectively. A threshold of 5000 was set for Stem cells and Epithelial cells. As for the mitochondrial content, the threshold ranged from 10 to 20% for all cell types. Cells that passed this filtering step were renormalized, imputed/smoothed with MAGIC and classified again with singleR. The first 10 principal components were used to obtain the Uniform Manifold Approximation and Projection (UMAP) for visualization purposes. Cells were assigned to clusters using FindClusters Seurat function (resolution = 1.2). A focused analysis was performed on the lymphoid and myeloid lineages separately. The expression of marker gene signatures from Hurskainen et al. was summarized by taking the average MAGIC score of its constituent genes and then used to refine the cell type annotation manually (Hurskainen et al., 2021). Pseudobulk differential expression analysis was performed for each cell type using DESEq2 with lfcShrink fold change shrinkage, as described above (Love et al., 2014). Functional enrichment analysis was performed over gene sets defined in

the Molecular Signatures Database (MSigDB) hallmark gene set collection, Gene Ontology database, and KEGG. The rotation-based approach for enrichment implemented in the R package limma was used to represent the null distribution (D. Wu et al., 2010). The max-mean enrichment statistic, under restandardization, was considered for competitive testing (Efron & Tibshirani, 2007).

Molecular biology

Gene expression analysis by RT-qPCR

RNA extraction

Cells were washed with PBS, resuspended in 500 µl Trizol and placed in a 1.5 mL Eppendorf tube, whereas tissue samples were homogenized using a Percellys instrument. 100 µl of chloroform were added and tubes were centrifuged at 15000×g at RT for 10 min. From the two liquid phases generated, the fraction with less density was transferred into new tubes. After adding 200 µl of 70% ethanol, the RNA extraction was followed using the PureLink RNA mini kit. DNAse treatment was performed using on-column DNase treatment following manufacturer's instructions. RNA purity and concentration were determined by measuring absorbance at 260 nM and 280 nM using a NanoDrop 2000 spectrophotometer (Thermo Scientific).

Synthesis of cDNA

cDNA was obtained from 150 ng to 1 µg of purified RNA. First, RNA was incubated with random primers and dNTP at 65°C for 5 min and ramped down to 4°C in a BioRAD. Samples were put on ice and a mixture of RNAsin and SuperScript IV reverse transcriptase was added. Retrotranscription PCR was run with the following PCR program: 23°C for 10 min, 55°C for 10 min and 80°C for 10 min. Samples were stored for a maximum of 1 week at 4°C or for longer at -20°C.

RT-qPCR

3-15 ng of cDNA were mixed with 5 µl of SYBR green, 0.25 µl of each primer and up to 10 µl of ddH_2O. Primers are described in **Table M9**. For pre-mRNA analysis, primers were designed within the intron-exon junction using the USCS database (Zeisel et al., 2013).The mix was incubated in a Quant6 Flex (Thermofisher) with the following PCR program: an initial step of 50°C for 2 min and 95°C for 10 min; 40 cycles of 95°C for

15 sec and 60°C for 1 min; and a final step of 95°C for 15 sec, 60°C for 1 min and 95°C for 15 sec.

Samples were analysed in triplicates and normalized to HPRT, GAPDH and/or beta-Actin housekeeping genes. Analysis was done using the ΔCt method.

Table M9 I

Primers for RT-qPCR		
Gene	FW	RV
GAPDH	GGCCCGGAGTCTTAAGTATTAG	GGGCGCGAAAGTAAAGAAAG
HTRP	GAGAGCGTTGGGCTTACCTC	ATCGCTAATCACGACGCTGG
CIITA E16-18 (total)	TGCGTGTGATGGATGTCCAG	CCAAAGGGGATAGTGGGTGTC
CIITA-pI	ACAGGGACCATGGAGACCATAG	GGGTCGGCATCACTGTTAAGG
CIITA-pIII	GCCGGAGTTGCAAGACCATAG	GGGTCGGCATCACTGTTAAGG
CIITA-pIV	GAGACTGCATGCAGGCAGCAC	GGGTCGGCATCACTGTTAAGG
H2-Aa	TGCTTCCTGAGTTTGGCCAA	GGAACACAGTCGCTTGAGGA
H2-Ab	ACAGCTTATTAGGAATGGGGACT	CACGGTGATGGGACTCTTCA
H2-Eb	TGTCACGGTCGAGTGGAAAG	AAGTAGATGAACAGCCCCGC
Pre-CIITA ex2	CTCTCTGCCTTTGCCTACCA	GAGATCCCAGATCCATGGTG
p38α EX2	GCATCGTGTGGCAGTTAAGA	GTCCTTTTGGCGTGAATGAT
p38α EX12	GCCCTCCCTCACTTCAGGAG	TGTGCTCGGCACTGGAGACC
TNFα	CCAGACCCTCACACTCAGATC	CACTTGGTGGTTTGCTACGAC
CD74	TTGCTGATGCGTCCAATGTC	GGGTCATGTTGCCGTACTTG
HDAC6	CCCAATCTAGCGGAGGTAAAG	CACTCTTGTCTCAGGGTTCAG
Colec12	GCCAACAATGACACCCTAGA	GGCCTGTGAGATAGTGGTAATG
MARCO	CCAGTGCCCAAGAAGAGAAA	TGCTCCTGCAGATTGAGAAC
CD36	CTGGGACCATTGGTGATGAAA	CACCACTCCAATCCCAAGTAAG
FABP4	GCAGAAGTGGGATGGAAAGT	GTGGAAGTCACGCCTTTCATA
CCL9	CCCTCTCCTTCCTCATTCTTACA	AGTCTTGAAAGCCCATGTGAAA
CCR2	TAACTGTGTGATTGACAAGCACT	TGGAGAGATACCTTCGGAACTT
CXCL1	GCCAATGAGCTGCGCTGT	CCTTCAAGCTGTCCATGTTCTTG
CXCL2	GCTGTCAATGCCCTGAAGACCCTGC	GTACGATCCAGGCTTCCCGGGTG
IFNγ	CCTTCTTCAGCAACAGCAAGGC	GGGTTGTTGACCTCAAACTTGGC
IL10	TTTCAATTCCCTGGGTGAGAA	CTCCACTGCCTTGCTCTTATTTTC
IL12β (p40)	GGAAGCACGGCAGCAGAATA	AACTTGAGGGAGAAGRAGGAARGG
IL18	GACTCTTGCGTCAACTTCAAGG	CAGGCTGTCTTTTGTCAACGA
IL1B	GCAACTGTTCCTGAACTCAACT	ATCTTTTGGGGTCCGTCAACT
IL6	GAGGATACCACTCCCAACAGACC	AAGTGCATCATCGTTGTTCATACA
TGFβ	CTCCCGTGGCTTCTAGTGC	GCCTTAGTTTGGACAGGATCTG
DUSP1	GCTATTGACTTCATAGACT	TCTGCTTCACAAACTCAAAG
MKK6	GACCAGTTCCACGCCGCCTC	CGTCGCCCTCCCGGAAGAGT
CXCL12	TGCATCAGTGACGGTAAACCA	TTCTTCAGCCGTGCAACAATC
p15 (Cdkn2b)	AATCCAGGTCATGATGATGGG	GTGCACAGGTCTGGTAAGG
p21 (Cdkn1a)	CGTGGACAGTGAGCAGTT	GTCTCCGTGACGAAGTCAAA
p16ink4	ATGGAGTCCGCTGCAGACAG	ATCGGGGTACGACCGAAAG
p19arf	GGGTCGCAGGTTCTTGGTC	GTGCGGCCCTCTTCTCAA

mAct *	GATCTGGCTTTCCGGCTATT	CCCTATTTGTGTGGCCTCTT
mGAPDH *	GGCCCGGAGTCTTAAGTATTAG	GGGCGCGAAAGTAAAGAAAG
16S *	AGAGTTTGATCCTGGCTCAG	GWATTACCGCGGCKGCTG

** Primers for genomic DNA*

Protein analysis by western blot

Tissue and cell lysis for protein extraction

From tissue samples

A piece of snap frozen tissue was collected in a tube and 3 lysis balls were added together with 250-300 ul of RIPA Buffer (1% NP40, 0.5% sodium deoxycholate, 0.1% SDS, 50 mM Tris-HCl, 150 mM NaCl, 5 mM EDTA, 5 mM EGTA, 20 mM sodium fluoride, 1 mM PMSF, 1 mM sodium orthovanadate, 2.5 mM benzamidine, 10 µg/mL pepstatin A, 1 µM mycrocystin, 10 µg/mL leupeptin and 10 µg/mL aprotinin). Tissue was homogenized (Precellys 24 Tissue Homogenizer) and sample was transferred to a 1.5mL Eppendorf and kept on ice.

From cultured cells

Adherent cells on plates were washed twice with PBS and placed on ice. RIPA buffer was added and cells were collected using a scraper maintaining the plates on ice.

Protein extraction and quantification

Collected samples were incubated on ice for 10 min and, if indicated, they were sonicated to remove remaining membrane lipids. Next, the lysate was spun at maximum speed for 15 min at 4°C, and the supernatant was collected and either kept at -80°C or used for protein quantification. If the lysate was used for immunoprecipitation (IP), the same procedure was done using IP buffer (10 mM Tris/Cl pH7.5, 150 mM NaCl, 0.5 mM EDTA, 0.5% Nonidet P40 Substitute) instead of RIPA buffer.
Protein concentration was estimated using the RC DC protein assay kit I. 2 µl of protein sample was mixed with 25 µl of freshly prepared working reagent A (10 µl of Protein Assay Reagent S and 490 µl of Reagent A). Then, 200 µl of Protein Assay reagent C was added and the solution was incubated for 5 min at RT. Absorbance at 750 nm was measured using a spectrophotometer (BioTek, FLx800) and concentrations were calculated using a BSA standard curve, which was prepared and quantified in every experiment.

Protein detection by western blot

Loading buffer was added to the quantified samples, which were boiled for 5 min at 95°C. Proteins (15-40 µg) were separated by SDS-PAGE using 8%, 10%, 12% Laemmli gels, depending on the molecular weight of the proteins. After electrophoresis, proteins were transferred from the polyacrylamide gel to a nitrocellulose membrane using a wet transfer system (Bio-Rad). Ponceau Red was used to reversibly stain proteins in order to check transfer quality and was then washed out with dH2O. The membrane was blocked for 1 h with 5% non-fat milk in PBS+0.01% Tween at RT. Primary antibody was diluted with 5% BSA in PBS-0.01% Tween and incubated overnight at 4°C. Membranes were washed three times in PBS+0.01% Tween and incubated for 1 h at RT with the secondary antibody diluted in the same buffer containing 5% non-fat milk. Finally, membranes were washed three times with PBS+0.01% Tween. Proteins were detected using the Odyssey Infrared Imageing System. The antibodies used for western blot are indicated in **Table M10**.

MK2 immunoprecipitation (IP)

For MK2 IP, the MK2-Trap Agarose kit was used following the user's guide. In brief, BMDMs were cultured in 15 cm plates and treated with PH and LPS stimulated for 24 h as usual. Cells were lysed with IP buffer supplemented with protease inhibitor cocktail and 1 mM PMSF. The lysis suspension was sonicated with 4 pulses of 10 sec each with pauses of 5 sec. Tubes were placed on ice for 30 min. Next, samples were centrifuged at 17.000xg for 10 min at 4°C and transferred to a new tube with 300 µL of Dilution Buffer (10 mM Tris/Cl pH 7.5, 150 mM NaCl, 0.5 mM EDTA) supplemented with 1 mM PMSF and protease inhibitor cocktail. 50 µL of diluted lysate were kept as input fraction. The diluted lysate was resuspended with 50 µl of equilibrated MK2-beads or control-beads and left on rotation overnight at 4°. Next day, samples were washed as stated in the kit's instructions, and finally resuspended in 30-50 µL of SDS-sample buffer and boiled for 5 min at 95°C. Beads were sedimented by centrifugation at 2500xg for 2 min at 4°C and samples were run in a NuPAGE 3-8% Tris-Acetate gradient gel.

Table M10 |

Western blot antibodies			
Antibody	Species	Company	Reference
p38α	Mouse	Santa Cruz	SC81621
Tubulin	Mouse	Sigma	T9026
p-MK2 (T334)	Rabbit	Cell Signalling	3007S
p-Stat1 (Ser727)	Rabbit	Cell Signalling	8826S
acetyl-α-Tubulin (Lys40)	Rabbit	Cell Signalling	5335T
HDAC6	Rabbit	Cell Signalling	7612S
acetyl-H3K9	Rabbit	Cell Signalling	9649T
MK2	Rabbit	Cell Signalling	3042
p-p38 (T180-Y182)	Rabbit	Cell Signalling	4631S
p-CREB (S133)	Mouse	Cell Signalling	9196S
p-eIF4E (S209)	Rabbit	Cell Signalling	9741S

Statistical analysis

All statistical analyses were performed using GraphPad Prism 9 software. Data is presented as mean ±standard error of the mean (SEM) unless otherwise indicated. Statistical significance was determined by the Student´s test for comparison of two groups. P-value (pval) was calculated and pval<0.05 was considered to be statistically significant. Pval is expressed in numbers or as *(pval ≤ 0.05), **(pval ≤ 0.01 and) ***(pval ≤ 0.001).

Commercial reagents and kits

Table M11 |

Reagent	Company	Reference
10% buffered formalin	Sigma	HT501128
Acrylamide 40% 29:1	BioRad	161-0146
Anti-CD28	BD Biosciences	553295
Anti-CD3	BD Biosciences	553058
Anti-PD1	BIOXCEL	BE0146
APS	Sigma	A3678
β-mercaptoethanol	Sigma	M7154
BSA	Sigma	A7906
Ceftriaxone disodium salt	Sigma	C5793
Cell trace CFSE Cell proliferation kit	Invitrogen	C34554
Celltrace Violet Cell proliferation kit	Invitrogen	C34557
Chloroform	Merck	1024451000
Clodronate liposomes	Liposoma B.V.	C-005
Collagenase A	Roche	20810727
Complete protease inhibitors	Roche	11873580001
Control agarose beads	Chromotek	Bab-20
Corn oil	Sigma	C8267
Countbright absolute conting beads	INVITROGEN	C36950
Dextran sodium sulfate (DSS)	MP Biochemicals	160110
Diaminobenzidine	Dako	K346811
Dispase II	Sigma	D4693
DMEM	Sigma	5796
DMSO	Sigma	D8418
DNAse	Sigma	D4513
dNTPs	ThermoFisher	R0192
DPX mounting media	Leica	3808600E
DTT	GE Healthcare	17-1318-02
Dynabeads Untouched Mouse CD4 Cells	Invitrogen	11415D
EDTA	Sigma	E46758
EGTA	Sigma	E4378
Ethanol	Panreac	1410861214
FBS	ThermoFisher	E6541L
Fludarabine (NSC 118218) 10mg	Sellekchem	S1491
FOXP3/Transcription factor Staining Buffer Kit	eBIOSCIENCE	00-5523-00
Glutamine	LabClinics	M11-004
Latex beads fluorescent yellow-green	Sigma	L4530
MEM Non-essential aminoacids 100X	Gibco	11140-035

Methanol	Panreac	1310911214
MK2-TRAP AGAROSE	Chromotek	mta
Nanodrop 2000 Spectrophotometer	Thermo Scientific	
Neon Transfection system kit	ThermoFisher	MPK10025
Nitrocellulose membrane 0.2 mm	GE Healthcare	10600002
NP40	AppliChem	A16960250
NuPAGE 3-8% Tris-Acetate gradient gel	INVITROGEN	EA0378BOX
Optimem	Gibco	31985-070
OVA 323-339	Invivogen	vac-isq
Paraformaldehyde 16%	Electron Microscopy Sciences	15710
Pepstatin A	Sigma	P4265
Peroxidase blocking buffer	Dako	S2023
Ponceau Red	Sigma	P3504
Proteinase K	Roche	3115852001
PureLink on column DNAse	Invitrogen	121-85-010
PureLink RNA mini kit	INVITROGEN	12183018A
PureProteome Magnetic stand (8well)	Millipore	LSKMAGS08
Random primers	Invitrogen	48190-011
RC DC Protein Assay Kit I	Dako	S2023
Recombinant murine IL-2	Peprotech	212-12
Rnase A	Roche	10109142001
RNAsin 2500U	Promega	N211
RPMI 1640	Sigma-Aldrich	R8758
SDS	Sigma	71725
Shielded I.V Catheter 24G	BD	381811
siRNA HDAC6 s67425	Thermofisher	4390771
Sodium citrate	MERK	1064485000
Sodium pyruvate	Sigma-Aldrich	P2256
Stem Pro Accutase	Thermofisher	A1110501
Superfrost glass slides	VWR	J1800AMNZ
Superscript IV reverse transcriptase	Invitrogen	18090010
SYBR Select master mix	ThermoFisher	4472942
TEMED	Sigma	T9281
Trizol	ThermoFisher	15596026
Ultracomp eBEADS	INVITROGEN	01-2222-42
Vacuum filter Stericup QuickRelease Millipore express 0,22um 500ml	Merck	S2GPU05RE

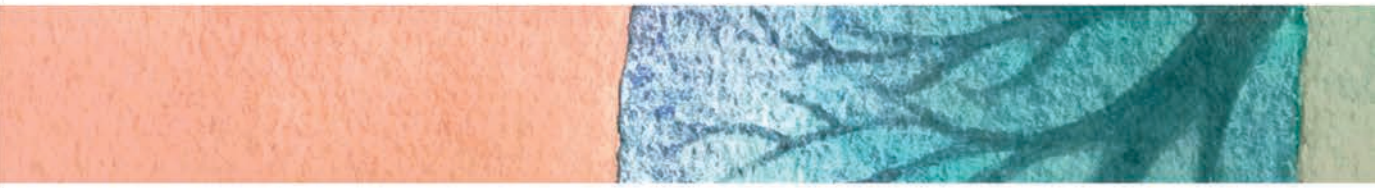


Results

SECTION 1

Myeloid p38α in melanoma and lung metastasis

Myeloid cells are important players in the immunosuppressive response of tumors. In this project, we have studied whether the kinase p38α in myeloid cells participates in the process of tumor immunosuppression. To address this, we have used a *LysM*^{Cre} model crossed with a p38α$^{fl/fl}$ strain, in which the exons 2 and 3 of the *MAPK14* gene encoding p38α are flanked by loxp sites, from now on referred to as p38αΔ^{Lys} (**Figure R1A**). Lysozyme M or LysM is an enzyme that is expressed mainly in some cells of the myeloid lineage (Abram et al., 2014). The deletion of p38α was double-checked in each experiment by PCR in newborn mice and by western blot of p38α in peritoneal macrophages at the end of each experiment (**Figure R1B**).

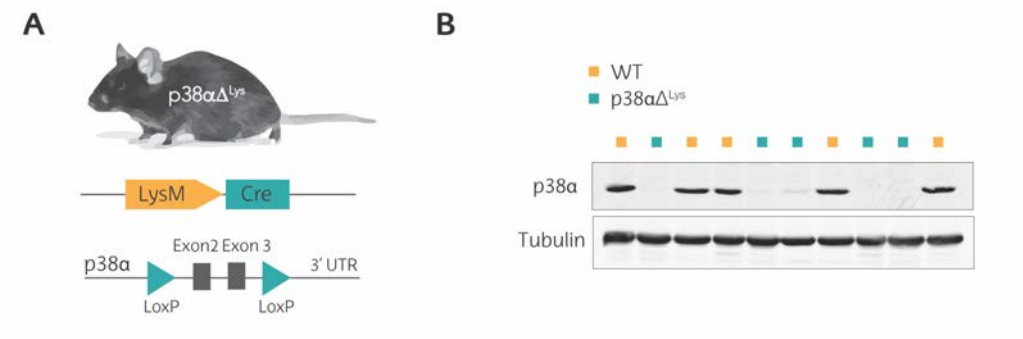

FIGURE R1. p38αΔ^{Lys} mice delete p38α in myeloid cells.
A. p38αΔ^{Lys} mice express Cre recombinase under the transcriptional control of the LysM promoter, which is only expressed in some myeloid cells. The MAPK14 (encoding p38α) exons 2 and 3 are flanked by LoxP sites, which are cleaved by Cre. **B**. Western blotting of p38α in peritoneal macrophages extracted from different WT and p38αΔ^{Lys} mice.

Primary melanoma growth is unaffected by myeloid p38α

We first studied whether myeloid p38α could be involved in the development of melanoma, a highly immunogenic type of cancer. Immunotherapies are extensively used to treat these tumors, but patients develop resistance due to a certain degree of immunosuppression. We explored whether the inhibition of p38α in myeloid cells could be beneficial to overcome immunosuppression and ameliorate the response to therapies. To this end, we used B16/F10 cells to study primary melanoma growth in

mice. The B16/F10 cell line is widely used as a model of metastatic melanoma in immune-oncology studies (Nakamura et al., 2002). We monitored the growth of subcutaneous tumors in WT and p38αΔ^{Lys} mice. However, we observed no differences in tumor growth between these two groups (**Figure R2A**), thereby indicating that myeloid p38α is not involved in primary melanoma tumor formation in mice. We also wondered whether p38α inhibition could boost the effect of the immunotherapy treatment. To this end, we induced subcutaneous B16/F10 tumors in WT mice and treated them with the checkpoint inhibitor anti-PD1, combined with or without the p38α inhibitor PH-797804. Our results showed that the anti-PD1 treatment effectively maintained the tumors smaller than those in mice treated with vehicle. However, we p38α inhibitor had no effect nor did it boost the effect of anti-PD1 therapy (**Figure R2B**).

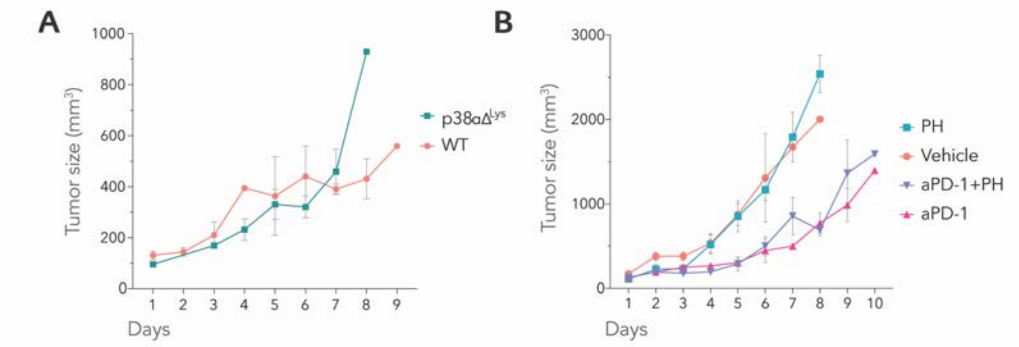

Figure R2. Myeloid p38α does not affect primary melanoma growth.
A. B16/F10-OVA subcutaneous tumor growth in WT and p38αΔ^{Lys} mice. For this experiment, B16-F10-OVA were used to increase tumor immunogenicity. (n=12). **B**. B16/F10 subcutaneous tumor growth in WT mice treated with or without the p38a inhibitor PH797804 (PH), the anti-PD1 checkpoint inhibitor, or the combination of both inhibitors (n=14). Data shown as mean ±SEM.

We conclude that myeloid-specific deletion of p38α or systemic inhibition of p38α has no effect on the development of primary melanoma tumors and does not boost the effect of anti-PD1 therapy.

Lung metastasis is affected in myeloid specific p38α deletion

It has been reported that primary tumors can release molecular factors that can prepare the metastatic niche prior to the metastasis, the lung being one of the most frequent sites of metastasis (Obenauf & Massagué, 2015). Previous studies on pre-metastatic niche formation have reported the importance of myeloid cells in this

process, given their immunosuppressive capacity (Gabrilovich et al., 2012; Hanahan & Coussens, 2012). To study the effect of myeloid p38α on metastatic melanoma, we first used a spontaneous metastasis model by resectioning primary B16/F10 subcutaneous tumors when they reached 100-200 mm^3. We left the animals for up to 40 days and carefully analysed the lungs, lymph nodes, kidneys, liver and spleen for the presence of metastasis. However, we did not observe metastasis in any of these organs. We therefore decided to use the melanoma metastatic cell line B16-F10 and generated experimental lung metastasis by intravenous tail vein injection in WT and p38αΔ^{Lys} animals. Mice were left 21 days for lung metastasis to form (**Figure R3A**). We observed a reduction of the metastatic burden in p38αΔ^{Lys} mice, pointing at the contribution of myeloid p38α in the formation of lung metastasis (**Figure R3B-C**). Of note, 5 WT animals died before day 21, possibly due to a high lung metastatic burden, and thus further pointing to the protective role of myeloid p38α deletion. Curiously, this reduction in lung metastasis was not observed in p38αΔ^{Lys} males, thus we used female mice for the further characterization of the function of myeloid p38α in lung tumorigenesis.

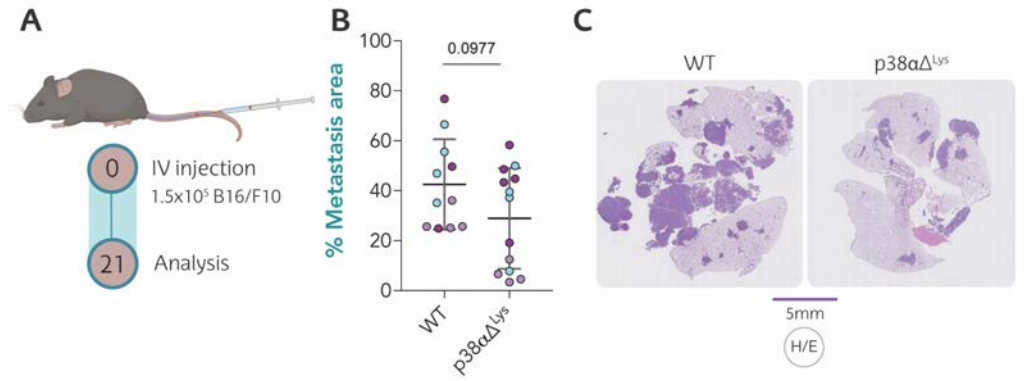

Figure R3. p38αΔ^{Lys} mice produce less lung metastasis.
A. Experimental metastasis model in which B16/F10 cells are injected intravenously and analysis is performed 21 days after injection. **B**. Metastasis area quantification of B16/F10 lung metastasis in WT and p38αΔ^{Lys} mice at day 21 of three independent experiments shown in different colours (n=24). Data shown as mean±SD. **C**. Representative Haematoxylin/Eosin (H/E) images from WT and p38αΔ^{Lys} mice with lung metastasis at day 21.

Next, we addressed whether changes in the recruitment of immune cell populations or changes in myeloid or lymphoid cell proportions could be responsible for the reduced lung metastasis in the p38αΔ^{Lys} mice. We performed FACS analysis of the immune cell populations from both WT and p38αΔ^{Lys} animals using either lungs with metastasis or lungs in basal conditions. We optimized a FACS panel of antibodies, which allowed us to classify the vast majority of immune cell populations of this organ.

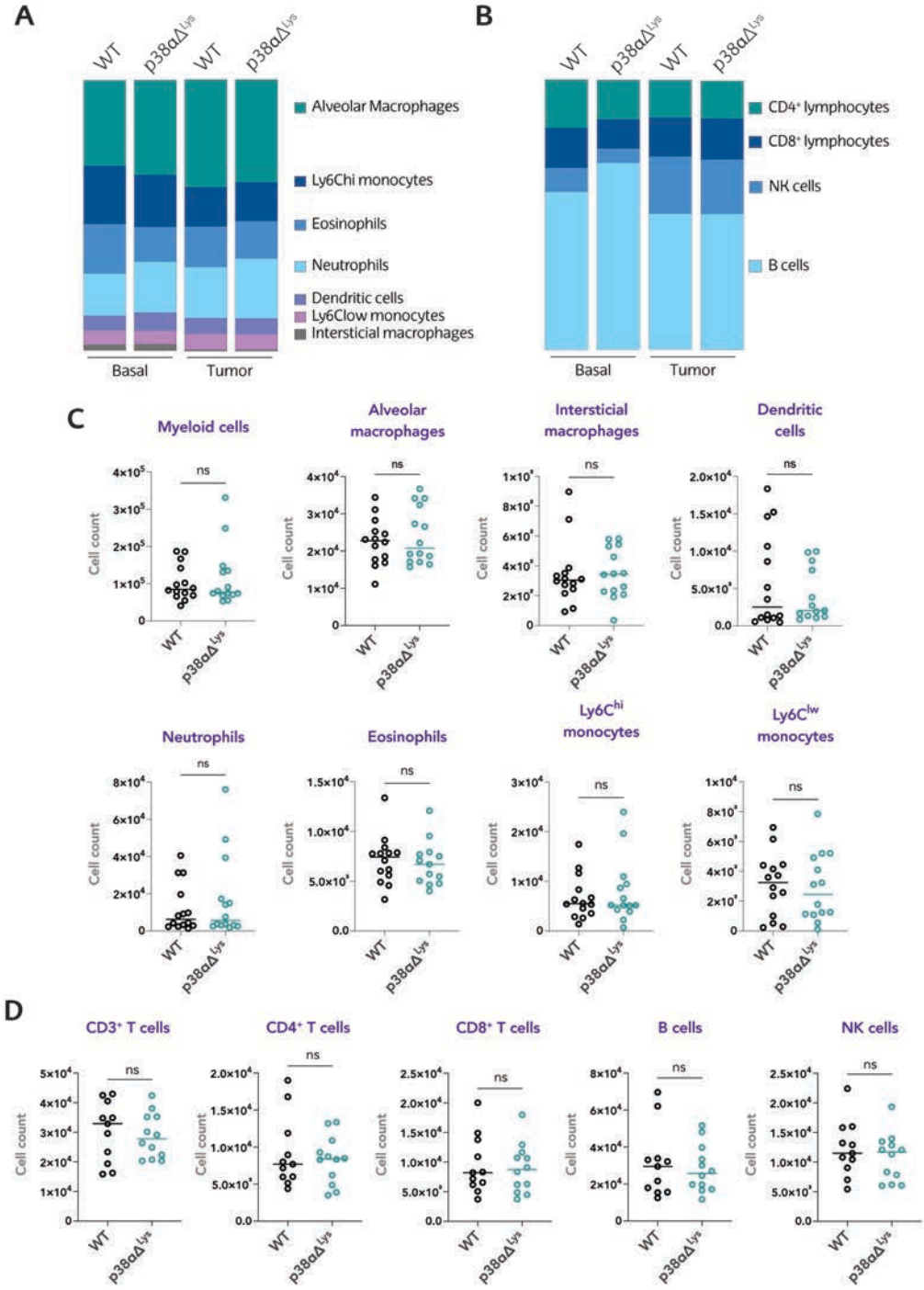
A
WT
p38αΔLys
WT
p38αΔLys
Alveolar Macrophages
Ly6Chi monocytes
Eosinophils
Neutrophils
Dendritic cells
Ly6Clow monocytes
Intersticial macrophages
Basal
Tumor
B
CD4+ lymphocytes
CD8+ lymphocytes
NK cells
B cells
C
Myeloid cells
Alveolar macrophages
Intersticial macrophages
Dendritic cells
Neutrophils
Eosinophils
Ly6Chi monocytes
Ly6Clw monocytes
Cell count
ns
D
CD3+ T cells
CD4+ T cells
CD8+ T cells
B cells
NK cells

FIGURE R4. p38αΔ^{Lys} and WT mice maintain the same lung immune populations.
A-B. Percentages of myeloid and lymphoid cell populations in WT and p38αΔ^{Lys} mice in lungs with and without metastasis. Lungs were analysed by FACS at day 21 after B16/F10 cell injection. Results are indicated as percentages of CD45^{+} cells. Each cell type is coloured as shown in the legend. **C-D**. Total cell number analysis of myeloid (C) and lymphoid (D) populations in a lung lobe in WT and p38αΔ^{Lys} mice with lung metastasis at day 21. Data shown as mean from mice of 3 independent experiments.

The myeloid cell populations analysed included alveolar macrophages (AMs), peritoneal macrophages, CD11b+ and CD103+ DCs, inflammatory monocytes and circulating monocytes, eosinophils and neutrophils. The lymphoid cell populations include CD4^{+} and CD8^{+} T cells, NK cells and B cells. No significant differences in terms of frequencies in the myeloid populations were observed between WT and p38αΔ^{Lys} mice, thereby indicating that the deletion of p38α in myeloid cells does not affect the proportions of any particular myeloid population in the lungs, either in basal conditions or in tumors (**Figure R4A**). Similar observations were seen in cells from the lymphoid lineage, where frequencies were very similar between genotypes, except for a slight but not significant increase in B cells only in basal conditions in p38αΔ^{Lys} mice (**Figure R4B**). These results were confirmed with cell count analysis, which revealed very similar total cell numbers between WT and p38αΔ^{Lys} animals with lung metastasis (**Figure 4RC-D**). This indicates that the observed reduction in lung metastasis is probably due to the effect of p38α deletion on the functional capacities of myeloid cells rather than on their ability to recruit or somewhat change the immune cell populations in the lungs.

We next addressed whether the deletion of p38α in myeloid cells could change the activation profiles of the T lymphocytes. To this end, we used FACS to analyse the naïve, effector and central memory T cells using the markers CD44 and CD62L. We observed a significant increase both in effector CD8^{+} and CD4^{+} T cells in the p38αΔ^{Lys} animals, both in basal and in tumor conditions (**Figure R5A**). This is a relevant finding as effector CD4^{+} and CD8^{+} cells are the main anti-tumoral cells in the tumor microenvironment that cause tumor cell death. These observations support that although immune cell proportions do not differ between p38αΔ^{Lys} and WT mice, the activity of T lymphocytes is modified in the p38αΔ^{Lys} mice towards a more anti-tumoral state, which could ultimately lead to a reduction in lung tumors. Interestingly, this was also observed in basal conditions, indicating that p38α myeloid deletion also enhances T cell activation at basal levels. Of interest, the increase of effector cells in tumors was accompanied by an increase in Regulatory CD4^{+} T cells in the p38αΔ^{Lys} mice, probably due to a compensatory mechanism to counteract the effector activation (**Figure R5B**). These changes point to the involvement of myeloid p38α in

the regulation of T cell activation. By keeping T cell activation low, myeloid p38α may contribute to the immune tolerance of the lungs.

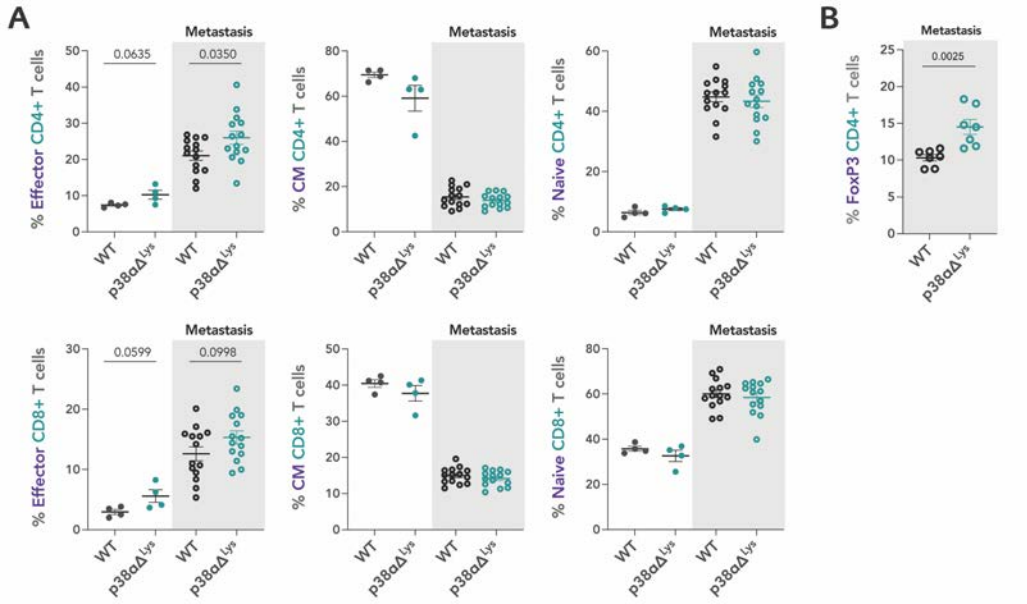

Figure R5. Effector T cells are increased in p38αΔ^{Lys} lungs.
A. FACS analysis of the activation profile of T lymphocytes in lungs with and without metastasis from WT and p38αΔ^{Lys} mice, represented as percentage of the total CD4^{+} T cells (above) and CD8^{+} T cells (below). Effector cells defined as CD62L^{low}, CD44^{hi}, central memory (CM) defined as CD62L^{hi}, CD44^{hi}, and naïve cells as CD62L^{hi}, CD44^{low}. Data shown as mean ±SEM from mice of two independent experiments. **B**. Percentage of FoxP3 positive cells from CD4^{+} T cells in lungs with tumor from WT and p38αΔ^{Lys} mice. Data shown as mean ±SEM.

AMs from p38αΔ^{Lys} mice are transcriptionally different

The FACS analysis indicated that immune cell populations were not modified in terms of numbers in the p38αΔ^{Lys} animals. We next sought to determine whether p38α deletion induced gene expression changes in myeloid cells that could affect tumor formation and/or increase T cell effector activity. To this end, we performed a sc-RNA-Seq analysis of the total immune cell population of the lungs. We induced B16/F10 metastasis in WT and p38αΔ^{Lys} animals and then FACS-sorted the CD45^{+} cell fraction of the lungs from both tumor-free and tumor-bearing mice. To be able to observe early changes and to avoid gene expression differences potentially related to the differential tumour size, we did the analysis at an early stage of the lung metastasis growth (11 days after cell inoculation). The analysis allowed us to identify up to 16 different cell populations, including AMs, interstitial macrophages, type 1 neutrophils, type 2 neutrophils, monocytes, type 1 DC, type 2 DC, B cells, pro-B cells, γδ T cells,

NK cells, $CD4^+$ T cells, $CD8^+$ cells, T-regs and ILC2 (**Figure R6A**). As expected, we did not observe particular changes in cell populations, thereby confirming the results obtained by FACS analysis. However, in terms of transcriptional profile, AMs differed substantially between genotypes, both with and without tumors (**Figure R6B**). Gene expression analysis of the AM subpopulation confirmed these observations. We found that, in basal conditions, 432 genes were differentially expressed in $p38\alpha\Delta^{Lys}$ AMs compared with WT, while in tumor conditions, 417 genes changed between $p38\alpha\Delta^{Lys}$ and WT AMs. These observations suggest that most of the changes in gene expression induced by p38α deletion in AMs that affect tumor growth are already present in basal conditions. Of interest, no significant gene expression differences were observed in the lymphoid cell populations detected. Therefore, we focused on the sc-RNA-Seq analysis of the myeloid cell lineage.

Closer analysis by re-clustering the myeloid compartment confirmed that AMs were the cell population with major transcriptional profile changes in the $p38\alpha\Delta^{Lys}$ mice both in basal and tumor conditions (**Figure R6C**). Enhanced MKK6 expression is a known readout of p38α deletion in a variety of cells (Ambrosino et al., 2003). Feature plot representation of MKK6 expression in myeloid cells confirmed that AMs had a high expression of the gene compared to other myeloid cell populations, such as neutrophils, monocytes and eosinophils, thereby confirming effective p38α deletion in AMs (**Figure R6D**). Furthermore, AMs have been described as myeloid cells that express high levels of *LysM* gene (Abram et al., 2014; J. Shi et al., 2018). Also, previous observations from our lab using a Tomato-EGFP reporter $LysM^{Cre}$ mouse, whose cells switch from Tomato to EGFP expression when LysM is expressed, showed that AMs had around 95% expression of EGFP, followed by 83% in neutrophils, 45% in monocytes, 30% in DCs and 12% in eosinophils (Rivas et al., *unpublished*). These observations support the notion that these AMs are the population with the highest p38α deletion levels in the $p38\alpha\Delta^{Lys}$ mice and hence, they can therefore make an important contribution to the changes that lead to reduced lung metastasis.

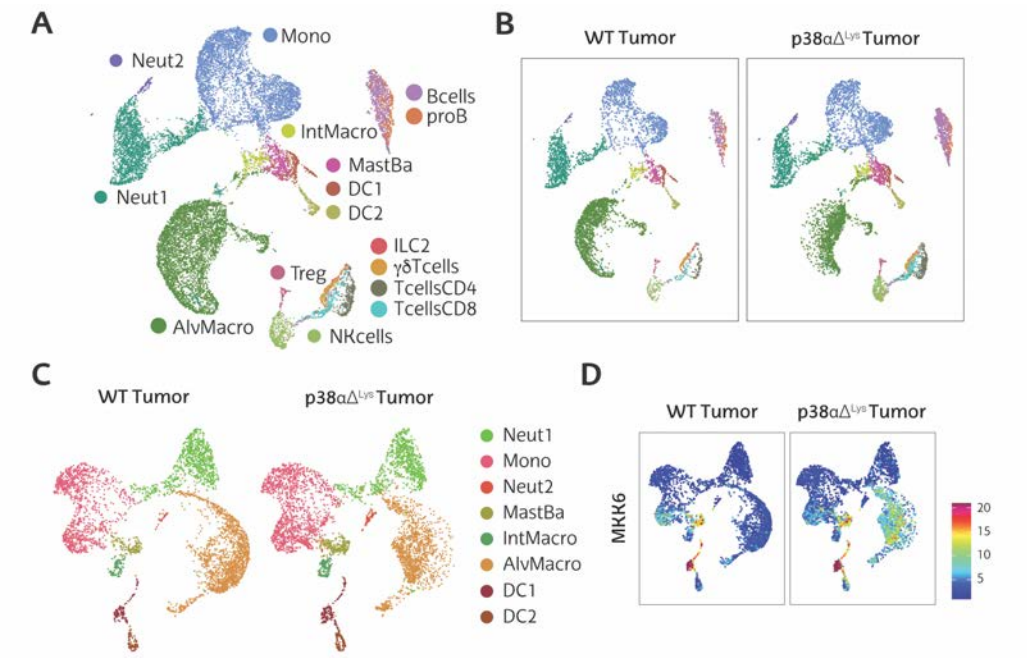

Figure R6. p38αΔ^{Lys} mice have changes in AM transcriptional profile.
A. Uniform Manifold Approximation and Projection (UMAP) plot representation of all immune cell population clusters in sc-RNA-Seq data analysis of CD45+ cells sorted from WT and p38αΔ^{Lys} mice with and without lung tumors. Mice with lung tumors were analysed 11 days post B16/F10 intravenous inoculation. Data shows Mono=monocytes, Neut=neutrophils, InMacro=interstitial macrophages, Bcells=B cells, proB=pro-B cells, MastBa=mast/basophil cells, DC=dendritic cells, AlvMacro=AMs, Treg=regulatory T cells, ILC2=innate lymphoid cells, gdTcells=gd T cells, NKcells=NK cells, TcellsCD4=CD4+ T cells, TcellsCD8= CD8+ T cells. **B**. UMAP plots comparing all WT and p38αΔLys immune cell populations in lungs with tumors. **C**. UMAP representation of myeloid cell population re-clustering comparing lungs with tumors from WT and p38αΔLys mice. Abbreviations defined in (A). **D**. Feature plot of myeloid cell populations showing MKK6 expression in WT versus p38αΔ^{Lys} mice with lung tumors. The intensity of expression is expressed by the colouring indicated in the legend.

Crucial AM functions are disrupted in the p38αΔ^{Lys} mice

AMs are tissue resident macrophages that are very abundant in the lungs. Our results from the sc-RNA-Seq suggested that p38α deletion induces transcriptional changes compared to the WT. Therefore, we decided to further explore the effects of p38α deletion specifically in AMs. To mitigate the dropout problem of the sc-RNA-Seq data and increase gene coverage, we performed a bulk RNA Sequencing (RNA-Seq) analysis of WT versus p38αΔ^{Lys}-derived AMs. We collected AMs from Bronchoalveolar Lavage (BAL) (**Figure R7A**) at 11 days after cell inoculation, thus replicating the same conditions used for the sc-RNA-Seq. FACS analysis confirmed that AMs accounted for >98% of the cells in BAL fluid both in basal and tumor conditions, demonstrating that

BAL extraction is a clean way of isolating AMs (**Figure R7B**). We used RT-qPCR to check that p38α was effectively deleted in these cells (**Figure R7C**).

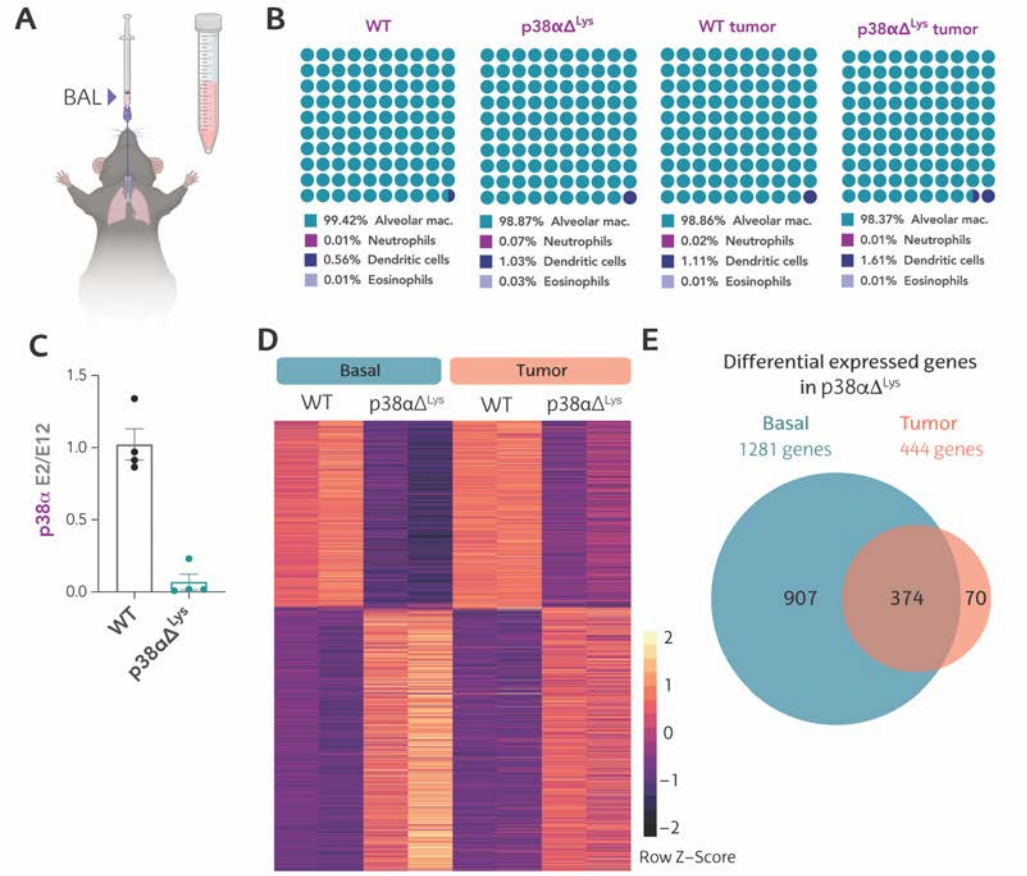

Figure R7. AMs from p38αΔ^{Lys} mice are transcriptionally different.
A. Procedure to perform a Bronchoalveolar lavage (BAL) extraction from mice to isolate AMs. **B**. 10x10 dot plot representing percentages of cell populations in BAL from WT and p38αΔ^{Lys} mice with and without lung tumors analysed by FACS. Mice with tumors were analysed 11 days post B16/F10 intravenous inoculation. Each cell type is coloured as shown in the legend. **C**. p38α mRNA analysis in WT and p38αΔ^{Lys} AMs extracted from BAL fluid. **D**. Heatmap representation of the differentially expressed genes across WT and p38αΔ^{Lys} AMs extracted from WT and p38αΔ^{Lys} mice with and without lung tumors. Each duplicate represents a pool of 2 mice. Represented genes passed the filtering of FC›1.5, and FDR‹0.05 (of p38αΔ^{Lys} relative to WT) and are ordered by FC in ascending order. Relative expression is represented by colour and indicated in the legend. **E**. Venn diagram indicating the overlap of genes differentially expressed in p38αΔ^{Lys} AMs in basal and tumor conditions compared to WT. Represented genes passed the filtering of FC›1.5, and FDR‹0.05 (of p38αΔ^{Lys} relative to WT).

Similar to what we observed in the sc-RNA-Seq experiment, RNA-Seq showed that AMs are highly different in terms of gene expression between genotypes (**Figure R7D**). Between WT and p38αΔ^{Lys} AMs, a total of 1281 genes changed in basal

conditions (fold change (FC)>1.5 and false discovery rate (FDR)<0.05). Of these genes, 740 were upregulated while 541 were downregulated. In AMs from lung tumors, we found a total of 444 genes were altered between WT and p38αΔ^{Lys}, 317 of them upregulated and 127 downregulated. The vast majority of the changes in gene expression observed in the p38αΔ^{Lys} mice with lung metastasis were also present in basal conditions (**Figure R7E**). Therefore, tumor formation did not greatly affect the gene expression of the AMs, as only 22 and 19 genes were found up- and downregulated, respectively, in AM from lung tumors compared with basal conditions in the WT and the p38αΔ^{Lys} mice. Moreover, most of these genes were melanocyte-related genes such as *SLC45A2*, *TYRP1* and *melan-A*, thereby suggesting the possible tumor cell phagocytosis by the AMs or the residual presence of B16/F10 cells in the BAL sample. In any case, the dramatic changes in gene expression observed in p38αΔ^{Lys} AMs highlight the importance of p38α in the homeostasis of this cell population, which can ultimately determine the growth of the lung tumor.

To study the functional implications of p38α deletion in AMs, we performed gene set enrichment analysis (GSEA). Curiously, the enriched gene sets in p38αΔ^{Lys} AMs were very similar between cells coming from lungs with and without tumors. Few changes were linked to the tumors in the p38αΔ^{Lys} AMs. These comprised mainly a decrease gene ontology (GO) of complement factors and pyrimidine metabolism, and an increase in the Wnt signalling pathway (**Figure R8A**). The most relevant GO terms with possible implications for tumor formation and lung immunity were found enriched in p38αΔ^{Lys} AMs of both basal and tumor conditions. Amongst these, we identified the enrichment of GO terms associated with antigen presentation via the major histocompatibility complex II (MHCII) as one of the main upregulated pathways. We also found a decrease in phagocytosis and pattern recognition, and a reduction in cholesterol and lipid storage. Further analysis of the functional implications of the dysregulation of these pathways in p38αΔ^{Lys} AMs is described below. Additionally, HDAC activity was also found upregulated in p38αΔ^{Lys} AMs, thereby pointing to the increase in general chromatin acetylation as a possible mechanism that affects gene expression in p38αΔ^{Lys} AMs (**Figure R8B**).

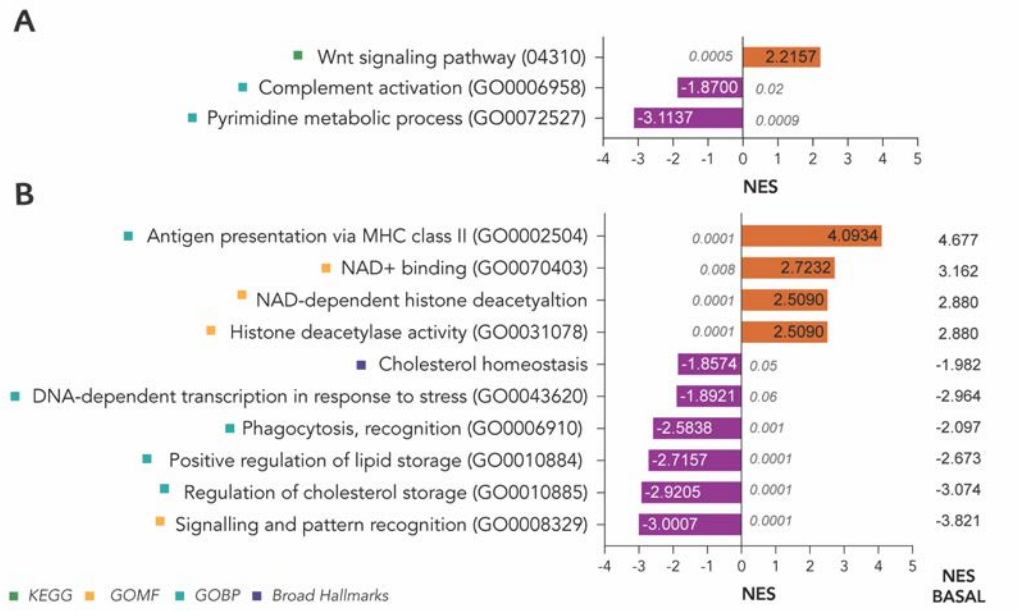

FIGURE R8. Crucial AM functions are potentially affected in p38αΔ^{Lys} mice.
A. Gene Set Enrichment Analysis (GSEA) of the RNA-Seq analysis in AMs, showing selected Gene Ontology (GO) terms that are enriched only in AMs of p38αΔ^{Lys} lungs with tumors versus all other conditions. pval of the selected GO terms is depicted next to each bar. **B**. GSEA analysis of the RNA-Seq analysis showing selected GO terms commonly enriched in p38αΔ^{Lys} AMs in basal and tumor conditions. Normalized Enrichment Score (NES) value represented in graph bars is from comparison of AMs from p38αΔLys vs WT in tumor conditions. NES of comparison between p38αΔ^{Lys} vs WT in basal conditions is shown at the right of the bars. pval of each depicted GO terms is indicated next to each bar. Different GO groups are depicted in the colours indicated in the legend.

Antigen presentation is a crucial process by which professional APCs can activate the adaptive immunity. The enhanced antigen presentation via MHCII observed in p38αΔ^{Lys} AMs could explain the increase in effector CD4^{+} T cells that we observed by FACS analysis. Specifically, a considerable number of genes involved in antigen presentation, such as subunits of the MHCII like *H2-Eb1*, *H2-Aa*, *H2-Ab* or *CD74*, amongst others, were highly upregulated in p38αΔ^{Lys} AMs (**Figure R9A, Supplementary Table 1**). The co-stimulatory molecule *CD80* was also upregulated in tumor conditions together with a downregulation of the checkpoint inhibitor *CD274* (PD-L1) in both basal and tumor conditions, thereby pointing at a higher capacity of these cells to activate the adaptive immune response. Feature plots of some of these genes in the AM population from the sc-RNA-Seq confirmed their dysregulation (**Figure R10**). On the other hand, we found decreased pattern recognition and phagocytosis in the p38αΔ^{Lys}. These observations would suggest an impaired capacity of these cells to recognise and phagocytose external particles, both crucial functions of AMs. The expression of macrophage scavenger receptors like *CD68*, *FABP4*, *CD36*

and *MARCO* were found to be downregulated in p38αΔ^{Lys} AMs, together with other genes involved in pattern recognition such as *TLR7, Clec7a* and *Colec12* and genes of the complement system like *C5ar*, *C1qa* and *C1qc* (**Figure R9B-C, Supplementary Table 2**). Feature plots of some of these genes illustrate their dysregulation also in the AM population predicted in the sc-RNA-Seq analysis, further confirming the results (**Figure R10**).

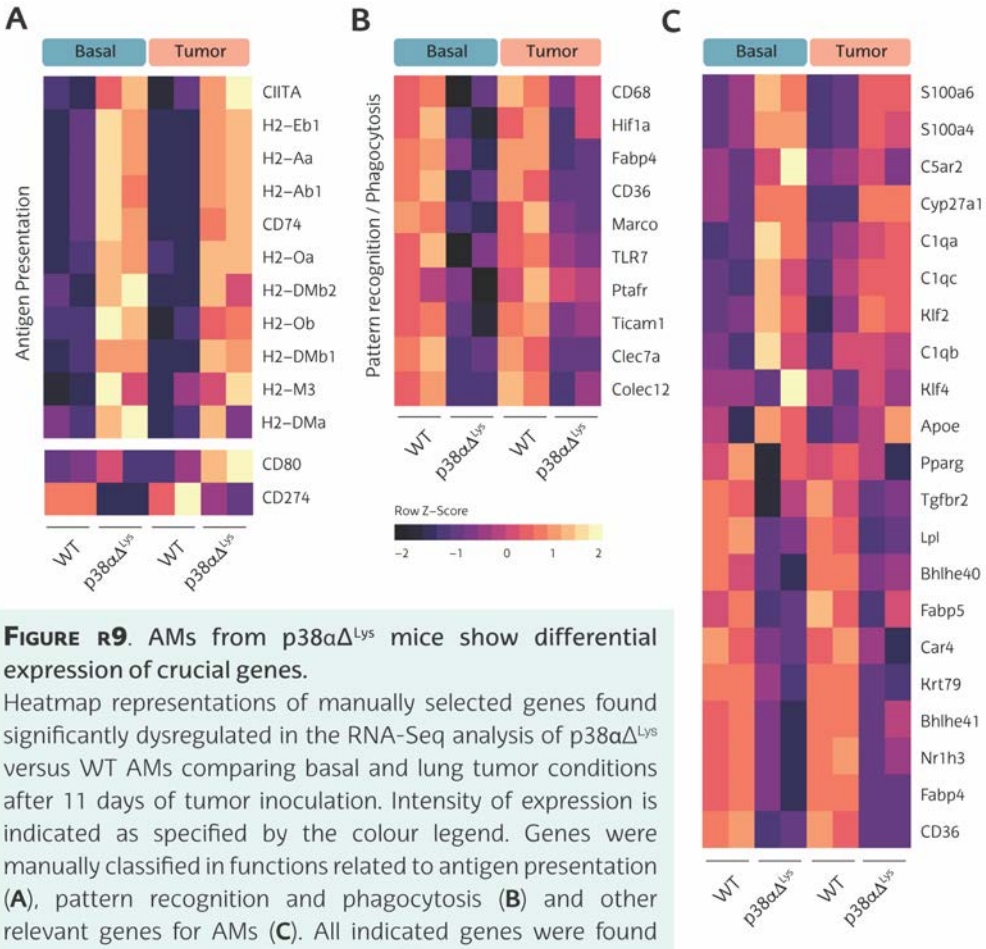

FIGURE R9. AMs from p38αΔ^{Lys} mice show differential expression of crucial genes.
Heatmap representations of manually selected genes found significantly dysregulated in the RNA-Seq analysis of p38αΔ^{Lys} versus WT AMs comparing basal and lung tumor conditions after 11 days of tumor inoculation. Intensity of expression is indicated as specified by the colour legend. Genes were manually classified in functions related to antigen presentation (**A**), pattern recognition and phagocytosis (**B**) and other relevant genes for AMs (**C**). All indicated genes were found significant by pval > 0.05. The pval and FC of the top 100 up- and downregulated genes is shown in Supplementary Tables 1-2.

Cholesterol metabolism is a crucial process in AMs to keep the airways clean of surfactant (Hawgood & Poulain, 2001). The reduction of cholesterol and lipid storage pathways in p38αΔ^{Lys} AMs pointed to a general decreased capacity to metabolize cholesterol and lipids, which is probably relevant since AMs rely mainly on lipid oxidation as their energy source. Cholesterol and lipid metabolism are regulated by PPARγ signalling in AMs. This receptor has been described as a key transcription

factor in the regulation of important processes in AMs (A. D. Baker, Malur, Barna, Kavuru, et al., 2010). Although the decrease in *PPARγ* of p38αΔ^{Lys} AMs was not significant in the RNA-Seq results and rather small in the sc-RNA-Seq data, we detected changes in known PPARγ transcriptional targets in p38αΔ^{Lys} AMs such as the increase in *Lpl*, *CD36*, *Cyp27a1*, *ApoE* and the decrease in *NR1H3* (**Figure R9C** and **R10**). These findings suggested that p38αΔ^{Lys} AMs show dysregulated PPARγ signalling, which can affect some of their crucial functions. Furthermore, we observed that transcription factors described to be important for AM identity and self-maintenance such as *Car4*, *Bhlhe40*, *Bhlh41*, *Krt79*, *Fabp4*, *Klf2* and *Klf4,* were highly downregulated in the p38αΔ^{Lys} AMs. Interestingly, the CD200-CD200R axis, which is key for maintaining the immune-suppressive functions of AMs, was also downregulated in the p38αΔ^{Lys} AMs (**Figure R10**).

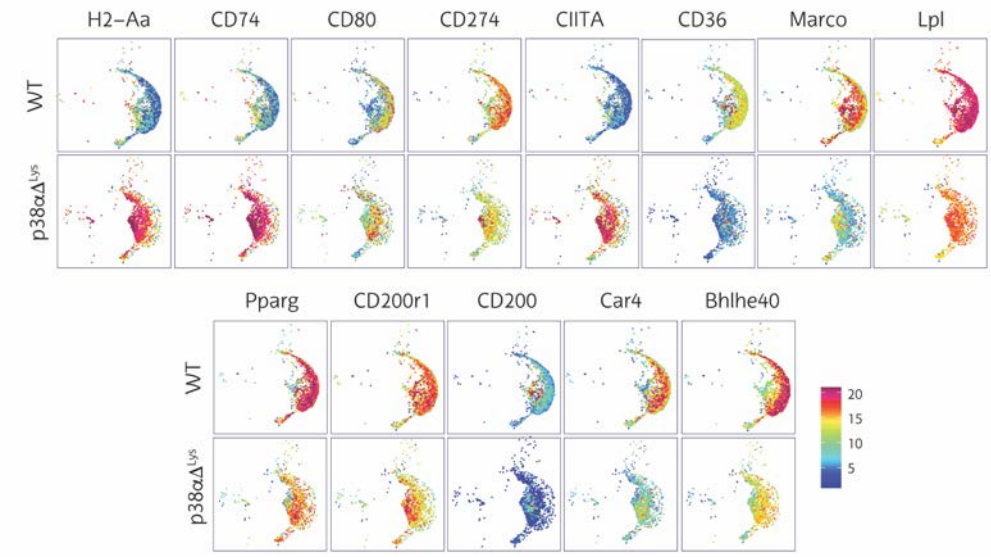

Figure R10. sc-RNA-Seq analysis of the AM sub-cluster confirms gene expression changes found in the RNA-Seq.
Feature plots of representative genes involved in antigen presentation, phagocytosis, pattern recognition and other genes in p38αΔ^{Lys} versus WT AM cell population defined by sc-RNA-Seq analysis. Intensity of expression is indicated in the colour legend.

AMs are highly involved in the regulation of lung homeostasis by maintaining a certain level of immune suppression and tolerance. Our results indicate that p38α controls several crucial functions of AMs already in tumor-free lungs. The deletion of p38α in AMs promotes changes in basal conditions that can ultimately affect tumor formation in the lungs and probably also influence the outcome of other inflammatory conditions. Amongst the changes that can affect tumor growth, the increase in antigen

presentation via MHCII could be responsible for the reduced tumor formation and thus deserves further study.

p38αΔ^{Lys} AMs have increased antigen presentation capacity

Validation by RT-qPCR of several genes found in the RNA-Seq confirmed the upregulation of *S100A6* and the downregulation of *Colec12*, *MARCO*, *CD36*, *FABP4* and *CD200* (**Figure R11**). These genes are related to the capacity of macrophages to recognise foreign particles and some of them are also involved in phagocytosis. However, antigen processing and presentation through MHCII was the highest enriched GO term in the p38αΔ^{Lys} AMs. RT-qPCR validation confirmed that AMs from p38αΔ^{Lys} mice expressed higher levels of the MHCII subunits *H2-Aa*, *H2-Ab*, *H2-Eb*, *CD74* (**Figure R11**). We also confirmed the upregulation of *OX40L*, a known co-stimulatory molecule expressed by APCs to activate CD4^{+} T cells.

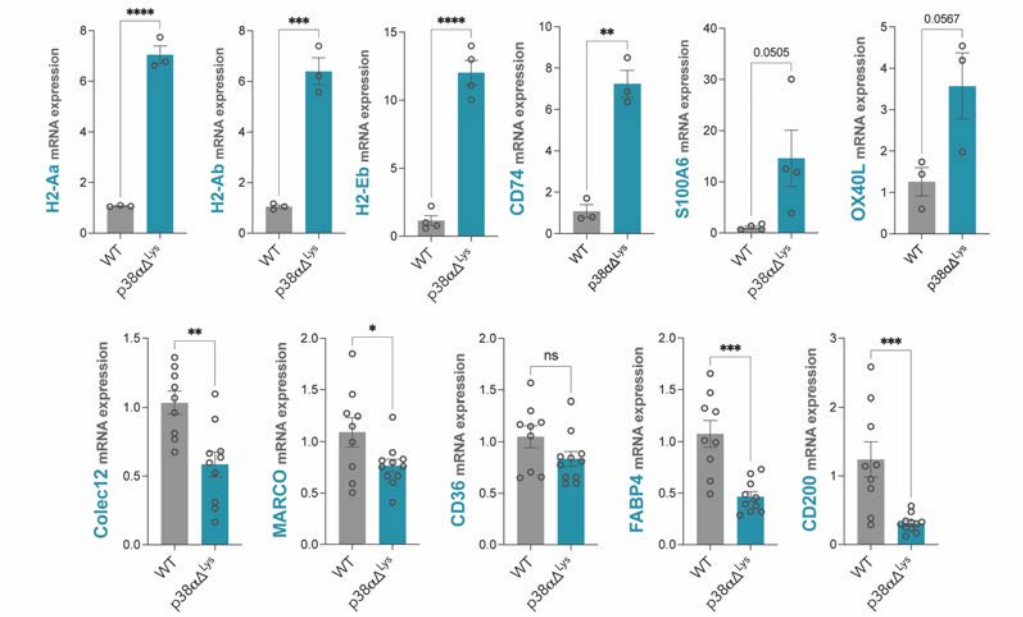

Figure R11. AMs from p38αΔ^{Lys} mice have an increase in MHCII gene expression.
RT-qPCR analysis in isolated AMs from WT and p38αΔ^{Lys} mice in basal conditions of some representative genes found upregulated (above) and downregulated (below) in the RNA-Seq analysis. Data shown as mean ±SEM.

To obtain evidence that p38αΔ^{Lys} AMs have an increased capacity for antigen presentation and the activation of CD4^{+} T cells, we used the Ovalbumin (OVA)-OT-II system, which is based on the specificity of the MHCII-CD4 T-cell receptor (TCR) synapse. OT-II are genetically modified mice so that the TCR of all their CD4^{+} T cells is unique for the OVA antigen (Barnden et al., 1998). Therefore, CD4^{+} T cells from

these animals will become activated and proliferate only if they are presented the OVA antigen in a MHCII molecule. For these assay, AMs from WT and p38αΔ^{Lys} animals were extracted from BAL fluid and loaded with OVA overnight with or without LPS stimulation. Violet-tracker-labelled CD4^{+} T cells were isolated from OT-II mice and were added to the AM cultures. After 7 days, T cell proliferation was measured by FACS (**Figure R12A**). The results showed that CD4^{+} T cells that were co-cultured with p38αΔ^{Lys} AMs or incubated with WT AMs in the presence of a p38α inhibitor showed increased proliferation (**Figure R12B**). Moreover, expression of activation markers like CD25 or, to a lesser extent, of CD69 were increased in CD4^{+} T cells co-cultured with p38αΔ^{Lys} AMs (**Figure R12C**). These results suggest that the observed increase in effector CD4^{+} T cells in lungs of p38αΔ^{Lys} animals could be due to the increased expression of MHCII in these AMs. Therefore, we decided to further study the molecular mechanisms by which p38α regulates antigen presentation.

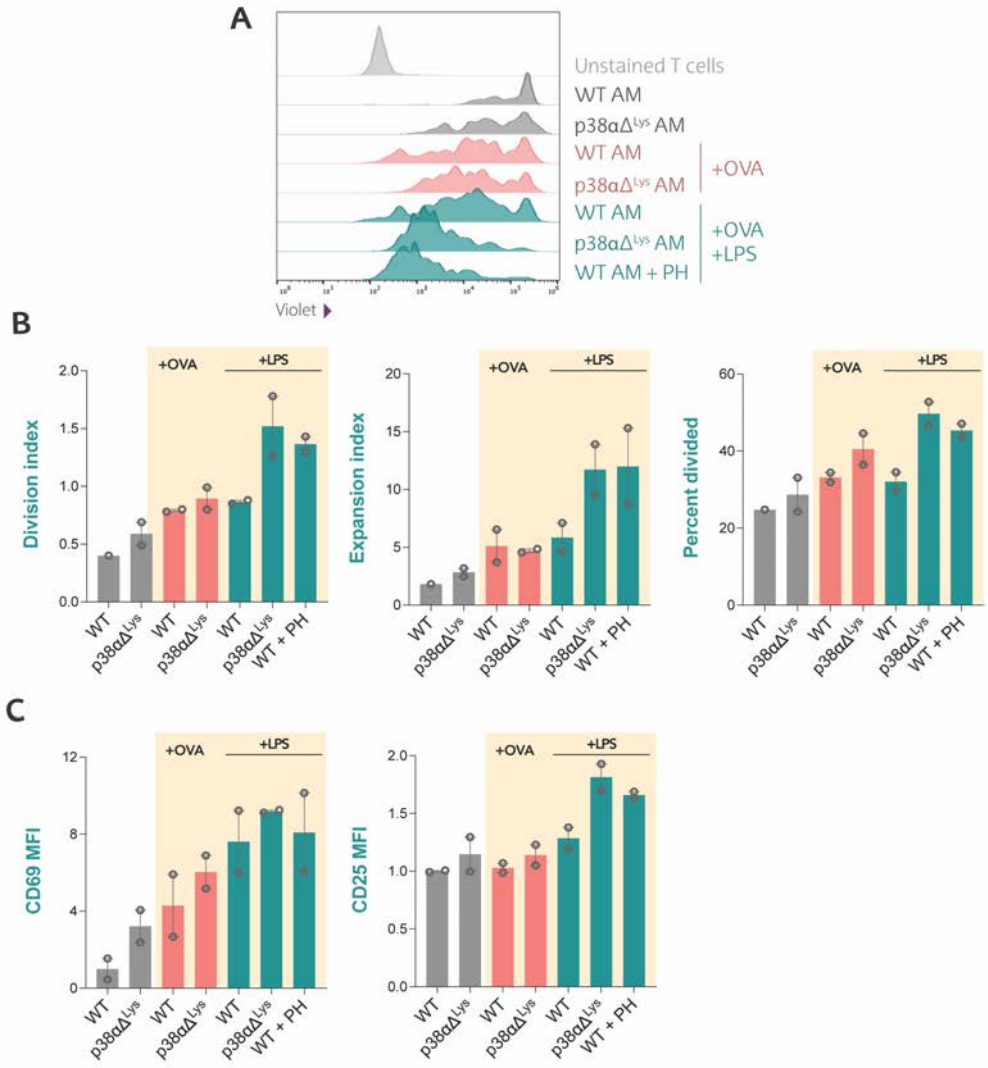

Figure R12. p38α-deficient AMs show an enhanced capacity to activate the adaptive immune response.
A. Representative FACS plots of Violet fluorescent CD4+ T cells extracted from OT-II TCR mice co-cultured for 7 days with AMs from p38αΔ^{Lys} and WT mice with or without the addition of the p38α inhibitor PH797804 (PH). AMs were pre-incubated overnight with OVA or LPS+OVA prior to the addition of the CD4+ T cells. **B.** Quantification of cell proliferation indexes of CD4+ T cells co-cultured with AMs from p38αΔ^{Lys} and WT mice with or without the addition of the p38α inhibitor PH pre-stimulated with OVA, OVA+LPS or not stimulated. **C.** Mean fluorescence intensity (MFI) quantification of T cell activation markers in CD4+ T cells from the co-cultures in (**B**).

We confirmed that increased MHCII mRNA levels translated into a higher expression of MHCII at the membrane of p38αΔ^{Lys} AMs. FACS analysis of lungs confirmed that MHCII levels were highly upregulated in the p38αΔ^{Lys} AMs both in basal conditions and in lungs with tumors (**Figure R13A**). Given that AMs are highly regulated by factors produced in their niche, we questioned whether some factors from the alveolar niche could trigger the p38α-mediated down-regulation of MHCII. To this end, we analysed MHCII expression in another type of tissue-resident macrophage, namely peritoneal macrophages. These cells are found in the specialized niche of the peritoneal cavity, and had an effective deletion of p38α in the p38αΔ^{Lys} model (**Figure R1B**). However, FACS analysis of both WT and p38αΔ^{Lys} peritoneal macrophages showed similarly high levels of MHCII expression (**Figure R13B**). This observation indicates that the negative regulation of MHCII by p38α is restricted to the alveolar space and is probably niche-specific.

To determine whether the inhibition of p38α would suffice to increase MHCII expression in AMs *in vivo*, we treated WT mice for 2 weeks with the p38α inhibitor LY-2228820. We confirmed that the LY treatment increased MHCII expression levels in AMs compared to the mice treated with vehicle (**Figure R14A**). The treatment with LY also decreased the B16/F10 lung tumor burden in the animals (**Figure R14B**), suggesting that the pharmacological inhibition of p38α could reduce lung metastasis and that this effect could be mediated by the p38α regulation of MHCII in AMs.

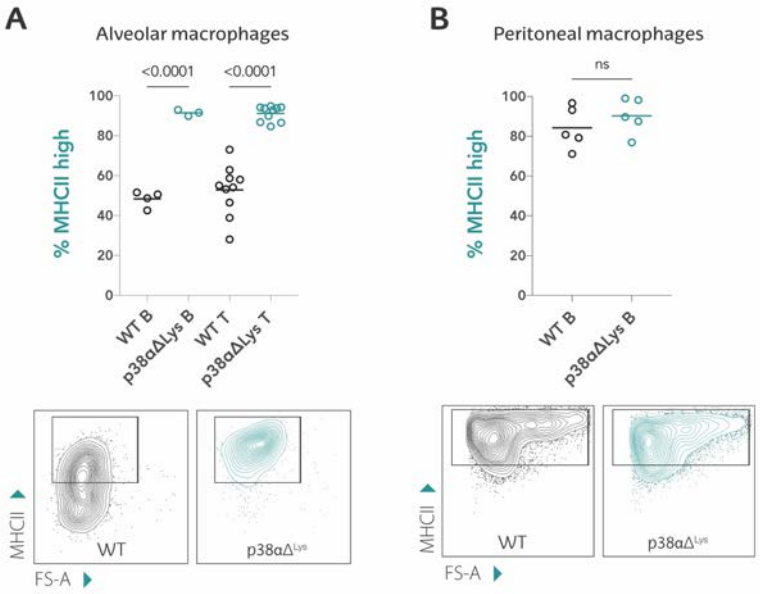

Figure R13. MHCII upregulation in alveolar but not peritoneal macrophages from p38αΔLys mice.

A. FACS analysis of MHCII expression in alveolar macrophages from WT and p38αΔ^{Lys} mice in basal (B) and lung tumor conditions (T) (top) and representative FACS gating plot of MHCII and Forward-Scatter (FS-A) (bottom). **B**. FACS analysis of MHCII expression in peritoneal macrophages from WT and p38αΔ^{Lys} mice in basal conditions (B) (top) and representative FACS gating plot (bottom).

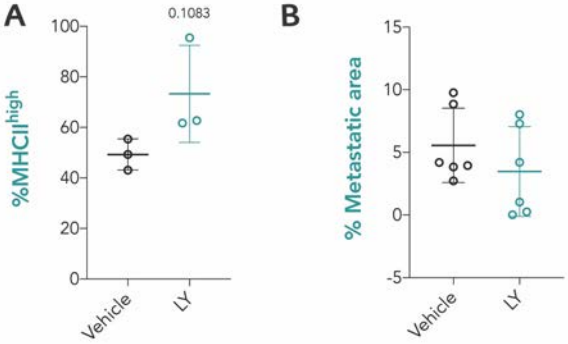

Figure R14. Pharmacological inhibition of p38α increases MHCII expression in AMs.

A. FACS analysis quantification of MHCII expression in AMs from mice treated by oral gavage for 15 days with vehicle or the p38α inhibitor LY2228820 (LY). **B**. Lung metastasis burden at day 21 after intravenous B16/F10 cell inoculation. Animals were treated for 15 days with LY starting at day 5 after tumor cell inoculation. Data shown as mean ±SD.

p38α-inhibited BMDMs upregulate MHCII

As p38α deletion in AMs increased antigen presentation mediated by MHCII, we studied the molecular mechanisms of MHCII regulation by p38α. Although AMs can be cultured *in vitro*, their numbers are limiting, thus we set up a model using bone marrow-derived macrophages (BMDMs). We used BMDMs from WT and p38αΔ^{Lys} mice and WT BMDMs pre-treated with p38α inhibitor PH. After 20-24h of LPS stimulation to activate the macrophages, we checked the membrane expression of MHCII by FACS analysis. In the absence of LPS, we observed no differences in MHCII expression between WT and p38αΔ^{Lys}-derived BMDMs or those treated with PH. LPS stimulation alone did not induce MHCII expression either. However, macrophages pre-treated with PH and stimulated with LPS showed a significant upregulation of MHCII (**Figure R15A**), suggesting that p38α regulates MHCII expression in BMDMs. To confirm the inhibition of the p38α pathway, we performed western blot of MK2, a main substrate of p38α. The addition of PH abolished the phosphorylation of MK2, confirming the inhibition of the p38α pathway (**Figure R15B**). However, in p38αΔ^{Lys}-derived BMDMs, although mRNA levels of p38α were reduced (Figure R13C), western blot revealed some p38α protein remaining, which was able to phosphorylate MK2 upon LPS treatment. These results indicated that BMDMs derived from p38αΔ^{Lys} animals did not induce the complete deletion of p38α so these cells were not a suitable system in which to study MHCII regulation. Furthermore, we treated the BMDMs from WT animals with another inhibitor of p38α, LY-2228820, and two different PROTACs, NR-7h and NR-11c, which induce p38α degradation (Donoghue et al. 2020, Cubillos-Rojas et al., *in preparation*). In all cases, p38α inhibition led to increased MHCII expression in BMDMs (**Figure R15D**). Additionally, FACS analysis of MHC class I (MHCI) showed no differences in BMDMs upon p38α inhibition, thereby indicating that p38α specifically regulates MHCII expression only (**Figure R15E**). These results indicate that BMDMs are a good model in which study the regulation of MHCII by p38α.

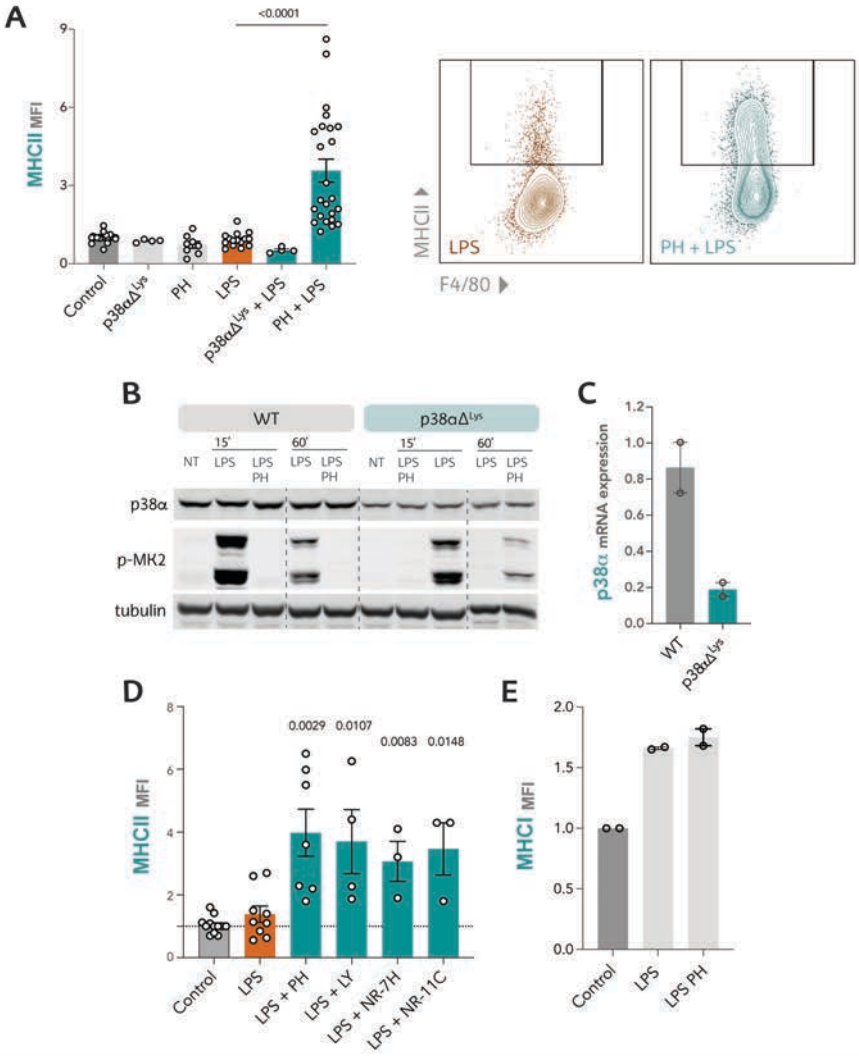

Figure R15. Inhibition of p38α in BMDMs upregulates MHCII.

A. Mean fluorescence intensity (MFI) quantification of MHCII expression in BMDMs from WT or p38 αΔ^{Lys} mice after 24 h of treatment with LPS and with or without pre-treatment of p38α inhibitor PH797804 (PH) (left), and representative FACS plot of MHCII/F4-80 expression in the indicated samples (right). **B**. Western blot of p38α and the phosphorylation of its substrate MK2 in WT and p38αΔ^{Lys}-derived BMDMs stimulated with LPS for the indicated times and with or without PH. C. RT-qPCR of p38α mRNA in WT and p38αΔ^{Lys}-derived BMDM. **D.** MFI quantification of BMDMs cultured for 24 h with LPS in the presence of the p38α inhibitors PH or LY2228820 (LY) and the Protacs Nr-7h or NR-11c. p-val of t-student test against LPS condition is shown at the top of each bar. **E**. MFI quantification of MHCI expression in BMDMs after 24 h of LPS stimulation with or without PH.

LPS and TNFα increase MHCII expression in p38α-inhibited BMDMs

AMs are exposed to many different signals in the alveolar niche and these help to keep their tolerogenic state (Aegerter et al., 2022; Lavin et al., 2014). Amongst them, GM-CSF, together with TGFβ, is a main factor that maintains AM function and fitness. To test whether factors from the alveolar niche could be triggering p38α downregulation of MHCII, we treated BMDMs with recombinant cytokines and tested MHCII expression upon the inhibition of p38α. We included classical pro- and anti-inflammatory factors such as TNFα, IL10 and IL4. FACS analysis of MHCII after 24 h of cytokine treatment showed that only LPS and to a less extent, TNFα, increased MHCII when p38α was inhibited, while the rest of the cytokines and factors had little or no effect (**Figure R16A**).

LPS is a pro-inflammatory molecule found in the cell wall of gram-negative bacteria and it is used extensively to polarize macrophages to a classical inflammatory phenotype. LPS activates the p38α pathway in macrophages (Bode et al., 2012). Since lungs have commensal microbiota mainly composed of gram-negative bacteria (Yun et al., 2014), and the MHCII upregulation in p38α-inhibited BMDMs is dependent on LPS stimulation, we hypothesized that LPS from commensal bacteria could be involved in the regulation of MHCII in AMs *in vivo*. To test this notion, we treated WT and p38αΔ^{Lys} animals with Ceftriaxone (Cef), an antibiotic that depletes lung gram-negative bacteria (Dickson et al., 2018), and studied how this treatment affected MHCII levels in AMs. After 7 days of antibiotic treatment, we observed no differences in MCHII expression of AMs either from WT or p38αΔ^{Lys} animals compared to saline-treated animals (**Figure R16B**). RT-qPCR revealed a slight decrease in 16S bacterial RNA in the lungs of Cef-treated animals, thus supporting the effectivity of the treatment (**Figure R16C**). These results suggest that alternative factors probably activate p38α to keep low levels of MHCII expression in AMs *in vivo*.

Along this line, we questioned whether the p38α signalling that downregulated MHCII expression was dependent on some alveolar niche factor. We extracted AMs from BAL fluid and cultured them *ex-vivo* for different times (**Figure R16D**) in the absence of any niche factors, as for example GM-CSF signalling has been shown to affect MHCII levels. Surprisingly, we observed that MHCII expression levels were maintained constant for up to 8 days both in the p38αΔ^{Lys} and in WT AMs (**Figure R16E**). This result suggests that the regulation of MHCII by p38α is controlled in a cell-autonomous manner, and that it probably involves some kind of epigenetic memory.

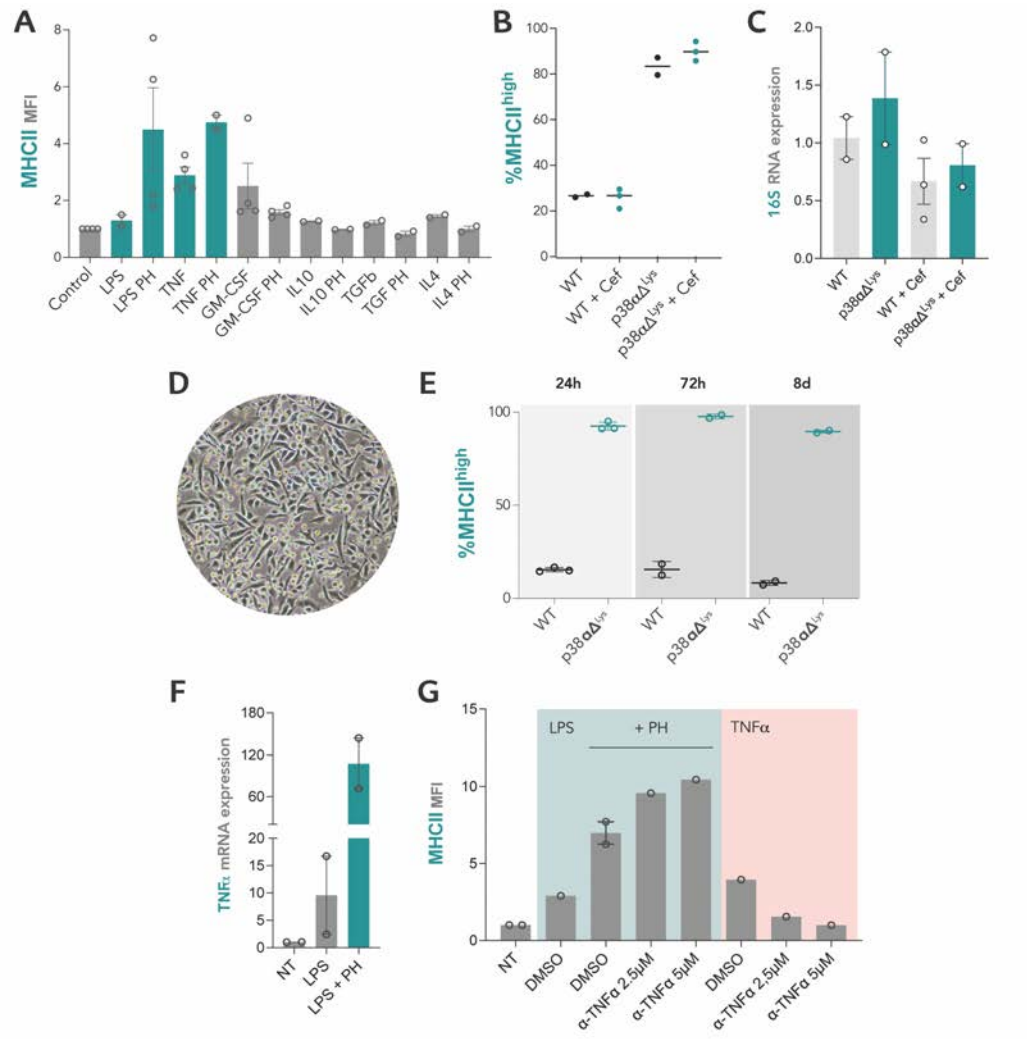

Figure R16. p38α-negatively regulates MHCII induced by LPS and TNFα in BMDMs.
A. MFI of MHCII expression in BMDMs stimulated for 24 h with the indicated cytokines and factors, and with or without p38α inhibition using PH797804 (PH). **B**. Percentage of MHCII+ AMs from lungs of WT and p38αΔ^{Lys} animals that received the antibiotic Ceftriaxone (Cef) for 7 days. **C**. RT-qPCR of bacterial 16S gene in whole lung lysates from WT and p38αΔ^{Lys} animals that received Cef for 7 days. **D.** Representative image of AMs after 5 days in culture. **E**. Analysis of MHCII expression in WT and p38αΔ^{Lys} AMs cultured for 24 h, 72 h and 8 days. **F**. RT-qPCR of TNFα expression in BMDMs treated for 24 h with LPS and with or without PH. **G**. MFI of MHCII expression in BMDMs pre-treated for 2 hours with anti-TNFα neutralizing antibody or DMSO and with or without PH and then stimulated with LPS (blue area) or TNFα (pink area) for 24 hours. Different concentrations of the anti-TNFα antibody were used and are shown under the bars. Data shown as mean ±SEM.

TNFα upregulated MHCII in BMDMs, and this process partially involved p38α (**Figure R14A**), and we observed that TNFα mRNA levels were highly upregulated in p38α-

inhibited BMDMs stimulated with LPS for 16 h (**Figure R16F**). Thus, we wondered whether a TNFα-autocrine feedback loop could be responsible for the upregulation of MCHII. We observed that the TNFα-induced increase in MHCII was strongly reduced by incubation with a TNFα neutralizing antibody, thereby proving that the neutralizing antibody works. However, the TNFα antibody did not abolish the MHCII upregulation observed in p38α-inhibited BMDMs stimulated with LPS; if anything, it had a slight additive effect (**Figure R16G**). This result rules out TNFα as being responsible for the upregulation of MHCII in p38α-inhibited BMDMs stimulated with LPS.

p38α regulates MHCII through the transcription activator CIITA

Next, we analysed the kinetics of MHCII mRNA upregulation in BMDMs treated with PH. We found that these cells overexpressed MHCII subunits *H2-Aa*, *H2-Ab* and *H2-Eb* at 14 and 18 h after LPS treatment (**Figure R17**). This finding confirms that MHCII upregulation is due to increased mRNA levels of MHCII both in p38αΔ^{Lys} AMs and in p38α-inhibited BMDMs.

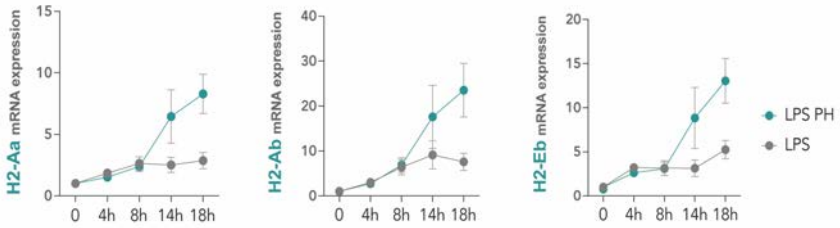

Figure R17. p38α inhibition increases in MHCII mRNA levels in macrophages.
RT-qPCR analysis of the different MHCII subunits in BMDMs pre-treated with or without the p38α inhibitor PH797804 (PH) for 2 hours and stimulated with LPS for the indicated times. Data represented as mean ±SEM.

Results from RNA-Seq in AMs showed considerable upregulation not only of the MHCII complex machinery, but also of Class II transcriptional activator (CIITA), a crucial transcriptional regulator of MHCII. In basal lungs and in lungs with tumors, *CIITA* was amongst the main hits in the RNA-Seq results (shrinked FC=7.93 adjusted pval=2.21×10^{-11}) (**Figure R9A**). Validation by RT-qPCR of total *CIITA* mRNA levels in AMs from p38αΔ^{Lys} mice confirmed the RNA-Seq results (**Figure R18A**). Furthermore, p38αΔ^{Lys} AMs expressed very high levels of three different transcripts of *CIITA*, namely *pI*, *pIII* and *pIV* (**Figure R18A**), thereby supporting the notion that p38α probably regulates MHCII through the regulation of *CIITA* transcription. Next, we performed

RT-qPCR on PH-treated BMDMs stimulated with LPS at different time points, and observed the upregulation of total *CIITA* mRNA as well as the transcripts *pIII* and *pIV* (**Figure R18B**). Similarly, TNFα stimulation induced the upregulation of *CIITA* transcripts *pIII* and *pIV* (**Figure R18C**). These results indicate that the increased MHCII in p38α-inhibited cells is probably due to increased MHCII transcription mediated by the upregulation of CIITA both in AMs and BMDMs.

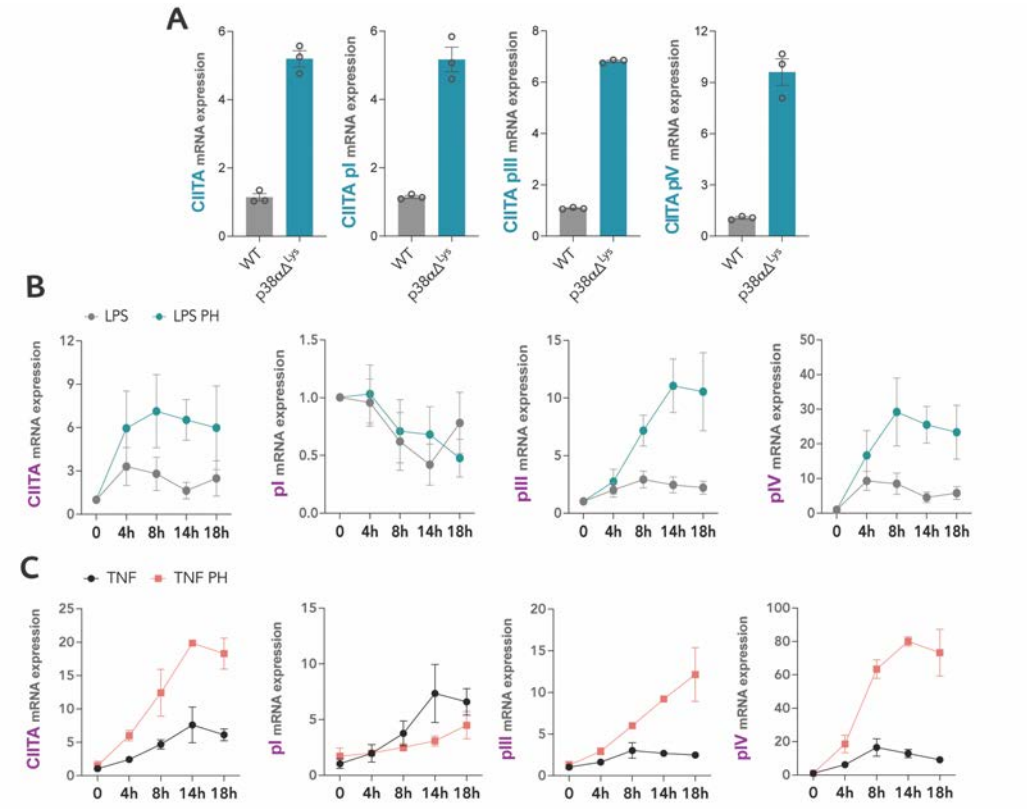

Figure R18. p38α inhibition increases CIITA mRNA levels in macrophages.
A. RT-qPCR analysis of total CIITA and different CIITA transcripts in AMs isolated from BAL of WT and p38αΔ^{Lys} mice in basal conditions. **B-C**. RT-qPCR analysis of total CIITA and different CIITA transcripts in BMDMs pre-incubated for 2 hours with or without the p38α inhibitor PH797804 (PH) and stimulated for the indicated times with LPS (**C**) and TNFα (**D**). Data represented as mean ±SEM.

Next, we studied the possibility that p38α could control CIITA expression by regulating *CIITA* mRNA stability, a role that has been reported for p38α (Canovas & Nebreda, 2021). We treated BMDMs with LPS for 16 h and then added Actinomycin D (ActD) to stop transcription. At 30 min, 90 min and 4 h after ActD treatment *CIITA* mRNA levels were analysed by RT-qPCR. The results indicated that p38α inhibition did not increase *CIITA* mRNA stability (**Figure R19A**). We also analysed the levels of

CIITA pre-mRNA using primers designed in the intronic regions of the gene to detect mRNA that had not undergone splicing yet (Zeisel et al., 2013). We observed a clear increase in *CIITA* pre-mRNA levels upon p38α inhibition of LPS-stimulated BMDMs (**Figure R19B**). This observation further supports the notion that p38α regulates the transcription of *CIITA*.

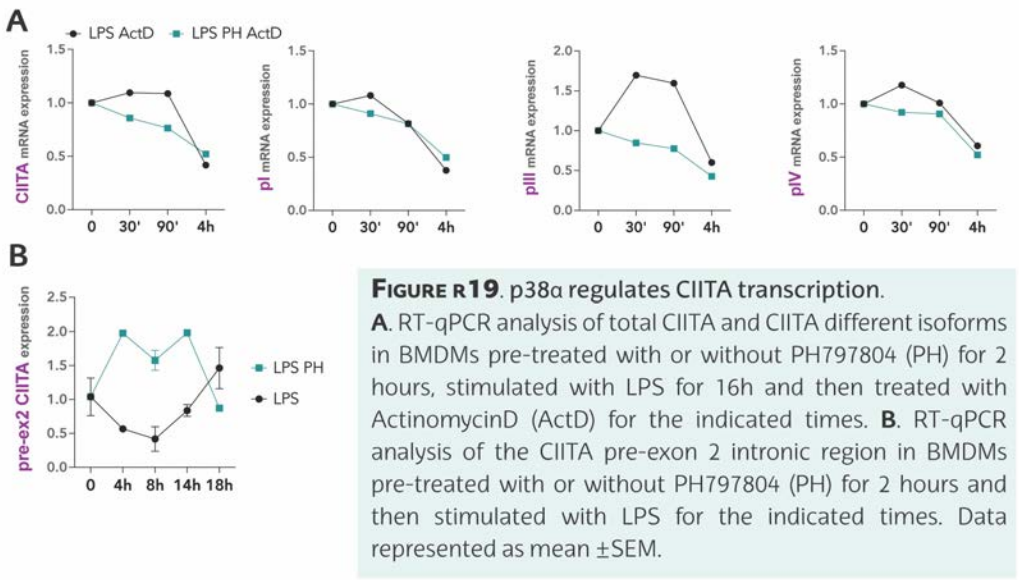

Figure R19. p38α regulates CIITA transcription.
A. RT-qPCR analysis of total CIITA and CIITA different isoforms in BMDMs pre-treated with or without PH797804 (PH) for 2 hours, stimulated with LPS for 16h and then treated with ActinomycinD (ActD) for the indicated times. **B**. RT-qPCR analysis of the CIITA pre-exon 2 intronic region in BMDMs pre-treated with or without PH797804 (PH) for 2 hours and then stimulated with LPS for the indicated times. Data represented as mean ±SEM.

STAT1 is not involved in p38α regulation of CIITA

CIITA transcription is known to be regulated by IFNγ signalling. Although results from RNA-Seq analysis showed no significant enrichment in the IFNγ response, we studied whether IFNγ signalling could be involved in p38α regulation of CIITA.

First, we observed that MHCII induction by IFNγ was not affected when p38α was inhibited in BMDMs (**Figure R20A**). Next, we addressed whether p38α could regulate STAT1, one of the main targets of IFNγ-signalling whose phosphorylation-dependent dimerization is known to activate CIITA transcription. We observed that IFNγ treatment did not induce MHCII upregulation in BMDMs derived from STAT1 KO mice, thereby confirming that IFNγ requires STAT1 to induce CIITA and consequently MHCII expression. However, STAT1-KO BMDMs treated with a p38α inhibitor showed an increase in MHCII when stimulated with LPS (**Figure R20B**). Moreover, AMs from STAT1-KO mice had similar levels of MHCII as their WT littermates (**Figure R20C**). Taken together, these observations indicate that p38α regulation of CIITA does not involve IFNγ signalling.

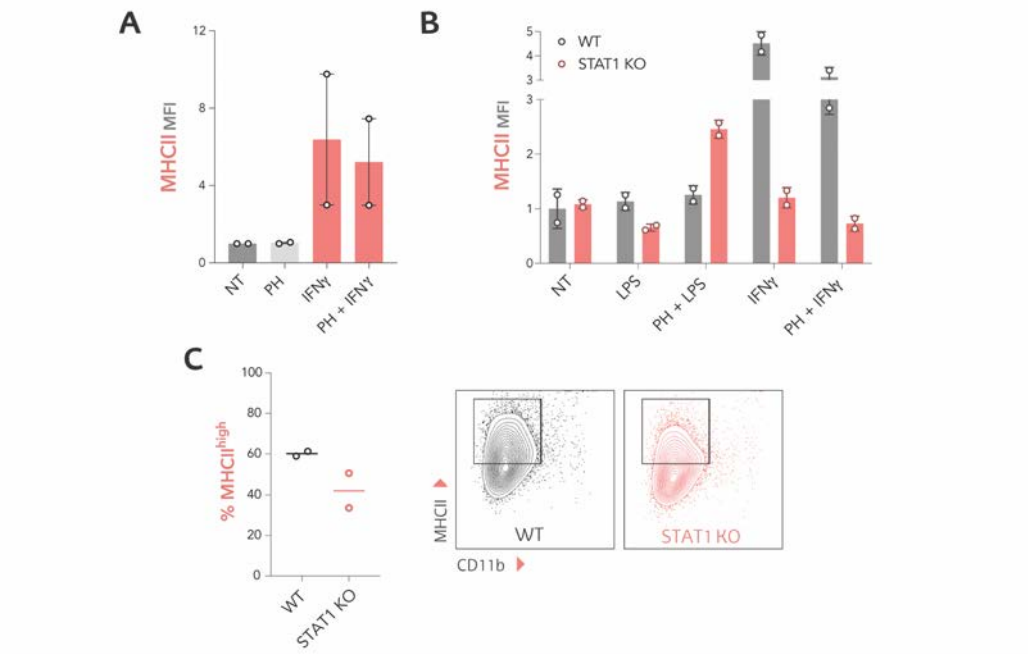

Figure R20. STAT1 is not involved in MHCII regulation by p38α.
A. MFI of MHCII expression in FACS analysis of WT BMDMs pre-treated for 2 h with or without the p38α inhibitor PH797804 (PH) and then stimulated with IFNγ for 24 h. NT=non treated control. **B**. MFI of MHCII expression in FACS analysis of BMDMs derived from STAT1 KO and WT littermates pre-treated with or without the p38α inhibitor PH797804 (PH) for 2 hours and stimulated with LPS or IFNγ for 24 h. NT=non treated control. **C.** Percentage of MHCII^{hi} AMs in lungs from STAT1 KO and WT animals analysed by FACS (left) and representative FACS gate plot of MHCII and CD11b expression (right).

p38α regulates CIITA through MK2

Next, we studied the p38α downstream signals that negatively regulate CIITA/MHCII expression. The three main substrates of p38α are the protein kinases MK2/3, MSK1/2 and MNK1/2. We used the chemical inhibitors PF-3644022 for MK2, SB-747651A for MSK1/2 and Tomivosertib for MNK1/2. We pre-treated BMDMs with the inhibitors and analysed MHCII expression 24 h after LPS stimulation. We observed that the MSK and MNK inhibitors did not increase LPS-induced MHCII expression. However, the inhibition of MK2 consistently increased the levels of MHCII to similar levels as those achieved by inhibition of p38α, thereby suggesting that p38α partially signals through MK2 to negatively regulate MHCII (**Figure R21A**). As with the p38α inhibitor, pre-treatment of BMDMs with the different inhibitors alone did not induce MCHII in the absence of LPS stimulation. We confirmed the effectivity and specificity of the different inhibitors on the p38α pathway by western blot. Thus, MSK inhibition reduced CREB phosphorylation and MNK inhibition reduced eif4E phosphorylation (**Figure R21B**).

Unfortunately, we could not detect the phosphorylation of HSP27, a main MK2 target, in BMDMs. However, we have confirmed in other cell lines that PF is a potent inhibitor of MK2 signalling.

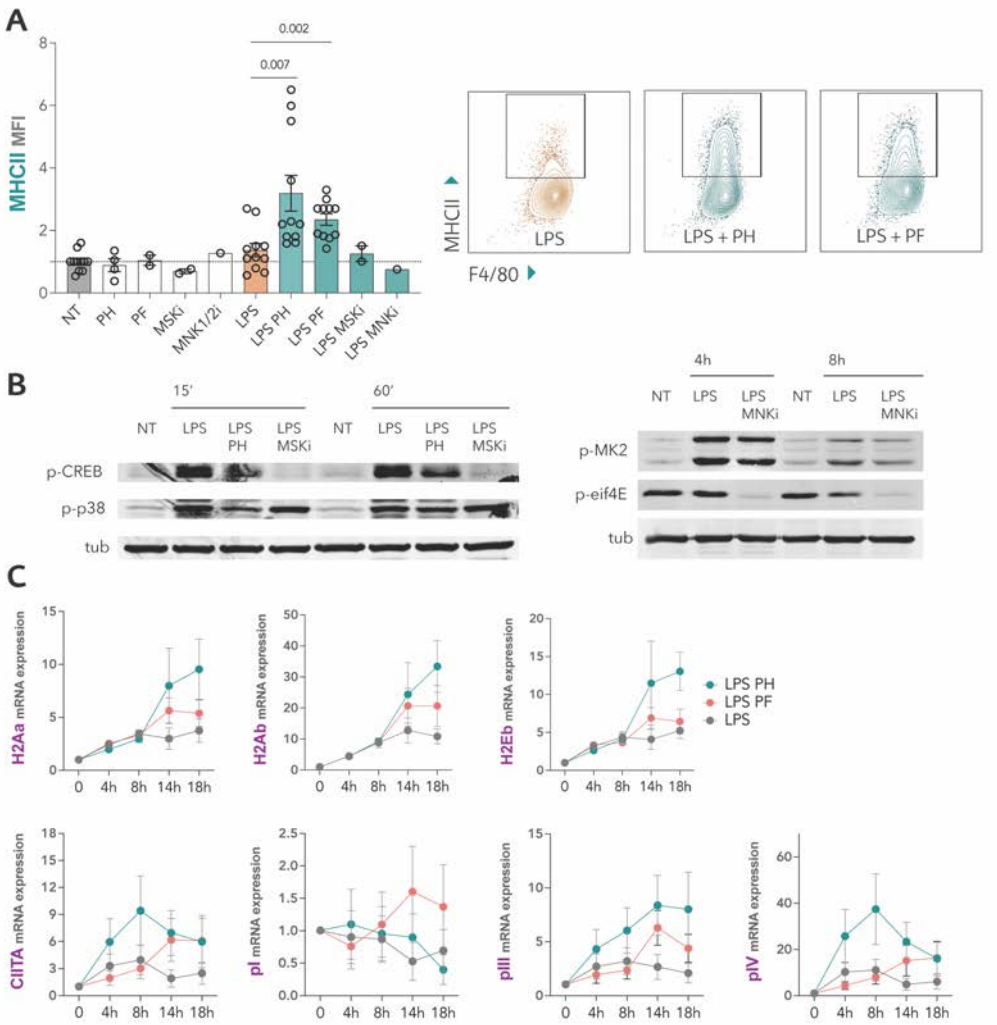

Figure R21. p38α signalling regulates MHCII expression though MK2.
A. MFI of MHCII expression analysed by FACS in BMDMs pre-treated for 2 h with or without the inhibitors of p38α PH797804 (PH), MK2 PF3644022 (MK2i), MSK1/2 (MSKi) or MNK1/2 (MNKi) (left). Representative FACS gate of MHCII expression treated with the indicates conditions (right). NT=non treated control. **B.** Western blots of the MSK1/2 target phospho-CREB (left) and the MNK1/2 target phospho-eif4E (right) in BMDMs pre-treated with the indicated inhibitors for 2 h and stimulated with LPS for the indicated times. **C**. RT-qPCR analysis of different MHCII subunits, CIITA total and CIITA isoforms in BMDMs pre-treated with or without PH and the MK2 inhibitor PF3644022 (PF) for 2 h and stimulated with LPS for the indicated times. Data shown as mean ±SEM.

Furthermore, we confirmed that mRNAs encoding the MHCII subunits *H2-Aa*, *H2-Ab* and *H2-Eb,* as well as *CIITA* were all upregulated upon MK2 inhibition, similar to what we observed in p38α-inhibited BMDMs (**Figure R21C**). However, the mRNA levels were lower compared with those observed upon inhibition of p38α. This observation thus suggests that MK2 is partially responsible for the negative regulation of CIITA by p38α.

p38α and HDAC6 regulate CIITA in a similar way

CIITA transcription is known to be regulated by chromatin epigenetic modifiers, including the HATs ATF2, p300, and CBP, chromatin remodelling complexes such as PRC2 or BRG1, and some HDACs (Abou El Hassan et al., 2015; Ni et al., 2008). Some of these regulators, for example ATF2, BRG1, p300, CBP and PRC2, have been described in the literature as possible substrates of the p38α pathway (Anwar et al., 2018; Canovas & Nebreda, 2021; H. Kawasaki et al., 2000; Meissner et al., 2007; Simone et al., 2004; Q. E. Wang et al., 2013). Furthermore, p38α was proposed to regulate IFNγ-dependent CIITA regulation in RAW 264.7 cells through histone acetylation (Yao et al., 2006). Our RNA-Seq results in AMs also connected p38α and HDAC activity in AMs (**Figure R8B**).

We decided to explore further the relevance of epigenetic modifications in the negative regulation of CIITA by p38α. To this end, we studied whether p38α positively regulates transcriptional silencers like HDACs or DNA methylation, or negatively regulates HATs such as p300, which is known to control CIITA and was recently described as a p38α substrate (De Maeyer et al., 2020). We used Trichostatin A (TSA) to inhibit class I and II HDACs, 5-Azacytidine (5-AZA) to inhibit DNA methylation and C646 to inhibit p300. The results indicated that the increased MHCII expression observed in LPS-treated BMDMs upon inhibition of p38α was not impaired by p300 inhibition and the MHCII restriction in LPS-treated BMDMs was not affected by the inhibition of DNA methylation. Surprisingly, TSA treatment sufficed to increase the LPS-induced expression of MHCII in the absence of p38α inhibitor, and also boosted the effect of p38α inhibition (**Figure R22A**). These findings support the notion that HDACs play an important role in the transcriptional regulation of MHCII, and point to a possible link between p38α signalling and HDACs.

The HDAC family of proteins consists of 18 members (King et al., 2021; Seto & Yoshida, 2014), and we wanted to elucidate which HDAC(s) could be responsible for MHCII upregulation upon p38α inhibition in macrophages. To the best of our knowledge, no specific HDAC has been linked to p38α or MK2 before. Our RNA-Seq

results in AMs indicated that some HDACs were expressed at higher levels in p38αΔ^{Lys} AMs while only few seemed to be significantly downregulated (**Figure R22B**).

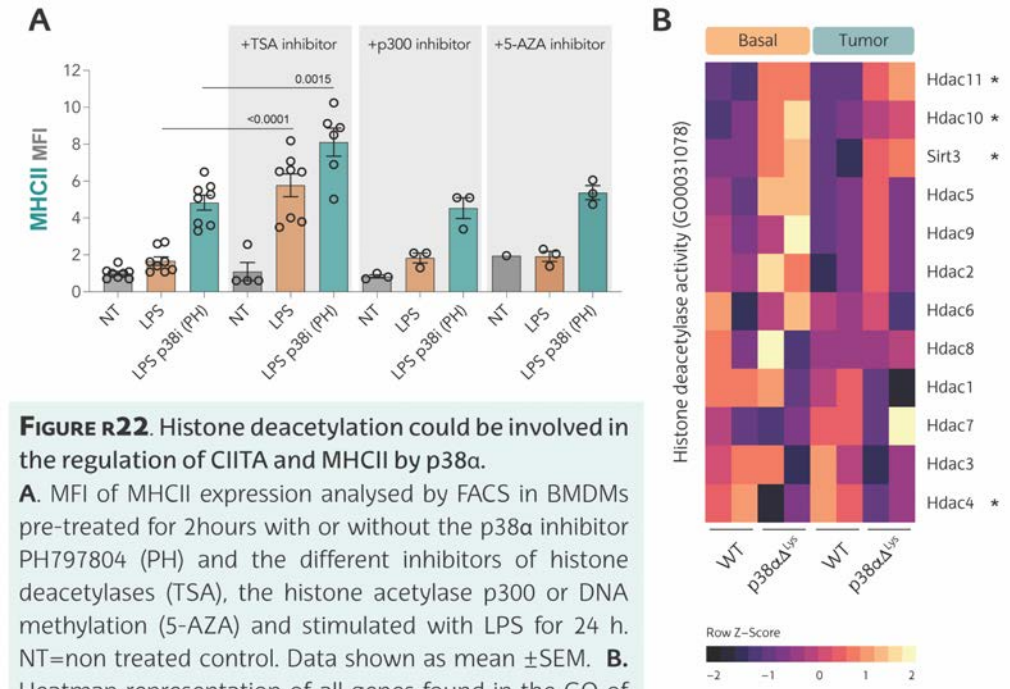

FIGURE R22. Histone deacetylation could be involved in the regulation of CIITA and MHCII by p38α.
A. MFI of MHCII expression analysed by FACS in BMDMs pre-treated for 2hours with or without the p38α inhibitor PH797804 (PH) and the different inhibitors of histone deacetylases (TSA), the histone acetylase p300 or DNA methylation (5-AZA) and stimulated with LPS for 24 h. NT=non treated control. Data shown as mean ±SEM. **B.** Heatmap representation of all genes found in the GO of histone deacetylate activity of the RNA-Seq analysis of p38αΔLys versus WT AMs comparing basal and lung tumor conditions after 11 days of B16/F10 cell inoculation. Relative expression is represented by colour and indicated in the legend. Statistically significant comparisons with a p.val<0.05 are indicated with a *.

To identify a specific p38α-regulated HDAC candidate, we took advantage of an analysis performed previously in the lab by Nuria Gutierrez-Prat. The study used the BioID system to find MK2-binding partners, and identified HDAC6 as an interactor of MK2 (Gutierrez-Prat, 2018). We observed that HDAC6 mRNA levels were not affected in the RNA-Seq of p38αΔ^{Lys} AMs. As CIITA regulation by p38α partially involves MK2, we tested the effect of the HDAC6 inhibitor Nexturastat A (NEX). Surprisingly, treatment with this inhibitor increased MHCII expression significantly when stimulating with LPS alone, thereby proving that HDAC6 activity, similar to that of p38α, inhibits MHCII expression upon LPS stimulation (**Figure R23A**). Western blot of acetyl-tubulin, a reported target of HDAC6 activity, confirmed the effective inhibition by both NEX and TSA (**Figure R23B**). To determine whether HDAC6 inhibition regulated MHCII expression though CIITA transcription, we analysed the *CIITA* mRNA at different time points during the NEX treatment. *CIITA* transcripts were upregulated

at 4 and 14 h similar to the upregulation observed in cells treated with LPS and inhibitors of p38α and MK2. We also observed the upregulation of *H2-Aa*, *H2-Ab* and *H2-Eb* at 14 h post-treatment, thereby supporting the notion that HDAC6 regulates MHCII through CIITA transcription, similar to p38α and MK2 (**Figure R23C**). These results point to a possible link between p38α and HDAC6 in the regulation of CIITA.

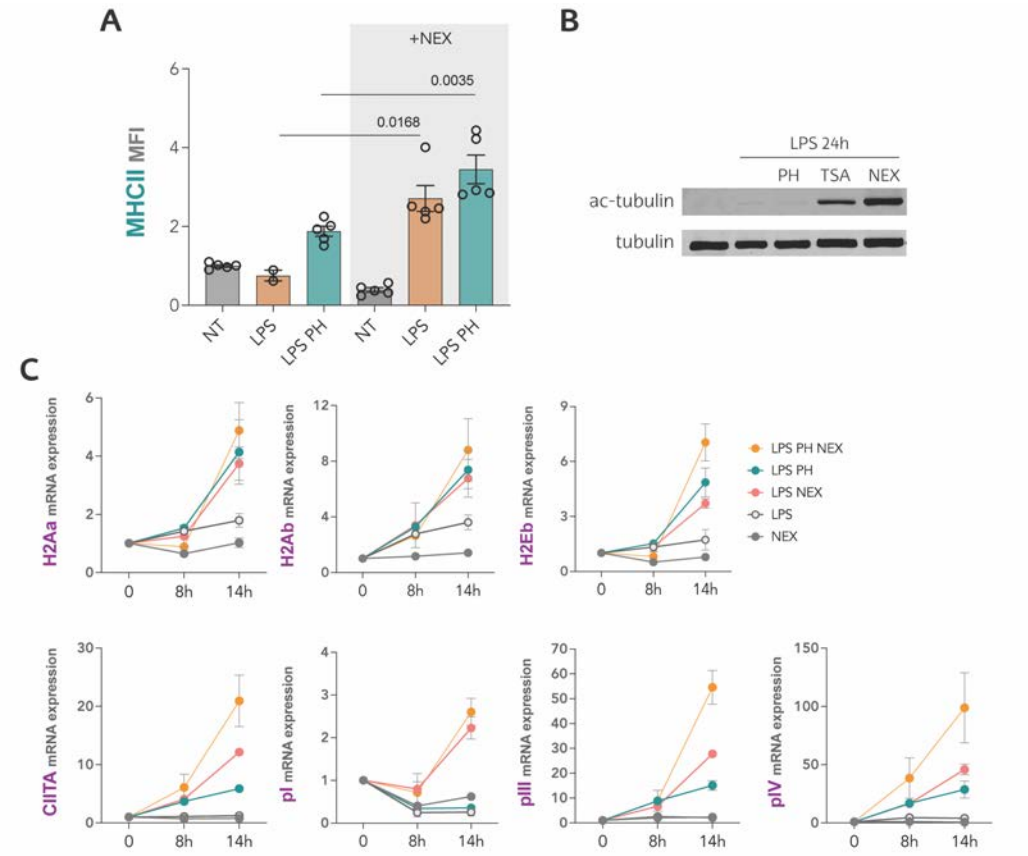

Figure R23. HDAC6 inhibition increases MHCII expression in BMDMs.
A. MFI of MHCII expression analysed by FACS in BMDMs treated for 24 h with LPS in the presence or absence of the p38α inhibitor PH797804 (PH) and the HDAC6 inhibitor Nexturastat (NEX). NT=non treated control. **B**. Western blot of acetyl-tubulin in BMDMs treated for 24 h with LPS and with PH, the histone deacetylase inhibitior TSA or Nex. **C**. RT-qPCR analysis of different MHCII subunits, CIITA total and CIITA isoforms in BMDMs pre-treated with PH and Nex for 2 h and stimulated with LPS for the indicated times. Data shown as mean ±SEM.

To confirm the involvement of HDAC6 in the regulation of CIITA, we used siRNAs targeting HDAC6. Primary BMDMs were electroporated with control or HDAC6 siRNAs, and after overnight recovery, they were stimulated with LPS. Analysis of MHCII expression 24 h after treatment confirmed the results previously seen using the HDAC6 inhibitor, as HDAC6 siRNA increased the levels of MHCII expression in LPS-

treated cells treated compared with the control siRNA (**Figure R24A**). We verified that HDAC6 mRNA levels were strongly reduced in the HDAC6 siRNA-treated cells, although about 20% remained (**Figure R24B**). This partial downregulation of HDAC6 could explain the milder effect on MHCII upregulation of the siRNA compared with the HDAC6 inhibitor NEX. Taken together, the suggest that HDAC6, possibly under the control of the p38α-MK2 pathway, regulates CIITA and MHCII expression.

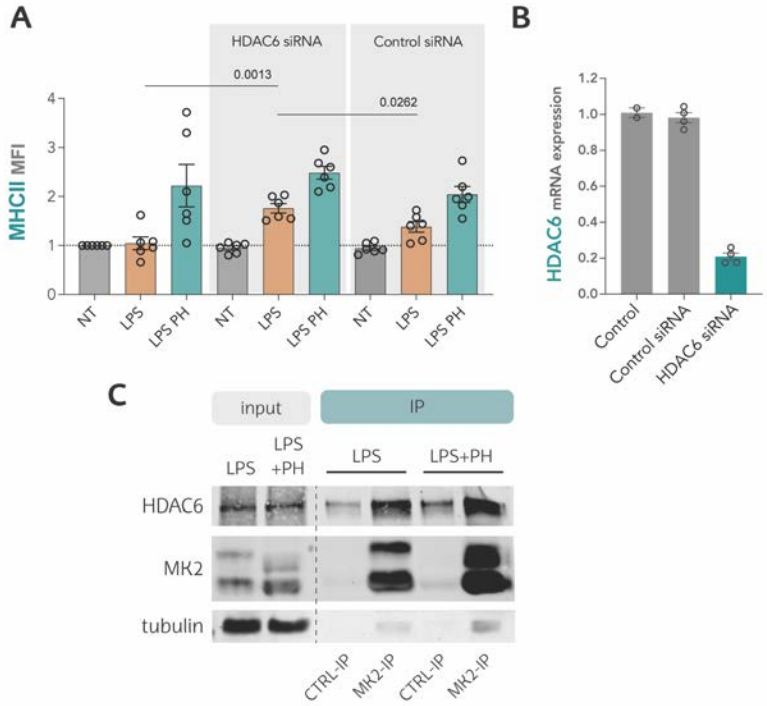

Figure R24. HDAC6 downregulation increases MHCII expression in BMDMs.
A. MFI of MHCII expression analysed by FACS in BMDMs electroporated with control or HDAC6-targeting siRNAs and then treated for 24 h with LPS in the presence or absence of the p38α inhibitor PH797804 (PH). NT=non treated control. **B**. RT-qPCR analysis of HDAC6 expression in BMDM treated with control or HDAC6 siRNAs. Data shown in A and B are mean ±SEM. **C**. BMDMs were treated with LPS in the presence or absence of PH, and then were immunoprecipitated (IP) with MK2 or control antibodies, and analysed by western blotting with the indicated antibodies. An aliquot of the total cell lysates was also run in the same gel (input).

To obtain further evidence of the link between MK2 and HDAC6 in BMDMs, we performed an MK2 IP in LPS-treated BMDMs, in the absence or presence of p38α inhibitor. Interestingly, we found that HDAC6 was enriched in the MK2 IP. Of note, HDAC6 was found to interact with MK2 even in p38α-inhibited cells, thereby suggesting that the regulation of HDAC6 activity by MK2 is independent of p38α activation (**Figure R24C**). Although preliminary, these results support a potentially interesting link between MK2 and HDAC6 activity in macrophages.

We conclude that the p38α/MK2 pathway regulates the transcription of CIITA and MHCII in macrophages, and this regulation probably involves HDAC6.

Phagocytosis is reduced in p38αΔ^{Lys} AMs

Our results showed that p38α plays a key role controlling the adaptive immune response in AMs through the regulation of antigen presentation via MHCII. However, RNA-Seq results also revealed a decrease in the GO terms associated with pattern recognition and phagocytosis. In fact, RT-qPCR validation in fresh AMs confirmed the downregulation of some of the mRNAs found in the RNA-Seq (**Figure R11**), suggesting that p38α KO AMs might have a decreased capacity to phagocytose. Given the importance of this process in tumor progression and inflammatory diseases, we tested whether the phagocytic capacity in AMs was regulated by p38α.

We first performed some optimization experiments using fluorescent beads. BMDMs were incubated for 30 min with 3 μm fluorescent latex beads and fluorescent macrophages were quantified by FACS (**Figure R25A**). We observed that p38α inhibition decreased the ability of BMDMs to ingest beads, also when cells were treated with LPS (**Figure R25B**). Next, we performed the same experiment using primary AMs extracted from WT and p38αΔ^{Lys} animals (**Figure R25C**). Similarly, we observed that both p38α-inhibited and p38αΔ^{Lys} AMs had a very reduced capacity to phagocytose beads, with or without LPS stimulation, thereby confirming a role for p38α in the regulation of phagocytosis (**Figure R25D**).

We next tested the ability of AMs to perform efferocytosis, a process by which macrophages phagocytose apoptotic cells. This process is important for the clearance function of AMs in the airways, and it has also been reported to be relevant for the immune-silent clearance of apoptotic cancer cells (Vaught et al., 2015; Y. Zhou et al., 2020). Jurkat cancer cells were stained with the CFSE tracker, then were treated with Etoposide for 16 h to induce apoptosis, (**Figure R25E**), and finally were co-cultured with fresh AMs. After 30 min, 3 h and 20 h, we analysed CFSE^{+} macrophages by FACS (**Figure R25F**). Consistent with the previous results, we observed a reduction in the efferocytosis capacity of p38α-inhibited AMs (**Figure R25G**). These results confirm that p38α regulates the process of phagocytosis in AMs, which is a crucial function of this tissue-specialised myeloid cell.

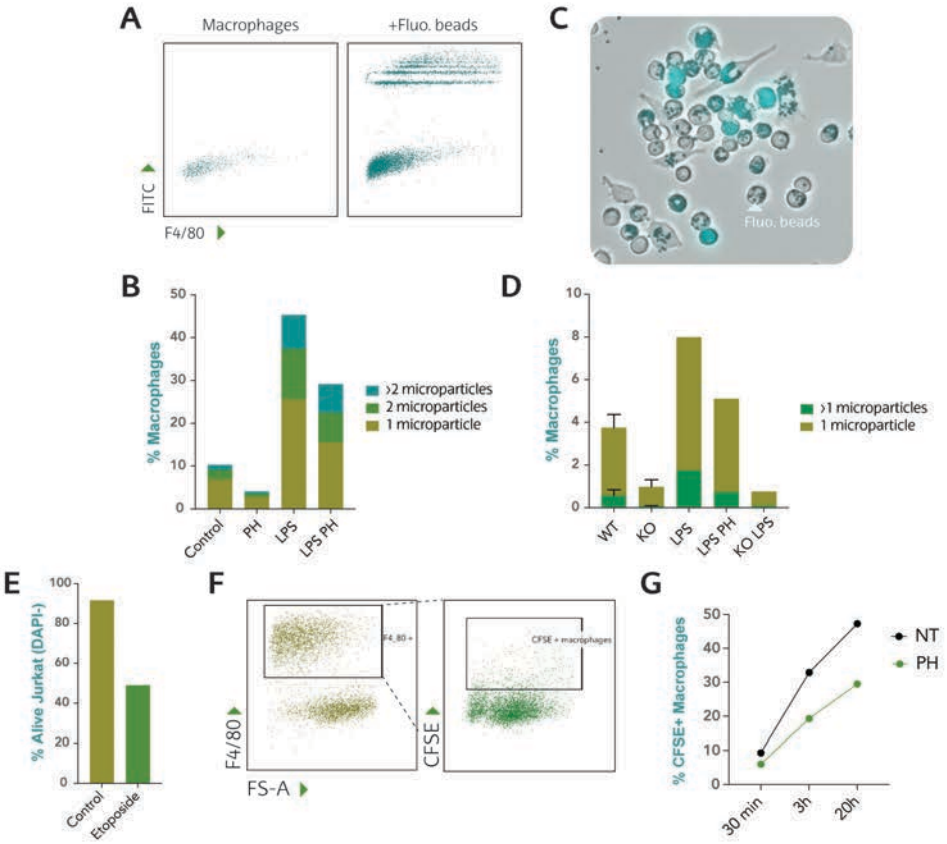

Figure R25. AMs from p38αΔ^{Lys} mice have reduced phagocytic capacity.
A. Representative FACS plots of BMDMs alone or incubated for 30 min with FITC-fluorescent beads. **B**. BMDM were treated for 24 h with LPS in the presence or absence of the p38α inhibitor PH797804 (PH), incubated with FITC-fluorescent beads for 30 min and the fluorescent-positive BMDMs were quantified by FACS. Cells were classified on their content of beads as indicated by colour. **C**. Representative image of AMs incubated ex-vivo for 24 h with fluorescent beads. **D**. AMs were treated for 24 h with LPS and with or without PH, incubated for 30 min with FITC-fluorescent beads and then fluorescent AMs were quantified by FACS. Cells were classified on their content of beads as indicated by colour. **E**. CFSE stained Jurkat cells were treated for 16 h with etoposide to induce apoptosis and DAPI negative cells were quantified by FACS in cells treated with or without etoposide. **F**. Gating strategy of phagocytic AMs cultured with CFSE+ Jurkat cells treated with etoposide (apoptotic CFSE+ Jurkat cells). **G**. Quantification of fluorescent AMs pre-treated or not with PH for 2 h and then co-cultured with apoptotic CFSE+ Jurkat cells for the indicated times.

SECTION 2

Myeloid p38α in lung inflammation

There is strong evidence in the literature supporting the relevance of p38α in myeloid cell functions and its involvement in inflammatory diseases. We have also observed that p38α deletion affects crucial functions of AMs in the lungs. Therefore, we sought to explore whether myeloid p38α participated in lung pathologies beyond tumorigenesis such as asthma and acute injury. In fact, although p38α chemical inhibitors have been used to study those diseases, the p38αΔ^{Lys} mouse model will allow us to determine specific functions of myeloid p38α in these pathologies.

Myeloid p38α is important in asthma

The use of p38α chemical inhibitors ameliorates inflammation in mouse models of asthma by reducing cytokine production. However, asthma is a disease in which both innate and adaptive immunity play crucial roles. Antigen presentation through MHCII is central for the activation of the inflammation cascade that ultimately leads to eosinophilic infiltration in the airways though the Th2 response. Given that p38α regulates MHCII expression in AMs, we examined whether p38α in AMs plays a role in asthma.

To explore this hypothesis, WT and p38αΔ^{Lys} mice were intranasally inoculated for 10 days with house dust mite (HDM) (**Figure R26A**), which is one of the main allergens causing asthma in humans. After HDM challenge, mice were sacrificed and the BAL fluid was analysed by FACS. UMAP representation of the FACS populations showed that mice treated with HDM had an expected higher infiltration of myeloid cells in the BAL fluid. Surprisingly, the infiltrating cells in the BAL fluid of WT and p38αΔ^{Lys} mice differed, with an increased proportion of eosinophils in p38αΔ^{Lys} mice (**Figure R26B**). This observation was confirmed by analysing total cell numbers, which showed an increase in total myeloid cells and an increase of around 15-fold of eosinophils in the p38αΔ^{Lys} mice (**Figure R26C**). We also observed increased numbers of neutrophils and DCs in these mice. On the other hand, AM numbers were maintained similar to the numbers at basal levels (**Figure R26D**). Importantly, we confirmed a sustained upregulation of the MHCII levels in AMs from p38αΔ^{Lys} mice, both in basal and asthma lungs, while AMs from WT animals showed increased MHCII expression levels in

asthma but without reaching the levels of p38αΔ^{Lys} mice (**Figure R26D**). These observations support the involvement of MHCII and antigen presentation in asthma, which can ultimately lead to eosinophil recruitment.

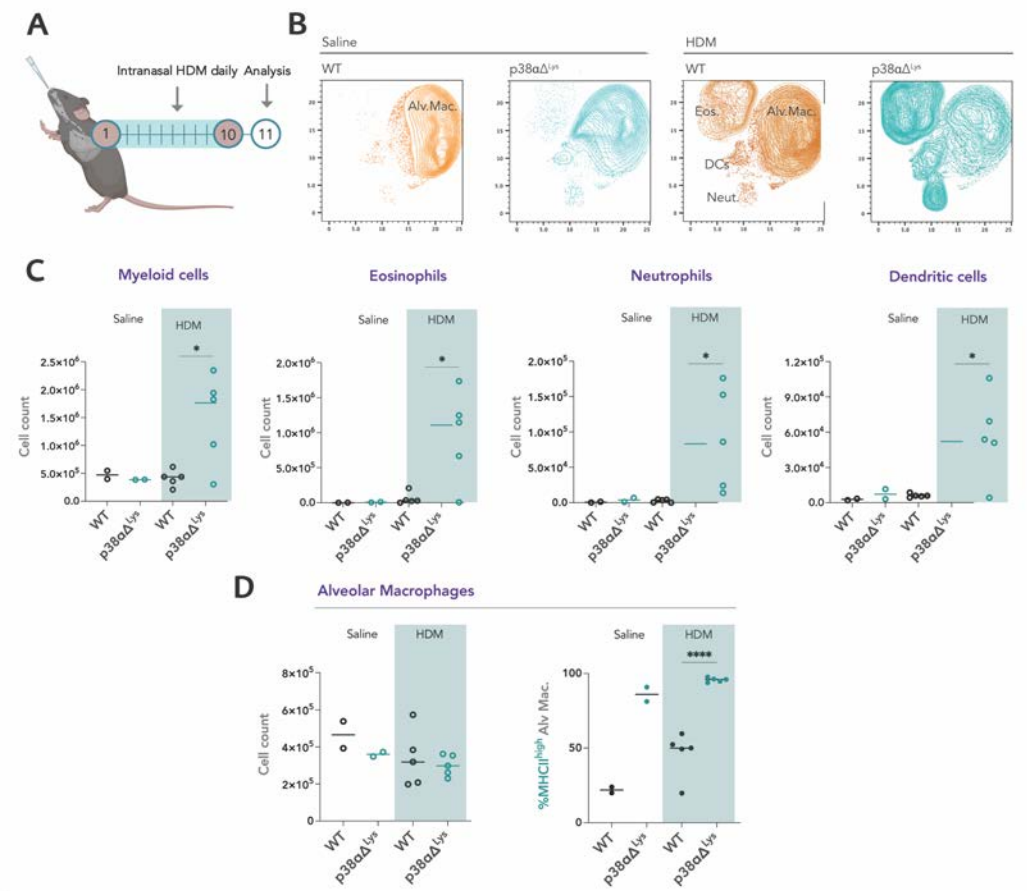

Figure R26. Enhanced immune cell infiltration in the lungs of p38αΔ^{Lys} mice with asthma. **A**. Asthma model consisted of 10 days intranasal inoculation of House dust mite (HDM) in WT and p38αΔ^{Lys} mice, which were analysed at day 11. **B**. UMAP representation of the FACS analysis of normalized CD45^{+} cells in BAL fluid from WT and p38αΔ^{Lys} mice with HDM or saline controls. Eos=eosinophils, DCs=Dendritic cells, Alv.Mac=alveolar macrophages, Neut=neutrophils. **C**. Quantification of the total number of different myeloid cell populations in BAL fluid from WT and p38αΔ^{Lys} mice with HDM-induced asthma compared to saline controls. **D**. Quantification of the total number of AMs and their MHCII expression levels in WT and p38αΔ^{Lys} mice with HDM-induced asthma or saline-treated controls.

Further histological analysis determined an increased perivascular and peribronchiolar infiltration of eosinophils in the p38αΔ^{Lys} mice (**Figure R27A-B**). Moreover, we observed a slight increase in CD45^{+} cell infiltration accompanied by an increase in Goblet cell metaplasia in these mice (**Figure R27C-D**). Goblet cells are responsible for the production of mucus and their metaplasia is a readout of asthma

severity. These observations point to a crucial role for myeloid p38α in asthma pathology and contrast with previous results using p38α chemical inhibitors in asthma models. The results also suggest that p38α contribute to the maintenance of a certain level of immune tolerance in lungs.

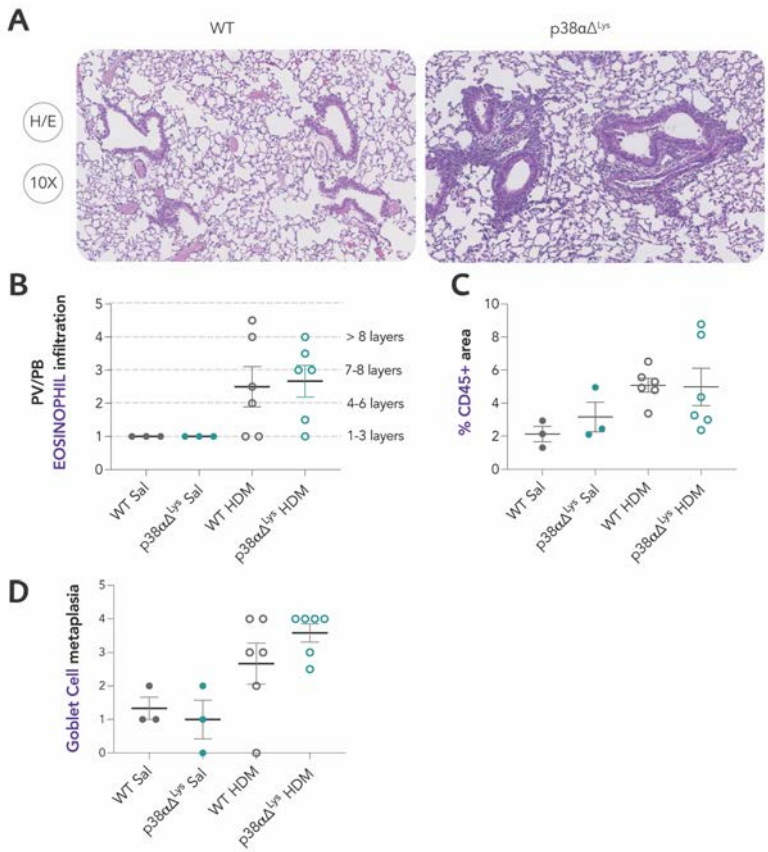

Figure R27. p38αΔ^{Lys} mice have worse asthma outcome.
A. Representative H/E staining of lung slices from WT and p38αΔ^{Lys} mice with House dust mite-induced asthma showing peribronchiolar eosinophilic infiltrates. **B**. Score quantification of perivascular and peribronchiolar eosinophilic infiltrates in lungs from WT and p38αΔ^{Lys} mice with HDM-induced asthma or saline controls. **C**. CD45^{+} cell quantification in whole lungs from WT and p38αΔ^{Lys} mice with HDM-induced asthma or saline controls. **D**. Score quantification of the Goblet cell metaplasia in bronchial areas from WT and p38αΔ^{Lys} mice with HDM-induced asthma or saline controls.

Myeloid p38α is important in LPS-induced acute lung injury

To further investigate the implication of p38α in the early innate immune response of the lungs in WT and p38αΔ^{Lys} animals, we induced acute lung inflammation by

intranasal administration of LPS. This model is widely used to study acute respiratory distress syndrome (ARDS), a major problem in humans (Diamond et al., 2022; Kabir et al., 2002). Given the acute nature of this immune challenge, the intranasal LPS model involves a macrophage function that is uncoupled from MHCII and antigen presentation, so it allows the study of p38α functions in AMs and other myeloid cells that regulate immune-suppression and tolerance.

We used LPS at 25 and 100 μg/dose to determine whether the phenotype was dose-dependent, and we analysed the BAL fluid by FACS 24 h after intranasal LPS administration (**Figure R28A**). Compared to mice treated with saline, LPS-treated animals had an increased level of immune cell infiltration in the BAL fluid, mainly neutrophils, which are the first cells to reach the site of inflammation in an acute response (**Figure R28B**). The levels of neutrophils in the BAL fluid were particularly elevated in the p38αΔ^{Lys} animals (**Figure R28C**), especially when using 100 μg of LPS, thereby confirming that the effect was dose-dependent. We also observed decreased numbers of AMs with 100 μg of LPS, suggesting that high inflammation levels cause this population to decrease, probably due to cell death (**Figure R28D**). However, high levels of MHCII were maintained throughout the experiment in the p38αΔ^{Lys} animals.

IHC analysis of the lungs determined that p38αΔ^{Lys} mice had an increased perivascular/peribronchiolar infiltration of neutrophils, which was confirmed by myeloperoxidase (MPO) staining (**Figure R29A-B**). Moreover, RT-qPCR of whole lung lysates showed increased expression of some cytokines and chemokines in the lungs of animals inoculated with 25 μg of LPS (**Figure R29C**). Interestingly, p38αΔ^{Lys} mice showed a slight increase in the neutrophil recruitment chemokine CXCL2 compared to the WT animals, which could explain the higher infiltration of neutrophils observed in those animals. These results support the relevance of myeloid p38α regulation in early events of acute inflammation in the lungs and points to a crucial function of p38α in the maintenance of an immunosuppressive phenotype in AMs. Further experiments should be performed to unravel the specific role of p38α in AMs in the pathophysiology of acute lung injury.

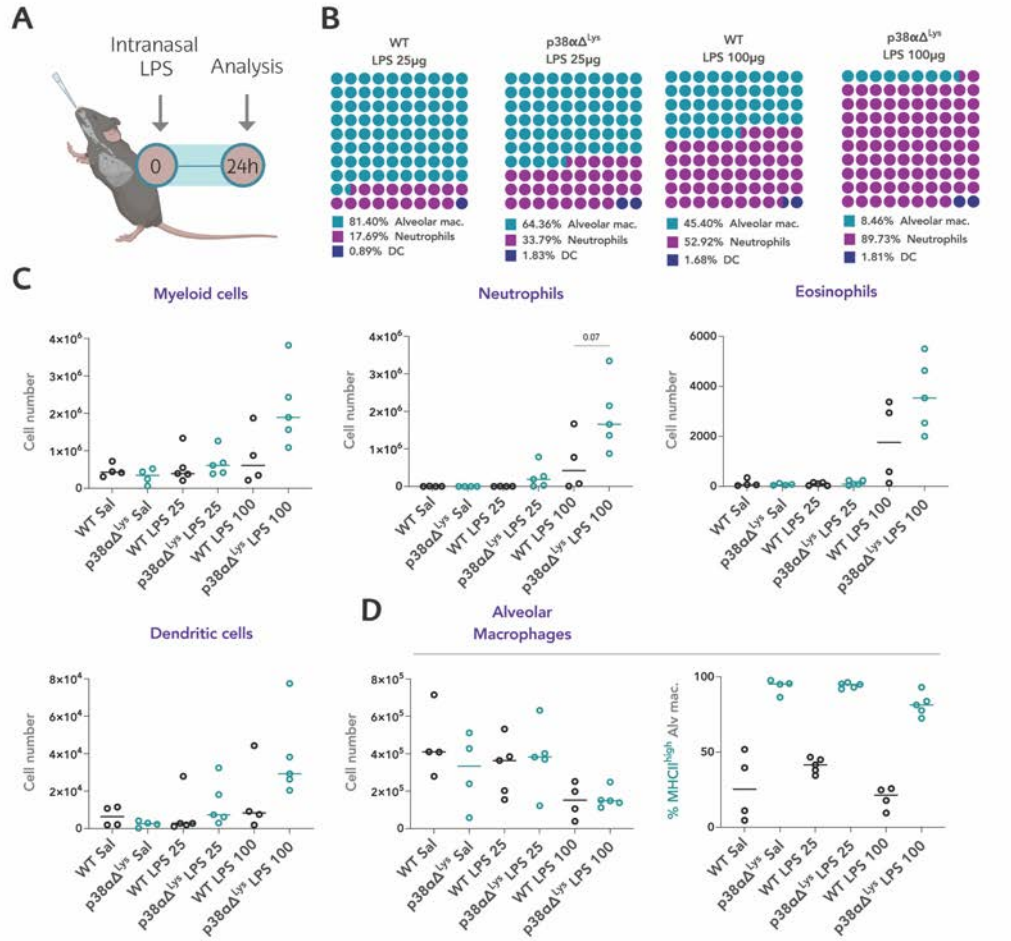

Figure R28. p38αΔ^{Lys} mice have a worse lung injury outcome.
A. Experimental model of acute lung inflammation was induced by LPS intranasal inoculation in WT and and p38αΔ^{Lys} mice and analysis was performed after 24 hours. **B**. 10x10 dot plot representation of the percentages of myeloid cells in BAL fluid extracted from WT and p38αΔ^{Lys} mice treated intranasally with the indicated doses of LPS. Data from two independent experiments (n=19). **C**. Total numbers of the indicated myeloid cell populations analysed by FACS in BAL fluid from WT and p38αΔ^{Lys} mice injected with saline or the indicated doses of LPS; 25=25 µg, 100=100 µg. **D**. Total number of AMs in BAL fluid and their MHCII expression levels in WT and p38αΔ^{Lys} mice treated with the indicated doses of LPS or saline.

The results of the asthma model and the LPS-acute lung disease are consistent with a role of p38α in AMs in the regulation of immune suppression. In both cases p38α downregulation in myeloid cells exacerbates the response to external agents, suggesting that the homeostatic levels of lung immune tolerance are somehow lost when p38α is inhibited. Taken together, these results support the notion that p38α contributes to a number of crucial functions in AMs, which are all implicated in

diseases that involve immune challenges such as cancer, asthma and acute lung injury.

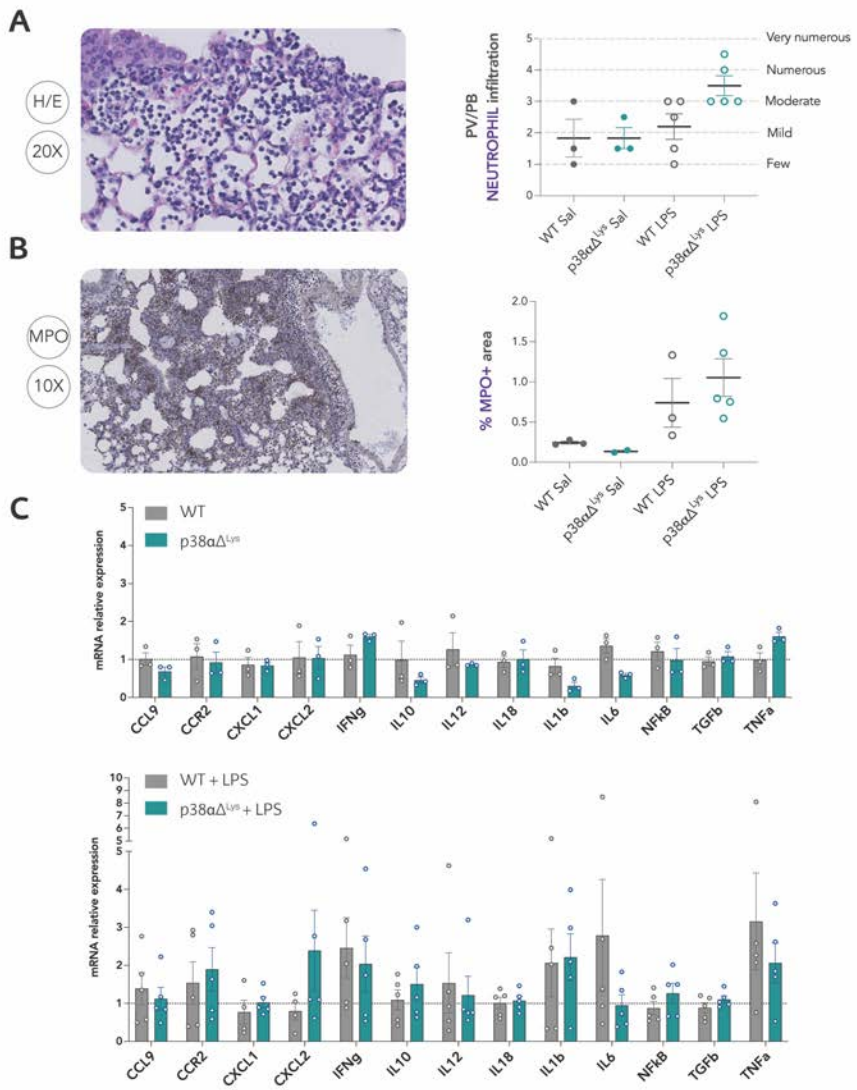

Figure R29. Enhanced immune cell infiltration in the lungs of p38αΔ^{Lys} mice with acute lung injury.

A. Representative H/E staining of lung slices from WT and p38αΔ^{Lys} mice treated with 25 μg of intranasal LPS to induce acute lung injury showing peribronchiolar neutrophilic infiltrates (left) and the score quantification (right). **B**. MPO^{+} cell quantification in whole lungs from WT and p38αΔ^{Lys} mice treated with 25 μg of LPS. **C**. RT-qPCR analysis of mRNAs encoding the indicated inflammatory cytokines in whole lung lysates from WT and p38αΔ^{Lys} mice inoculated with 25 μg of LPS. Data normalized to values of WT mice treated with saline and shown as mean ±SEM.

SECTION 3

In vivo effects of genetic p38α overexpression

This chapter describes the generation of a mouse model that mildly overexpresses p38α. This model was used to analyse whether a small increase in the activity of the p38α pathway affects either homeostatic or pathologic conditions *in vivo*.

Characterization of the p38α overexpressing mice

For the overexpression of p38α *in vivo*, we used a BAC transgenic mouse model of p38α (p38αBAC), which has several copies of the p38α-encoding genomic region integrated in the genome (**Figure R30A**), as described in Methods. For the general characterization of the model, we first analysed the expression of p38α in several tissues by RT-qPCR and western blot. We observed increased mRNA levels of p38α in most of the tissues analysed, including heart, kidney, spleen, colon and liver (**Figure R30B**). However, p38α protein levels did not seem to change much in the tissues from p38αBAC mice (**Figure R30C**).

Next, to study the activation of the p38α signalling pathway, we treated BMDMs isolated from both WT and p38αBAC mice with LPS. We observed an increase expression of p38α both by western blot and by RT-qPCR in BMDMs from p38αBAC mice (**Figure R31A-B**), which also showed increased phosphorylation of MK2, one of the main p38α substrates (**Figure R31A**). We also tested the effect of this increased signalling in the production of p38α-regulated cytokines such as IL6 and TNFα. However, no significant differences between genotypes were observed (**Figure R31B**). This finding suggests that BMDMs have mechanisms that regulate any fluctuations in the p38α pathway activity downstream of MK2 activation.

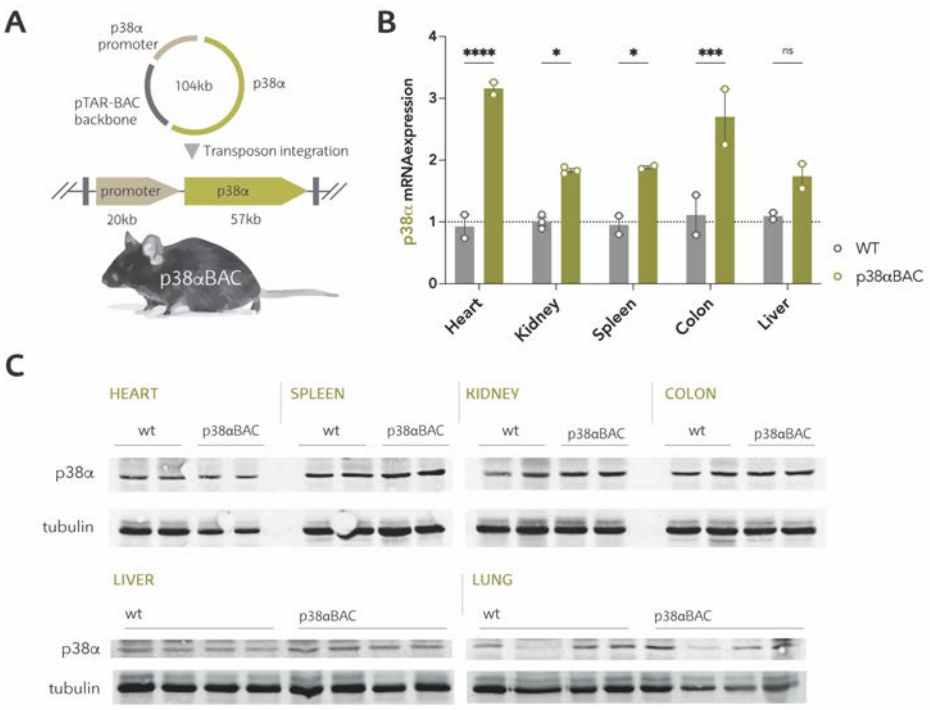

Figure R30. p38αBAC mice express higher levels of the p38α mRNA.
A. p38αBAC mice were engineered to have additional genomic copies of the whole p38α coding region integrated in the genome. **B**. RT-qPCR of p38α mRNA in different tissue lysates from p38α BAC mice compared to WT littermates. Data shown as mean ±SEM. **B**. Western blot of p38α in different tissue lysates from WT and p38αBAC mice.

p38α is involved in the upregulation of cell cycle inhibitors in the pancreas, spleen and liver during ageing (Wong et al., 2009). Since our results indicated a higher expression of p38α in these organs in p38αBAC mice (**Figure R30B**), we examined whether p38α overexpression could have the opposite effect. Although anatomopathological analysis of the p38αBAC mice and their tissues during ageing (until 24 months) showed no apparent differences with WT mice, RT-qPCR analysis revealed that aged p38αBAC mice expressed higher levels of the cell cycle inhibitors p15, p16 and p19 in the liver and spleen (**Figure R32**). These results were in line with previous work (Wong et al., 2009). Hence, the p38α pathway could be important for healthy ageing. However, further research is required to understand the underlying molecular mechanisms and possible implications.

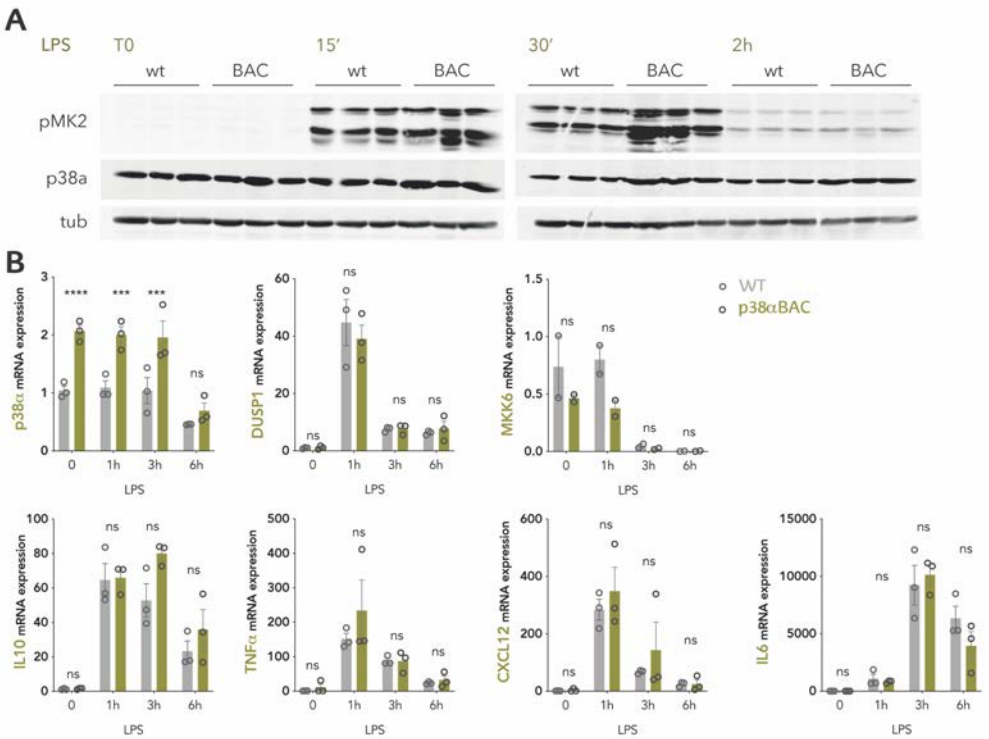

Figure R31. p38α pathway activity and cytokine expression in BMDMs from p38αBAC mice. **A**. BMDMs were generated from WT and p38αBAC mice and were stimulated with LPS for 15 min, 30 min and 2 h, and then analysed by western blot with the indicated antibodies. **B**. BMDMs were generated from WT and p38αBAC mice and the expression of several p38α-regulated cytokines was analysed by RT-qPCR after stimulation with LPS for the indicated times. Data shown as mean ±SEM.

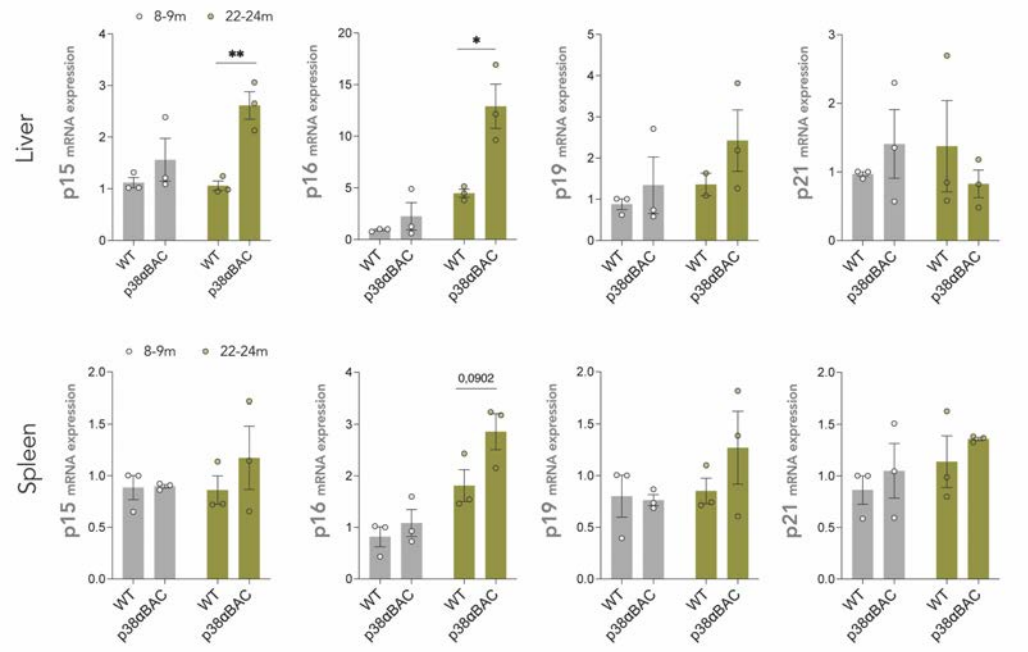

Figure R32. Enhanced expression of cell cycle inhibitors in aged tissues from p38αBAC mice. RT-qPCR analysis of the indicated cell cycle inhibitor-encoding mRNAs in liver and spleen lysates from WT and p38αBAC mice of 8-9 months and 22-24 months. Data shown as mean ±SEM.

p38αBAC mice have a worse response to liver and colon injuries

It has been reported that mice deficient for p38α in mature hepatocytes are protected against CCl_4-induced acute liver injury (Fortier et al., 2019). To study whether p38α overexpression affects this process, we generated "homozygous" p38αBAC$^{+/+}$ mice, which have an increased number of p38α copies. These animals were injected with CCl_4 i.p., and 48 h later various readouts of acute liver injury were analysed. p38αBAC$^{+/+}$ mice had a higher necrotic area in the liver (**Figure R33A**) and a slight increase in the liver-injury marker ALT in the serum (**Figure R33B**), thereby suggesting a higher susceptibility to liver damage upon p38α expression. Moreover, we observed that the CCl_4 treatment induced the phosphorylation of p38α in the liver, and that p38αBAC$^{+/+}$ mice showed increased p38α phosphorylation compared to the WT animals (**Figure R33C**). In contrast to a previous study (Fortier et al., 2019), we did not observe any changes in liver proliferative areas by bromodeoxyuridine (BrDU) staining (**Figure R33D**). These results support the notion that p38α pathway is involved in acute liver injury, in agreement with previously published work.

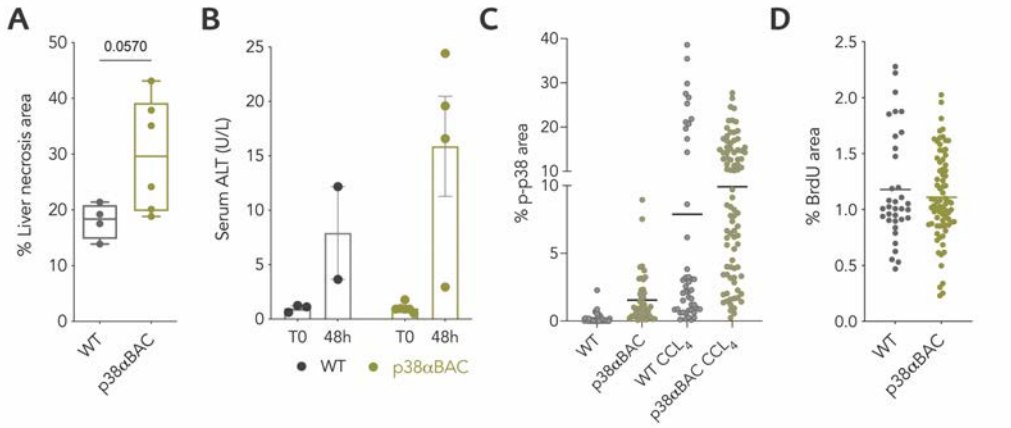

Figure R33. Increased necrosis in p38αBAC mice with acute liver injury.
A. Quantification of necrotic areas in the livers from WT and homozygous p38αBAC+/+ mice 48 h after i.p. injection of CCl_4 to induce acute liver injury. **B**. Alanine Aminotransferase (ALT) quantification in sera from WT and p38αBAC$^{+/+}$ mice extracted right before or 48 h after CCl_4 treatment. U/L=units per litre. **C.** Immunohistochemistry quantification of phospho-p38α in livers from WT and p38αBAC+/+ mice at basal levels (untreated) or with liver injury. **D**. IHC quantification of BrDU staining in livers from WT and p38αBAC$^{+/+}$ mice with CCl_4-induced liver injury, which were injected with BrDU i.p. 2 h before sacrifice.

We also wanted to determine the possible effect of p38α overexpression on colon inflammation, given that previous reports from our group have described the importance of this pathway in colitis (Gupta et al., 2014; Youssif et al., 2018). We treated p38αBAC mice with dextran sodium sulphate (DSS) in drinking water for 6 days to induce colitis and annotated the weight of the animals every day as a readout for colon inflammation severity. DSS-treated p38αBAC animals showed a stronger reduction in weight (**Figure R34A**) and also a slight increase in epithelial damage, as measured by haematoxylin/eosin (H/E) staining (**Figure R34B-C**). These observations support the notion that p38α contributes to the colon epithelia damage induced by inflammatory diseases.

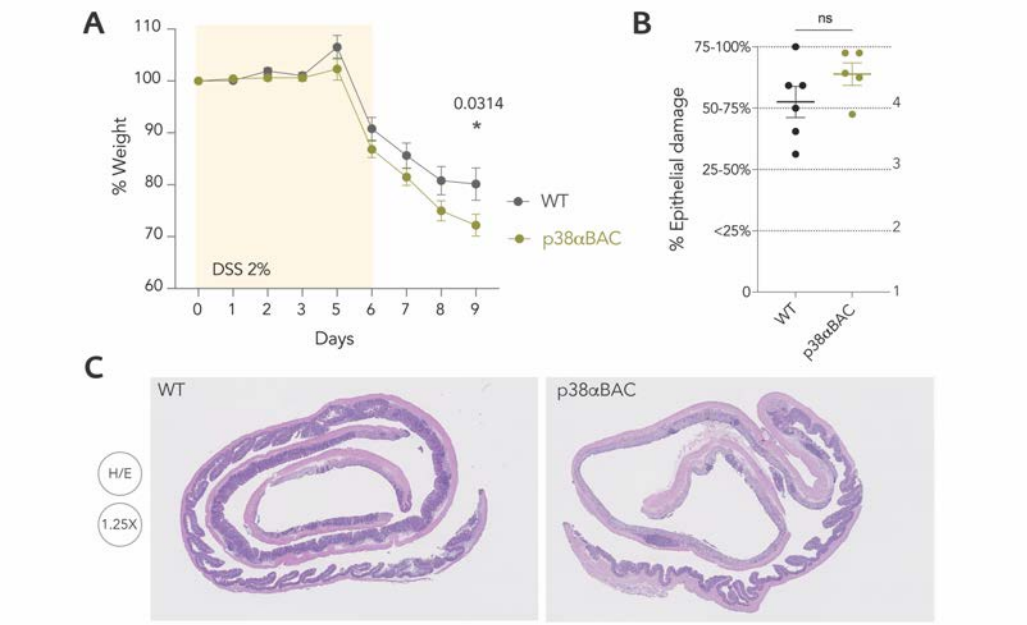

Figure R34. Increased DSS-induced colitis in p38αBAC mice.
A. Percentage of weight loss normalized to day 0 during treatment with DSS in drinking water to induce colitis in WT and p38αBAC mice. **B**. Epithelial damage score of colons from WT and p38α BAC mice at day 9 after DSS-treatment. **C**. Representative images of "swiss roll" IHC colons from WT and p38αBAC mice treated with DSS in drinking water and analysed at day 9 showing inflammation and intestinal crypt loss.

p38αBAC mice have decreased MHCII expression in AMs

Finally, we examined whether p38α overexpression could affect primary tumor growth and lung metastasis formation. To this end, we generated subcutaneous B16/F10 tumors. We observed no differences in tumor growth between WT and p38αBAC animals (**Figure R35A**). On the other hand, in a model of experimental lung metastasis with B16-F10 cells, we observed an increased metastatic burden in p38αBAC$^{+/+}$ mice (**Figure R35B**). Curiously, we also observed decreased expression of MHCII in AMs from these animals (**Figure R35C**), in agreement with the observations in p38αΔ^{Lys} animals and the use of a p38α inhibitor *in vivo*. Moreover, we checked the activation profiles of T cells by FACS and observed a decrease in the effector CD4^{+} and CD8^{+} T cells in tumor-bearing lungs from p38αBAC$^{+/+}$ mice (**Figure R35D**). These cells had an increased naïve profile, consistent with the downregulation of MHCII in AMs. These results support the importance of p38α for the regulation of antigen presentation by AMs and the subsequent activation of the adaptive anti-tumor immunity, which can ultimately control lung tumor progression.

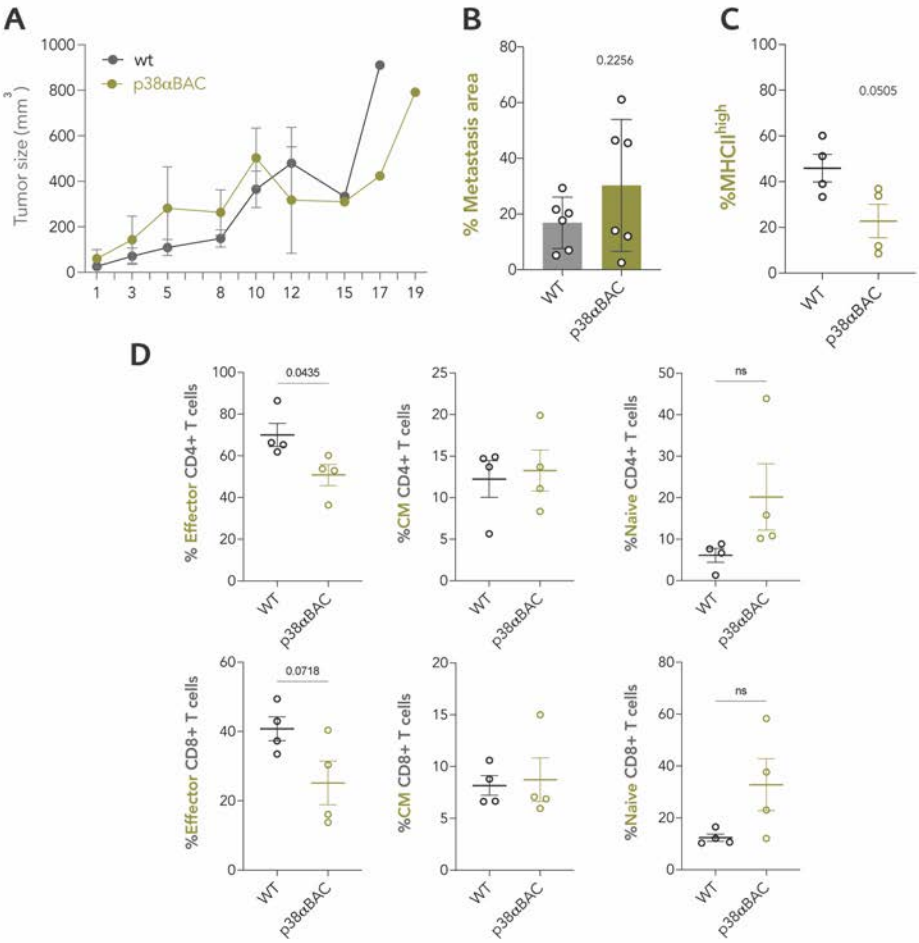

Figure R35. p38αBAC mice have reduced MHCII in AMs and increased lung metastasis. **A**. Subcutaneous tumor growth induced by B16/F10 cells in WT and p38αBAC mice (n=12). **B**. Lung metastasis induced 21 days after intravenous injection of B16/F10 cells in WT and p38α BAC$^{+/+}$ mice. **C**. FACS analysis of MHCII expression in AMs from lungs with tumors of WT and p38α BAC$^{+/+}$ mice. **D**. Percentage of activation profiles of CD4+ and CD8+ T cells in lungs with tumors from WT and p38αBAC$^{+/+}$ mice. Effector cells defined as CD62L^{low}, CD44^{hi}, central memory (CM) defined as CD62L^{hi}, CD44^{hi}, and naïve cells as CD62L^{hi}, CD44^{low}. (CM=central memory). Data shown as mean ±SEM or ±SD.

Discussion

The kinase p38α has long been studied for its capacity to regulate inflammation and immunity. However, initial experiments linking p38α to the production of inflammatory cytokines like TNFα and IL6 have probably misled and generalized the association of p38α activity to proinflammatory responses. This has been challenged over time, since a number of studies reported that its functions depend on the context and type of cell. In this thesis, we have focused on the specific contribution of p38α in myeloid cells to the response of lungs to tumor metastasis and different inflammation challenges. We have found that p38α is crucial in maintaining the homeostasis and immune tolerance of the lungs, with an especially important role of this protein in AMs, which can impact the outcome of lung inflammatory diseases and tumorigenesis.

Role of myeloid p38α in lung metastasis

Our results indicate that p38α does not seem to play a role in primary melanoma tumor formation, and its inhibition did not boost the effect of immune checkpoint inhibitors. Furthermore, in a mouse model of experimental lung metastasis by intravenous injection of B16/F10 cells, we found that p38αΔ^{Lys} mice had a reduced lung tumor burden, indicating that myeloid p38α promotes lung metastasis (**Figure R3**). It could be argued whether the intravenous metastasis model is indeed a model of lung metastasis or just a model of lung tumorigenesis, since the cells do not go through the early stages of the metastatic process (Zeeshan & Mutahir, 2017). In fact, experiments from our group have shown reduced lung tumorigenesis in p38αΔ^{Lys} mice using other models, such as intratracheal injection of mKLC KRAS^{G12V} lung cancer cells or intravenous inoculation of Lewis lung carcinoma (LLC) cells (Vitos-Faleato, 2017, Rivas et al, unpublished), supporting the idea that myeloid p38α facilitates lung tumorigenesis. The reduction in lung tumors observed in p38αΔ^{Lys} mice was accompanied by an increased number of effector CD4$^+$ and CD8$^+$ T cells in the lungs of p38αΔ^{Lys} mice (**Figure R5**). This suggests that the reduction in tumors in p38αΔ^{Lys} mice was given by the increase in effector T cells. However, this hypothesis should be confirmed, for instance, by using antibodies against CD4$^+$ and CD8$^+$ cell populations.

In our lung metastasis studies, we only observed a decrease in lung tumors comparing WT and p38αΔ^{Lys} female mice but not in male mice. However, we validated relevant genes that appeared differentially expressed in the RNA-Seq results from female mice using AMs derived from both p38αΔ^{Lys} males and females, including MHCII (**Figure R11**). Besides, the increase in MHCII in p38αΔ^{Lys} mice by FACS was also observed in male mice, indicating that, for some reason, the increase in MHCII by itself might not

be sufficient to reduce lung tumor growth in p38αΔ^{Lys} males. These results suggest that myeloid p38α could regulate lung tumor progression possibly in a hormone-dependent manner. Strikingly, a study using p38αΔLys mice to model multiple sclerosis also reported differences between males and females, and showed that female myeloid cells depend more on p38α for the expression of proinflammatory genes (Krementsov et al., 2014). In humans, differences in metastasis have also been observed between sexes, and have been attributed to sexual dimorphism, genetic differences and sexual hormones (Farach-Carson et al., 2017; Sagerup et al., 2011; Stabellini et al., 2022). On the other hand, to make use of the whole p38αΔ^{Lys} mouse colony, male littermates were normally used to obtain BMDMs for *in vitro* experiments to study the MHCII regulation by p38α, although we confirmed that female-derived BMDMs also upregulated MHCII upon LPS stimulation in p38α inhibited cells. In addition, male mice were used for the HDM-induced asthma and LPS-induced acute lung injury models. Since inflammation experiments in males supported the role of myeloid p38α in promoting immunosuppression, the female-only effect in tumor decrease might be due to some tumor-specific factor(s).

It should be noted that the extent of lung tumor reduction in p38αΔ^{Lys} mice was slightly variable and not always significant. We hypothesize that this could be due to the mouse housing conditions, which can affect their microbiome and result in alterations of the immune response, as has been reported by others (Burberry et al., 2020; Dickson et al., 2018). Of note, we observed an increase in T-regs in lungs with tumors of p38αΔ^{Lys} mice (**Figure R5**), and T-regs seem to be also slightly increased in basal lungs, supporting a tumor-independent effect. The increased number of T-regs could be due to a compensatory mechanism due to the increase in effector T cells (Chen & Mellman, 2013). However, the delicate balance of effector and T-regs, which we argue can be affected by the basal inflammation state of the animals, might be tilted somehow and cause variability in the phenotype.

We observed that the numbers of different immune cell populations did not change in the lungs with tumors of p38αΔ^{Lys} mice compared to WT mice (**Figure R4**). For this reason, we performed transcriptomics analysis to find differences between immune populations of WT and p38αΔ^{Lys} mice that could explain the differences in tumorigenesis. Using both sc-RNA-Seq and RNA-Seq technologies, we concluded that the LysM-Cre directed deletion of p38α mainly affected AMs. Strikingly, one of the most interesting observations was that strong transcriptional differences between the two genotypes were already present in lungs without tumors (**Figure R7**). The formation of tumors did not seem to produce major changes in the transcriptional

profile of AMs, either in WT or p38αΔ^{Lys} mice, suggesting that the homeostatic changes caused by p38α deletion in myeloid cells was responsible for the reduce tumorigenesis. This restricted plasticity of AMs in pathologies and, in general, of tissue-resident macrophages in comparison with the bone-marrow derived macrophages, has also been reported by others. A recent study showed that AMs promote invasion of NSCLC tumors, but have few chromatin and transcriptional changes in response to tumors, most of them related to antigen presentation and tissue remodelling (Casanova-Acebes et al., 2021). It has been proposed that the reduced plasticity of tissue-resident macrophages is caused by their prolonged residency in the tissue, together with their self-renewal capacities (Guilliams & Svedberg, 2021). This restricted plasticity has been favoured by evolution to safeguard the homeostasis of the tissue (Guilliams & Svedberg, 2021).

Role of p38α in AMs and lung immunity

Amongst the changes in RNA-Seq transcriptomic analysis, we found a very significant increase in the antigen presentation capacity via MHCII of the p38αΔ^{Lys} AMs (**Figure R7-8-9**). Since antigen presentation provides the signals for T cell activation, we assume that the increase in effector T cells in the lungs of p38αΔ^{Lys} mice is probably given by the increased MHCII in AMs. Tissue-resident macrophages are known to locally potentiate recruited T cells after DC-priming in the lymph nodes (T. Kawasaki et al., 2022; Low et al., 2020). The MHCII increase in p38αΔ^{Lys} AMs was supported by experiments using the p38α inhibitor LY, which also increased MHCII in AMs, although less than the p38αΔ^{Lys}, and slightly decreased the lung tumor load (**Figure R14**). The milder effectivity of LY could be due to its difficulty to reach the restricted alveolar space. In this regard, preliminary experiments using intratracheal administration of clodronate liposomes have shown promising results specifically targeting AM, so experiments using liposome-encapsulated compounds are worth trying to selectively inhibit p38α in AMs and decrease lung tumor burden. Besides, p38αBAC mice, which overexpress p38α, present decreased expression of MHCII in AMs and a reduced effector phenotype in lung T cells (**Figure R35**), supporting a connexion between MHCII levels in AMs and the activation phenotype of the T cells in the lungs. Notwithstanding that the p38αBAC model leads to the potential ubiquitous overexpression of the p38α protein while p38αΔ^{Lys} mice bear specific p38α deletion in myeloid cells, these observations further support that p38α promotes the development of lung metastasis and provide support for the potential use of p38α inhibitors to treat this pathology.

Bioinformatic analysis of the RNA-Seq data in AMs showed that, apart from the striking increase in antigen presentation by MHCII, there was an unexpected limited amount of classical M1-like macrophage polarization factors that could favour an anti-tumoral response in the lungs of p38αΔ^{Lys} mice. Instead, we observed that several processes related to intrinsic functions of AMs were dysregulated in p38αΔ^{Lys} mice (**Figure R7**). This observation goes in line with the view that the M1/M2-like classification is a simplistic way of defining the complex plasticity of macrophages *in vivo*. AMs are a very specialized cell type with important functions to maintain lung immunosuppression and avoid unnecessary inflammation. To sustain immune tolerance, AMs maintain antigen presentation restricted and have a substantial "immune-silent" phagocytic capacity (Aegerter et al., 2022; Roberts et al., 2017). In this sense, p38α seems to be implicated in these tolerogenic functions both by restricting MHCII and its co-stimulatory molecules CD80, OX40L, and by increasing PD-L1 (**Figure R8-9**). Functional studies of antigen presentation *in vitro* proved that p38αΔ^{Lys} AMs have a higher capacity to induce T cell proliferation and activation (**Figure R12**). Also, p38α maintains the CD200-CD200R signalling axis (**Figure R9**), which is crucial to maintain firm adhesion to the lung epithelium and immunosuppression in AMs (Bissonnette et al., 2020). When this signal is lost by epithelial damage, AMs become activated. Previous literature has reported the activation of p38α signalling downstream of CD200 in macrophages (B. Zhu et al., 2019), pointing at the cross-regulation of both molecules. Moreover, TGFβRII or MARCO, which are known to cause TAM immunosuppression by inducing T regs in lung tumors (Fleur et al., 2021), were also found downregulated in the p38αΔ^{Lys} mice (**Figure R9**). This loss of tolerance, however, did not impair p38αΔ^{Lys} mouse health, as they suffered no particular lung inflammatory alterations. However, these animals were housed in very clean conditions. The lung immune tolerance capacity was indeed challenged by using mouse models that trigger lung inflammation like HDM-induced asthma or LPS-induced acute lung injury, where we observed an exacerbated inflammatory response in the p38αΔ^{Lys} mice in both models (**Figure R26-R29**), supporting the idea that p38α in AMs maintains immune tolerance and restricts lung inflammation. It seems likely that the same immunosuppressive mechanisms provided by p38α to prevent massive immune reactions are harnessed by cancer cells to facilitate lung tumor formation.

We observed a reduction of phagocytosis markers and a reduced capacity in *in vitro* functional studies both using genetic deletion or chemical inhibition of p38α (**Figure R25**). Since internalization of antigens is required for their subsequent presentation, the reduction of phagocytic capacity and certain pattern recognition receptors in

p38αΔ^{Lys} AMs seemed to contradict the observed increase in antigen presentation. This apparent contradiction could be due a p38α-independent negative feedback mechanism limits the increase in antigen presentation or contribute to, as some authors propose, a "defence-ready" strategy of the cells to be ready to fight against persistent immune challenges (Martin et al., 2021). The function of p38α in phagocytosis has been studied before using mainly chemical inhibitors in assays of fluorescently-labelled bacteria, pressure-induced or bead phagocytosis, showing either an increase or no effect upon p38α inhibition (Bewley et al., 2016; Blander & Medzhitov, 2004; Kang et al., 2008; X. Li et al., 2003; Scheraga et al., 2020; Shiratsuchi & Basson, 2005). The discrepancy between those studies and our observations can be due to different reasons. In contrast to other studies, which used peritoneal macrophages or the THP-1 cell line (Blander & Medzhitov, 2004; Shiratsuchi & Basson, 2005), we used primary AMs, which have been exposed to life-long prolonged alveolar signals that can affect their phagocytic capacity. Moreover, we observed a reduced phagocytosis in BMDMs upon p38α inhibition with PH, while published data showed no effect in the phagocytosis of BMDMs inhibiting p38α with SB203580 (X. Li et al., 2003) or with SCIO469 and VX745 (Bewley et al., 2016). This suggests that the type of chemical inhibitor affects the outcome, which is supported by an interesting study showing that different pharmacologic inhibitors of p38α produce contradictory effects in the expression of inflammatory factors by macrophages (Raza et al., 2017).

Moreover, we observed that that p38α-inhibited AMs had a decreased efferocytosis (**Figure R25**), an immune-silent engulfment of apoptotic cells. In fact, some anti-tumoral drugs aim at decreasing efferocytosis and promote a pro-inflammatory environment by for instance blocking the "eat-me" signals in cancer cells (Y. Zhou et al., 2020). In our experiments, the decreased efferocytosis in p38α-inhibited AMs was accompanied by an increase in effector $CD4^+$ and $CD8^+$ T cells in lungs of p38αΔLys mice, a relation that has frequently been observed by others in conditions where immunosuppression is lost (Chao et al., 2010; Cook et al., 2013; Jinushi et al., 2009; Loeser et al., 2007; Paolino et al., 2014). Previous studies have reported in a human dermal model of acute inflammation, that p38α reduces efferocytosis by controlling the expression of TIM-4 in macrophages (De Maeyer et al., 2020). Others have shown no effect of p38α inhibition in human COPD-derived AMs or monocyte-derived macrophages (Bewley et al., 2016). The reasons for these discrepancies can be similar to the ones stated before for phagocytosis. Thus, although p38α can clearly regulate phagocytosis and efferocytosis, whether it promotes it or not depends on the context, as other functions of p38α (Canovas & Nebreda, 2021). In our case, the reduced phagocytic capacity of AMs provides further evidence that immune tolerance is lost in lungs of p38αΔ^{Lys} mice.

The RNA-Seq data revealed that the expression of known targets of PPARγ, a main transcription factor in AMs, was affected in the AMs from p38αΔ^{Lys} mice (**Figure R9-10**). These changes were comparable to the ones described in a PPARγ KO AMs (A. D. Baker, Malur, Barna, Ghosh, et al., 2010). Using the LysM-Cre model, these authors showed that the deletion of PPARγ in AMs decreases LXRα and increases CYP27A1 and ApoE, which our data nicely reproduced, together with other PPARγ described targets such as LPL or CD36 (A. D. Baker, Malur, Barna, Kavuru, et al., 2010; T. H. Kim et al., 2013) (**Figure R9-10**). This suggests that PPARγ could be regulated by p38α,as it has been described in other systems (Ptasinska et al., 2007; Puigserver et al., 2001; Schild et al., 2006). There is also evidence of p38α activation by GM-CSF, a known activator of PPARγ in AMs (Rolli-Derkinderen et al., 2003; Schneider et al., 2014; Suzuki et al., 2001). Besides, the dysregulation in PPARγ signaling is consistent with processes involved in cholesterol and lipid metabolism being affected in AMs from p38αΔ^{Lys} mice, as shown by a decrease in GO related to cholesterol homeostasis and lipid storage in the RNA-Seq analysis (**Figure R8**), which predicts a lower capacity of AMs to catabolize those lipids. Similar effects were reported in the PPARγ KO AMs, in which dysregulation of lipid metabolism affected their ability to catabolize pulmonary surfactant (A. D. Baker, Malur, Barna, Ghosh, et al., 2010). Since lipid catabolism is associated to immunosuppressive and tolerogenic functions (R. Y. Ma et al., 2022), this result supports that p38αΔ^{Lys} mice have a reduced immunosuppression. The maintenance of lung surfactant homeostasis and the metabolic profile of AMs, however, have not been explored in our p38αΔ^{Lys} mice yet.

AMs from p38αΔ^{Lys} mice also have a significant downregulation in genes, markers and transcription factors that have been described to have crucial functions, such as Car4, Bhlhe40, Blhehe41, Fabp5, Fabp4, Krt79 (**Figure R9-10**) (Aegerter et al., 2022; Lavin et al., 2014; Rauschmeier et al., 2019). Interestingly, genes that are important for AM self-renewal capacity, such as Klf2 and Klf4, were found upregulated. This suggests that p38α may control not only the main functions of AMs, but also their cellular identity. Furthermore, a previous sc-RNA-seq study described subclassifications of AMs based on proliferative capacity and inflammatory programing (Mould et al., 2019). This distinction could be applied to our sc-RNA-Seq data to determine whether the deletion of p38α skews AMs to one of those newly described subpopulations. Besides, lung recruited macrophages, which appear in the lungs when there are perturbations in the homeostasis and are described to be more inflammatory than tissue resident macrophages (Aegerter et al., 2022), express a combination of markers which are curiously found upregulated in p38αΔ^{Lys} AMs, such as increased S100A6,

S100A4, APOe and C5ar and decreased MARCO (**Figure R9-10**). One possible interpretation could be that the absence of p38α leads to AM death, which results in a life-long increased recruitment to maintain the pool of macrophages in lungs of p38αΔ^{Lys} mice. This would be supported by the observation that p38αΔ^{Lys}-derived AMs proliferate worse in culture. Lineage tracing experiments should be performed to investigate this possibility.

MHCII regulation by p38α in macrophages

Transcriptomic and FACS analysis showed that p38α restricts the expression of MHCII in AMs (**Figure R11 and R13**). Of note, the negative regulation of MHCII by p38α seems to be AM-specific, since peritoneal macrophages from p38αΔ^{Lys} mice do not show this effect (**Figure R13**). This supports the context-specific regulation of p38α of diverse biological processes and, at the same time, the finely-tuned regulation of MHCII in different APCs. However, we have not been able to identify the alveoli-specific signal that could trigger this downregulation (**Figure R16**), and culture of primary AMs revealed that the negative regulation of MHCII by p38α is maintained ex-vivo for up to 8 days (**Figure R16**), probably though a mechanism of epigenetic memory, which could involve HDAC6 activity.

Studies using BMDMs have led us to propose a model in which the activity of p38α and MK2, triggered by LPS in BMDMs, regulates CIITA expression probably via HDAC6, which silences CIITA. This leads to the inhibition of MHCII transcription and reduced antigen presentation capacity (**Figure D1**). Although we have seen that CIITA/MHCII regulation by p38α is robust amongst AMs and BMDMs, the implication of HDAC6 remains to be validated in AMs *in vivo*. Based on the RNA-Seq results, HDAC6 mRNA seems unchanged in p38αΔ^{Lys} AMs (**Figure R22**), suggesting that it could be post-translationally regulated by p38α. Interestingly, we observed a very significant upregulation of HDAC11 and to a less extent, HDAC10 or HDAC5 (**Figure R22**). We argue that the increased expression of HDACs in p38αΔ^{Lys} AMs could be due to a compensatory mechanism resulting from the proposed HDAC6 inhibition by p38α. Curiously, HDAC6 and HDAC11 have been described to form a complex that regulates IL-10 in APCs (Cheng et al., 2014), supporting the idea that different HDACs may interact in macrophages.

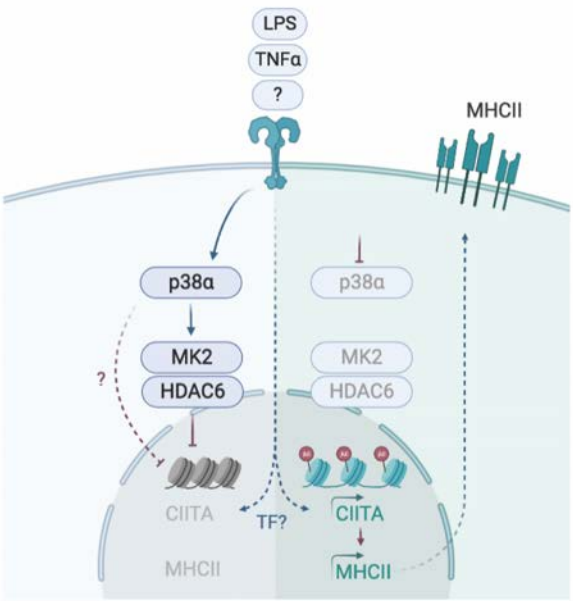

Figure D1. Proposed model of CIITA/MHCII regulation by p38α in macrophages.
The kinase p38α controls CIITA transcription partially though its substrate MK2, which regulates the gene silencer HDAC6. This ultimately regulates MHCII expression in macrophages and their capacity to perform antigen presentation. In BMDMs, this regulation is triggered by LPS or TNFα, which activate p38α and probably regulate some additional CIITA transciption factor. Designed with Biorender.

The use of BMDMs to model AMs has some limitations. First of all, the different developmental origin of the cells could alter the regulation of the pathways, especially given the context-dependency of p38α. This is illustrated by the fact that in comparison to AMs, BMDMs from p38αΔ^{Lys} mice did not completely delete p38α and did not overexpress MHCII (**Figure R15**). This might be because the LysM promoter is not fully expressed or the Cre-mediated cleavage of MAPK14 is less efficient in BMDMs. On the other hand, the requirement for LPS or TNFα to induce MHCII overexpression in p38α-inhibited BMDMs (**Figure R15**) contrasts with the constitutive overexpression of MHCII observed in p38αΔ^{Lys} AMs (**Figure R13**). BMDMs might need LPS or TNFα to surpass an activation threshold that keeps their inflammation capacity low, or to lead to the activation of a CIITA transcription factor (**Figure D1**), since the sole inhibition of p38α in BMDMs did not induce MHCII upregulation. Another difference between AMs and BMDMs is the differential regulation of CIITA isoforms by p38α. While all three isoforms are active in p38αΔ^{Lys} AMs, p38α-inhibited BMDMs have increased pIII and pIV but not pI upon stimulation with LPS or TNFα (**Figure R18**). Again, this could be due to their different developmental origin or to the different timings, as CIITA mRNA in BMDMs was only checked up to 24 h (**Figure R18**). The fact

that p38αΔ^{Lys} AMs show a general activation of all three CIITA promoters suggest that p38α is a general regulator of CIITA, more than a promoter specific regulator as described for IFNγ. This supports that CIITA regulation by p38α could involve HDACs like HDAC6, whose specific inhibition in BMDMs affects the expression of all CIITA isoforms upon LPS treatment (**Figure R23**).

The p38α and the MK2 inhibitors gave very similar phenotypes in the transcriptional regulation of CIITA/MHCII both by FACS and at mRNA level (**Figure R21**). However, we observed that the induction of CIITA and MCHII by the MK2 inhibitor was partial compared to the one induced by the p38α inhibitor. This suggests that p38α could have a MK2-independent role in the regulation of CIITA. One hypothesis is that the alternative silencing of CIITA by p38α could be done by HDAC4, found to be significantly downregulated in the RNA-Seq of AMs (**Figure R22**). Another possibility could be that p38α regulates the transcription factor USF1, which was found upregulated in the p38αΔ^{Lys} AMs, and has been involved in the transcriptional regulation of CIITA (Muhlethaler-Mottet et al., 1998).

HDACs are known to regulate antigen presentation at different levels (Woan et al., 2012). Previous literature using the RAW 264.7 cell line provide evidence for the regulation of CIITA by p38α mediated by HDACs (Yao et al., 2006). Although those experiments were restricted to the regulation of CIITA pIV by IFNγ, we have found that p38α also regulates pI and pIII of CIITA. Our TSA experiments in BMDMs proved the implication of HDACs in the expression of CIITA (**Figure R22**), but did not provide a direct link to p38α. Given the nature of studying a negative regulation, it becomes difficult to prove causality since rescue experiments were not possible. However, the fact that the inhibition of both p38α and HDACs resulted in very similar patterns of CIITA and MHCII regulation support that they could functionally interact. We also noticed a slight additive effect on MHCII expression upon combining TSA or NEX inhibitors with the p38α inhibitor (**Figure R22-23**). This might be due to the HDAC inhibition additionally affecting the transcription of MHCII independently of CIITA, which is known to be also regulated by histone modifiers (Wright & Ting, 2006). Finally, the preliminary IP experiment showing MK2-HDAC6 interaction is an interesting finding that could be worth of further characterization (**Figure R24**). However, the complex forms also upon p38α inhibition suggesting that the interaction is not affected by MK2 phosphorylation. HDAC6 phosphorylation by MK2 is unlikely, since HDAC6 does not have MK2 phosphorylation motifs (Hornbeck et al., 2015), and the hypothesis could be that upon activation MK2 determines the nuclear localization

of HDAC6, which is described to have some cytoplasmic localization (Seto & Yoshida, 2014).

Myeloid p38α in lung inflammatory diseases

The role of p38α in maintaining lung immunosuppression is further supported by the results in the models of lung inflammation with HDM or LPS, which have an exacerbated inflammatory response in p38αΔ^{Lys} mice (**Figure R26-29**). However, these results do not agree with previously published literature, where the use of several p38α chemical inhibitors was shown to ameliorate inflammatory symptoms in preclinical models of asthma, COPD and acute lung injury. Published asthma studies used the p38α inhibitors SB239063 (Bao et al., 2017; L. Liang et al., 2013; Underwood et al., 2000), SB202190 (Choudhury et al., 2002), SD-282 (J. Y. Ma et al., 2008; Nath et al., 2006), SB203580 (Escott et al., 2000; Q. Wu et al., 2018) and CHF6297 (Martucci et al., 2017). Preclinical models of acute lung inflammation and COPD also used different p38α inhibitors, such as M39 (Nick et al., 2000, 2002) or SB203580 (D. Li et al., 2018). On the other hand, we have used a genetic deletion of p38α in myeloid cells, which has allowed us to study the contribution of p38α specifically in those cells to the biology of asthma and inflammation. However, we cannot rule out that systemic p38α inhibitors affecting other lung epithelial and immune cells could have different effects in this pathology. For instance, a study modelling COPD in mice using LPS and cigarette smoke show that increased expression of p38α in type II alveolar epithelial cells was responsible for the severity of the disease (Amano et al., 2014). Thus, the type of p38α inhibition and, more specifically, the cell type in which p38α is inhibited can have either pro- or anti-inflammatory roles, which could explain the modest effect of p38 MAPK inhibitors in clinical trials. Noteworthy, other published studies using LysM-Cre-mediated genetic deletion of p38α have also shown unexpected increased inflammation in models or arthritis and skin injury (Guma et al., 2012; C. Kim et al., 2008), demonstrating that genetic deletion offers mechanistic information which is not necessarily consistent with the use of pharmacological inhibitors. Besides, we have used HDM to induce asthma, which is a physiological allergen that better models asthma in humans, while the majority of published studies using p38α inhibition use OVA to induce the disease. Finally, given that a major player in asthma is antigen presentation by MHCII via macrophages and DCs, which is the first event that triggers the Th2 inflammatory response (Tang et al., 2022), we think that MHCII regulation by p38α should be taken into account in lung inflammatory diseases such as asthma in which p38α inhibitors are tested.

p38α overexpression *in vivo*

The association of p38α with biological and pathological processes is commonly performed though the use of pharmacological inhibitors, knock-down and KO studies. Although genetic downregulation models are very useful, the direct implication of p38α in a pathological condition can be further supported with experiments of overexpression. There are some published studies using models of p38α intrinsic activation but, to our knowledge, an *in vivo* p38α-overexpression model using BAC constructs has not been reported before. A recent study with mice expressing an inducible and constitutively active p38α showed a 40% mortality and dramatic loss of body weight in the mice, although no particular histological differences were observed (Darlyuk-Saadon et al., 2021). In contrast to those results, p38αBAC mice neither show any health problems in homeostasis nor we observe histological differences in the tissues analysed. This is probably due to the fact that p38αBAC mice show small increases in p38α mRNA levels that did not particularly enhance the quantity of the protein in several mouse tissues (**Figure R30**). Similarly, BMDMs from p38αBAC mice show a slightly increased MK2 phosphorylation, which does not lead to increased expression of the downstream inflammatory mediators. This probably means that the cells have mechanisms to keep the p38α protein expression at certain levels as well as to regulate the pathway activity fluctuations (**Figure R31**).

Experiments using p38αBAC mice confirmed the published role of p38α in several physiological and pathological conditions, including the regulation of CDK inhibitors in ageing spleen and liver (Wong et al., 2009), the CCl_4-induced acute liver damage (Fortier et al., 2019) and the DSS-induced colitis (Youssif et al., 2018) (**Figures R32-34**). Although we have not tested the proposed molecular mechanisms, our experiments support the potential use of the p38αBAC mice to study diseases in which p38α can be implicated. Most importantly, the p38αBAC model has provided additional evidence for the negative regulation of MHCII by p38α in AMs, as increased levels of p38α resulted in lower levels of MHCII in AMs (**Figure R35**). However, increased protein levels of p38α in AMs from p38αBAC mice have not been verified yet. The increase in MHCII was nicely accompanied by a decrease in effector $CD4^+$ and $CD8^+$ T cells and an increase in lung tumors, supporting the causality between levels of MHCII in AMs, the number of effector T cells and the lung tumor burden. Interestingly, the published study using constitutively active p38α also shows differences in the lungs, as an increase in M2-like markers in AMs such as iNOS and Arg1 (Darlyuk-Saadon et al., 2021). This data is consistent with our findings that p38α regulates the immunosuppressive phenotype of AMs.

Altogether, we have shown that the p38α kinase in myeloid cells contributes to the intrinsic properties of lung immune homeostasis by regulating crucial functions of AMs. Most importantly, by regulating MHCII through CIITA transcription, p38α regulates the immunosuppressive functions of AMs, and this ultimately determines the outcome of lung inflammatory diseases and cancer.

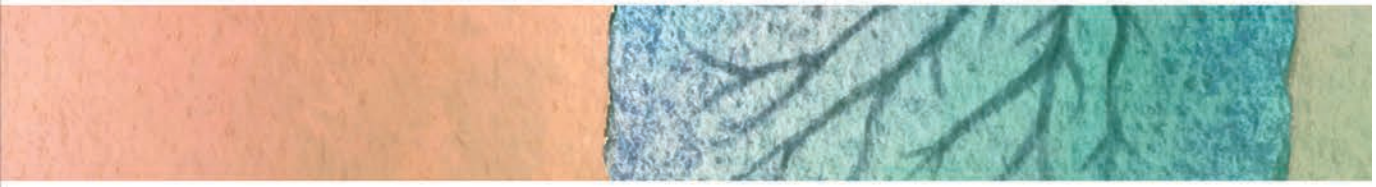

Conclusions

- Myeloid p38α does not affect primary melanoma tumor development.
- Myeloid p38α facilitates lung tumor metastasis by controlling immune suppression in the lung.
- p38α regulates crucial physiological processes in alveolar macrophages that can affect tumor progression in the lung.
- p38α regulates antigen presentation via MHCII in macrophages through transcriptional regulation of CIITA probably involving MK2 and HDAC6.
- Myeloid p38α has a protective role in asthma and acute lung injury.
- Overexpression of p38α is sufficient to induce increased MHCII expression in alveolar macrophages.

Supplementary material

Supplementary Table 1 | Top 100 upregulated genes in RNA-Seq of p38$\alpha\Delta^{Lys}$ AMs

100 top upregulated genes found in p38$\alpha\Delta^{Lys}$ (KO) AMs compared to WT AMs in tumor conditions and values for the same genes in basal conditions. Genes are classified in descending order of the FC.shrinked in the KOvsWT Tumor condition. pval.adj=p value adjusted, FC.shrinked= fold change shrinked.

Gene symbol	KOvsWT Tumor pval.adj	KOvsWT Tumor FC.shrinked	KOvsWT Basal pval.adj	KOvsWT Basal FC.shrinked
Map2k6	0,00000	62,453	0,00000	58,494
Cfap161	0,00000	22,417	0,00000	13,608
Stk32c	0,00000	11,699	0,00000	9,346
Zfp273	0,00001	10,014	0,00155	3,081
Cbx8	0,00000	9,331	0,00000	7,729
D930048N14Rik	0,00000	8,633	0,00103	3,256
Gm10384	0,00000	8,078	0,00000	5,922
Ciita	0,00000	7,935	0,00000	5,961
Fbxo31	0,00000	7,447	0,00000	7,910
Dclk3	0,00051	6,576	0,00001	22,809
H2-Eb1	0,00000	6,424	0,00000	5,036
Kif5c	0,00047	5,879	0,00013	5,982
H2-Aa	0,00000	5,720	0,00000	4,579
Slc7a4	0,00000	5,120	0,00000	4,186
H2-Ab1	0,00000	5,064	0,00000	4,177
Syt3	0,00057	4,989	0,00479	2,574
Tnfsf10	0,00009	4,951	0,00000	9,785
Mir5107	0,00000	4,792	0,00000	3,543
Sall2	0,00001	4,733	0,00000	6,924
Cd74	0,00000	4,629	0,00000	3,903
Klhl33	0,00036	4,621	0,00000	8,536
Cyp27a1	0,00000	4,578	0,00000	2,816
Ndrg1	0,00000	4,410	0,00000	7,503
Sorl1	0,00000	4,249	0,00000	4,818
Zfp395	0,00000	4,201	0,00000	7,122
S100a6	0,00000	4,137	0,00000	5,226
Gpr171	0,00002	4,126	0,00003	3,925
G0s2	0,00000	4,093	0,00000	4,826
Akap5	0,00068	4,029	0,00002	5,841
Zfp61	0,00000	3,952	0,00001	3,659
Tspan13	0,00000	3,893	0,00000	4,543
Tfap4	0,00051	3,760	0,00002	5,640
Ccdc166	0,00004	3,674	0,00005	3,410
Tsc22d3	0,00000	3,626	0,00000	2,900
Hmga2-ps1	0,00025	3,602	0,00004	4,140
Zfp760	0,00004	3,581	0,00018	2,891
Sgsh	0,00001	3,530	0,00000	9,382
Bmf	0,00015	3,529	0,00000	7,500
Hhex	0,00006	3,522	0,00000	5,557
Sox12	0,00253	3,515	0,00937	2,324
Gbp8	0,00004	3,499	0,00228	2,267
Il15	0,00001	3,496	0,00002	3,209

Svip	0,00324	3,486	0,00046	5,182
Lpar5	0,00150	3,445	0,00000	8,175
Arhgap22	0,00000	3,377	0,00000	3,021
H2-Oa	0,00000	3,360	0,00000	3,552
Amer1	0,00002	3,342	0,00031	2,623
S100a4	0,00000	3,328	0,00000	4,427
Klhl42	0,00000	3,236	0,00000	3,316
Tmem71	0,00000	3,224	0,00001	2,574
Ksr1	0,00003	3,136	0,00025	2,608
Ephx1	0,00000	3,133	0,00000	2,910
Prkcb	0,00000	3,123	0,00002	2,806
Tnfsf13b	0,00001	3,067	0,00000	3,992
Spred2	0,00007	3,020	0,00268	2,142
Zfp870	0,00088	2,954	0,01225	1,931
Hnmt	0,00421	2,947	0,00009	5,098
Trim65	0,00000	2,904	0,00000	2,931
4930431P03Rik	0,00178	2,888	0,00860	2,110
Sap25	0,00000	2,856	0,00002	2,386
Eif4e3	0,00013	2,851	0,00000	4,410
Castor2	0,00004	2,849	0,00388	1,906
H2-DMb1	0,00000	2,845	0,00000	2,316
Mtus1	0,00226	2,836	0,00001	4,901
Aoah	0,00038	2,817	0,00140	2,360
Hdac11	0,00258	2,816	0,00018	3,998
Sh3pxd2a	0,00004	2,804	0,00000	3,809
Frmd4b	0,00054	2,796	0,00001	3,597
Rab3a	0,00123	2,773	0,00127	2,584
Card14	0,00317	2,768	0,00007	4,995
Zfp658	0,00178	2,664	0,00000	5,375
Clec2l	0,00250	2,633	0,00050	2,803
Dnajc28	0,00147	2,631	0,00372	2,130
BC051537	0,00191	2,629	0,00040	2,986
Cldn1	0,00011	2,603	0,00008	2,512
Vash1	0,00000	2,602	0,00011	1,898
Atp23	0,00374	2,574	0,00069	3,079
Pstk	0,00118	2,571	0,00007	3,017
Lrrc25	0,00080	2,555	0,00103	2,327
2810021J22Rik	0,00039	2,512	0,00096	2,194
Fbxo21	0,00005	2,497	0,00000	2,701
Rhobtb2	0,00185	2,487	0,00009	3,106
Arl4c	0,00004	2,485	0,00000	2,871
Mettl7a1	0,00007	2,476	0,00007	2,370
Traf3ip3	0,00091	2,435	0,00000	3,341
Rgs2	0,00129	2,429	0,00001	3,378
Zfp770	0,00004	2,426	0,00007	2,237
Scarf1	0,00935	2,397	0,00172	2,955
Sobp	0,00675	2,391	0,00081	3,041
Rarg	0,00510	2,363	0,00026	3,190
Etaa1	0,00005	2,360	0,00012	2,128
Ptprs	0,00013	2,357	0,00085	1,985
Lrrcc1	0,00359	2,336	0,00824	1,967
Zbtb18	0,00010	2,333	0,00001	2,500
Mvb12b	0,00001	2,319	0,00013	1,958

Mfap3l	0,00360	2,317	0,00003	3,405
Tlr3	0,00118	2,308	0,00054	2,297
H2-DMb2	0,00118	2,304	0,00007	2,643
Ccdc142	0,00018	2,301	0,00090	1,972
AI467606	0,00109	2,299	0,00002	2,832

Supplementary Table 2 | Top 100 downregulated genes in RNA-Seq of p38αΔ^{Lys} AMs
100 top downregulated genes found in p38αΔ^{Lys} (KO) AMs compared to WT AMs in tumor conditions and values for the same genes in basal conditions. Genes are classified in ascending order of the FC.shrinked in the KOvsWT Tumor condition. pval.adj=p value adjusted, FC.shrinked= fold change shrinked.

Gene symbol	KOvsWT Tumor pval.adj	KOvsWT Tumor FC.shrinked	KOvsWT Basal pval.adj	KOvsWT Basal FC.shrinked
Egfem1	0,00000	-68,018	0,00000	-34,145
Cd200	0,00000	-14,214	0,00000	-14,930
Efr3b	0,00000	-8,271	0,00000	-8,144
Cspg4	0,00000	-7,763	0,00000	-5,339
Plin1	0,00000	-6,150	0,00013	-3,882
Colec12	0,00000	-5,921	0,00000	-9,949
Met	0,00005	-4,665	0,00000	-9,111
Pdk4	0,00000	-4,378	0,00000	-4,704
Awat1	0,00004	-3,980	0,00001	-4,644
Zfyve9	0,00031	-3,379	0,00008	-3,729
Fstl1	0,00000	-3,305	0,00000	-3,293
Fabp4	0,00000	-3,199	0,00000	-3,220
Cav1	0,00000	-3,155	0,00001	-2,742
Plk3	0,00000	-3,074	0,00000	-4,531
Nabp1	0,00021	-2,967	0,01225	-1,843
Pex11a	0,00004	-2,895	0,00005	-2,760
Marco	0,00002	-2,878	0,00000	-3,968
Fzd8	0,00005	-2,822	0,00000	-3,565
Slc39a2	0,00000	-2,751	0,00004	-2,367
Cd36	0,00000	-2,643	0,00000	-3,239
Rgcc	0,00360	-2,629	0,00262	-2,580
Lyz2	0,00000	-2,617	0,00000	-2,353
Phlda3	0,00018	-2,615	0,00059	-2,256
A930017K11Rik	0,00412	-2,442	0,00015	-3,439
Celsr3	0,00086	-2,416	0,00824	-1,825
Clec7a	0,00000	-2,377	0,00000	-2,641
Cyfip2	0,00263	-2,341	0,00000	-5,603
Rhov	0,00812	-2,339	0,00067	-3,230
Efnb2	0,00602	-2,323	0,00003	-4,213
Zfp503	0,00215	-2,322	0,00000	-3,677
Zfp36	0,00005	-2,289	0,01133	-1,583
Sqle	0,00017	-2,275	0,00082	-1,960
Krt79	0,00009	-2,225	0,00023	-2,013
Ctsk	0,00069	-2,220	0,00002	-2,572
Bag3	0,00094	-2,167	0,00011	-2,367

Sgk1	0,00023	-2,153	0,00007	-2,192
Casz1	0,00003	-2,129	0,00024	-1,857
Tbc1d2	0,00039	-2,112	0,00182	-1,820
Plk2	0,01686	-2,099	0,00274	-3,315
Clec4n	0,00322	-2,076	0,00117	-2,156
Chrm3	0,01613	-2,042	0,00027	-3,830
Ric1	0,00049	-2,027	0,00001	-2,353
Naip2	0,00031	-1,985	0,00000	-2,502
Fbxl5	0,00289	-1,984	0,00003	-2,598
Fasn	0,00012	-1,971	0,00005	-1,986
Map6	0,01266	-1,941	0,00015	-3,005
Top1	0,00185	-1,929	0,00000	-3,060
Lrp12	0,00200	-1,928	0,00000	-2,688
Hsd17b7	0,00377	-1,916	0,00001	-2,749
Cpeb4	0,00191	-1,908	0,00000	-3,650
Plekhg1	0,00081	-1,892	0,00000	-2,685
Olr1	0,00189	-1,872	0,00001	-2,455
Sc5d	0,00137	-1,870	0,00000	-2,463
Car4	0,01330	-1,868	0,00708	-1,938
Ubqln1	0,00001	-1,857	0,00000	-2,028
Plcb1	0,00637	-1,844	0,00058	-2,165
Fosl1	0,02983	-1,840	0,00016	-4,477
Maoa	0,00091	-1,839	0,02086	-1,476
Sde2	0,00534	-1,836	0,00011	-2,360
Dnajb9	0,00400	-1,829	0,00028	-2,135
Gm11545	0,02046	-1,777	0,00407	-2,106
Lrrc59	0,00017	-1,768	0,00000	-2,106
Cdr2	0,00292	-1,760	0,00164	-1,784
Id2	0,02556	-1,755	0,00018	-3,024
Gmppb	0,00108	-1,755	0,03257	-1,415
St6galnac4	0,00707	-1,748	0,00087	-2,006
Ptgir	0,02631	-1,726	0,00009	-3,119
Sesn2	0,01389	-1,726	0,00013	-2,485
Kdelr2	0,00412	-1,715	0,00577	-1,652
Igf2bp2	0,00430	-1,698	0,00163	-1,788
Tob2	0,00289	-1,698	0,00000	-2,318
Gnat3	0,03753	-1,694	0,00891	-2,479
Tapt1	0,00880	-1,646	0,00001	-2,437
Nr1h3	0,02642	-1,642	0,00027	-2,520
Cyp51	0,02983	-1,641	0,02091	-1,703
Eef1e1	0,00598	-1,629	0,00438	-1,656
Nsf	0,00791	-1,628	0,03154	-1,469
Gdf15	0,04983	-1,627	0,00597	-2,415
Fnip2	0,01993	-1,622	0,00003	-2,641
Serpine1	0,02790	-1,621	0,00010	-2,705
Adm	0,04481	-1,618	0,00137	-3,957
Sh2b2	0,02036	-1,612	0,00043	-2,216
Alas1	0,01776	-1,609	0,00030	-2,202
Hmgcr	0,02897	-1,608	0,00154	-2,152
Pprc1	0,00243	-1,593	0,00002	-1,956
E030018B13Rik	0,05441	-1,589	0,00119	-4,064
Plin2	0,01444	-1,584	0,01482	-1,584
Tfrc	0,01973	-1,581	0,00000	-3,440

Atp2a2	0,00315	-1,580	0,00013	-1,840
Srebf2	0,00123	-1,573	0,00018	-1,698
Samd4b	0,00200	-1,572	0,00055	-1,671
Pcyt1a	0,00510	-1,568	0,00086	-1,732
Hfm1	0,05398	-1,548	0,00544	-2,800
Tuba4a	0,00706	-1,545	0,00881	-1,536
Ptges	0,06381	-1,543	0,02760	-1,848
Ero1a	0,02897	-1,541	0,00019	-2,321
Ppard	0,05334	-1,538	0,00154	-2,462
Frk	0,05669	-1,531	0,02995	-1,715
Taf7	0,04953	-1,531	0,00227	-2,238
Ear6	0,05433	-1,529	0,01224	-1,913
Ddb1	0,00098	-1,528	0,00194	-1,500

References

Abou El Hassan, M., Yu, T., Song, L., & Bremner, R. (2015). Polycomb Repressive Complex 2 Confers BRG1 Dependency on the CIITA Locus. *Journal of Immunology (Baltimore, Md. : 1950)*, *194*(10), 5007–5013.

Abram, C. L., Roberge, G. L., Hu, Y., & Lowell, C. A. (2014). Comparative analysis of the efficiency and specificity of myeloid-Cre deleting strains using ROSA-EYFP reporter mice. *Journal of Immunological Methods*, *408*, 89.

Adams, R. H., Porras, A., Alonso, G., Jones, M., Vintersten, K., Panelli, S., Valladares, A., Perez, L., Klein, R., & Nebreda, A. R. (2000). Essential role of p38α MAP kinase in placental but not embryonic cardiovascular development. *Molecular Cell*, *6*(1), 109–116.

Aegerter, H., Lambrecht, B. N., & Jakubzick, C. V. (2022). Biology of lung macrophages in health and disease. *Immunity*, *55*(9), 1564–1580.

Aguilera, K. Y., Rivera, L. B., Hur, H., Carbon, J. G., Toombs, J. E., Goldstein, C. D., Dellinger, M. T., Castrillon, D. H., & Brekken, R. A. (2014). Collagen signaling enhances tumor progression after anti-VEGF therapy in a murine model of pancreatic ductal adenocarcinoma. *Cancer Research*, *74*(4), 1032–1044.

Alam, M. S., Gaida, M. M., Bergmann, F., Lasitschka, F., Giese, T., Giese, N. A., Hackert, T., Hinz, U., Hussain, S. P., Kozlov, S. V., & Ashwell, J. D. (2015). Selective inhibition of the p38 alternative activation pathway in infiltrating T cells inhibits pancreatic cancer progression. *Nature Medicine*, *21*(11), 1337–1343.

Allard, B., Panariti, A., & Martin, J. G. (2018). Alveolar Macrophages in the Resolution of Inflammation, Tissue Repair, and Tolerance to Infection. *Frontiers in Immunology*, *9*, 1777.

Amano, H., Murata, K., Matsunaga, H., Tanaka, K., Yoshioka, K., Kobayashi, T., Ishida, J., Fukamizu, A., Sugiyama, F., Sudo, T., Kimura, S., Tatsumi, K., & Kasuya, Y. (2014). P38 Mitogen-activated protein kinase accelerates emphysema in mouse model of chronic obstructive pulmonary disease. *Journal of Receptors and Signal Transduction*, *34*(4), 299–306.

Ambrosino, C., Mace, G., Galban, S., Fritsch, C., Vintersten, K., Black, E., Gorospe, M., & Nebreda, A. R. (2003). Negative Feedback Regulation of MKK6 mRNA Stability by p38α Mitogen-Activated Protein Kinase. *Molecular and Cellular Biology*, *23*(1), 370.

Ananieva, O., Darragh, J., Johansen, C., Carr, J. M., McIlrath, J., Park, J. M., Wingate, A., Monk, C. E., Toth, R., Santos, S. G., Iversen, L., & Arthur, J. S. C. (2008). The kinases MSK1 and MSK2 act as negative regulators of Toll-like receptor signaling. *Nature Immunology 2008 9:9*, *9*(9), 1028–1036.

Anderson, N. M., & Simon, M. C. (2020). The tumor microenvironment. *Current Biology*, *30*(16), R921–R925.

Anwar, T., Arellano-Garcia, C., Ropa, J., Chen, Y. C., Kim, H. S., Yoon, E., Grigsby, S., Basrur, V., Nesvizhskii, A. I., Muntean, A., Gonzalez, M. E., Kidwell, K. M., Nikolovska-Coleska, Z., & Kleer, C. G. (2018). p38-mediated phosphorylation at T367 induces EZH2 cytoplasmic localization to promote breast cancer metastasis. *Nature Communications*, *9*(1).

Aran, D., Looney, A. P., Liu, L., Wu, E., Fong, V., Hsu, A., Chak, S., Naikawadi, R. P.,

Wolters, P. J., Abate, A. R., Butte, A. J., & Bhattacharya, M. (2019). Reference-based analysis of lung single-cell sequencing reveals a transitional profibrotic macrophage. *Nature Immunology*, *20*(2), 163–172.
Ardain, A., Marakalala, M. J., & Leslie, A. (2020). Tissue-resident innate immunity in the lung. *Immunology*, *159*(3), 245–256.
Arthur, J. S. C., & Ley, S. C. (2013). Mitogen-activated protein kinases in innate immunity. *Nature Reviews Immunology 2013 13:9*, *13*(9), 679–692.
Arthur, J. S., & Ley, S. C. (2013). Mitogen-activated protein kinases in innate immunity. *Nat Rev Immunol*, *13*(9), 679–692.
Aubas, P., Cosso, B., Godard, P., Michel, F. B., & Clot, J. (1984). Decreased suppressor cell activity of alveolar macrophages in bronchial asthma. *The American Review of Respiratory Disease*, *130*(5), 875–878.
Baker, A. D., Malur, A., Barna, B. P., Ghosh, S., Kavuru, M. S., Malur, A. G., & Thomassen, M. J. (2010). Targeted PPARγ deficiency in alveolar macrophages disrupts surfactant catabolism. *Journal of Lipid Research*, *51*(6), 1325.
Baker, A. D., Malur, A., Barna, B. P., Kavuru, M. S., Malur, A. G., & Thomassen, M. J. (2010). PPARγ regulates the expression of cholesterol metabolism genes in alveolar macrophages. *Biochemical and Biophysical Research Communications*, *393*(4), 682–687.
Baker, E. H., & Baines, D. L. (2018). Airway Glucose Homeostasis: A New Target in the Prevention and Treatment of Pulmonary Infection. *Undefined*, *153*(2), 507–514.
Balhara, J., & Gounni, A. S. (2012). The alveolar macrophages in asthma: a double-edged sword. *Mucosal Immunology*, *5*(6), 605–609.
Bao, A., Yang, H., Ji, J., Chen, Y., Bao, W., Li, F., Zhang, M., Zhou, X., Li, Q., & Ben, S. (2017). Involvements of p38 MAPK and oxidative stress in the ozone-induced enhancement of AHR and pulmonary inflammation in an allergic asthma model. *Respiratory Research*, *18*(1), 1–12.
Barclay, A. N., & Van Den Berg, T. K. (2014). The interaction between signal regulatory protein alpha (SIRPα) and CD47: structure, function, and therapeutic target. *Annual Review of Immunology*, *32*, 25–50.
Barnden, M. J., Allison, J., Heath, W. R., & Carbone, F. R. (1998). Defective TCR expression in transgenic mice constructed using cDNA-based α- and β-chain genes under the control of heterologous regulatory elements. *Immunology and Cell Biology*, *76*(1), 34–40.
Barnes, T. A., & Amir, E. (2017). HYPE or HOPE: the prognostic value of infiltrating immune cells in cancer. *British Journal of Cancer*, *117*(4), 451.
Batlle, R., Andrés, E., Gonzalez, L., Llonch, E., Igea, A., Gutierrez-Prat, N., Berenguer-Llergo, A., & Nebreda, A. R. (2019). Regulation of tumor angiogenesis and mesenchymal-endothelial transition by p38α through TGF-β and JNK signaling. *Nature Communications*, *10*(1), 3071.
Bayne, L. J., Beatty, G. L., Jhala, N., Clark, C. E., Rhim, A. D., Stanger, B. Z., & Vonderheide, R. H. (2012). Tumor-derived granulocyte-macrophage colony-stimulating factor regulates myeloid inflammation and T cell immunity in pancreatic cancer. *Cancer Cell*, *21*(6), 822–835.

Bedoret, D., Wallemacq, H., Marichal, T., Desmet, C., Calvo, F. Q., Henry, E., Closset, R., Dewals, B., Thielen, C., Gustin, P., De Leval, L., Van Rooijen, N., Le Moine, A., Vanderplasschen, A., Cataldo, D., Drion, P. V., Moser, M., Lekeux, P., & Bureau, F. (2009). Lung interstitial macrophages alter dendritic cell functions to prevent airway allergy in mice. *The Journal of Clinical Investigation*, *119*(12), 3723–3738.

Benoit, M., Desnues, B., & Mege, J.-L. (2008). Macrophage polarization in bacterial infections. *Journal of Immunology (Baltimore, Md. : 1950)*, *181*(6), 3733–3739.

Bewley, M. A., Belchamber, K. B. R., Chana, K. K., Budd, R. C., Donaldson, G., Wedzicha, J. A., Brightling, C. E., Kilty, I., Donnelly, L. E., Barnes, P. J., Singh, D., Whyte, M. K. B., Dockrell, D. H., Gaw, A., Mayer, R. J., Tal-Singer, R., Salmon, M., & Roubenoff, R. (2016). Differential Effects of p38, MAPK, PI3K or Rho Kinase Inhibitors on Bacterial Phagocytosis and Efferocytosis by Macrophages in COPD. *PLOS ONE*, *11*(9), e0163139.

Bhattacharya, S., Qian, J., Tzimas, C., Baker, D. P., Koumenis, C., Diehl, J. A., & Fuchs, S. Y. (2011). Role of p38 Protein Kinase in the Ligand-independent Ubiquitination and Down-regulation of the IFNAR1 Chain of Type I Interferon Receptor. *The Journal of Biological Chemistry*, *286*(25), 22069.

Bhavsar, P., Hew, M., Khorasani, N., Torrego, A., Barnes, P. J., Adcock, I., & Chung, K. F. (2008). Relative corticosteroid insensitivity of alveolar macrophages in severe asthma compared with non-severe asthma. *Thorax*, *63*(9), 784–790.

Bissonnette, E. Y., Lauzon-Joset, J. F., Debley, J. S., & Ziegler, S. F. (2020). Cross-Talk Between Alveolar Macrophages and Lung Epithelial Cells is Essential to Maintain Lung Homeostasis. *Frontiers in Immunology*, *11*.

Biswas, S. K., Allavena, P., & Mantovani, A. (2013). Tumor-associated macrophages: functional diversity, clinical significance, and open questions. *Seminars in Immunopathology*, *35*(5), 585–600.

Blanck, G. (2002). Components of the IFN-gamma signaling pathway in tumorigenesis. *Archivum Immunologiae et Therapiae Experimentalis*, *50*(3), 151–158.

Blander, J. M., & Medzhitov, R. (2004). Regulation of Phagosome Maturation by Signals from Toll-Like Receptors. *Science*, *304*(5673), 1014–1018.

Blum, J. S., Wearsch, P. A., & Cresswell, P. (2013). Pathways of Antigen Processing. *Annual Review of Immunology*, *31*, 443.

Bode, J. G., Ehlting, C., & Häussinger, D. (2012). The macrophage response towards LPS and its control through the p38MAPK–STAT3 axis. *Cellular Signalling*, *24*(6), 1185–1194.

Boss, J. M., & Jensen, P. E. (2003). Transcriptional regulation of the MHC class II antigen presentation pathway. *Current Opinion in Immunology*, *15*(1), 105–111.

Boulton, T. G., & Cobb, M. H. (1991). Identification of multiple extracellular signal-regulated kinases (ERKs) with antipeptide antibodies. *Cell Regulation*, *2*(5), 357–371.

Branchett, W. J., Cook, J., Oliver, R. A., Bruno, N., Walker, S. A., Stölting, H., Mack, M., O'Garra, A., Saglani, S., & Lloyd, C. M. (2021). Airway macrophage-intrinsic TGF-β1 regulates pulmonary immunity during early-life allergen exposure.

Journal of Allergy and Clinical Immunology, *147*(5), 1892–1906.
Budczies, J., von Winterfeld, M., Klauschen, F., Bockmayr, M., Lennerz, J. K., Denkert, C., Wolf, T., Warth, A., Dietel, M., Anagnostopoulos, I., Weichert, W., Wittschieber, D., & Stenzinger, A. (2015). The landscape of metastatic progression patterns across major human cancers. *Oncotarget*, *6*(1), 570–583.
Burberry, A., Wells, M. F., Limone, F., Couto, A., Smith, K. S., Keaney, J., Gillet, G., van Gastel, N., Wang, J. Y., Pietilainen, O., Qian, M., Eggan, P., Cantrell, C., Mok, J., Kadiu, I., Scadden, D. T., & Eggan, K. (2020). C9orf72 suppresses systemic and neural inflammation induced by gut bacteria. *Nature 2020 582:7810*, *582*(7810), 89–94.
Busch, C., Favret, J., Geirsdóttir, L., Molawi, K., & Sieweke, M. (2019). Isolation and Long-term Cultivation of Mouse Alveolar Macrophages. *Bio-Protocol*, *9*(14).
Busch, R., Rinderknecht, C. H., Roh, S., Lee, A. W., Harding, J. J., Burster, T., Hornell, T. M. C., & Mellins, E. D. (2005). Achieving stability through editing and chaperoning: regulation of MHC class II peptide binding and expression. *Immunological Reviews*, *207*, 242–260.
Bustamante-Marin, X. M., & Ostrowski, L. E. (2017). Cilia and Mucociliary Clearance. *Cold Spring Harbor Perspectives in Biology*, *9*(4).
Butler, A., Hoffman, P., Smibert, P., Papalexi, E., & Satija, R. (2018). Integrating single-cell transcriptomic data across different conditions, technologies, and species. *Nature Biotechnology 2018 36:5*, *36*(5), 411–420.
Buxadé, M., Encabo, H. H., Riera-Borrull, M., Quintana-Gallardo, L., López-Cotarelo, P., Tellechea, M., Martínez-Martínez, S., Redondo, J. M., Martín-Caballero, J., Flores, J. M., Bosch, E., Rodríguez-Fernández, J. L., Aramburu, J., & López-Rodríguez, C. (2018). Macrophage-specific MHCII expression is regulated by a remote Ciita enhancer controlled by NFAT5. *Journal of Experimental Medicine*, *215*(11), 2901–2918.
Byun, J. S., & Gardner, K. (2013). Wounds that will not heal: pervasive cellular reprogramming in cancer. *The American Journal of Pathology*, *182*(4), 1055–1064.
Campisi, L. (2017). In vitro Antigen-presentation Assay for Self- and Microbial-derived Antigens. *BIO-PROTOCOL*, *7*(11).
Canovas, B., & Nebreda, A. R. (2021). Diversity and versatility of p38 kinase signalling in health and disease. *Nature Reviews. Molecular Cell Biology*, *22*(5), 346–366.
Carey, B., & Trapnell, B. C. (2010). The molecular basis of pulmonary alveolar proteinosis. *Clinical Immunology (Orlando, Fla.)*, *135*(2), 223–235.
Casanova-Acebes, M., Dalla, E., Leader, A. M., LeBerichel, J., Nikolic, J., Morales, B. M., Brown, M., Chang, C., Troncoso, L., Chen, S. T., Sastre-Perona, A., Park, M. D., Tabachnikova, A., Dhainaut, M., Hamon, P., Maier, B., Sawai, C. M., Agulló-Pascual, E., Schober, M., … Merad, M. (2021). Tissue-resident macrophages provide a pro-tumorigenic niche to early NSCLC cells. *Nature*, *595*(7868), 578–584.
Casbon, A. J., Reynau, D., Park, C., Khu, E., Gan, D. D., Schepers, K., Passegué, E., & Werb, Z. (2015). Invasive breast cancer reprograms early myeloid

differentiation in the bone marrow to generate immunosuppressive neutrophils. *Proceedings of the National Academy of Sciences of the United States of America*, *112*(6), E566–E575.

Cassetta, L., & Kitamura, T. (2018). Targeting Tumor-Associated Macrophages as a Potential Strategy to Enhance the Response to Immune Checkpoint Inhibitors. *Frontiers in Cell and Developmental Biology*, *6*(APR).

Chakarov, S., Lim, H. Y., Tan, L., Lim, S. Y., See, P., Lum, J., Zhang, X. M., Foo, S., Nakamizo, S., Duan, K., Kong, W. T., Gentek, R., Balachander, A., Carbajo, D., Bleriot, C., Malleret, B., Tam, J. K. C., Baig, S., Shabeer, M., … Ginhoux, F. (2019). Two distinct interstitial macrophage populations coexist across tissues in specific subtissular niches. *Science*, *363*(6432).

Chandler, K. J., Chandler, R. L., Broeckelmann, E. M., Hou, Y., Southard-Smith, E. M., & Mortlock, D. P. (2007). Relevance of BAC transgene copy number in mice: transgene copy number variation across multiple transgenic lines and correlations with transgene integrity and expression. *Mammalian Genome : Official Journal of the International Mammalian Genome Society*, *18*(10), 693–708.

Chang, C. H., Fontes, J. D., Peterlin, M., & Flavell, R. A. (1994). Class II transactivator (CIITA) is sufficient for the inducible expression of major histocompatibility complex class II genes. *The Journal of Experimental Medicine*, *180*(4), 1367–1374.

Chang, C. H., Guerder, S., Hong, S. C., Van Ewijk, W., & Flavell, R. A. (1996). Mice lacking the MHC class II transactivator (CIITA) show tissue-specific impairment of MHC class II expression. *Immunity*, *4*(2), 167–178.

Chao, M. P., Alizadeh, A. A., Tang, C., Myklebust, J. H., Varghese, B., Gill, S., Jan, M., Cha, A. C., Chan, C. K., Tan, B. T., Park, C. Y., Zhao, F., Kohrt, H. E., Malumbres, R., Briones, J., Gascoyne, R. D., Lossos, I. S., Levy, R., Weissman, I. L., & Majeti, R. (2010). Anti-CD47 antibody synergizes with rituximab to promote phagocytosis and eradicate non-Hodgkin lymphoma. *Cell*, *142*(5), 699–713.

Chelen, C. J., Fang, Y., Freeman, G. J., Secrist, H., Marshall, J. D., Hwang, P. T., Frankel, L. R., DeKruyff, R. H., & Umetsu, D. T. (1995). Human alveolar macrophages present antigen ineffectively due to defective expression of B7 costimulatory cell surface molecules. *The Journal of Clinical Investigation*, *95*(3), 1415–1421.

Chen, D. S., & Mellman, I. (2013). Oncology meets immunology: The cancer-immunity cycle. *Immunity*, *39*(1), 1–10.

Cheng, F., Lienlaf, M., Perez-Villarroel, P., Wang, H.-W., Lee, C., Woan, K., Woods, D., Knox, T., Bergman, J., Pinilla-Ibarz, J., Kozikowski, A., Seto, E., Sotomayor, E. M., & Villagra, A. (2014). Divergent roles of histone deacetylase 6 (HDAC6) and histone deacetylase 11 (HDAC11) on the transcriptional regulation of IL10 in antigen presenting cells. *Molecular Immunology*, *60*(1), 44–53.

Choi, N. M., Majumder, P., & Boss, J. M. (2011). Regulation of major histocompatibility complex class II genes. *Current Opinion in Immunology*, *23*(1), 81–87.

Chou, S. D., Khan, A. N. H., Magner, W. J., & Tomasi, T. B. (2005). Histone acetylation

regulates the cell type specific CIITA promoters, MHC class II expression and antigen presentation in tumor cells. *International Immunology*, *17*(11), 1483–1494.

Choudhury, B. K., Wild, J. S., Alam, R., Klinman, D. M., Boldogh, I., Dharajiya, N., Mileski, W. J., & Sur, S. (2002). In Vivo Role of p38 Mitogen-Activated Protein Kinase in Mediating the Anti-inflammatory Effects of CpG Oligodeoxynucleotide in Murine Asthma. *The Journal of Immunology*, *169*(10), 5955–5961.

Clausen, B. E., Burkhardt, C., Reith, W., Renkawitz, R., & Förster, I. (1999). Conditional gene targeting in macrophages and granulocytes using LysMcre mice. *Transgenic Research*, *8*(4), 265–277.

Coelho, M. A., de Carné Trécesson, S., Rana, S., Zecchin, D., Moore, C., Molina-Arcas, M., East, P., Spencer-Dene, B., Nye, E., Barnouin, K., Snijders, A. P., Lai, W. S., Blackshear, P. J., & Downward, J. (2017). Oncogenic RAS Signaling Promotes Tumor Immunoresistance by Stabilizing PD-L1 mRNA. *Immunity*, *47*(6), 1083-1099.e6.

Coffelt, S. B., Wellenstein, M. D., & De Visser, K. E. (2016). Neutrophils in cancer: neutral no more. *Nature Reviews. Cancer*, *16*(7), 431–446.

Collins, A. V., Brodie, D. W., Gilbert, R. J. C., Iaboni, A., Manso-Sancho, R., Walse, B., Stuart, D. I., van der Merwe, P. A., & Davis, S. J. (2002). The Interaction Properties of Costimulatory Molecules Revisited. *Immunity*, *17*(2), 201–210.

Cook, R. S., Jacobsen, K. M., Wofford, A. M., DeRyckere, D., Stanford, J., Prieto, A. L., Redente, E., Sandahl, M., Hunter, D. M., Strunk, K. E., Graham, D. K., & Earp, H. S. (2013). MerTK inhibition in tumor leukocytes decreases tumor growth and metastasis. *The Journal of Clinical Investigation*, *123*(8), 3231–3242.

Cortez-Retamozo, V., Etzrodt, M., Newton, A., Ryan, R., Pucci, F., Sio, S. W., Kuswanto, W., Rauch, P. J., Chudnovskiy, A., Iwamoto, Y., Kohler, R., Marinelli, B., Gorbatov, R., Wojtkiewicz, G., Panizzi, P., Mino-Kenudson, M., Forghani, R., Figueiredo, J. L., Chen, J. W., … Pittet, M. J. (2013). Angiotensin II drives the production of tumor-promoting macrophages. *Immunity*, *38*(2), 296–308.

Cotechini, T., Atallah, A., & Grossman, A. (2021). Tissue-Resident and Recruited Macrophages in Primary Tumor and Metastatic Microenvironments: Potential Targets in Cancer Therapy. *Cells*, *10*(4).

Coussens, L. M., Zitvogel, L., & Palucka, A. K. (2013). Neutralizing tumor-promoting chronic inflammation: a magic bullet? *Science (New York, N.Y.)*, *339*(6117), 286–291.

Cresswell, P. (1994). Assembly, transport, and function of MHC class II molecules. *Annual Review of Immunology*, *12*(1), 259–291.

Cuadrado, A., & Nebreda, A. R. (2010). Mechanisms and functions of p38 MAPK signalling. *Biochemical Journal*, *429*(3), 403–417.

Cuenda, A., & Rousseau, S. (2007). p38 MAP-kinases pathway regulation, function and role in human diseases. *Biochimica et Biophysica Acta*, *1773*(8), 1358–1375.

Cuenda, A., & Sanz-Ezquerro, J. J. (2017). p38γ and p38δ: From Spectators to Key Physiological Players. *Trends in Biochemical Sciences*, *42*(6), 431–442.

Curtis, M., Kenny, H. A., Ashcroft, B., Mukherjee, A., Johnson, A., Zhang, Y., Helou, Y., Batlle, R., Liu, X., Gutierrez, N., Gao, X., Yamada, S. D., Lastra, R., Montag, A., Ahsan, N., Locasale, J. W., Salomon, A. R., Nebreda, A. R., & Lengyel, E. (2019). Fibroblasts Mobilize Tumor Cell Glycogen to Promote Proliferation and Metastasis. *Cell Metabolism*, *29*(1), 141-155.e9.

Curtsinger, J. M., Lins, D. C., & Mescher, M. F. (2003). Signal 3 determines tolerance versus full activation of naive CD8 T cells: dissociating proliferation and development of effector function. *The Journal of Experimental Medicine*, *197*(9), 1141–1151.

Curtsinger, J. M., Schmidt, C. S., Mondino, A., Lins, D. C., Kedl, R. M., Jenkins, M. K., & Mescher, M. F. (1999). Inflammatory cytokines provide a third signal for activation of naive CD4+ and CD8+ T cells. *Journal of Immunology (Baltimore, Md. : 1950)*, *162*(6), 3256–3262.

Dahl, M., Bauer, A. K., Arredouani, M., Soininen, R., Tryggvason, K., Kleeberger, S. R., & Kobzik, L. (2007). Protection against inhaled oxidants through scavenging of oxidized lipids by macrophage receptors MARCO and SR-AI/II. *Journal of Clinical Investigation*, *117*(3), 757–764.

Daniel, B., Czimmerer, Z., Halasz, L., Boto, P., Kolostyak, Z., Poliska, S., Berger, W. K., Tzerpos, P., Nagy, G., Horvath, A., Hajas, G., Cseh, T., Nagy, A., Sauer, S., Francois-Deleuze, J., Szatmari, I., Bacsi, A., & Nagy, L. (2020). The transcription factor EGR2 is the molecular linchpin connecting STAT6 activation to the late, stable epigenomic program of alternative macrophage polarization. *Genes & Development*, *34*(21–22), 1474–1492.

Darlyuk-Saadon, I., Heng, C. K. M., Bai, C., Gilad, N., Yu, W. P., Meng Huang Mok, M., Wong, W. S. F., & Engelberg, D. (2021). Expression of a constitutively active p38α mutant in mice causes early death, anemia, and accumulation of immunosuppressive cells. *FEBS Journal*, *288*(13), 3978–3999.

Davies, L. C., Jenkins, S. J., Allen, J. E., & Taylor, P. R. (2013). Tissue-resident macrophages. *Nature Immunology*, *14*(10), 986–995.

De Maeyer, R. P. H., van de Merwe, R. C., Louie, R., Bracken, O. V., Devine, O. P., Goldstein, D. R., Uddin, M., Akbar, A. N., & Gilroy, D. W. (2020). Blocking elevated p38 MAPK restores efferocytosis and inflammatory resolution in the elderly. *Nature Immunology*, *21*(6), 615–625.

DeNardo, D. G., & Ruffell, B. (2019). Macrophages as regulators of tumour immunity and immunotherapy. *Nature Reviews. Immunology*, *19*(6), 369–382.

Denzin, L. K., & Cresswell, P. (1995). HLA-DM induces CLIP dissociation from MHC class II alpha beta dimers and facilitates peptide loading. *Cell*, *82*(1), 155–165.

Dérijard, B., Hibi, M., Wu, I. H., Barrett, T., Su, B., Deng, T., Karin, M., & Davis, R. J. (1994). JNK1: a protein kinase stimulated by UV light and Ha-Ras that binds and phosphorylates the c-Jun activation domain. *Cell*, *76*(6), 1025–1037.

DeSandro, A., Nagarajan, U. M., & Boss, J. M. (1999). The bare lymphocyte syndrome: molecular clues to the transcriptional regulation of major histocompatibility complex class II genes. *American Journal of Human Genetics*, *65*(2), 279–286.

Devaiah, B. N., & Singer, D. S. (2013). CIITA and Its Dual Roles in MHC Gene

Transcription. *Frontiers in Immunology*, *4*(DEC).
Diamond, M., Feliciano, H. L. P., Sanghavi, D., & Mahapatra, S. (2022). Acute Respiratory Distress Syndrome. *StatsPearls[Internet]*. https://www.ncbi.nlm.nih.gov/books/NBK436002/
Dickson, R. P., Erb-Downward, J. R., Falkowski, N. R., Hunter, E. M., Ashley, S. L., & Huffnagle, G. B. (2018). The Lung Microbiota of Healthy Mice Are Highly Variable, Cluster by Environment, and Reflect Variation in Baseline Lung Innate Immunity. *American Journal of Respiratory and Critical Care Medicine*, *198*(4), 497–508.
Dillekås, H., Rogers, M. S., & Straume, O. (2019). Are 90% of deaths from cancer caused by metastases? *Cancer Medicine*, *8*(12), 5574.
Dobin, A., Davis, C. A., Schlesinger, F., Drenkow, J., Zaleski, C., Jha, S., Batut, P., Chaisson, M., & Gingeras, T. R. (2013). STAR: ultrafast universal RNA-seq aligner. *Bioinformatics (Oxford, England)*, *29*(1), 15–21.
Donoghue, C., Cubillos-Rojas, M., Gutierrez-Prat, N., Sanchez-Zarzalejo, C., Verdaguer, X., Riera, A., & Nebreda, A. R. (2020). Optimal linker length for small molecule PROTACs that selectively target p38α and p38β for degradation. *European Journal of Medicinal Chemistry*, *201*.
Dranoff, G., Crawford, A. D., Sadelain, M., Ream, B., Rashid, A., Bronson, R. T., Dickersin, G. R., Bachurski, C. J., Mark, E. L., Whitsett, J. A., & Mulligan, R. C. (1994). Involvement of granulocyte-macrophage colony-stimulating factor in pulmonary homeostasis. *Science (New York, N.Y.)*, *264*(5159), 713–716.
Duan, W., Chan, J. H. P., McKay, K., Crosby, J. R., Choo, H. H., Leung, B. P., Karras, J. G., & Wong, W. S. F. (2005). Inhaled p38alpha mitogen-activated protein kinase antisense oligonucleotide attenuates asthma in mice. *American Journal of Respiratory and Critical Care Medicine*, *171*(6), 571–578.
Efron, B., & Tibshirani, R. (2007). On testing the significance of sets of genes. *Https://Doi.Org/10.1214/07-AOAS101*, *1*(1), 107–129.
Engblom, C., Pfirschke, C., & Pittet, M. J. (2016). The role of myeloid cells in cancer therapies. *Nature Reviews Cancer*, *16*(7), 447–462.
Escott, K. J., Belvisi, M. G., Birrell, M. A., Webber, S. E., Foster, M. L., & Sargent, C. A. (2000). Effect of the p38 kinase inhibitor, SB 203580, on allergic airway inflammation in the rat. *British Journal of Pharmacology*, *131*(2), 173–176.
Etzerodt, A., Moulin, M., Doktor, T. K., Delfini, M., Mossadegh-Keller, N., Bajenoff, M., Sieweke, M. H., Moestrup, S. K., Auphan-Anezin, N., & Lawrence, T. (2020). Tissue-resident macrophages in omentum promote metastatic spread of ovarian cancer. *The Journal of Experimental Medicine*, *217*(4).
Fadok, V. A., Bratton, D. L., & Henson, P. M. (2001). Phagocyte receptors for apoptotic cells: Recognition, uptake, and consequences. *Journal of Clinical Investigation*, *108*(7), 957–962.
Farach-Carson, M. C., Li, S. H., Nalty, T., & Satcher, R. L. (2017). Sex Differences and Bone Metastases of Breast, Lung, and Prostate Cancers: Do Bone Homing Cancers Favor Feminized Bone Marrow? *Frontiers in Oncology*, *7*(AUG), 163.
Farc, O., & Cristea, V. (2021). An overview of the tumor microenvironment, from cells to complex networks (Review). *Experimental and Therapeutic Medicine*, *21*(1),

1–1.

Fares, J., Fares, M. Y., Khachfe, H. H., Salhab, H. A., & Fares, Y. (2020). Molecular principles of metastasis: a hallmark of cancer revisited. *Signal Transduction and Targeted Therapy 2020 5:1*, *5*(1), 1–17.

Fathi, M., Johansson, A., Lundborg, M., Orre, L., Sköld, C. M., & Camner, P. (2001). Functional and morphological differences between human alveolar and interstitial macrophages. *Experimental and Molecular Pathology*, *70*(2), 77–82.

Fidler, I. J., & Poste, G. (2008). The "seed and soil" hypothesis revisited. *The Lancet Oncology*, *9*(8), 808.

Fleur, L. La, Botling, J., He, F., Pelicano, C., Zhou, C., He, C., Palano, G., Mezheyeuski, A., Micke, P., Ravetch, J. V., Karlsson, M. C. I., & Sarhan, D. (2021). Targeting MARCO and IL37R on immunosuppressive macrophages in lung cancer blocks regulatory T cells and supports cytotoxic lymphocyte function. *Cancer Research*, *81*(4), 956–967.

Fooksman, D. R., Vardhana, S., Vasiliver-Shamis, G., Liese, J., Blair, D. A., Waite, J., Sacristán, C., Victora, G. D., Zanin-Zhorov, A., & Dustin, M. L. (2010). Functional Anatomy of T Cell Activation and Synapse Formation. *Annual Review of Immunology*, *28*(1), 79–105.

Fortier, M., Cadoux, M., Boussetta, N., Pham, S., Donné, R., Couty, J. P., Desdouets, C., & Celton-Morizur, S. (2019). Hepatospecific ablation of p38α MAPK governs liver regeneration through modulation of inflammatory response to CCl4-induced acute injury. *Scientific Reports 2019 9:1*, *9*(1), 1–12.

Freshney, N. W., Rawlinson, L., Guesdon, F., Jones, E., Cowley, S., Hsuan, J., & Saklatvala, J. (1994). Interleukin-1 activates a novel protein kinase cascade that results in the phosphorylation of Hsp27. *Cell*, *78*(6), 1039–1049.

Fricker, M., & Gibson, P. G. (2017). Macrophage dysfunction in the pathogenesis and treatment of asthma. *European Respiratory Journal*, *50*(3), 1700196.

Fujimori, T., Grabiec, A. M., Kaur, M., Bell, T. J., Fujino, N., Cook, P. C., Svedberg, F. R., Macdonald, A. S., Maciewicz, R. A., Singh, D., & Hussell, T. (2015). The Axl receptor tyrosine kinase is a discriminator of macrophage function in the inflamed lung. *Mucosal Immunology*, *8*(5), 1021–1030.

Gabrilovich, D. I., Ostrand-Rosenberg, S., & Bronte, V. (2012). Coordinated regulation of myeloid cells by tumours. *Nature Reviews. Immunology*, *12*(4), 253–268.

Gaestel, M. (2016). MAPK-Activated Protein Kinases (MKs): Novel Insights and Challenges. *Frontiers in Cell and Developmental Biology*, *3*(JAN).

Gaffey, K., Reynolds, S., Plumb, J., Kaur, M., & Singh, D. (2013). Increased phosphorylated p38 mitogenactivated protein kinase in COPD lungs. *European Respiratory Journal*, *42*(1), 28–41.

Gajewski, T. F., Schreiber, H., & Fu, Y. X. (2013). Innate and adaptive immune cells in the tumor microenvironment. *Nature Immunology*, *14*(10), 1014–1022.

Galli, S. J., Borregaard, N., & Wynn, T. A. (2011). Phenotypic and functional plasticity of cells of innate immunity: macrophages, mast cells and neutrophils. *Nature Immunology*, *12*(11), 1035–1044.

Ganesh, K., & Massagué, J. (2021). Targeting metastatic cancer. *Nature Medicine*,

27(1), 34–44.
Gautiar, E. L., Shay, T., Miller, J., Greter, M., Jakubzick, C., Ivanov, S., Helft, J., Chow, A., Elpek, K. G., Gordonov, S., Mazloom, A. R., Ma'Ayan, A., Chua, W. J., Hansen, T. H., Turley, S. J., Merad, M., Randolph, G. J., Best, A. J., Knell, J., … Benoist, C. (2012). Gene-expression profiles and transcriptional regulatory pathways that underlie the identity and diversity of mouse tissue macrophages. *Nature Immunology*, *13*(11), 1118–1128.
Gerhard, G. M., Bill, R., Messemaker, M., Klein, A. M., & Pittet, M. J. (2021). Tumor-infiltrating dendritic cell states are conserved across solid human cancers. *The Journal of Experimental Medicine*, *218*(1).
Gomez Perdiguero, E., Klapproth, K., Schulz, C., Busch, K., Azzoni, E., Crozet, L., Garner, H., Trouillet, C., De Bruijn, M. F., Geissmann, F., & Rodewald, H. R. (2015). Tissue-resident macrophages originate from yolk-sac-derived erythro-myeloid progenitors. *Nature*, *518*(7540), 547–551.
Gordon, S. (2003). Alternative activation of macrophages. *Nature Reviews. Immunology*, *3*(1), 23–35.
Gordon, S. B., & Read, R. C. (2002). Macrophage defences against respiratory tract infections. *British Medical Bulletin*, *61*, 45–61.
Goritzka, M., Makris, S., Kausar, F., Durant, L. R., Pereira, C., Kumagai, Y., Culley, F. J., Mack, M., Akira, S., & Johansson, C. (2015). Alveolar macrophage-derived type I interferons orchestrate innate immunity to RSV through recruitment of antiviral monocytes. *The Journal of Experimental Medicine*, *212*(5), 699–714.
Gorki, A.-D., Symmank, D., Zahalka, S., Lakovits, K., Hladik, A., Langer, B., Maurer, B., Sexl, V., Kain, R., & Knapp, S. (2021). Murine ex vivo cultured alveolar macrophages provide a novel tool to study tissue-resident macrophage behavior and function. *BioRxiv*, 2021.02.11.430791.
Granot, Z., Henke, E., Comen, E. A., King, T. A., Norton, L., & Benezra, R. (2011). Tumor entrained neutrophils inhibit seeding in the premetastatic lung. *Cancer Cell*, *20*(3), 300.
Gschwend, J., Sherman, S. P. M., Ridder, F., Feng, X., Liang, H. E., Locksley, R. M., Becher, B., & Schneider, C. (2021). Alveolar macrophages rely on GM-CSF from alveolar epithelial type 2 cells before and after birth. *The Journal of Experimental Medicine*, *218*(10).
Gui, J., Zahedi, F., Ortiz, A., Cho, C., Katlinski, K. V., Alicea-Torres, K., Li, J., Todd, L., Zhang, H., Beiting, D. P., Sander, C., Kirkwood, J. M., Snow, B. E., Wakeham, A. C., Mak, T. W., Diehl, J. A., Koumenis, C., Ryeom, S. W., Stanger, B. Z., … Fuchs, S. Y. (2020). Activation of p38α stress-activated protein kinase drives the formation of the pre-metastatic niche in the lungs. *Nature Cancer*, *1*(6), 603–619.
Guilliams, M., De Kleer, I., Henri, S., Post, S., Vanhoutte, L., De Prijck, S., Deswarte, K., Malissen, B., Hammad, H., & Lambrecht, B. N. (2013). Alveolar macrophages develop from fetal monocytes that differentiate into long-lived cells in the first week of life via GM-CSF. *The Journal of Experimental Medicine*, *210*(10), 1977–1992.
Guilliams, M., & Svedberg, F. R. (2021). Does tissue imprinting restrict macrophage

plasticity? *Nature Immunology*, *22*(2), 118–127.

Guma, M., Hammaker, D., Topolewski, K., Corr, M., Boyle, D. L., Karin, M., & Firestein, G. S. (2012). Antiinflammatory functions of p38 in mouse models of rheumatoid arthritis: advantages of targeting upstream kinases MKK-3 or MKK-6. *Arthritis and Rheumatism*, *64*(9), 2887–2895.

Gupta, J., delBarcoBarrantes, I., Igea, A., Sakellariou, S., Pateras, I. S., Gorgoulis, V. G., & Nebreda, A. R. (2014). Dual function of p38α MAPK in colon cancer: suppression of colitis-associated tumor initiation but requirement for cancer cell survival. *Cancer Cell*, *25*(4), 484–500.

Gupta, J., & Nebreda, A. R. (2015). Roles of p38α mitogen-activated protein kinase in mouse models of inflammatory diseases and cancer. *The Febs Journal*, *282*(10), 1841.

Gurusamy, D., Henning, A. N., Yamamoto, T. N., Yu, Z., Zacharakis, N., Krishna, S., Kishton, R. J., Vodnala, S. K., Eidizadeh, A., Jia, L., Kariya, C. M., Black, M. A., Eil, R., Palmer, D. C., Pan, J. H., Sukumar, M., Patel, S. J., & Restifo, N. P. (2020). Multi-phenotype CRISPR-Cas9 Screen Identifies p38 Kinase as a Target for Adoptive Immunotherapies. *Cancer Cell*, *37*(6), 818-833.e9.

Gutierrez-Prat, N. (2018). *Molecular basis of p38alpha MAPK signaling*.

Gyory, I., Wu, J., Fejér, G., Seto, E., & Wright, K. L. (2004). PRDI-BF1 recruits the histone H3 methyltransferase G9a in transcriptional silencing. *Nature Immunology*, *5*(3), 299–308.

Hafemeister, C., & Satija, R. (2019). Normalization and variance stabilization of single-cell RNA-seq data using regularized negative binomial regression. *Genome Biology*, *20*(1), 1–15.

Han, J., Lee, J. D., Bibbs, L., & Ulevitch, R. J. (1994). A MAP kinase targeted by endotoxin and hyperosmolarity in mammalian cells. *Science (New York, N.Y.)*, *265*(5173), 808–811.

Han, J., Wu, J., & Silke, J. (2020). An overview of mammalian p38 mitogen-activated protein kinases, central regulators of cell stress and receptor signaling. *F1000Research*, *9*.

Hanahan, D. (2022). Hallmarks of Cancer: New Dimensions. *Cancer Discovery*, *12*(1), 31–46.

Hanahan, D., & Coussens, L. M. (2012). Accessories to the Crime: Functions of Cells Recruited to the Tumor Microenvironment. In *Cancer Cell* (Vol. 21, Issue 3, pp. 309–322).

Hanahan, D., & Weinberg, R. A. (2011). Hallmarks of cancer: the next generation. *Cell*, *144*(5), 646–674.

Hao, Y., Hao, S., Andersen-Nissen, E., Mauck, W. M., Zheng, S., Butler, A., Lee, M. J., Wilk, A. J., Darby, C., Zager, M., Hoffman, P., Stoeckius, M., Papalexi, E., Mimitou, E. P., Jain, J., Srivastava, A., Stuart, T., Fleming, L. M., Yeung, B., … Satija, R. (2021). Integrated analysis of multimodal single-cell data. *Cell*, *184*(13), 3573-3587.e29.

Hashimoto, D., Chow, A., Noizat, C., Teo, P., Beasley, M. B., Leboeuf, M., Becker, C. D., See, P., Price, J., Lucas, D., Greter, M., Mortha, A., Boyer, S. W., Forsberg, E. C., Tanaka, M., van Rooijen, N., García-Sastre, A., Stanley, E. R., Ginhoux, F., …

Merad, M. (2013). Tissue-resident macrophages self-maintain locally throughout adult life with minimal contribution from circulating monocytes. *Immunity*, *38*(4), 792–804.
Hawgood, S., & Poulain, F. R. (2001). *THE PULMONARY COLLECTINS AND SURFACTANT METABOLISM*. www.annualreviews.org
Hengst, J. C., Kan-Mitchell, J., Kempf, R. A., Strumpf, I. J., Sharma, O. P., Kortes, V. L., & Mitchell, M. S. (1985). Correlation between cytotoxic and suppressor activities of human pulmonary alveolar macrophages. *Cancer Research*, *45*(1), 459–463.
Hiratsuka, S., Watanabe, A., Aburatani, H., & Maru, Y. (2006). Tumour-mediated upregulation of chemoattractants and recruitment of myeloid cells predetermines lung metastasis. *Nature Cell Biology*, *8*(12), 1369–1375.
Holling, T. M., Schooten, E., Langerak, A. W., & Van Den Elsen, P. J. (2004). Regulation of MHC class II expression in human T-cell malignancies. *Blood*, *103*(4), 1438–1444.
Holt, P. G. (1979). Alveolar macrophages. III. Studies on the mechanisms of inhibition of T-cell proliferation. *Immunology*, *37*(2), 437–445.
Holt, P. G., Oliver, J., Bilyk, N., McMenamin, C., McMenamin, P. G., Kraal, G., & Thepen, T. (1993). Downregulation of the antigen presenting cell function(s) of pulmonary dendritic cells in vivo by resident alveolar macrophages. *The Journal of Experimental Medicine*, *177*(2), 397–407.
Holt, P., & Leivers, S. (1985). ALVEOLAR MACROPHAGES: ANTIGEN PRESENTATION ACTIVITY *IN VIVO*. *Australian Journal of Experimental Biology and Medical Science*, *63*(1), 33–39.
Holtz, R., Choi, J. C., Petroff, M. G., Piskurich, J. F., & Murphy, S. P. (2003). Class II transactivator (CIITA) promoter methylation does not correlate with silencing of CIITA transcription in trophoblasts. *Biology of Reproduction*, *69*(3), 915–924.
Hornbeck, P. V., Zhang, B., Murray, B., Kornhauser, J. M., Latham, V., & Skrzypek, E. (2015). PhosphoSitePlus, 2014: mutations, PTMs and recalibrations. *Nucleic Acids Research*, *43*(Database issue), D512–D520.
Hu, J. F., Zhang, W., Zuo, W., Tan, H. Q., & Bai, W. (2020). Inhibition of the PD-1/PD-L1 signaling pathway enhances innate immune response of alveolar macrophages to mycobacterium tuberculosis in mice. *Pulmonary Pharmacology & Therapeutics*, *60*.
Hubo, M., Trinschek, B., Kryczanowsky, F., Tuettenberg, A., Steinbrink, K., & Jonuleit, H. (2013). Costimulatory molecules on immunogenic versus tolerogenic human dendritic cells. *Frontiers in Immunology*, *4*(APR), 82.
Hui, L., Bakiri, L., Mairhorfer, A., Schweifer, N., Haslinger, C., Kenner, L., Komnenovic, V., Scheuch, H., Beug, H., & Wagner, E. F. (2007). p38alpha suppresses normal and cancer cell proliferation by antagonizing the JNK-c-Jun pathway. *Nature Genetics*, *39*(6), 741–749.
Hulsen, T., de Vlieg, J., & Alkema, W. (2008). BioVenn - A web application for the comparison and visualization of biological lists using area-proportional Venn diagrams. *BMC Genomics*, *9*.
Huotari, J., & Helenius, A. (2011). Endosome maturation. *The EMBO Journal*, *30*(17),

3481–3500.
Hurskainen, M., Mižíková, I., Cook, D. P., Andersson, N., Cyr-Depauw, C., Lesage, F., Helle, E., Renesme, L., Jankov, R. P., Heikinheimo, M., Vanderhyden, B. C., & Thébaud, B. (2021). Single cell transcriptomic analysis of murine lung development on hyperoxia-induced damage. *Nature Communications*, *12*(1).
Hussell, T., & Bell, T. J. (2014). Alveolar macrophages: plasticity in a tissue-specific context. *Nature Reviews. Immunology*, *14*(2), 81–93.
Igea, A., & Nebreda, A. R. (2015). The stress kinase p38?? as a target for cancer therapy. *Cancer Research*, *75*(19), 3997–4002.
Ina, Y., Takada, K., Yamamoto, M., Morishita, M., & Yoshikawa, K. (1991). Antigen-presenting capacity of alveolar macrophages and monocytes in pulmonary tuberculosis. *The European Respiratory Journal*, *4*(1), 88–93.
Italiani, P., & Boraschi, D. (2014). From Monocytes to M1/M2 Macrophages: Phenotypical vs. Functional Differentiation. *Frontiers in Immunology*, *5*(OCT).
Itoh-Lindstrom, Y., Piskurich, J. F., Felix, N. J., Wang, Y., Brickey, W. J., Platt, J. L., Koller, B. H., & Ting, J. P. (1999). Reduced IL-4-, lipopolysaccharide-, and IFN-gamma-induced MHC class II expression in mice lacking class II transactivator due to targeted deletion of the GTP-binding domain. *Journal of Immunology (Baltimore, Md. : 1950)*, *163*(5), 2425–2431.
Jaiswal, A. K., Makhija, S., Stahr, N., Sandey, M., Suryawanshi, A., Saxena, A., Dagur, P. K., McCoy, J. P., Levine, S. J., & Mishra, A. (2020). Dendritic Cell-Restricted Progenitors Contribute to Obesity-Associated Airway Inflammation via Adam17-p38 MAPK-Dependent Pathway. *Frontiers in Immunology*, *11*.
Jakubzick, C., Gautier, E. L., Gibbings, S. L., Sojka, D. K., Schlitzer, A., Johnson, T. E., Ivanov, S., Duan, Q., Bala, S., Condon, T., vanRooijen, N., Grainger, J. R., Belkaid, Y., Ma'ayan, A., Riches, D. W. H., Yokoyama, W. M., Ginhoux, F., Henson, P. M., & Randolph, G. J. (2013). Minimal differentiation of classical monocytes as they survey steady-state tissues and transport antigen to lymph nodes. *Immunity*, *39*(3), 599–610.
Jakubzick, C., Tacke, F., Llodra, J., van Rooijen, N., & Randolph, G. J. (2006). Modulation of dendritic cell trafficking to and from the airways. *Journal of Immunology (Baltimore, Md. : 1950)*, *176*(6), 3578–3584.
Janssen, W. J., Barthel, L., Muldrow, A., Oberley-Deegan, R. E., Kearns, M. T., Jakubzick, C., & Henson, P. M. (2011). Fas determines differential fates of resident and recruited macrophages during resolution of acute lung injury. *American Journal of Respiratory and Critical Care Medicine*, *184*(5), 547–560.
Jardine, L., Wiscombe, S., Reynolds, G., McDonald, D., Fuller, A., Green, K., Filby, A., Forrest, I., Ruchaud-Sparagano, M. H., Scott, J., Collin, M., Haniffa, M., & Simpson, A. J. (2019). Lipopolysaccharide inhalation recruits monocytes and dendritic cell subsets to the alveolar airspace. *Nature Communications*, *10*(1).
Jiang-Shieh, Y. F., Chien, H. F., Chang, C. Y., Wei, T. S., Chiu, M. M., Chen, H. M., & Wu, C. H. (2010). Distribution and expression of CD200 in the rat respiratory system under normal and endotoxin-induced pathological conditions. *Journal of Anatomy*, *216*(3), 407–416.
Jiménez-Garcia, L., Herránz, S., Luque, A., & Hortelano, S. (2015). Critical role of p38

MAPK in IL-4-induced alternative activation of peritoneal macrophages. *European Journal of Immunology*, *45*(1), 273–286.

Jin, M. Z., & Jin, W. L. (2020). The updated landscape of tumor microenvironment and drug repurposing. *Signal Transduction and Targeted Therapy 2020 5:1*, *5*(1), 1–16.

Jinushi, M., Sato, M., Kanamoto, A., Itoh, A., Nagai, S., Koyasu, S., Dranoff, G., & Tahara, H. (2009). Milk fat globule epidermal growth factor-8 blockade triggers tumor destruction through coordinated cell-autonomous and immune-mediated mechanisms. *The Journal of Experimental Medicine*, *206*(6), 1317–1326.

Josefowicz, S. Z., Niec, R. E., Kim, H. Y., Treuting, P., Chinen, T., Zheng, Y., Umetsu, D. T., & Rudensky, A. Y. (2012). Extrathymically generated regulatory T cells control mucosal TH2 inflammation. *Nature*, *482*(7385), 395–399.

Jurewicz, M. M., & Stern, L. J. (2018). Class II MHC antigen processing in immune tolerance and inflammation. *Immunogenetics 2018 71:3*, *71*(3), 171–187.

Kabir, K., Gelinas, J. P., Chen, M., Chen, D., Zhang, D., Luo, X., Yang, J. H., Carter, D., & Rabinovici, R. (2002). Characterization of a murine model of endotoxin-induced acute lung injury. *Shock (Augusta, Ga.)*, *17*(4), 300–303.

Kang, Y. J., Chen, J., Otsuka, M., Mols, J., Ren, S., Wang, Y., & Han, J. (2008). Macrophage deletion of p38alpha partially impairs lipopolysaccharide-induced cellular activation. *Journal of Immunology (Baltimore, Md. : 1950)*, *180*(7), 5075–5082.

Karwacz, K., Bricogne, C., MacDonald, D., Arce, F., Bennett, C. L., Collins, M., & Escors, D. (2011). PD-L1 co-stimulation contributes to ligand-induced T cell receptor down-modulation on CD8 $^{+}$ T cells. *EMBO Molecular Medicine*, *3*(10), 581–592.

Katlinski, K. V, Gui, J., Katlinskaya, Y. V, Ortiz, A., Chakraborty, R., Bhattacharya, S., Carbone, C. J., Beiting, D. P., Girondo, M. A., Peck, A. R., Puré, E., Chatterji, P., Rustgi, A. K., Diehl, J. A., Koumenis, C., Rui, H., & Fuchs, S. Y. (2017). Inactivation of Interferon Receptor Promotes the Establishment of Immune Privileged Tumor Microenvironment. *Cancer Cell*, *31*(2), 194–207.

Kawasaki, H., Schiltz, L., Chiu, R., Itakura, K., Taira, K., Nakatani, Y., & Yokoyama, K. K. (2000). ATF-2 has intrinsic histone acetyltransferase activity which is modulated by phosphorylation. *Nature*, *405*(6783), 195–200.

Kawasaki, T., Ikegawa, M., & Kawai, T. (2022). Antigen Presentation in the Lung. *Frontiers in Immunology*, *13*.

Keshet, Y., & Seger, R. (2010). The MAP kinase signaling cascades: a system of hundreds of components regulates a diverse array of physiological functions. *Methods in Molecular Biology (Clifton, N.J.)*, *661*, 3–38.

Kim, C., Sano, Y., Todorova, K., Carlson, B. A., Arpa, L., Celada, A., Lawrence, T., Otsu, K., Brissette, J. L., Arthur, J. S. C., & Park, J. M. (2008). The kinase p38α serves cell type–specific inflammatory functions in skin injury and coordinates pro- and anti-inflammatory gene expression. *Nature Immunology 2008 9:9*, *9*(9), 1019–1027.

Kim, S., Takahashi, H., Lin, W. W., Descargues, P., Grivennikov, S., Kim, Y., Luo, J. L.,

& Karin, M. (2009). Carcinoma-produced factors activate myeloid cells through TLR2 to stimulate metastasis. *Nature*, *457*(7225), 102–106.

Kim, T. H., Kim, M. Y., Jo, S. H., Park, J. M., & Ahn, Y. H. (2013). Modulation of the transcriptional activity of peroxisome proliferator-activated receptor gamma by protein-protein interactions and post-translational modifications. *Yonsei Medical Journal*, *54*(3), 545–559.

King, J., Patel, M., & Chandrasekaran, S. (2021). Metabolism, HDACs, and HDAC Inhibitors: A Systems Biology Perspective. *Metabolites*, *11*(11).

Kirby, A. C., Coles, M. C., & Kaye, P. M. (2009). Alveolar macrophages transport pathogens to lung draining lymph nodes. *Journal of Immunology (Baltimore, Md. : 1950)*, *183*(3), 1983–1989.

Knauf, U., Tschopp, C., & Gram, H. (2001). Negative regulation of protein translation by mitogen-activated protein kinase-interacting kinases 1 and 2. *Molecular and Cellular Biology*, *21*(16), 5500–5511.

Knebel, A., Haydon, C. E., Morrice, N., & Cohen, P. (2002). Stress-induced regulation of eukaryotic elongation factor 2 kinase by SB 203580-sensitive and -insensitive pathways. *The Biochemical Journal*, *367*(Pt 2), 525–532.

Knudsen, L., & Ochs, M. (2018). The micromechanics of lung alveoli: structure and function of surfactant and tissue components. *Histochemistry and Cell Biology*, *150*(6), 661–676.

Kolch, W. (2005). Coordinating ERK/MAPK signalling through scaffolds and inhibitors. *Nature Reviews. Molecular Cell Biology*, *6*(11), 827–837.

Kolli, D., Gupta, M. R., Sbrana, E., Velayutham, T. S., Chao, H., Casola, A., & Garofalo, R. P. (2014). Alveolar macrophages contribute to the pathogenesis of human metapneumovirus infection while protecting against respiratory syncytial virus infection. *American Journal of Respiratory Cell and Molecular Biology*, *51*(4), 502–515.

Kopf, M., Schneider, C., & Nobs, S. P. (2015). The development and function of lung-resident macrophages and dendritic cells. *Nat Immunol*, *16*(1), 36–44.

Kotlyarov, A., Neininger, A., Schubert, C., Eckert, R., Birchmeier, C., Volk, H. D., & Gaestel, M. (1999). MAPKAP kinase 2 is essential for LPS-induced TNF-alpha biosynthesis. *Nature Cell Biology*, *1*(2), 94–97.

Kowanetz, M., Wu, X., Lee, J., Tan, M., Hagenbeek, T., Qu, X., Yu, L., Ross, J., Korsisaari, N., Cao, T., Bou-Reslan, H., Kallop, D., Weimer, R., Ludlam, M. J. C., Kaminker, J. S., Modrusan, Z., Van Bruggen, N., Peale, F. V., Carano, R., … Ferrara, N. (2010). Granulocyte-colony stimulating factor promotes lung metastasis through mobilization of Ly6G+Ly6C+ granulocytes. *Proceedings of the National Academy of Sciences of the United States of America*, *107*(50), 21248–21255.

Kozmar, A., Greenlee-Wacker, M. C., & Bohlson, S. S. (2010). Macrophage Response to Apoptotic Cells Varies with the Apoptotic Trigger and Is Not Altered by a Deficiency in LRP Expression. *Journal of Innate Immunity*, *2*(3), 248.

Kratofil, R. M., Kubes, P., & Deniset, J. F. (2017). Monocyte Conversion During Inflammation and Injury. *Arteriosclerosis, Thrombosis, and Vascular Biology*, *37*(1), 35–42.

Krementsov, D. N., Noubade, R., Dragon, J. A., Otsu, K., Rincon, M., & Teuscher, C. (2014). Sex-specific control of central nervous system autoimmunity by p38 mitogen-activated protein kinase signaling in myeloid cells. *Annals of Neurology*, *75*(1), 50–66.

Kyriakis, J. M., Banerjee, P., Nikolakaki, E., Dai, T., Rubie, E. A., Ahmad, M. F., Avruch, J., & Woodgett, J. R. (1994). The stress-activated protein kinase subfamily of c-Jun kinases. *Nature*, *369*(6476), 156–160.

Landmann, S., Mühlethaler-Mottet, A., Bernasconi, L., Suter, T., Waldburger, J. M., Masternak, K., Arrighi, J. F., Hauser, C., Fontana, A., & Reith, W. (2001). Maturation of dendritic cells is accompanied by rapid transcriptional silencing of class II transactivator (CIITA) expression. *The Journal of Experimental Medicine*, *194*(4), 379–391.

Landsverk, O. J. B., Bakke, O., & Gregers, T. F. (2009). MHC II and the endocytic pathway: regulation by invariant chain. *Scandinavian Journal of Immunology*, *70*(3), 184–193.

Laplane, L., Duluc, D., Bikfalvi, A., Larmonier, N., & Pradeu, T. (2019). Beyond the tumour microenvironment. *International Journal of Cancer*, *145*(10), 2611–2618.

Latchman, Y. E., Liang, S. C., Wu, Y., Chernova, T., Sobel, R. A., Klemm, M., Kuchroo, V. K., Freeman, G. J., & Sharpe, A. H. (2004). PD-L1-deficient mice show that PD-L1 on T cells, antigen-presenting cells, and host tissues negatively regulates T cells. *Proceedings of the National Academy of Sciences*, *101*(29), 10691–10696.

Lauzon-Joset, J. F., Langlois, A., Lai, L. J. A., Santerre, K., Lee-Gosselin, A., Bosse, Y., Marsolais, D., & Bissonnette, E. Y. (2015). Lung CD200 Receptor Activation Abrogates Airway Hyperresponsiveness in Experimental Asthma. *American Journal of Respiratory Cell and Molecular Biology*, *53*(2), 276–284.

Lavin, Y., Winter, D., Blecher-Gonen, R., David, E., Keren-Shaul, H., Merad, M., Jung, S., & Amit, I. (2014). Tissue-resident macrophage enhancer landscapes are shaped by the local microenvironment. *Cell*, *159*(6), 1312–1326.

Lee, J. C., Laydon, J. T., McDonnell, P. C., Gallagher, T. F., Kumar, S., Green, D., McNulty, D., Blumenthal, M. J., Keys, J. R., Land Vatter, S. W., Strickler, J. E., McLaughlin, M. M., Siemens, I. R., Fisher, S. M., Livi, G. P., White, J. R., Adams, J. L., & Young, P. R. (1994). A protein kinase involved in the regulation of inflammatory cytokine biosynthesis. *Nature*, *372*(6508), 739–746.

Lee, J. D., Ulevitch, R. J., & Han, J. (1995). Primary structure of BMK1: A new mammalian MAP kinase. *Biochemical and Biophysical Research Communications*, *213*(2), 715–724.

LeibundGut-Landmann, S., Waldburger, J. M., Krawczyk, M., Otten, L. A., Suter, T., Fontana, A., Acha-Orbea, H., & Reith, W. (2004). Mini-review: Specificity and expression of CIITA, the master regulator of MHC class II genes. *European Journal of Immunology*, *34*(6), 1513–1525.

LeibundGut-Landmann, S., Waldburger, J. M., Reis e Sousa, C., Acha-Orbea, H., & Reith, W. (2004). MHC class II expression is differentially regulated in plasmacytoid and conventional dendritic cells. *Nature Immunology*, *5*(9), 899–

908.

León Machado, J. A., & Steimle, V. (2021). The mhc class ii transactivator ciita: Not (quite) the odd-one-out anymore among nlr proteins. *International Journal of Molecular Sciences*, *22*(3), 1–19.

Leung, S., Liu, X., Fang, L., Chen, X., Guo, T., & Zhang, J. (2010). The cytokine milieu in the interplay of pathogenic Th1/Th17 cells and regulatory T cells in autoimmune disease. *Cellular & Molecular Immunology 2010 7:3*, *7*(3), 182–189.

Li, B., Tan, T. B., Wang, L., Zhao, X. Y., & Tan, G. J. (2019). p38MAPK/SGK1 signaling regulates macrophage polarization in experimental autoimmune encephalomyelitis. *Aging*, *11*(3), 898–907.

Li, D., Ren, W., Jiang, Z., & Zhu, L. (2018). Regulation of the NLRP3 inflammasome and macrophage pyroptosis by the p38 MAPK signaling pathway in a mouse model of acute lung injury. *Molecular Medicine Reports*, *18*(5), 4399–4409.

Li, S., Liu, M., Do, M. H., Chou, C., Stamatiades, E. G., Nixon, B. G., Shi, W., Zhang, X., Li, P., Gao, S., Capistrano, K. J., Xu, H., Cheung, N. K. V., & Li, M. O. (2020). Cancer immunotherapy via targeted TGF-β signalling blockade in TH cells. *Nature*, *587*(7832), 121–125.

Li, X., Udagawa, N., Takami, M., Sato, N., Kobayashi, Y., & Takahashi, N. (2003). p38 Mitogen-Activated Protein Kinase Is Crucially Involved in Osteoclast Differentiation But Not in Cytokine Production, Phagocytosis, or Dendritic Cell Differentiation of Bone Marrow Macrophages. *Endocrinology*, *144*(11), 4999–5005.

Liang, L., Li, F., Bao, A., Zhang, M., Chung, K. F., & Zhou, X. (2013). Activation of p38 mitogen-activated protein kinase in ovalbumin and ozone-induced mouse model of asthma. *Respirology*, *18*, 20–29.

Liang, S. C., Greenwald, R. J., Latchman, Y. E., Rosas, L., Satoskar, A., Freeman, G. J., & Sharpe, A. H. (2006). PD-L1 and PD-L2 have distinct roles in regulating host immunity to cutaneous leishmaniasis. *European Journal of Immunology*, *36*(1), 58–64.

Liao, Y., Smyth, G. K., & Shi, W. (2019). The R package Rsubread is easier, faster, cheaper and better for alignment and quantification of RNA sequencing reads. *Nucleic Acids Research*, *47*(8).

Lichanska, A. M., & Hume, D. A. (2000). Origins and functions of phagocytes in the embryo. *Experimental Hematology*, *28*(6), 601–611.

Liechtenstein, T., Dufait, I., Lanna, A., Breckpot, K., & Escors, D. (2012). Modulating Co-Stimulation During Antigen Presentation to Enhance Cancer Immunotherapy. *Immunology Endocrine & Metabolic Agents - Medicinal Chemistry*, *12*(3), 224–235.

Liu, C. H., Liu, H., & Ge, B. (2017). Innate immunity in tuberculosis: host defense vs pathogen evasion. *Cellular & Molecular Immunology 2017 14:12*, *14*(12), 963–975.

Liu, L., Wei, Y., & Wei, X. (2017). The Immune Function of Ly6Chi Inflammatory Monocytes During Infection and Inflammation. *Current Molecular Medicine*, *17*(1), 4–12.

Liu, Q., Zhang, H., Jiang, X., Qian, C., Liu, Z., & Luo, D. (2017). Factors involved in cancer metastasis: a better understanding to "seed and soil" hypothesis. *Molecular Cancer 2017 16:1*, *16*(1), 1–19.

Lloberas, J., Valverde-Estrella, L., Tur, J., Vico, T., & Celada, A. (2016). Mitogen-activated protein kinases and mitogen kinase phosphatase 1: A critical interplay in macrophage biology. *Frontiers in Molecular Biosciences*, *3*(JUN), 28.

Lloyd, C. M., & Hawrylowicz, C. M. (2009). Regulatory T cells in asthma. *Immunity*, *31*(3), 438–449.

Loeser, S., Loser, K., Bijker, M. S., Rangachari, M., Van Der Burg, S. H., Wada, T., Beissert, S., Melief, C. J. M., & Penninger, J. M. (2007). Spontaneous tumor rejection by cbl-b-deficient CD8+ T cells. *The Journal of Experimental Medicine*, *204*(4), 879–891.

Lomas-Neira, J., Chung, C. S., Perl, M., Gregory, S., Biffl, W., & Ayala, A. (2006). Role of alveolar macrophage and migrating neutrophils in hemorrhage-induced priming for ALI subsequent to septic challenge. *American Journal of Physiology. Lung Cellular and Molecular Physiology*, *290*(1).

Lopez-Rodriguez, E., Gay-Jordi, G., Mucci, A., Lachmann, N., & Serrano-Mollar, A. (2017). Lung surfactant metabolism: early in life, early in disease and target in cell therapy. *Cell and Tissue Research*, *367*(3), 721–735.

Love, M. I., Huber, W., & Anders, S. (2014). Moderated estimation of fold change and dispersion for RNA-seq data with DESeq2. *Genome Biology*, *15*(12), 1–21.

Low, J. S., Farsakoglu, Y., Amezcua Vesely, M. C., Sefik, E., Kelly, J. B., Harman, C. C. D., Jackson, R., Shyer, J. A., Jiang, X., Cauley, L. S., Flavell, R. A., & Kaech, S. M. (2020). Tissue-resident memory T cell reactivation by diverse antigen-presenting cells imparts distinct functional responses. *Journal of Experimental Medicine*, *217*(8).

Loyher, P. L., Hamon, P., Laviron, M., Meghraoui-Kheddar, A., Goncalves, E., Deng, Z., Torstensson, S., Bercovici, N., De Chanville, C. B., Combadière, B., Geissmann, F., Savina, A., Combadière, C., & Boissonnas, A. (2018). Macrophages of distinct origins contribute to tumor development in the lung. *The Journal of Experimental Medicine*, *215*(10), 1–18.

Lu, T., Ramakrishnan, R., Altiok, S., Youn, J. I., Cheng, P., Celis, E., Pisarev, V., Sherman, S., Sporn, M. B., & Gabrilovich, D. (2011). Tumor-infiltrating myeloid cells induce tumor cell resistance to cytotoxic T cells in mice. *The Journal of Clinical Investigation*, *121*(10), 4015–4029.

Ma, J. Y., Medicherla, S., Kerr, I., Mangadu, R., Protter, A. A., & Higgins, L. S. (2008). Selective p38α mitogen-activated protein kinase inhibitor attenuates lung inflammation and fibrosis in IL-13 transgenic mouse model of asthma. *Journal of Asthma and Allergy*, *1*(1), 31.

Ma, L., & Chung, W. K. (2014). Quantitative Analysis of Copy Number Variants Based on Real-Time LightCycler PCR. *Current Protocols in Human Genetics*, *80*(1), 7.21.1-7.21.8.

Ma, R. Y., Black, A., & Qian, B. Z. (2022). Macrophage diversity in cancer revisited in the era of single-cell omics. *Trends in Immunology*, *43*(7), 546–563.

Machiels, B., Dourcy, M., Xiao, X., Javaux, J., Mesnil, C., Sabatel, C., Desmecht, D., Lallemand, F., Martinive, P., Hammad, H., Guilliams, M., Dewals, B., Vanderplasschen, A., Lambrecht, B. N., Bureau, F., & Gillet, L. (2017). A gammaherpesvirus provides protection against allergic asthma by inducing the replacement of resident alveolar macrophages with regulatory monocytes. *Nature Immunology*, *18*(12), 1310–1320.

Maik-Rachline, G., Lifshits, L., & Seger, R. (2020). Nuclear P38: Roles in Physiological and Pathological Processes and Regulation of Nuclear Translocation. *International Journal of Molecular Sciences*, *21*(17), 6102.

Martin, F. P., Jacqueline, C., Poschmann, J., & Roquilly, A. (2021). Alveolar Macrophages: Adaptation to Their Anatomic Niche during and after Inflammation. *Cells 2021, Vol. 10, Page 2720*, *10*(10), 2720.

Martinez, E. C., Garg, R., & van Drunen Littel-van den Hurk, S. (2019). Innate immune protection from pneumonia virus of mice induced by a novel immunomodulator is prolonged by dual treatment and mediated by macrophages. *Antiviral Research*, *171*.

Martinez, F. O., & Gordon, S. (2014). The M1 and M2 paradigm of macrophage activation: time for reassessment. *F1000prime Reports*, *6*.

Martucci, C., Miglietta, D., Puviani, V., Allen, A. D., Carnini, C., Patacchini, R., Facchinetti, F., Civelli, M., Villetti, G., & Pappani, A. (2017). Effects of CHF6297, a potent and selective p38α MAPK inhibitor, in murine models of steroid resistant lung inflammation. *European Respiratory Journal*, *50*(suppl 61), OA4831.

Mass, E., Ballesteros, I., Farlik, M., Halbritter, F., Günther, P., Crozet, L., Jacome-Galarza, C. E., Händler, K., Klughammer, J., Kobayashi, Y., Gomez-Perdiguero, E., Schultze, J. L., Beyer, M., Bock, C., & Geissmann, F. (2016). Specification of tissue-resident macrophages during organogenesis. *Science (New York, N.Y.)*, *353*(6304).

McCombs, C. C., Michalski, J. P., & Light, R. W. (1984). Specificity of Immunosuppression by Human Alveolar Cells. *Http://Dx.Doi.Org/10.3109/01902148409087914*, *7*(3–4), 211–222.

McCombs, C. C., Michalski, J. P., Westerfield, B. T., & Light, R. W. (1982). Human alveolar macrophages suppress the proliferative response of peripheral blood lymphocytes. *Chest*, *82*(3), 266–271.

Meissner, J. D., Chang, K. C., Kubis, H. P., Nebreda, A. R., Gros, G., & Scheibe, R. J. (2007). The p38alpha/beta mitogen-activated protein kinases mediate recruitment of CREB-binding protein to preserve fast myosin heavy chain IId/x gene activity in myotubes. *The Journal of Biological Chemistry*, *282*(10), 7265–7275.

Menard, G., & Bissonnette, E. Y. (2000). Priming of alveolar macrophages by leukotriene D(4): potentiation of inflammation. *American Journal of Respiratory Cell and Molecular Biology*, *23*(4), 572–577.

Ménard, G., Turmel, V., & Bissonnette, E. Y. (2007). Serotonin modulates the cytokine network in the lung: involvement of prostaglandin E2. *Clinical and Experimental Immunology*, *150*(2), 340–348.

Meng, A., Zhang, X., & Shi, Y. (2014). Role of p38 MAPK and STAT3 in lipopolysaccharide-stimulated mouse alveolar macrophages. *Experimental and Therapeutic Medicine*, *8*(6), 1772–1776.

Mills, C. D., Kincaid, K., Alt, J. M., Heilman, M. J., & Hill, A. M. (2000). M-1/M-2 macrophages and the Th1/Th2 paradigm. *Journal of Immunology (Baltimore, Md. : 1950)*, *164*(12), 6166–6173.

Misharin, A. V., Morales-Nebreda, L., Mutlu, G. M., Budinger, G. R. S., & Perlman, H. (2013). Flow Cytometric Analysis of Macrophages and Dendritic Cell Subsets in the Mouse Lung. *American Journal of Respiratory Cell and Molecular Biology*, *49*(4), 503–510.

Mohan, J. F., Petzold, S. J., & Unanue, E. R. (2011). Register shifting of an insulin peptide-MHC complex allows diabetogenic T cells to escape thymic deletion. *The Journal of Experimental Medicine*, *208*(12), 2375–2383.

Molawi, K., Wolf, Y., Kandalla, P. K., Favret, J., Hagemeyer, N., Frenzel, K., Pinto, A. R., Klapproth, K., Henri, S., Malissen, B., Rodewald, H. R., Rosenthal, N. A., Bajenoff, M., Prinz, M., Jung, S., & Sieweke, M. H. (2014). Progressive replacement of embryo-derived cardiac macrophages with age. *The Journal of Experimental Medicine*, *211*(11), 2151–2158.

Moosavi, S. M., Prabhala, P., & Ammit, A. J. (2017). Role and regulation of MKP-1 in airway inflammation. *Respiratory Research*, *18*(1).

Morimoto, Y., Toyota, M., Satoh, A., Murai, M., Mita, H., Suzuki, H., Takamura, Y., Ikeda, H., Ishida, T., Sato, N., Tokino, T., & Imai, K. (2004). Inactivation of class II transactivator by DNA methylation and histone deacetylation associated with absence of HLA-DR induction by interferon-gamma in haematopoietic tumour cells. *British Journal of Cancer*, *90*(4), 844–852.

Morris, A. C., Beresford, G. W., Mooney, M. R., & Boss, J. M. (2002). Kinetics of a gamma interferon response: expression and assembly of CIITA promoter IV and inhibition by methylation. *Molecular and Cellular Biology*, *22*(13), 4781–4791.

Morris, A. C., Spangler, W. E., & Boss, J. M. (2000). Methylation of class II trans-activator promoter IV: a novel mechanism of MHC class II gene control. *Journal of Immunology (Baltimore, Md. : 1950)*, *164*(8), 4143–4149.

Morris, P., Shaman, J., Attaya, M., Amaya, M., Goodman, S., Bergman, C., Monaco, J. J., & Mellins, E. (1994). An essential role for HLA-DM in antigen presentation by class II major histocompatibility molecules. *Nature*, *368*(6471), 551–554.

Mould, K. J., Barthel, L., Mohning, M. P., Thomas, S. M., McCubbrey, A. L., Danhorn, T., Leach, S. M., Fingerlin, T. E., O'Connor, B. P., Reisz, J. A., D'Alessandro, A., Bratton, D. L., Jakubzick, C. V., & Janssen, W. J. (2017). Cell Origin Dictates Programming of Resident versus Recruited Macrophages during Acute Lung Injury. *American Journal of Respiratory Cell and Molecular Biology*, *57*(3), 294–306.

Mould, K. J., Jackson, N. D., Henson, P. M., Seibold, M., & Janssen, W. J. (2019). Single cell RNA sequencing identifies unique inflammatory airspace macrophage subsets. *JCI Insight*, *4*(5).

Mu, X., Li, Y., & Fan, G. C. (2021). Tissue-Resident Macrophages in the Control of

Infection and Resolution of Inflammation. *Shock (Augusta, Ga.)*, *55*(1), 14–23.
Mudgett, J. S., Ding, J., Guh-Siesel, L., Chartrain, N. A., Yang, L., Gopal, S., & Shen, M. M. (2000). Essential role for p38alpha mitogen-activated protein kinase in placental angiogenesis. *Proceedings of the National Academy of Sciences of the United States of America*, *97*(19), 10454–10459.
Muhlethaler-Mottet, A., Berardino, W. Di, Otten, L. A., & Mach, B. (1998). Activation of the MHC class II transactivator CIITA by interferon-gamma requires cooperative interaction between Stat1 and USF-1. *Immunity*, *8*(2), 157–166.
Muhlethaler-Mottet, A., Otten, L. A., Steimle, V., & Mach, B. (1997). Expression of MHC class II molecules in different cellular and functional compartments is controlled by differential usage of multiple promoters of the transactivator CIITA. *The EMBO Journal*, *16*(10), 2851–2860.
Murali, K., & Rao, K. (2001). MAP kinase activation in macrophages. *Journal of Leukocyte Biology*, *69*(1), 3–10.
Murphy, S. P., Holtz, R., Lewandowski, N., Tomasi, T. B., & Fuji, H. (2002). DNA alkylating agents alleviate silencing of class II transactivator gene expression in L1210 lymphoma cells. *Journal of Immunology (Baltimore, Md. : 1950)*, *169*(6), 3085–3093.
Murray, P. J., Allen, J. E., Biswas, S. K., Fisher, E. A., Gilroy, D. W., Goerdt, S., Gordon, S., Hamilton, J. A., Ivashkiv, L. B., Lawrence, T., Locati, M., Mantovani, A., Martinez, F. O., Mege, J. L., Mosser, D. M., Natoli, G., Saeij, J. P., Schultze, J. L., Shirey, K. A., … Wynn, T. A. (2014). Macrophage activation and polarization: nomenclature and experimental guidelines. *Immunity*, *41*(1), 14–20.
Nakamura, K., Yoshikawa, N., Yamaguchi, Y., Kagota, S., Shinozuka, K., & Kunitomo, M. (2002). Characterization of mouse melanoma cell lines by their mortal malignancy using an experimental metastatic model. *Life Sciences*, *70*, 791–798.
Nath, P., Leung, S.-Y., Williams, A., Noble, A., Chakravarty, S. D. S., Luedtke, G. R., Medicherla, S., Higgins, L. S., Protter, A., & Chung, K. F. (2006). Importance of p38 mitogen-activated protein kinase pathway in allergic airway remodelling and bronchial hyperresponsiveness. *European Journal of Pharmacology*, *544*(1–3), 160–167.
Nathan, C. (2006). Neutrophils and immunity: challenges and opportunities. *Nature Reviews. Immunology*, *6*(3), 173–182.
Neamatallah, T. (2019). Mitogen-Activated Protein Kinase Pathway: A Critical Regulator in Tumor-associated Macrophage Polarization. *Journal of Microscopy and Ultrastructure*, *7*(2), 53.
Neupane, A. S., Willson, M., Chojnacki, A. K., Vargas E Silva Castanheira, F., Morehouse, C., Carestia, A., Keller, A. E., Peiseler, M., DiGiandomenico, A., Kelly, M. M., Amrein, M., Jenne, C., Thanabalasuriar, A., & Kubes, P. (2020). Patrolling Alveolar Macrophages Conceal Bacteria from the Immune System to Maintain Homeostasis. *Cell*, *183*(1), 110-125.e11.
Ni, Z., Hassan, M. A. El, Xu, Z., Yu, T., & Bremner, R. (2008). The chromatin-remodeling enzyme BRG1 coordinates CIITA induction through many interdependent distal enhancers. *Nature Immunology*, *9*(7), 785–793.

Ni, Z., Karaskov, E., Yu, T., Callaghan, S. M., Der, S., Park, D. S., Xu, Z., Pattenden, S. G., & Bremner, R. (2005). Apical role for BRG1 in cytokine-induced promoter assembly. *Proceedings of the National Academy of Sciences of the United States of America*, *102*(41), 14611–14616.

Nick, J. A., Young, S. K., Arndt, P. G., Lieber, J. G., Suratt, B. T., Poch, K. R., Avdi, N. J., Malcolm, K. C., Taube, C., Henson, P. M., & Worthen, G. S. (2002). Selective Suppression of Neutrophil Accumulation in Ongoing Pulmonary Inflammation by Systemic Inhibition of p38 Mitogen-Activated Protein Kinase. *The Journal of Immunology*, *169*(9), 5260–5269.

Nick, J. A., Young, S. K., Brown, K. K., Avdi, N. J., Arndt, P. G., Suratt, B. T., Janes, M. S., Henson, P. M., & Worthen, G. S. (2000). Role of p38 Mitogen-Activated Protein Kinase in a Murine Model of Pulmonary Inflammation. *The Journal of Immunology*, *164*(4), 2151–2159.

Nickerson, K., Sisk, T. J., Inohara, N., Yee, C. S. K., Kennell, J., Cho, M. C., Yannie, P. J., Núñez, G., & Chang, C. H. (2001). Dendritic cell-specific MHC class II transactivator contains a caspase recruitment domain that confers potent transactivation activity. *The Journal of Biological Chemistry*, *276*(22), 19089–19093.

Nielsen, S. R., & Schmid, M. C. (2017). Macrophages as Key Drivers of Cancer Progression and Metastasis. *Mediators of Inflammation*, *2017*.

Noy, R., & Pollard, J. W. (2014). Tumor-associated macrophages: from mechanisms to therapy. *Immunity*, *41*(1), 49–61.

Nurieva, R., Thomas, S., Nguyen, T., Martin-Orozco, N., Wang, Y., Kaja, M.-K., Yu, X.-Z., & Dong, C. (2006). T-cell tolerance or function is determined by combinatorial costimulatory signals. *The EMBO Journal*, *25*(11), 2623–2633.

Obenauf, A. C., & Massagué, J. (2015). Surviving at a distance: organ specific metastasis. *Trends in Cancer*, *1*(1), 76–91.

Ochs, M., Hegermann, J., Lopez-Rodriguez, E., Timm, S., Nouailles, G., Matuszak, J., Simmons, S., Witzenrath, M., & Kuebler, W. M. (2020). On top of the alveolar epithelium: Surfactant and the glycocalyx. In *International Journal of Molecular Sciences* (Vol. 21, Issue 9). MDPI AG.

Olman, M. A., Mcdonald, C., Asosingh, K., Hasday, J. D., Southern, B. D., Crish, J. F., Perelas, A., Scheraga, R. G., Abraham, S., & Grove, L. M. (2022). *Switching Pneumonia via MAPK Molecular Pathway TRPV4 Protects the Lung from Bacterial*.

Otten, L. A., Steimle, V., Bontron, S., & Mach, B. (1998). Quantitative control of MHC class II expression by the transactivator CIITA. *European Journal of Immunology*, *28*(2), 473–478.

Oumouna, M., Weitnauer, M., Mijošek, V., Schmidt, L. M., Eigenbrod, T., & Dalpke, A. H. (2015). Cell-contact dependent inhibition of monocytes by airway epithelial cells and reversion by infection with Respiratory Syncytial Virus. *Immunobiology*, *220*(11), 1240–1245.

Ouyang, W., & O'Garra, A. (2019). IL-10 Family Cytokines IL-10 and IL-22: from Basic Science to Clinical Translation. *Immunity*, *50*(4), 871–891.

Paget, S. (n.d.). *DISTRIBUTION OF SECONDARY GROWTHS IN CANCER OF THE*

BREAST.

Paolino, M., Choidas, A., Wallner, S., Pranjic, B., Uribesalgo, I., Loeser, S., Jamieson, A. M., Langdon, W. Y., Ikeda, F., Fededa, J. P., Cronin, S. J., Nitsch, R., Schultz-Fademrecht, C., Eickhoff, J., Menninger, S., Unger, A., Torka, R., Gruber, T., Hinterleitner, R., … Penninger, J. M. (2014). The E3 ligase Cbl-b and TAM receptors regulate cancer metastasis via natural killer cells. *Nature*, *507*(7493), 508–512.

Patnaik, A., Haluska, P., Tolcher, A. W., Erlichman, C., Papadopoulos, K. P., Lensing, J. L., Beeram, M., Molina, J. R., Rasco, D. W., Arcos, R. R., Kelly, C. S., Wijayawardana, S. R., Zhang, X., Stancato, L. F., Bell, R., Shi, P., Kulanthaivel, P., Pitou, C., Mulle, L. B., … Goetz, M. P. (2016). A First-in-Human Phase I Study of the Oral p38 MAPK Inhibitor, Ralimetinib (LY2228820 Dimesylate), in Patients with Advanced Cancer. *Clinical Cancer Research*, *22*(5), 1095–1102.

Pelaia, C., Vatrella, A., Gallelli, L., Lombardo, N., Sciacqua, A., Savino, R., & Pelaia, G. (2021). Role of p38 Mitogen-Activated Protein Kinase in Asthma and COPD: Pathogenic Aspects and Potential Targeted Therapies. *Drug Design, Development and Therapy*, *15*, 1275–1284.

Pelaia, C., Vatrella, A., Sciacqua, A., Terracciano, R., & Pelaia, G. (2020). Role of p38-mitogen-activated protein kinase in COPD: pathobiological implications and therapeutic perspectives. *Expert Review of Respiratory Medicine*, *14*(5), 485–491.

Perdiguero, E. G., & Geissmann, F. (2016). The development and maintenance of resident macrophages. *Nature Immunology*, *17*(1), 2–8.

Pietersma, A., Tilly, B. C., Gaestel, M., De Jong, N., Lee, J. C., Koster, J. F., & Sluiter, W. (1997). p38 mitogen activated protein kinase regulates endothelial VCAM-1 expression at the post-transcriptional level. *Biochemical and Biophysical Research Communications*, *230*(1), 44–48.

Piskurich, J. F., Lin, K. I., Lin, Y., Wang, Y., Ting, J. P. Y., & Calame, K. (2000). BLIMP-I mediates extinction of major histocompatibility class II transactivator expression in plasma cells. *Nature Immunology*, *1*(6), 526–532.

Pittet, M. J., Michielin, O., & Migliorini, D. (2022). Clinical relevance of tumour-associated macrophages. *Nature Reviews Clinical Oncology 2022 19:6*, *19*(6), 402–421.

Popper, H. (2017). Normal Lung. *Pathology of Lung Disease*, 7–20.

Ptasinska, A., Wang, S., Zhang, J., Wesley, R. A., & Danner, R. L. (2007). Nitric oxide activation of peroxisome proliferator-activated receptor gamma through a p38 MAPK signaling pathway. *FASEB Journal : Official Publication of the Federation of American Societies for Experimental Biology*, *21*(3), 950–961.

Pu, Z., Lovitch, S. B., Bikoff, E. K., & Unanue, E. R. (2004). T cells distinguish MHC-peptide complexes formed in separate vesicles and edited by H2-DM. *Immunity*, *20*(4), 467–476.

Puigserver, P., Rhee, J., Lin, J., Wu, Z., Yoon, J. C., Zhang, C. Y., Krauss, S., Mootha, V. K., Lowell, B. B., & Spiegelman, B. M. (2001). Cytokine stimulation of energy expenditure through p38 MAP kinase activation of PPARgamma coactivator-1. *Molecular Cell*, *8*(5), 971–982.

Qian, B. Z., & Pollard, J. W. (2010). Macrophage diversity enhances tumor progression and metastasis. *Cell*, *141*(1), 39–51.
Radosevich, M., Jager, M., & Ono, S. J. (2007). Inhibition of MHC class II gene expression in uveal melanoma cells is due to methylation of the CIITA gene or an upstream activator. *Experimental and Molecular Pathology*, *82*(1), 68–76.
Rajaram, M. V. S., Arnett, E., Azad, A. K., Guirado, E., Ni, B., Gerberick, A. D., He, L. Z., Keler, T., Thomas, L. J., Lafuse, W. P., & Schlesinger, L. S. (2017). M. tuberculosis-Initiated Human Mannose Receptor Signaling Regulates Macrophage Recognition and Vesicle Trafficking by FcRγ-Chain, Grb2, and SHP-1. *Cell Reports*, *21*(1), 126–140.
Ramanathan, S., Dubois, S., Chen, X.-L., Leblanc, C., Ohashi, P. S., & Ilangumaran, S. (2011). Exposure to IL-15 and IL-21 enables autoreactive CD8 T cells to respond to weak antigens and cause disease in a mouse model of autoimmune diabetes. *Journal of Immunology (Baltimore, Md. : 1950)*, *186*(9), 5131–5141.
Rauschmeier, R., Gustafsson, C., Reinhardt, A., A-Gonzalez, N., Tortola, L., Cansever, D., Subramanian, S., Taneja, R., Rossner, M. J., Sieweke, M. H., Greter, M., Månsson, R., Busslinger, M., & Kreslavsky, T. (2019). Bhlhe40 and Bhlhe41 transcription factors regulate alveolar macrophage self-renewal and identity. *The EMBO Journal*, *38*(19).
Ray, A. L., Castillo, E. F., Morris, K. T., Nofchissey, R. A., Weston, L. L., Samedi, V. G., Hanson, J. A., Gaestel, M., Pinchuk, I. V., & Beswick, E. J. (2016). Blockade of MK2 is protective in inflammation-associated colorectal cancer development. *International Journal of Cancer*, *138*(3), 770–775.
Raza, A., Crothers, J. W., McGill, M. M., Mawe, G. M., Teuscher, C., & Krementsov, D. N. (2017). Anti-inflammatory roles of p38α MAPK in macrophages are context dependent and require IL-10. *Journal of Leukocyte Biology*, *102*(5), 1219.
Redente, E. F., Dwyer-Nield, L. D., Merrick, D. T., Raina, K., Agarwal, R., Pao, W., Rice, P. L., Shroyer, K. R., & Malkinson, A. M. (2010). Tumor progression stage and anatomical site regulate tumor-associated macrophage and bone marrow-derived monocyte polarization. *The American Journal of Pathology*, *176*(6), 2972–2985.
Reith, W., LeibundGut-Landmann, S., & Waldburger, J. M. (2005). Regulation of MHC class II gene expression by the class II transactivator. *Nature Reviews. Immunology*, *5*(10), 793–806.
Reith, W., Steimle, V., & Mach, B. (1995). Molecular defects in the bare lymphocyte syndrome and regulation of MHC class II genes. *Immunology Today*, *16*(11), 539–546.
Remy, G., Risco, A. M., Iñesta-Vaquera, F. A., González-Terán, B., Sabio, G., Davis, R. J., & Cuenda, A. (2010). Differential activation of p38MAPK isoforms by MKK6 and MKK3. *Cellular Signalling*, *22*(4), 660–667.
Renda, T., Baraldo, S., Pelaia, G., Bazzan, E., Turato, G., Papi, A., Maestrelli, P., Maselli, R., Vatrella, A., Fabbri, L. M., Zuin, R., Marsico, S. A., & Saetta, M. (2008). Increased activation of p38 MAPK in COPD. *The European Respiratory Journal*, *31*(1), 62–69.
Reyskens, K. M. S. E., & Arthur, J. S. C. (2016). Emerging Roles of the Mitogen and

Stress Activated Kinases MSK1 and MSK2. *Frontiers in Cell and Developmental Biology*, *4*(JUN).

Riberdy, J. M., Newcomb, J. R., Surman, M. J., Barbosat, J. A., & Cresswell, P. (1992). HLA-DR molecules from an antigen-processing mutant cell line are associated with invariant chain peptides. *Nature*, *360*(6403), 474–477.

Riihimäki, M., Thomsen, H., Sundquist, K., Sundquist, J., & Hemminki, K. (2018). Clinical landscape of cancer metastases. *Cancer Medicine*, *7*(11), 5534.

Rincón, M., & Davis, R. J. (2009). Regulation of the immune response by stress-activated protein kinases. *Immunological Reviews*, *228*(1), 212–224.

Roberts, A. W., Lee, B. L., Deguine, J., John, S., Shlomchik, M. J., & Barton, G. M. (2017). Tissue-Resident Macrophages Are Locally Programmed for Silent Clearance of Apoptotic Cells. *Immunity*, *47*(5), 913-927.e6.

Roche, P. A., & Furuta, K. (2015). The ins and outs of MHC class II-mediated antigen processing and presentation. *Nature Reviews Immunology 2015 15:4*, *15*(4), 203–216.

Rolli-Derkinderen, M., Machavoine, F., Baraban, J. M., Grolleau, A., Beretta, L., & Dy, M. (2003). ERK and p38 inhibit the expression of 4E-BP1 repressor of translation through induction of Egr-1. *Journal of Biological Chemistry*, *278*(21), 18859–18867.

Rosenberg, H. F., Dyer, K. D., & Foster, P. S. (2013). Eosinophils: changing perspectives in health and disease. *Nature Reviews. Immunology*, *13*(1), 9–22.

Rouse, J., Cohen, P., Trigon, S., Morange, M., Alonso-Llamazares, A., Zamanillo, D., Hunt, T., & Nebreda, A. R. (1994). A novel kinase cascade triggered by stress and heat shock that stimulates MAPKAP kinase-2 and phosphorylation of the small heat shock proteins. *Cell*, *78*(6), 1027–1037.

Russell, R. E. K., Culpitt, S. V., DeMatos, C., Donnelly, L., Smith, M., Wiggins, J., & Barnes, P. J. (2002). Release and activity of matrix metalloproteinase-9 and tissue inhibitor of metalloproteinase-1 by alveolar macrophages from patients with chronic obstructive pulmonary disease. *American Journal of Respiratory Cell and Molecular Biology*, *26*(5), 602–609.

Sade-Feldman, M., Jiao, Y. J., Chen, J. H., Rooney, M. S., Barzily-Rokni, M., Eliane, J. P., Bjorgaard, S. L., Hammond, M. R., Vitzthum, H., Blackmon, S. M., Frederick, D. T., Hazar-Rethinam, M., Nadres, B. A., Van Seventer, E. E., Shukla, S. A., Yizhak, K., Ray, J. P., Rosebrock, D., Livitz, D., … Hacohen, N. (2017). Resistance to checkpoint blockade therapy through inactivation of antigen presentation. *Nature Communications*, *8*(1).

Sagerup, C. M. T., Småstuen, M., Johannesen, T. B., Helland, Å., & Brustugun, O. T. (2011). Sex-specific trends in lung cancer incidence and survival: a population study of 40 118 cases. *Thorax*, *66*(4), 301–307.

Sajti, E., Link, V. M., Ouyang, Z., Spann, N. J., Westin, E., Romanoski, C. E., Fonseca, G. J., Prince, L. S., & Glass, C. K. (2020). Transcriptomic and epigenetic mechanisms underlying myeloid diversity in the lung. *Nature Immunology 2020 21:2*, *21*(2), 221–231.

Satija, R., Farrell, J. A., Gennert, D., Schier, A. F., & Regev, A. (2015). Spatial reconstruction of single-cell gene expression data. *Nature Biotechnology 2015*

33:5, *33*(5), 495–502.
Satoh, A., Toyota, M., Ikeda, H., Morimoto, Y., Akino, K., Mita, H., Suzuki, H., Sasaki, Y., Kanaseki, T., Takamura, Y., Soejima, H., Urano, T., Yanagihara, K., Endo, T., Hinoda, Y., Fujita, M., Hosokawa, M., Sato, N., Tokino, T., & Imai, K. (2004). Epigenetic inactivation of class II transactivator (CIITA) is associated with the absence of interferon-gamma-induced HLA-DR expression in colorectal and gastric cancer cells. *Oncogene*, *23*(55), 8876–8886.
Sceneay, J., Chow, M. T., Chen, A., Halse, H. M., Wong, C. S. F., Andrews, D. M., Sloan, E. K., Parker, B. S., Bowtell, D. D., Smyth, M. J., & Möller, A. (2012). Primary tumor hypoxia recruits CD11b+/Ly6Cmed/Ly6G+ immune suppressor cells and compromises NK cell cytotoxicity in the premetastatic niche. *Cancer Research*, *72*(16), 3906–3911.
Sceneay, J., Smyth, M. J., & Möller, A. (2013). The pre-metastatic niche: finding common ground. *Cancer Metastasis Reviews*, *32*(3–4), 449–464.
Scheraga, R. G., Abraham, S., Grove, L. M., Southern, B. D., Crish, J. F., Perelas, A., Mcdonald, C., Asosingh, K., Hasday, J. D., & Olman, M. A. (2020). TRPV4 Protects the Lung from Bacterial Pneumonia via MAPK Molecular Pathway Switching. *The Journal of Immunology*, *204*, 1310–1321.
Schild, R. L., Sonnenberg-Hirche, C. M., Schaiff, W. T., Bildirici, I., Nelson, D. M., & Sadovsky, Y. (2006). The kinase p38 regulates peroxisome proliferator activated receptor-gamma in human trophoblasts. *Placenta*, *27*(2–3), 191–199.
Schneider, C., Nobs, S. P., Kurrer, M., Rehrauer, H., Thiele, C., & Kopf, M. (2014). Induction of the nuclear receptor PPAR-γ by the cytokine GM-CSF is critical for the differentiation of fetal monocytes into alveolar macrophages. *Nature Immunology*, *15*(11), 1026–1037.
Schooten, E., Klous, P., Van Den Elsen, P. J., & Holling, T. M. (2005). Lack of MHC-II expression in activated mouse T cells correlates with DNA methylation at the CIITA-PIII region. *Immunogenetics*, *57*(10), 795–799.
Schulz, C., Perdiguero, E. G., Chorro, L., Szabo-Rogers, H., Cagnard, N., Kierdorf, K., Prinz, M., Wu, B., Jacobsen, S. E. W., Pollard, J. W., Frampton, J., Liu, K. J., & Geissmann, F. (2012). A lineage of myeloid cells independent of Myb and hematopoietic stem cells. *Science (New York, N.Y.)*, *336*(6077), 86–90.
Seto, E., & Yoshida, M. (2014). Erasers of Histone Acetylation: The Histone Deacetylase Enzymes. *Cold Spring Harbor Perspectives in Biology*, *6*(4), a018713.
Sette, A., Ceman, S., Kubo, R. T., Sakaguchi, K., Appella, E., Hunt, D. F., Davis, T. A., Michel, H., Shabanowitz, J., Rudersdorf, R., Grey, H. M., & DeMars, R. (1992). Invariant chain peptides in most HLA-DR molecules of an antigen-processing mutant. *Science (New York, N.Y.)*, *258*(5089), 1801–1804.
Shapouri-Moghaddam, A., Mohammadian, S., Vazini, H., Taghadosi, M., Esmaeili, S. A., Mardani, F., Seifi, B., Mohammadi, A., Afshari, J. T., & Sahebkar, A. (2018). Macrophage plasticity, polarization, and function in health and disease. *Journal of Cellular Physiology*, *233*(9), 6425–6440.
Sharma, S. K., Chintala, N. K., Vadrevu, S. K., Patel, J., Karbowniczek, M., & Markiewski, M. M. (2015). Pulmonary Alveolar Macrophages Contribute to the

Premetastatic Niche by Suppressing Antitumor T Cell Responses in the Lungs. *The Journal of Immunology*, *194*(11), 5529–5538.

Shellito, J., & Kaltreider, H. B. (1985). Heterogeneity of immunologic function among subfractions of normal rat alveolar macrophages. II. Activation as a determinant of functional activity. *The American Review of Respiratory Disease*, *131*(5), 678–683.

Shi, J., Hua, L., Harmer, D., Li, P., & Ren, G. (2018). Cre Driver Mice Targeting Macrophages. *Methods in Molecular Biology (Clifton, N.J.)*, *1784*, 263.

Shi, Q., Cheng, L., Liu, Z., Hu, K., Ran, J., Ge, D., & Fu, J. (2015). The p38 MAPK inhibitor SB203580 differentially modulates LPS-induced interleukin 6 expression in macrophages. *Central-European Journal of Immunology*, *40*(3), 276.

Shin, J. S., Ebersold, M., Pypaert, M., Delamarre, L., Hartley, A., & Mellman, I. (2006). Surface expression of MHC class II in dendritic cells is controlled by regulated ubiquitination. *Nature*, *444*(7115), 115–118.

Shinohara, M., Ohyama, N., Murata, Y., Okazawa, H., Ohnishi, H., Ishikawa, O., & Matozaki, T. (2006). CD47 regulation of epithelial cell spreading and migration, and its signal transduction. *Cancer Science*, *97*(9), 889–895.

Shiratsuchi, H., & Basson, M. D. (2005). Activation of p38 MAPKalpha by extracellular pressure mediates the stimulation of macrophage phagocytosis by pressure. *American Journal of Physiology. Cell Physiology*, *288*(5).

Simone, C., Forcales, S. V., Hill, D. A., Imbalzano, A. N., Latella, L., & Puri, P. L. (2004). p38 pathway targets SWI-SNF chromatin-remodeling complex to muscle-specific loci. *Nature Genetics*, *36*(7), 738–743.

Snelgrove, R. J., Goulding, J., Didierlaurent, A. M., Lyonga, D., Vekaria, S., Edwards, L., Gwyer, E., Sedgwick, J. D., Barclay, A. N., & Hussell, T. (2008). A critical function for CD200 in lung immune homeostasis and the severity of influenza infection. *Nature Immunology*, *9*(9), 1074–1083.

Sonali, J., & Leonidas C., P. (2014). Mnk kinase pathway: Cellular functions and biological outcomes. *World Journal of Biological Chemistry*, *5*(3), 321.

Soroosh, P., Doherty, T. A., Duan, W., Mehta, A. K., Choi, H., Adams, Y. F., Mikulski, Z., Khorram, N., Rosenthal, P., Broide, D. H., & Croft, M. (2013). Lung-resident tissue macrophages generate Foxp3+ regulatory T cells and promote airway tolerance. *The Journal of Experimental Medicine*, *210*(4), 775–788.

Stabellini, N., Bruno, D. S., Dmukauskas, M., Barda, A. J., Cao, L., Shanahan, J., Waite, K., Montero, A. J., & Barnholtz-Sloan, J. S. (2022). Sex Differences in Lung Cancer Treatment and Outcomes at a Large Hybrid Academic-Community Practice. *JTO Clinical and Research Reports*, *3*(4).

Steimle, V., Siegrist, C. A., Mottet, A., Lisowska-Grospierre, B., & Mach, B. (1994). Regulation of MHC class II expression by interferon-gamma mediated by the transactivator gene CIITA. *Science (New York, N.Y.)*, *265*(5168), 106–109. http://www.ncbi.nlm.nih.gov/pubmed/8016643

Stern, N., Riklis, S., Kalina, M., & Tietz, A. (1986). The catabolism of lung surfactant by alveolar macrophages. *Biochimica et Biophysica Acta*, *877*(3), 323–333.

Strickland, D., Kees, U. R., & Holt, P. G. (1996). Regulation of T-cell activation in the

lung: isolated lung T cells exhibit surface phenotypic characteristics of recent activation including down-modulated T-cell receptors, but are locked into the G0/G1 phase of the cell cycle. *Immunology*, *87*(2), 242–249.

Stuart, T., Butler, A., Hoffman, P., Hafemeister, C., Papalexi, E., Mauck, W. M., Hao, Y., Stoeckius, M., Smibert, P., & Satija, R. (2019). Comprehensive Integration of Single-Cell Data. *Cell*, *177*(7), 1888-1902.e21.

Suarez-Lopez, L., Sriram, G., Kong, Y. W., Morandell, S., Merrick, K. A., Hernandez, Y., Haigis, K. M., & Yaffe, M. B. (2018). MK2 contributes to tumor progression by promoting M2 macrophage polarization and tumor angiogenesis. *Proceedings of the National Academy of Sciences of the United States of America*, *115*(18), E4236–E4244.

Sun, F., Xiao, G., & Qu, Z. (2017). Murine Bronchoalveolar Lavage. *Bio-Protocol*, *7*(10).

Suzuki, K., Hasegawa, T., Sakamoto, C., Zhou, Y.-M., Hato, F., Hino, M., Tatsumi, N., & Kitagawa, S. (2001). Cleavage of Mitogen-Activated Protein Kinases in Human Neutrophils Undergoing Apoptosis: Role in Decreased Responsiveness to Inflammatory Cytokines. *The Journal of Immunology*, *166*(2), 1185–1192.

Svedberg, F. R., Brown, S. L., Krauss, M. Z., Campbell, L., Sharpe, C., Clausen, M., Howell, G. J., Clark, H., Madsen, J., Evans, C. M., Sutherland, T. E., Ivens, A. C., Thornton, D. J., Grencis, R. K., Hussell, T., Cunoosamy, D. M., Cook, P. C., & MacDonald, A. S. (2019). The lung environment controls alveolar macrophage metabolism and responsiveness in type 2 inflammation. *Nature Immunology*, *20*(5), 571–580.

Swiecki, M., & Colonna, M. (2015). The multifaceted biology of plasmacytoid dendritic cells. *Nature Reviews. Immunology*, *15*(8), 471–485.

T'Jonck, W., Guilliams, M., & Bonnardel, J. (2018). Niche signals and transcription factors involved in tissue-resident macrophage development. *Cellular Immunology*, *330*, 43–53.

Tamura, K., Sudo, T., Senftleben, U., Dadak, A. M., Johnson, R., & Karin, M. (2000). Requirement for p38α in Erythropoietin Expression: A Role for Stress Kinases in Erythropoiesis. *Cell*, *102*(2), 221–231.

Tang, X. Z., Kreuk, L. S. M., Cho, C., Metzger, R. J., & Allen, C. D. C. (2022). Bronchus-associated macrophages efficiently capture and present soluble inhaled antigens and are capable of local Th2 cell activation. *ELife*, *11*.

Tarasov, A., Vilella, A. J., Cuppen, E., Nijman, I. J., & Prins, P. (2015). Sambamba: fast processing of NGS alignment formats. *Bioinformatics (Oxford, England)*, *31*(12), 2032–2034.

The lungs at the frontlines of immunity. (2014). *Nature Immunology 2015 16:1*, *16*(1), 17–17.

Thepen, T., McMenamin, C., Oliver, J., Kraal, G., & Holt, P. G. (1991). Regulation of immune response to inhaled antigen by alveolar macrophages: differential effects of in vivo alveolar macrophage elimination on the induction of tolerance vs. immunity. *European Journal of Immunology*, *21*(11), 2845–2850.

Thepen, T., Van Rooijen, N., & Kraal, G. (1989). Alveolar macrophage elimination in vivo is associated with an increase in pulmonary immune response in mice. *The*

Journal of Experimental Medicine, *170*(2), 499–509.

Tie, Y., Tang, F., Wei, Y. quan, & Wei, X. wei. (2022). Immunosuppressive cells in cancer: mechanisms and potential therapeutic targets. *Journal of Hematology & Oncology 2022 15:1*, *15*(1), 1–33.

Trempolec, N., Dave-Coll, N., & Nebreda, A. R. (2013). SnapShot: p38 MAPK substrates. *Cell*, *152*(4).

Tzavlaki, K., & Moustakas, A. (2020). TGF-β Signaling. *Biomolecules 2020, Vol. 10, Page 487*, *10*(3), 487.

Underwood, D. C., Osborn, R. R., Kotzer, C. J., Adams, J. L., Lee, J. C., Webb, E. F., Carpenter, D. C., Bochnowicz, S., Thomas, H. C., Hay, D. W., & Griswold, D. E. (2000). SB 239063, a potent p38 MAP kinase inhibitor, reduces inflammatory cytokine production, airways eosinophil infiltration, and persistence. *The Journal of Pharmacology and Experimental Therapeutics*, *293*(1), 281–288.

Ural, B. B., Yeung, S. T., Damani-Yokota, P., Devlin, J. C., de Vries, M., Vera-Licona, P., Samji, T., Sawai, C. M., Jang, G., Perez, O. A., Pham, Q., Maher, L., Loke, P., Dittmann, M., Reizis, B., & Khanna, K. M. (2020). Identification of a nerve-associated, lung-resident interstitial macrophage subset with distinct localization and immunoregulatory properties. *Science Immunology*, *5*(45).

Van den Elsen, P. J., Van der Stoep, N., Viëtor, H. E., Wilson, L., Van Zutphen, M., & Gobin, S. J. P. (2000). Lack of CIITA expression is central to the absence of antigen presentation functions of trophoblast cells and is caused by methylation of the IFN-gamma inducible promoter (PIV) of CIITA. *Human Immunology*, *61*(9), 850–862.

Van Der Stoep, N., Biesta, P., Quinten, E., & Van Den Elsen, P. J. (2002). Lack of IFN-gamma-mediated induction of the class II transactivator (CIITA) through promoter methylation is predominantly found in developmental tumor cell lines. *International Journal of Cancer*, *97*(4), 501–507.

van Dijk, D., Sharma, R., Nainys, J., Yim, K., Kathail, P., Carr, A. J., Burdziak, C., Moon, K. R., Chaffer, C. L., Pattabiraman, D., Bierie, B., Mazutis, L., Wolf, G., Krishnaswamy, S., & Pe'er, D. (2018). Recovering Gene Interactions from Single-Cell Data Using Data Diffusion. *Cell*, *174*(3), 716-729.e27.

Van Hove, H., Martens, L., Scheyltjens, I., De Vlaminck, K., Pombo Antunes, A. R., De Prijck, S., Vandamme, N., De Schepper, S., Van Isterdael, G., Scott, C. L., Aerts, J., Berx, G., Boeckxstaens, G. E., Vandenbroucke, R. E., Vereecke, L., Moechars, D., Guilliams, M., Van Ginderachter, J. A., Saeys, Y., & Movahedi, K. (2019). A single-cell atlas of mouse brain macrophages reveals unique transcriptional identities shaped by ontogeny and tissue environment. *Nature Neuroscience*, *22*(6), 1021–1035.

Van Oud, A., & Van Furth, R. (1979). *ORIGIN, KINETICS, AND CHARACTERISTICS OF PULMONARY MACROPHAGES IN THE NORMAL STEADY STATE*.

Vaught, D. B., Stanford, J. C., & Cook, R. S. (2015). Efferocytosis creates a tumor microenvironment supportive of tumor survival and metastasis. *Cancer Cell & Microenvironment*, *2*(1).

Vecchiarelli, A., Dottorini, M., Pietrella, D., Monari, C., Retini, C., Todisco, T., & Bistoni, F. (2012). Role of human alveolar macrophages as antigen-presenting

cells in Cryptococcus neoformans infection. *Https://Doi.Org/10.1165/Ajrcmb.11.2.8049074*, *11*(2), 130–137.
Veldhuizen, R., Nag, K., Orgeig, S., & Possmayer, F. (1998). The role of lipids in pulmonary surfactant. *Biochimica et Biophysica Acta*, *1408*(2–3), 90–108.
Ventura, J. J., Tenbaum, S., Perdiguero, E., Huth, M., Guerra, C., Barbacid, M., Pasparakis, M., & Nebreda, A. R. (2007). p38alpha MAP kinase is essential in lung stem and progenitor cell proliferation and differentiation. *Nature Genetics*, *39*(6), 750–758.
Vergote, I., Heitz, F., Buderath, P., Powell, M., Sehouli, J., Lee, C. M., Hamilton, A., Fiorica, J., Moore, K. N., Teneriello, M., Golden, L., Zhang, W., Pitou, C., Bell, R., Campbell, R., Farrington, D. L., Bell-McGuinn, K., & Wenham, R. M. (2020). A randomized, double-blind, placebo-controlled phase 1b/2 study of ralimetinib, a p38 MAPK inhibitor, plus gemcitabine and carboplatin versus gemcitabine and carboplatin for women with recurrent platinum-sensitive ovarian cancer. *Gynecologic Oncology*, *156*(1), 23–31.
Vinay, D. S., Ryan, E. P., Pawelec, G., Talib, W. H., Stagg, J., Elkord, E., Lichtor, T., Decker, W. K., Whelan, R. L., Kumara, H. M. C. S., Signori, E., Honoki, K., Georgakilas, A. G., Amin, A., Helferich, W. G., Boosani, C. S., Guha, G., Ciriolo, M. R., Chen, S., … Kwon, B. S. (2015). Immune evasion in cancer: Mechanistic basis and therapeutic strategies. *Seminars in Cancer Biology*, *35 Suppl*, S185–S198.
Vitos-Faleato, J. (2017). *Role of p38alpha in lung tumor progression*.
Wagner, E. F., & Nebreda, Á. R. (2009). Signal integration by JNK and p38 MAPK pathways in cancer development. *Nature Reviews. Cancer*, *9*(8), 537–549.
Waldburger, J. M., Suter, T., Fontana, A., Acha-Orbea, H., & Reith, W. (2001). Selective abrogation of major histocompatibility complex class II expression on extrahematopoietic cells in mice lacking promoter IV of the class II transactivator gene. *The Journal of Experimental Medicine*, *194*(4), 393–406.
Wang, H., Pan, J., Barsky, L., Jacob, J. C., Zheng, Y., Gao, C., Wang, S., Zhu, W., Sun, H., Lu, L., Jia, H., Zhao, Y., Bruns, C., Vago, R., Dong, Q., & Qin, L. (2021). Characteristics of pre-metastatic niche: the landscape of molecular and cellular pathways. *Molecular Biomedicine*, *2*(1), 3.
Wang, Q. E., Han, C., Zhao, R., Wani, G., Zhu, Q., Gong, L., Battu, A., Racoma, I., Sharma, N., & Wani, A. A. (2013). p38 MAPK- and Akt-mediated p300 phosphorylation regulates its degradation to facilitate nucleotide excision repair. *Nucleic Acids Research*, *41*(3), 1722–1733.
Wculek, S. K., & Malanchi, I. (2015). Neutrophils support lung colonization of metastasis-initiating breast cancer cells. *Nature*, *528*(7582), 413–417.
Westphalen, K., Gusarova, G. A., Islam, M. N., Subramanian, M., Cohen, T. S., Prince, A. S., & Bhattacharya, J. (2014). Sessile alveolar macrophages communicate with alveolar epithelium to modulate immunity. *Nature*, *506*(7489), 503–506.
Woan, K. V., Sahakian, E., Sotomayor, E. M., Seto, E., & Villagra, A. (2012). Modulation of antigen-presenting cells by HDAC inhibitors: implications in autoimmunity and cancer. *Immunology and Cell Biology*, *90*(1), 55–65.
Wong, E. S. M., Le Guezennec, X., Demidov, O. N., Marshall, N. T., Wang, S. T.,

Krishnamurthy, J., Sharpless, N. E., Dunn, N. R., & Bulavin, D. V. (2009). p38MAPK Controls Expression of Multiple Cell Cycle Inhibitors and Islet Proliferation with Advancing Age. *Developmental Cell*, *17*(1), 142–149.

Wright, K. L., & Ting, J. P. Y. (2006). Epigenetic regulation of MHC-II and CIITA genes. *Trends in Immunology*, *27*(9), 405–412.

Wu, D., Lim, E., Vaillant, F., Asselin-Labat, M. L., Visvader, J. E., & Smyth, G. K. (2010). ROAST: rotation gene set tests for complex microarray experiments. *Bioinformatics*, *26*(17), 2176–2182.

Wu, Q., Gu, Y., Tang, Y., Hu, X., & Dong, L. (2018). Therapeutic effects of p38 mitogen-activated protein kinases inhibitor SB203580 on airway inflammation in a mouse model of asthma. *Chinese Journal of Microbiology and Immunology*, *38*(7), 511–517.

Wu, W. C., Sun, H. W., Chen, H. T., Liang, J., Yu, X. J., Wu, C., Wang, Z., & Zheng, L. (2014). Circulating hematopoietic stem and progenitor cells are myeloid-biased in cancer patients. *Proceedings of the National Academy of Sciences of the United States of America*, *111*(11), 4221–4226.

Xu, Y., Wang, X., Liu, L., Wang, J., Wu, J., & Sun, C. (2022). Role of macrophages in tumor progression and therapy (Review). *International Journal of Oncology*, *60*(5).

Yan, H. H., Pickup, M., Pang, Y., Gorska, A. E., Li, Z., Chytil, A., Geng, Y., Gray, J. W., Moses, H. L., & Yang, L. (2010). Gr-1+CD11b+ myeloid cells tip the balance of immune protection to tumor promotion in the premetastatic lung. *Cancer Research*, *70*(15), 6139–6149.

Yang, Y., Kim, S. C., Yu, T., Yi, Y. S., Rhee, M. H., Sung, G. H., Yoo, B. C., & Cho, J. Y. (2014). Functional roles of p38 mitogen-activated protein kinase in macrophage-mediated inflammatory responses. *Mediators of Inflammation*, *2014*.

Yao, Y., Xu, Q., Kwon, M.-J., Matta, R., Liu, Y., Hong, S.-C., & Chang, C.-H. (2006). ERK and p38 MAPK signaling pathways negatively regulate CIITA gene expression in dendritic cells and macrophages. *Journal of Immunology (Baltimore, Md. : 1950)*, *177*(1), 70–76.

Yona, S., Kim, K. W., Wolf, Y., Mildner, A., Varol, D., Breker, M., Strauss-Ayali, D., Viukov, S., Guilliams, M., Misharin, A., Hume, D. A., Perlman, H., Malissen, B., Zelzer, E., & Jung, S. (2013). Fate mapping reveals origins and dynamics of monocytes and tissue macrophages under homeostasis. *Immunity*, *38*(1), 79–91.

Young, M. R., Endicott, R. A., Duffie, G. P., & Wepsic, H. T. (1987). Suppressor Alveolar Macrophages in Mice Bearing Metastatic Lewis Lung Carcinoma Tumors. *Journal of Leukocyte Biology*, *42*(6), 682–688.

Youssif, C., Cubillos-Rojas, M., Comalada, M., Llonch, E., Perna, C., Djouder, N., & Nebreda, A. R. (2018). Myeloid p38α signaling promotes intestinal IGF-1 production and inflammation-associated tumorigenesis. *EMBO Molecular Medicine*, *10*(7).

Yu, J., Angelin-Duclos, C., Greenwood, J., Liao, J., & Calame, K. (2000). Transcriptional repression by blimp-1 (PRDI-BF1) involves recruitment of

histone deacetylase. *Molecular and Cellular Biology*, *20*(7), 2592–2603.
Yu, X., Buttgereit, A., Lelios, I., Utz, S. G., Cansever, D., Becher, B., & Greter, M. (2017). The Cytokine TGF-β Promotes the Development and Homeostasis of Alveolar Macrophages. *Immunity*, *47*(5), 903-912.e4.
Yun, Y., Srinivas, G., Kuenzel, S., Linnenbrink, M., Alnahas, S., Bruce, K. D., Steinhoff, U., Baines, J. F., & Schaible, U. E. (2014). Environmentally determined differences in the murine lung microbiota and their relation to alveolar architecture. *PloS One*, *9*(12).
Zeeshan, R., & Mutahir, Z. (2017). Cancer metastasis - tricks of the trade. *Bosnian Journal of Basic Medical Sciences*, *17*(3), 172–182.
Zeisel, A., Yitzhaky, A., Bossel Ben-Moshe, N., & Domany, E. (2013). An accessible database for mouse and human whole transcriptome qPCR primers. *Bioinformatics (Oxford, England)*, *29*(10), 1355–1356.
Zhang, X., of, D. M.-T. J. of P. A. J., & 2008, undefined. (2008). Macrophage activation by endogenous danger signals. *Wiley Online Library*, *214*(2), 161–178.
Zheng, G. X. Y., Terry, J. M., Belgrader, P., Ryvkin, P., Bent, Z. W., Wilson, R., Ziraldo, S. B., Wheeler, T. D., McDermott, G. P., Zhu, J., Gregory, M. T., Shuga, J., Montesclaros, L., Underwood, J. G., Masquelier, D. A., Nishimura, S. Y., Schnall-Levin, M., Wyatt, P. W., Hindson, C. M., … Bielas, J. H. (2017). Massively parallel digital transcriptional profiling of single cells. *Nature Communications 2017 8:1*, *8*(1), 1–12.
Zheng, T., Zhang, B., Chen, C., Ma, J., Meng, D., Huang, J., Hu, R., Liu, X., Otsu, K., Liu, A. C., Li, H., Yin, Z., & Huang, G. (2018). Protein kinase p38α signaling in dendritic cells regulates colon inflammation and tumorigenesis. *Proceedings of the National Academy of Sciences of the United States of America*, *115*(52), E12313–E12322.
Zhou, G., Bao, Z. Q., & Dixon, J. E. (1995). Components of a new human protein kinase signal transduction pathway. *The Journal of Biological Chemistry*, *270*(21), 12665–12669.
Zhou, Y., Yao, Y., Deng, Y., & Shao, A. (2020). Regulation of efferocytosis as a novel cancer therapy. *Cell Communication and Signaling 2020 18:1*, *18*(1), 1–11.
Zhu, B., Yu, Y., Liu, X., Han, Q., Kang, Y., & Shi, L. (2019). CD200 Modulates S. aureus-Induced Innate Immune Responses Through Suppressing p38 Signaling. *International Journal of Molecular Sciences*, *20*(3).
Zhu, Y., Herndon, J. M., Sojka, D. K., Kim, K. W., Knolhoff, B. L., Zuo, C., Cullinan, D. R., Luo, J., Bearden, A. R., Lavine, K. J., Yokoyama, W. M., Hawkins, W. G., Fields, R. C., Randolph, G. J., & DeNardo, D. G. (2017). Tissue-Resident Macrophages in Pancreatic Ductal Adenocarcinoma Originate from Embryonic Hematopoiesis and Promote Tumor Progression. *Immunity*, *47*(2), 323-338.e6.
Zissel, G., Homolka, J., Schlaak, J., Schlaak, M., & Müller-Quernheim, J. (1996). Anti-inflammatory cytokine release by alveolar macrophages in pulmonary sarcoidosis. *American Journal of Respiratory and Critical Care Medicine*, *154*(3 Pt 1), 713–719.
Zou, W. (2005). Immunosuppressive networks in the tumour environment and their

therapeutic relevance. *Nature Reviews Cancer 2005 5:4*, *5*(4), 263–274.
Zuniga, E. I., McGavern, D. B., & Oldstone, M. B. A. (2008). Antigen Presentation. *Encyclopedia of Virology*, 121–126.